FACULDADE DE CIÊNCIAS E TECNOLOGIA
UNIVERSIDADE NOVA DE LISBOA
Departamento de Química

requimte
rede de química e tecnologia

Universidade Nova de Lisboa

Faculdade de Ciências de Tecnologia

Author: MsC. Elisabete De Jesus Oliveira Marques

New Fluorescent Chemosensors based on bio-inspired ligands and Macrocycles: From single molecules to nanoparticles

PhD em Biotecnologia

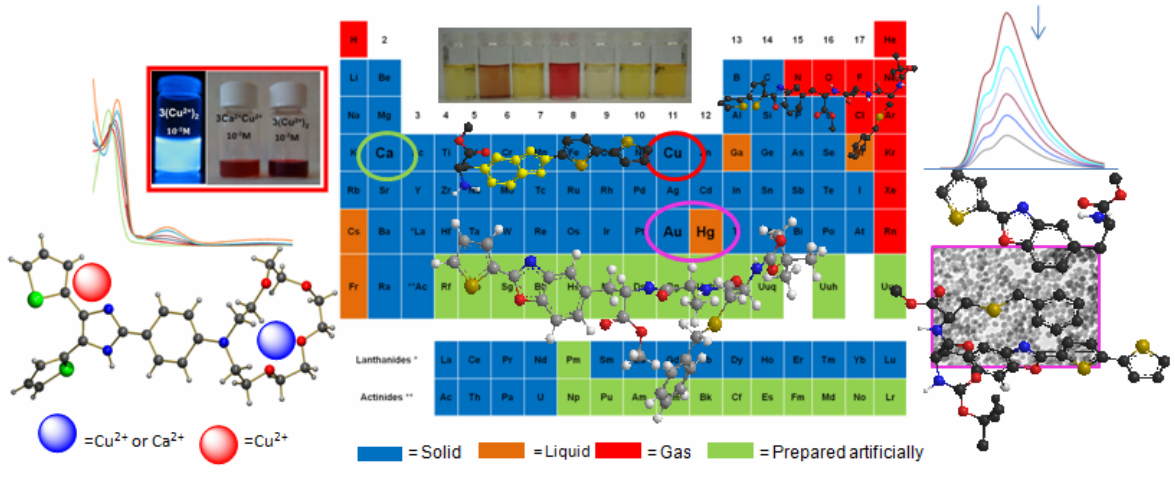

Supervisor: Dr.Carlos Lodeiro (FCT-UNL/U.VIGO)

Co-Supervisor (s): Dra. Susana Costa (UMINHO)

Dra. Isabel Moura (REQUIMTE-FCT-UNL)

Lisboa, 2010

Ph.D dissertation in Biotecnologia by Elisabete De Jesus Oliveira Marques
Title: New Fluorescent Chemosensors based on bio-inspired ligands and Macrocycles: From single molecules to nanoparticles
Author: Elisabete De Jesus Oliveira Marques
Printed by Lápices 4

FACULDADE DE CIÊNCIAS E TECNOLOGIA
UNIVERSIDADE NOVA DE LISBOA
Departamento de Química

requimte
rede de química e tecnologia

Universidade Nova de Lisboa
Faculdade de Ciências de Tecnologia

Author: MsC. Elisabete De Jesus Oliveira Marques

New Fluorescent Chemosensors based on bio-inspired ligands and Macrocycles: From single molecules to nanoparticles

PhD em Biotecnologia

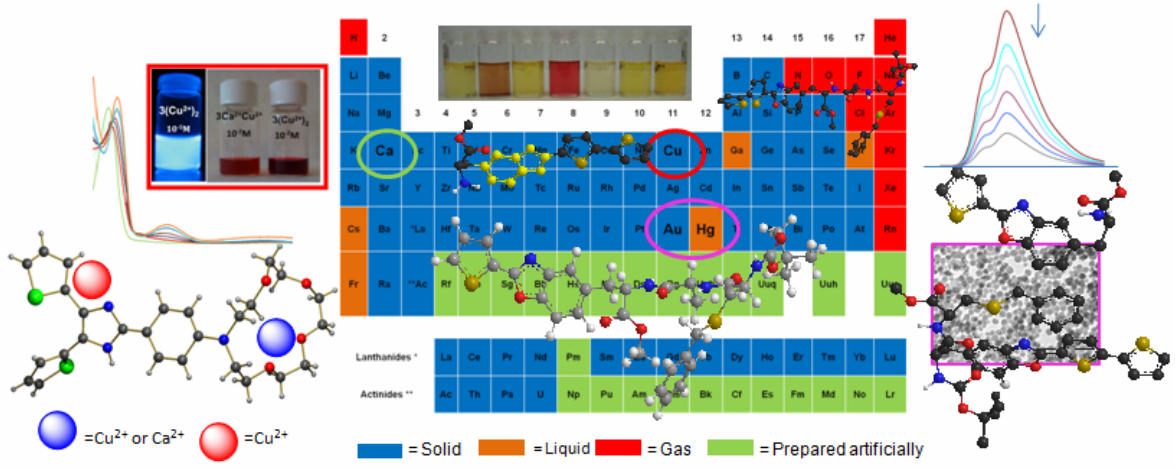

Dissertação apresentada para obtenção do grau de Doutor em Biotecnologia pela Universidade Nova de Lisboa, Faculdade de Ciências e Tecnologia.

A presente dissertação foi preparada no âmbito do protocolo de acordo bilateral de educação avançada (ERASMUS) entre a Universidad de Vigo e a Universidade Nova de Lisboa.

Lisboa, 2010

“Life is not easy for any of us. But what of that? We must have perseverance and above all confidence in ourselves. We must believe that we are gifted for something and that this thing must be attained”

Marie Curie

To Patrique and my mother

ACKNOWLEDGEMENTS

During my PhD I had the pleasure and lucky to know many people, where which one contributed for the increase of my knowledge. Thus I would like to thank the support of many people.

I'm eternally grateful to Dr. Carlos Lodeiro, my supervisor, for their support and guidance in difficult times, and be always present in the most important moments of my scientific life. There are no words to describe all his dedication, kindness and friendship shown during these past years. I thank you from my heart for everything.

I'm gratefully to Dr. José Capelo for is guidance on MALDI-TOF-MS studies, his friendship and support in the BIOSCOPE group.

I would like to thank to my co-supervisor, Dra. Susana Costa for her support during the three months that I spent in Minho University; all her guidance and help, during my PhD; thank to the entire chemistry group of Prof. M.Manuela Raposo.

I would like to thank also to my co-supervisor Dra. Isabel Moura.

I would like to thank to Dra. Teresa Avilés by the speak about science and good atmosphere in the laboratory 412.

I'm gratefully to the REQUIMTE, New University of Lisbon by the host, allowing the development of research work.

I would like to thank to Prof. Dr. Luca Prodi to welcome me in his research group in Bologna, to Dra. Nelsi Zaccheroni for her great support in the nanoparticle synthesis and fluorescence studies; to Dra. M. Teresa Gandolfi, to Riccardo, Damiano and Sara.

I'm gratefully to Prof. Dr. Juan Carlos Mejuto from Vigo University, Ourense.

Thanks to all my laboratory colleagues in the BIOSCOPE group, who became friends and made me fell as a part of a great group, Bruno, Cristina, Javier, Jorge, Júlio, Marco, Ricardo, Gonçalo e Dr. Mário Dinis; specially my friend and colleague Hugo, which always gave me support and his friendship, and it is a pleasure work with him.

I would like to thank to Dr. Cristina Nuñez by the help in X-Ray diffraction, to Dr. Pablo Gonzalez by the EPR studies, to Dr. Olalla Nieto by the DFT calculations and to MsC. Luz Fernandes by the help in the MALDI studies.

I thank to FC-MCTES (Portugal) by my PhD grant SFRH/BD/35905/2007, by the project PTDC/QUI/66250/2006, “Desenvolvimento de novos compostos heterocicíclos como sensores químicos luminescentes e colorimétricos: detecção de aniões e catiões metálicos”; to the University of Vigo by the Project VICOUK914-122P64702 “Sintese y aplicación de novos sensores químicos de fluorescencia para la determinación de biomoleculas y metales de interés medioambiental”; and Xunta de Galicia, Spain by the Project 09CSA04338PR (in Biomedicine) “Aplicación de Nanopartículas activas inxectadas por ultrasonidos no tratamento de mostra para a identificación rápida de proteínas e biomarcadores de tecidos biológicos”; and specially to Fundação Calouste Gulbenkian (Portugal), for the National Prize in criativity and quality in reseach activity, 2008.

Finally the most important thanks go to my family, my husband Patrique, my mother, my father and my sister. Without them none of this would be possible, they always gave me the strength needed to move on and continue this difficult research way. Especially to my husband, who always accompanied me, supported me and followed me even when we had to change of city. He suffered and laughed with me in difficult and happy times during this PhD.

ABSTRACT

Due to the importance of the development of new fluorescent compounds with multifunctional applications in environmental and analytical sciences, nano-scale technologies and bio-medicine, the research summarized in this PhD project was focused on the synthesis of new bio-inspired sensors, containing alanine, trypthophan and cysteine amino acids, provided with benzoxazole chromophores; exploration of its photophysical properties as fluorescence markers and chemosensors, and finally in the synthesis of new gold and silica nanoparticles with emissive properties. At the same time, different macrocyclic compounds bearing anthracene, or furyl, aryl or thienyl moieties linked to an imidazo-aza-crown ether were exploited for the synthesis of solid inorganic complexes and their use as fluorescent chemosensors for metal ions and anions was undertaken.

The benzoxazole ring was selected as fluorescence probe for peptide skeleton due to the biological activity, antifungal, antimicrobial and anticancer properties, and also due to the higher emission fluorescence which makes it a good candidate for molecular recognition, biomarkers or biosensors.

Several studies on the metal ion association constants and by density functional theory (DFT) were performed.

The association of the synthesized compounds to more structured nanoparticles could increase the sensibility of the chemosensor and also its capability for sensing. In our case, incorporation of the cysteine amino acid made them good candidates for linkage to gold surface nanoparticles. However, in same cases due to the energy transfer from the metal core, the emission fluorescence of these decorated nanoparticles was quenched. Taking into account this phenomenon, different commercial light transparent LUDOX© silica nanoparticles were prepared and studied, containing the emissive peptides.

This PhD dissertation is divided in eight chapters; and a brief description of each chapter is presented.

Chapter 1 shows a brief introduction to general fluorescent chemosensors and definitions, mechanisms of detection, chemosensors based on macrocyclic ligands, chemosensors containing bio-inspired units, from single amino acids to peptide chains; some aspects on the biological applications on emissive chromophores; the importance on the detection and quantification of metal ions; and finally a short introduction concerning the synthesis and applications of silica and gold nanoparticles and their advantages.

In **Chapter 2** is described the photophysical studies of a new macrocyclic ligand (**L**) containing an anthracene as pendant arm, and its characterization. The sensing capability of

Abstract

L towards alkaline (Na^+, K^+, Li^+), alkaline earth (Ca^{2+}, Mg^{2+}), transition and post-transition (Cr^{3+},Cu^{2+} and Zn^{2+}, Cd^{2+}, Hg^{2+} and Al^{3+}) metal ions were performed by Uv-vis and fluorescent emission spectrocopy. An increase in the fluorescence emission (CHEF effect) was observed in methanol and in mixtures methanol/water in the presence of Cd^{2+} (5.0-fold), Zn^{2+} (4.5-fold), Cr^{3+} (2.0-fold) and Al^{3+} (1.8-fold). This work was published in: *Inorganica Chimica Acta*, **2007,** 360, 2734-2743.

In **Chapter 3** is presented the synthesis of several metal complexes with three new aza-crown ether macrocycles bearing furyl, aryl or thienyl moieties linked to an imidazo-crown system (**1**, **2** and **3**) and its chemical characterization by elemental analysis, infrared, absorption and emission spectroscopy, X-Ray crystal diffraction, and MALDI-TOF-MS spectrometry. The sensing capability of all ligands were studied in the presence of Ca^{2+}, Cu^{2+}, Ni^{2+}, Hg^{2+} and F^-. For compounds **2** and **3** was observed an increase in the emission fluorescence with Ca^{2+} and Cu^{2+}. Moreover, compound **3** showed a colorimetric characteristic with Cu^{2+}. Submitted to *Inorganic Chemistry*, **2010**.

In **Chapter 4** is described the photophysicial studies of highly emissive fluorescent probes based on unnatural alanine derivatives bearing the benzoxazole unit as chromophore at the side chain, functionalized with different moieties, such as, thiophene (**2a**-**2d**) or trimethoxybenzaldehyde (**2e**-**2f**). The incorporation of different units into the benzoxazole modulates the fluorescence quantum yield, being the thiophene derivatives the most emissive compounds. For all compounds was observed a quenching effect with Cu^{2+}, Ni^{2+} and Hg^{2+}, as shown by absorption and emission fluorescence spectroscopy. Taking into account the complexation constants obtained it was postulated that probably the first metal ion takes place in the carboxylic acid group and the second one around the chomophore. This work was published in: *Sensors*, **2007,** 7, 2096-2114.

Chapter 5 shows the synthesis and photophysical studies with new benzoxazolyalanine derivatives bearing (oligo)thiophene units at the side chain (**4a**-**6a**). All compounds were highly fluorescent, making them good candidates for application as fluorescent probes. This work was published in: *Tetrahedron Letters,* **2008,** 49, 5258-5261.

Due to the highly fluorescent quantum yield shown by the compounds reported in chapter 5 all were titrated with metal ions, and the synthesis of the metal complexes, with Cu^{2+}, Ni^{2+} and Hg^{2+} was performed. These results are summarized in **Chapter 6**. The complexes were characterized by elemental analysis, Uv-Vis and fluorescence spectroscopy in solution and solid state. Some studies by DFT confirm our coordination hypothesis. In order to increase the knowledge of the coordination site an angular bis-alanine system, **L4**, bearing two units

of alanine-benzoxazole linked by a thiophene unit was explored towards Cu^{2+}, Ni^{2+} and Hg^{2+} metal ions. Manuscript submitted to *Inorganica Chimica Acta*, **2010**.

Chapter 7 summarizes the synthesis of six new emissive di and tri-peptides derivatives containing benzoxazolyl-alanine, trypthophan and cysteine amino acids (**L1**-**L4**, **L6**-**L7**), and two previously reported in chapter **5** benzoxazolyl alanine derivates (**L** and **L5**). Photophysical studies on the interaction towards transition and post-transition metal ions (Cu^{2+}; Ni^{2+}; Ag^{+}; Zn^{2+}; Cd^{2+}; Hg^{2+} and Pb^{2+}) by absorption and fluorescence emission spectroscopy, and by MALDI-TOF-Ms spectrometry were performed. In general, all compounds showed a good interaction with Hg^{2+}. Gold(0) nanoparticles decorated with ligands **L**, **L1** and **L3,** were synthesized by common reductive procedures, and emissive silica nanoparticles were synthesized using compounds **L5-L7** linked through a silane spacer. The silica core were based on commercial LUDOX© nanoparticles, in different ligand:nanoparticle ratios. All nanoparticles obtained were characterized by dynamic light-scattering (DLS), transmission electron microscopy (TEM), UV-vis absorption and emission spectroscopy. TEM images revealed the formation of gold nanoparticles between 2.4 and 10 nm, and silica nanoparticles, with size between 14 and 24 nm. The interaction with metal ions was also performed using the silica nanoparticles as supramolecular chemosensors, being selective for Ag^{+} and Hg^{2+}.

The general conclusions of this research work can be found in **Chapter 8**.

RESUMO

Devido ao desenvolvimento e importância de novos compostos fluorescentes com aplicações multifuncionais em ciência do ambiente, em ciências analíticas, tecnologia de nano-escala e bio-medicina, o trabalho de investigação apresentado neste projecto de Doutoramento incide na síntese de novos sensores bio-inspirados, contendo aminoácidos, como a alanina, cisteina e triptofano, conjugados ao cromóforo benzoxazole; foram exploradas as suas propriedades fotofísicas, como marcadores fluorescentes e sensores químicos, e finalmente na síntese de nanopartículas de ouro e sílica com propriedades emissivas.

De igual modo, foi explorado a síntese de complexes sólidos inorgânicos, bem como as suas propriedades como sensores químicos na presença de iões metálicos e aniões, de compostos macrocíclicos contendo unidades antraceno; furano, arilo ou tiofeno ligados a um éter imidazo-aza-coroa.

O anel aromático benzozazole foi seleccionado como sonda fluorescente na estrutura peptídica, devido à sua actividade biológica, antifúngica, antimicrobial e anticancerígena; e também devido à sua elevada emissão de fluorescência. Todas estas propriedades, torna-o um bom candidato para reconhecimento molecular, biomarcadores e biosensores.

Por conseguinte, foram efectuados estudos de constantes de associação a iões metálicos e também por teoria funcional de densidade (DFT).

A associação dos compostos sintetizados a nanopartículas poderá aumentar a sensibilidade do sensor químico, bem como a sua capacidade sensitiva. No presente trabalho, a incorporação do aminoácido cisteina na cadeia peptídica dos compostos tornou-os bons candidados para ligação a superfícies de nanopartículas de ouro. No entanto, em alguns casos devido à transferência de energia proveniente do centro metálico, ocorreu a supressão de emissão de fluorescência dos compostos “decorados”. Devido a este fenómeno, foram sintetizados e estudados péptidos emissivos ancorados a nanopartículas transparentes comerciais de sílica LUDOX©.

Esta dissertação de Doutoramento está dividida em oito capítulos, e de seguida é apresentada uma breve descrição de cada capítulo.

No **Capítulo 1** é apresentada uma breve introdução sobre sensores químicos fluorescentes gerais e definições, mecanismos de detecção, sensores químicos baseados em ligandos macrocíclicos, sensores químicos compostos por unidades bio-inspiradas, desde aminoácidos simples a cadeias peptídicas; alguns aspectos de aplicações biológicas dos cromóforos emissivos; a importância da detecção e quantificação de iões metálicos; e

finalmente uma breve introdução acerca da síntese e aplicações das nanopartículas de ouro e silica e as suas vantagens.

No **Capítulo 2** são descritos os estudos fotofísicos e a caracterização de um novo ligando macrocíclico (**L**) contendo como braço pendente uma unidade antraceno. A avaliação da capacidade sensorial de **L** na presença de iões metálicos alcalinos (Na^+, K^+, Li^+), alcalino-terrosos (Ca^{2+}, Mg^{2+}), de transição de pós-transição (Cr^{3+},Cu^{2+} and Zn^{2+}, Cd^{2+}, Hg^{2+} and Al^{3+}) foi efectuada por espectroscopias de absorção e de emissão de fluorescência. Em metanol e em misturas metanol/água, foi observado um aumento da intensidade de emissão (efeito CHEF) na presença dos iões metálicos Cd^{2+} (5.0-vezes), Zn^{2+} (4.5-vezes), Cr^{3+} (2.0-vezes) and Al^{3+} (1.8-vezes). Este trabalho foi publicado em: *Inorganica Chimica Acta*, **2007,** 360, 2734-2743.

No **Capítulo 3** é apresentada a síntese e caracterização (por análise elementar, espectroscopias de infravermelho, absorção e emissão de fluorescência, difracção Raios-X, e espectroscopia de MALDI-TOF-MS) de complexos metálicos com três novos macrociclos éter aza-coroa contendo unidades furano, arilo e tiofeno ligadas a um sistema imizado-coroa (**1**, **2** e **3**).
A capacidade sensorial de todos os ligandos foi estudada na presença de Ca^{2+}, Cu^{2+}, Ni^{2+}, Hg^{2+} e F^-. Nos compostos 2 e 3 foi observado um aumento da intensidade de emissão de fluorescência com Ca^{2+} e Cu^{2+}. O composto 3 apresentou características colorimétricas com Cu^{2+}. Submetido ao *Inorganic Chemistry*, **2010**.

No **Capítulo 4** são descritos os estudos fotofísicos de sondas altamente fluorescentes compostos por derivados não naturais da alanina contendo, o cromóforo benzoxazole funcionalizado com diferentes unidades, como o tiofeno (**2a**-**2d**) ou o trimetoxibenzaldeido (**2e**-**2f**).
A introdução de diferentes unidades no cromóforo benzoxazole modula o rendimento quântico de fluorescência, sendo os mais emissivos os compostos derivados do tiofeno. Em todos os compostos foi observado por espectroscopias de absorção e de emissão de fluorescência uma supressão da intensidade de emissão com Cu^{2+}, Ni^{2+} and Hg^{2+}. Com base nas constantes de complexação obtidas foi postulado que provavelmente o primeiro ião metálico liga-se ao grupo ácido carboxílico, e o segundo em torno do cromóforo. Este trabalho foi publicado em: *Sensors*, **2007,** 7, 2096-2114.

O **Capítulo 5** apresenta a síntese e os estudos fotofísicos de novos derivados benzoxazole-alanina contendo na cadeia lateral, unidades de (oligo)tiofeno (**4a**-**6a**). Todos os compostos demonstraram propriedades altamente fluorescentes, tornando-os bons candidatos como

sondas fluorescentes. Este trabalho foi publicado em: *Tetrahedron Letters,* **2008,** 49, 5258-5261.

Devido ao elevado rendimento quântico de fluorescência demostrado pelos compostos no **Capítulo 5**, todos foram titulados com iões metálicos, e procedeu-se à síntese de complexos metálicos, com Cu^{2+}, Ni^{2+} e Hg^{2+}. Estes resultados estão sumarizados no **Capítulo 6.**
Os complexos foram caracterizados por análise elementar, espectroscopias de absorção e de emissão de fluorescência em solução e estado sólido. Os estudos por DFT confirmam a hipótese de coordenação apresentada. Tendo como objectivo incrementar o conhecimento do local de coordenção pelo metal, um sistema angular to tipo bis-alanina L4, contendo duas unidades de alanina-benzoxazole ligados por uma unidade tiofeno foi estudado na presença de iões metálicos como o Cu^{2+}, Ni^{2+} e Hg^{2+}. Manuscrito submetido ao *Inorganica Chimica Acta*, **2010**.

O **Capítulo 7** sumariza a síntese de seis novos derivados de di e tripéptidos contendo aminoácidos como a benzoxazolil-alanina, o triptofano e a cisteina (**L1**-**L4**, **L6**-**L7**), e dois derivados de benzoxazolil-alanina, já apresentados no Capítulo 5 (**L** and **L5**). Os estudos fotofísicos dos ligandos na presença de iões metálicos de transição e pós-transição (Cu^{2+}; Ni^{2+}; Ag^{+}; Zn^{2+}; Cd^{2+}; Hg^{2+} and Pb^{2+}) foram monitorizados por espectroscopias de absorção e de emissão de fluorescência e MALDI-TOF-MS.
Em geral, todos os compostos apresentaram uma boa interacção com Hg^{2+}. Nanopartículas de ouro(0) “decoradas” com os ligandos **L**, **L1** e **L3** foram obtidas pelo método de síntese redutiva; nanopartículas emissivas de sílica foram sintetizadas com os compostos **L5-L7** ligados por um espaçador silano. O centro de sílica é baseado em nanopartículas comerciais LUDOX©, com diferentes razões ligando: nanopartículas.
Todas as nanopartículas obtidas foram caracterizadas por "dynamic light-scattering” (DLS), microscopia de transmissão electrónica (TEM) e espectroscopias de absorção e de emissão de fluorescência. As imagens TEM revelaram a formação de nanopartículas de ouro entre 2.4 e 10 nm, e nanopartículas de sílica, de tamanho entre 14 e 24 nm. A interacção com iões metálicos foi também realizada usando como sensores químicos supramoleculares, as nanopartículas de sílica, sendo selectivas para Ag^{+} e Hg^{2+}.
As conclusões gerais deste trabalho de investigação poder-se-ão encontrar no **Capítulo 8**.

COMPOUNDS

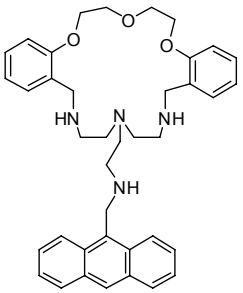

L

Figure 1.- Macrocycle discussed in Chapter 2.

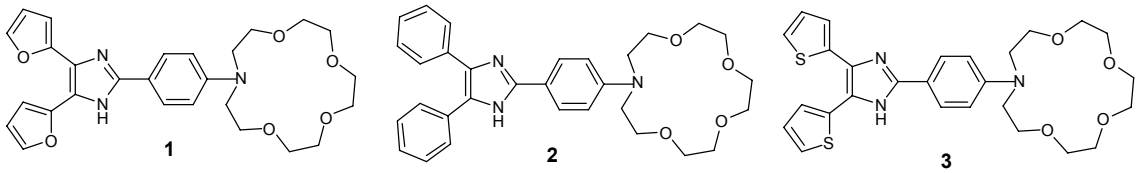

1 2 3

Figure 2.- 15-crown-5-imidazo crown ethers derivates discussed in Chapter 3.

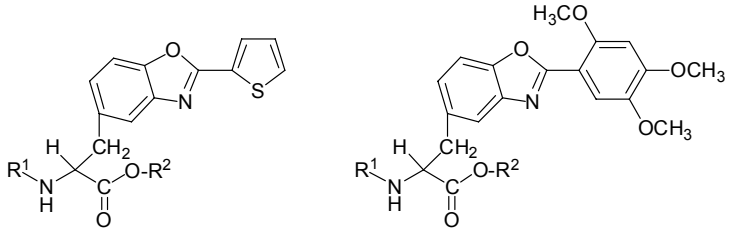

2 a R^1 = Boc, R^2 = CH_3
b R^1 = Boc, R^2 = H
c R^1 = H, R^2 = CH_3
d R^1 = R^2 = H

2 e R^1 = Boc, R^2 = CH_3
f R^1 = Boc, R^2 = H
g R^1 = R^2 = H

Figure 3.- Alanine derivatives discussed in Chapter 4.

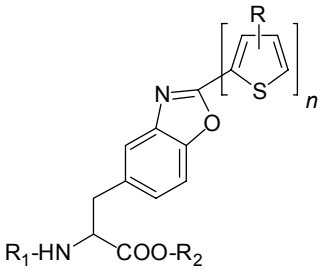

4 *n* = 1, R = $(CH_2O)_2$
5 *n* = 2, R = H
6 *n* = 3, R = H

a R_1= Boc, R_2 = Me
b R_1= Boc, R_2 = H
c R_1= R_2 = H

Figure 4.- (Oligo)thienylbenzoxazolyl-alanine derivatives **4a-c** to **6a-c** discussed in Chapter 5.

Compounds

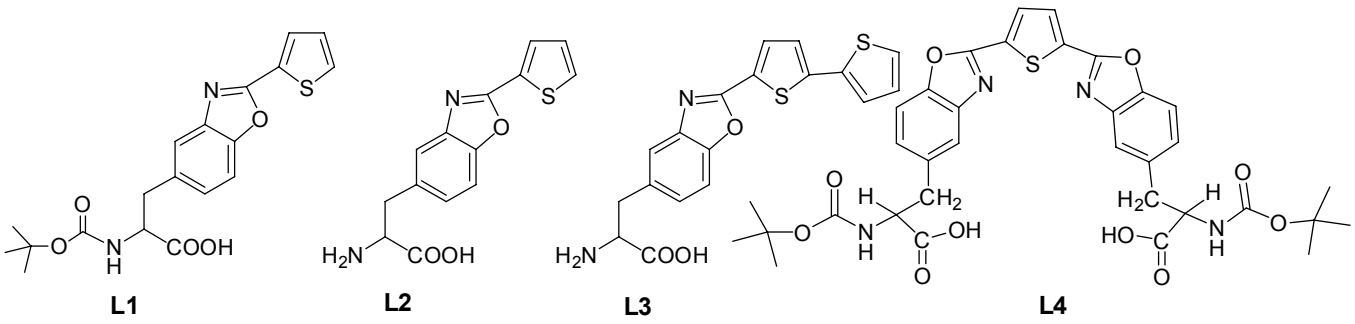

Figure 5 .- Alanine derivatives discussed in Chapter 6.

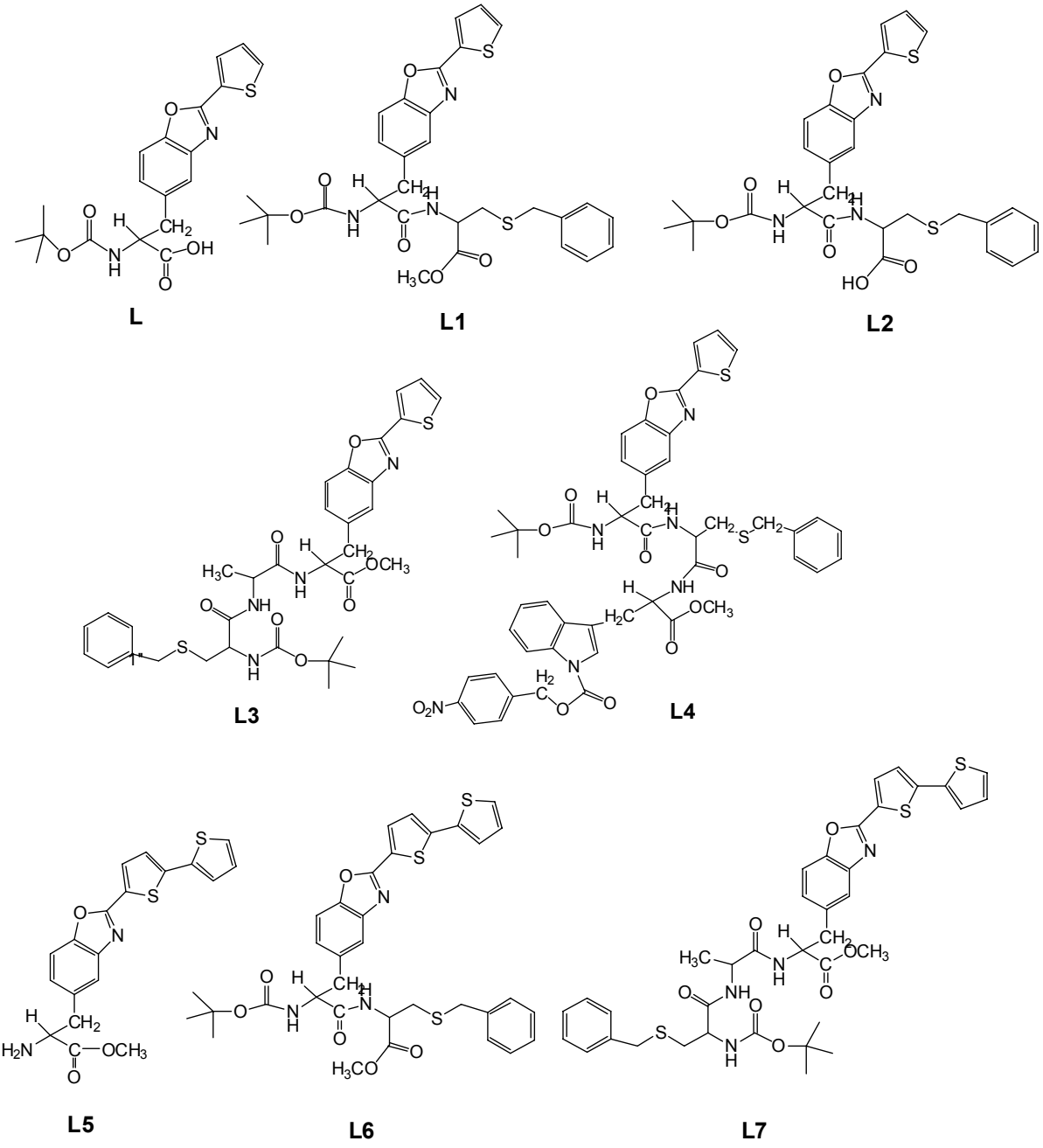

Figure 6 .- Amino acids and peptide sensors discussed in Chapter 7.

ABBREVIATIONS

ε	Molar extinction coefficient
λ	Wavelength
ν	Wave number
^{13}C-NMR	Carbon nuclear magnetic ressonance
^{1}H-NMR	Proton nuclear magnetic ressonance
AgNPs	Silver nanoparticles
Ala	Alanine
AuNPs	Gold nanoparticles
BOT	Benzoxazol-thiophene
BOTT	Benzoxazol- bithiophene
CHEF	Chelation enhancement of the fluorescence emission
CHEQ	Chelation enhancement of the quenching emission
Cys	Cysteine
DCC	N,N'-Dicyclohexylcarbodiimide
DDNs	Dye-doped silica nanoparticles
DE	Delayed extraction
DFT	Density Functional Theory
DL	Detection limits
DLS	Dynamic ligth-scattering
DMF	Dymetilformamide
DSP	Dithiobis(succinimidylpropionate)
EET	Electronic energy transfer
EPR	Electron paramagnetic resonance
eT	Electron transfer
ET	Electronic transfer
FRET	Fluorescence resonance energy transfer
FSR	Fluorophore-Spacer- Receptor
FT	Tetraoctylammonium bromide
HOBt	1-Hydroxybenzotriazole
HOMO	Highest occupied molecular orbital
IR	Infrared
LMCT	Ligand-metal charge-transfer transition
LUMO	Lowest unoccupied molecular orbital
MALDI-MS	Matrix Assisted Laser Desorption Ionization-Mass Spectrometry
MLCT	Metal-to ligand charge transfer transition
NP	Nanoparticles

Abbreviations

PET	Photoinduced electron transfer
pI	Isoelectric point
QL	Quantification limits
RMM	Reverse-micelle microemulsion
SiNPs	Silica nanoparticles
TEM	Transmission electronic microscopy
TEOS	Tetraethoxysilane
TFA	Trifluoracetic acid
TLC	Thin layer chromatography
TMOS	Tetramethoxysysilane
Trp	Tryptophan
UV	Ultra-violet
UV-Vis	Ultraviolet- visible
Φ_F	Fluorescent quantum yield
τ	Lifetime

CONTENTS

INDEX OF FIGURES

Index of Figures

INDEX OF SCHEMES

Index of Schemes

INDEX OF TABLES

Chapter 1

Introduction

"If I have seen further it is by standing on the shoulders of giants"

Sir Isaac Newton, 1643-1727

Index

1.1 - Supramolecular Chemistry: Fluorescent Chemosensors.

In the middle of the 19th century G. Stokes reported that the fluorescence emission spectrum appears at a longer wavelength than the excitation spectra[1], and with this physical observation known as "Stokes shift" started the key conceptual basis for the fluorimetric analysis.

The development of new chemosensors changed dramatically since the pioneering work of Czarnik[2], and these modifications altered substantially the analytical applications in chemical analysis.[3]

One of the first papers reporting the uses of luminescence as an analytical tool appears later in 1923. Harvey reported in Science the minimum of concentration required of the molecule luciferin, **1**, a light-emitting biological dye found in some organisms capable of bioluminescence, to detect visible light.[4] Later Sousa and Larson described the concept of a fluorescence chemosensor using some functionalized naphthalene azacrown-ether ligands, **2**, for alkaline metal ion detection (Scheme 1.1).[5]

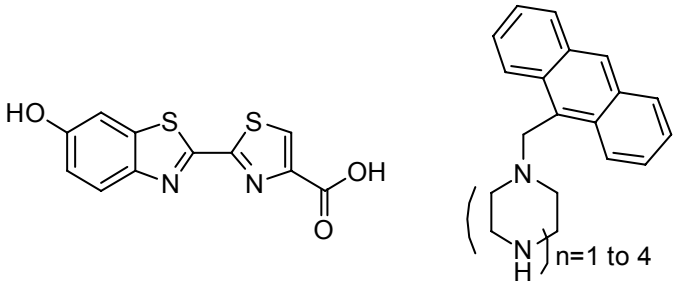

1 **2**

Scheme 1.1 – Structure of ligands **1** and **2**.

Since that, a fluorescent chemosensor can be defined as "a compound of abiotic origin that complexes to an analyte reversibly with a concomitant fluorescent signal transduction".[6,7] This classical definition cannot be confused with the more extended definition given by the IUPAC for a chemical sensor, "as a device that transform chemical information, ranging from the concentration of a specific sampler to total composition analysis into analytically useful signals"[8]

As was reported by A.P. de Silva and co-workers, a classical fluorescent chemosensor is constituted by three basic units: i) a receptor (responsible for molecule recognition), ii) a fluorophore (responsible for signaling the recognition) and iii) a spacer (a chemical brigde that links the receptor and the fluorophore controlling their separation and geometric

arrangement). [9,10] Sometimes, one part of the molecule can act by performing two or more aforementioned functions. From a structurally point of view fluorescent chemosensors can be classified into two general classes: *intrinsic*[11] chemosensors in which both functions (binding and signaling) are performed by the fluorophore (A; Scheme 1.2) and *conjugated* chemosensors in which binding/recognizing and signaling parts are separated by a spacer (FSR) (B; Scheme 1.2).

In all cases mentioned, a good fluorescent chemosensor must have a strong affinity and selectivity for the analyte, be photostable, and the environmental interferences should not disturb in the fluorescence signal.[12] The recognition can be occurs in four different ways: i) a chelation enhancement of the fluorescence emission (CHEF), ii) a chelation enhancement of the quenching emission (CHEQ), iii) formation of an *exciplex* or *excimer* probes (C; Scheme 1.2), and iv) as a chemodosimeters (D; Scheme 1.2).[13,14] The three first mechanism are reversible and the last one is irreversible.[14]

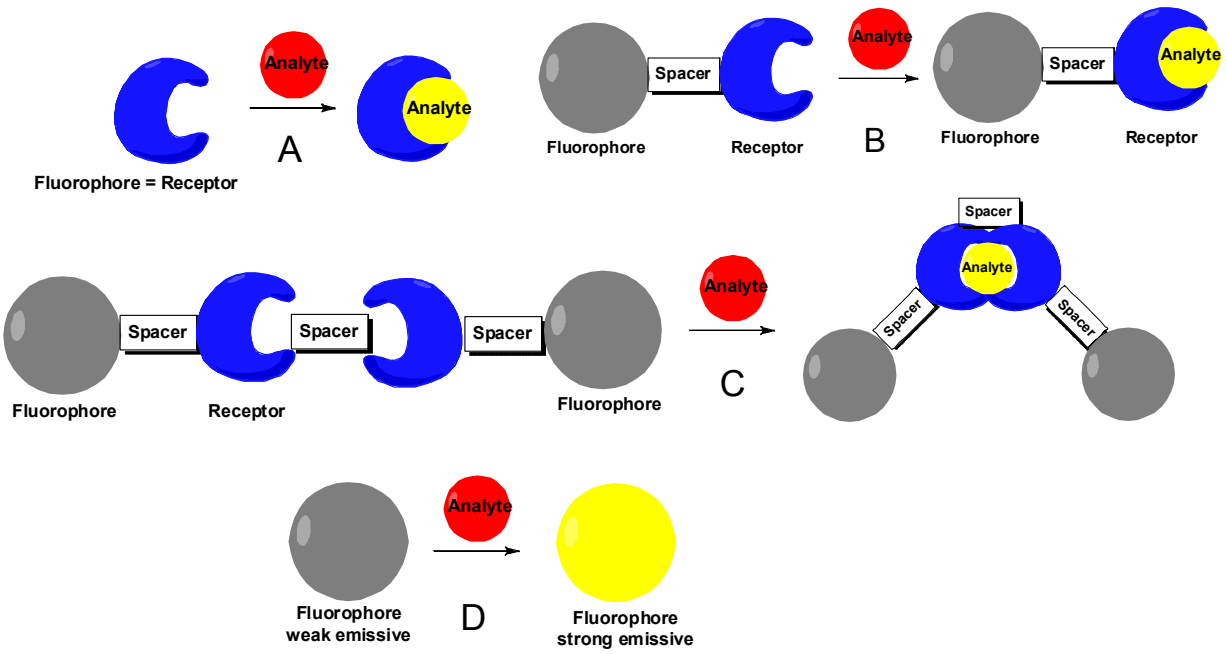

Scheme 1.2 – Schematic representation of the different approaches between the chemosensor and the analyte. (A) – Intrinsic Fluorescence probes, (B) – Fluorophore-spacer-receptor systems (Conjugated), (C) - exciplex or excimer probes, (D) - Chemodosimeters [14]

1.2 - Mechanisms of detection

Fluorescence is an important analytical tool to sense relevant species, for example metal ions and anions. This application can be useful for analytical purposes *in vitro* and *in vivo* studies.[3]
It is important to mention that different processes can occur: ones involving intramolecular and others intermolecular processes.

In an excited molecule radiative and non-radiative transition between electronic states can occur, for example, photon absorption, fluorescence, internal conversion, intersystem crossing, phosphorescence, delay fluorescence and triplet-triplet transitions (see Scheme 1.3).

Concerning the interaction with other molecules several photophysical processes can happen as for example, electron transfer, proton transfer, energy transfer, excimer or exciplex formation.[15]

In more detail, fluorescence is a radiative transition where an emission of a photon from the excited state to the ground state ocurrs. Based on Stoke´s rule mentioned below and the energy loss in the excited state due to the vibrational relaxation, the wavelength of the emission is always located at higher values.[15]

An internal conversion is a non-radiative transition that occurs between two electronic states with the same spin multiplicity, being described as a vibrational relaxation from the lowest vibrational level to the final electronic state.

In the same way, an intersystem crossing is also a non-radiative transition between two vibrational levels with the same energy, even if they are of different multiplicities, for example electronic transition from a S_1 state to T_n triplet state with the same energy. A special case is the phosphorescence being the transition from triplet state T_1. They occur preferably in low temperatures, because at room temperature the process is very slow comparing with the intersystem crossing and vibrational relaxation process. The lowest triplet state has an energy lower than the singlet state S_1, so the phosphorescence band appears at higher wavelength than the emission fluorescence.[15]

Delay fluorescence is contrary to the intersystem crossing, when the triplet state T_1 has a long lifetime, and the energy difference between S_1 and T_1 is small, the transition from T_1 to S_1 can occur. A rise in temperature increases the probability of the process occurence.[15]
Triplet-triplet transitions occur when a molecule in the excited state absorb another photon at different wavelength.[15]

In Scheme 1.3 are represented schematically the processes mentioned above.

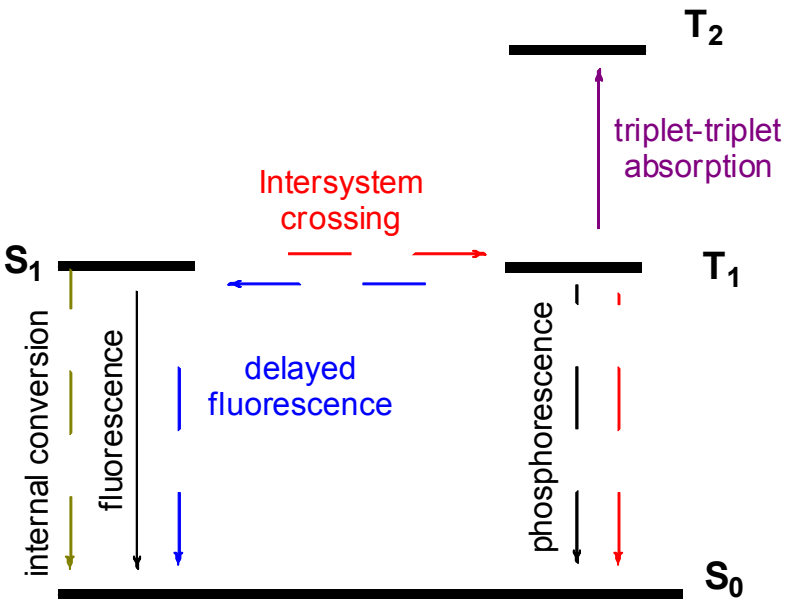

Scheme 1.3 – Photophysical processes, radiative and non-radiative transitions between electronic states of a molecule in the excited state in solution.[15]

There are many processes that can quench the fluorescence emission, like, double-bond torsion, low energy $n\pi^*$ levels, heavy metals, weak bonds, photoinduced electron transfer (PET) or electronic energy transfer (EET).[9]

When the fluorophore and the receptor (FSR) are electronically decoupled, any signaling mechanism has to occur by electronic transfer (ET) mechanisms.
A PET process happens when the receptor has nitrogen or other atoms, with a free lone pair of electrons, which can quench the luminescence by photoinduced transfer processes. On the other hand, this mechanims can be prevented by complexation or protonation of the lone pair located in the donor atoms.

In more details, in the PET-FSR, the HOMO of the receptor is energetically located between the HOMO and LUMO of the fluorophore. So, when promotion of an electron occurs from the HOMO to the LUMO of the fluorophore, happens a fast electron transfer, eT, from the receptor's HOMO to the HOMO of the fluorophore, promoting thus a quenching in the emission fluorescence.[14]

However, when the lone electron pair is engaged, the HOMO energy decreases, and the eT from the HOMO receptor to the HOMO fluorophore is switched off, resulting an emissive fluorescence (see Scheme 1.4). [14,14]

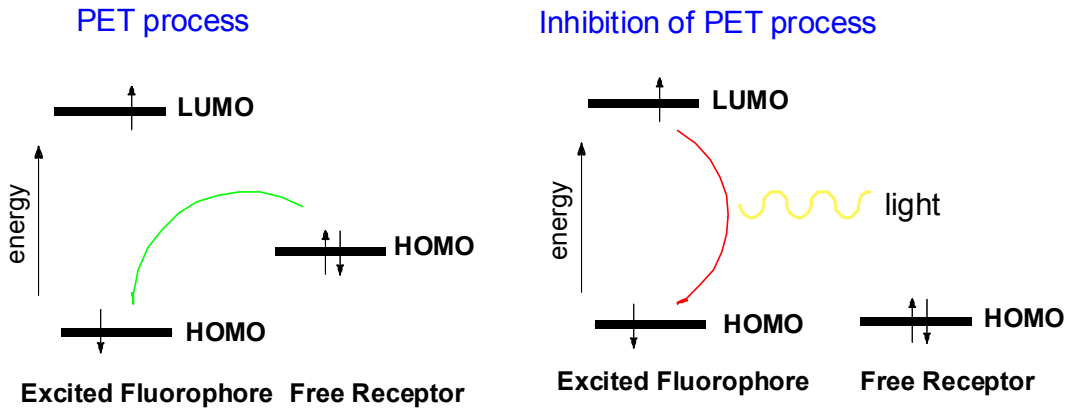

Scheme 1.4 – Schematic representation of an excited-state photoinduced electron transfer (PET) process and its inhibition. [14,15]

Finally the formation of excimers and exciplexes can occur when two or more fluorophores with a long lifetime, for example, pyrene and naphthalene, are present.[16,17,18]

The intramolecular/intermolecular excimer is formed in the excited state, by collision of an excited molecule/fluorophore that interacts with other identical molecule/fluorophore in the ground state.[15] The fluorescence band corresponding to an excimer is located at highest wavelengths than the monomer and normally is none vibrationally resolved. The monomer/excimer relationship is highly temperature dependent, with higher temperatures increasing the monomer formation.[15]

The exciplex formation occurs by the interaction of one molecule in the excited state with other different molecule or lone pair of electrons in the ground state, forming an excited complex. [15] The exciplex band changes with the solvent polarityas solvent polarity increases the band is red-shifted.

On the other hand, colorimetric molecular devices have attracted much scientific attention due to the so called “naked-eye” detection. This strategy reduces the use of expensive and complicated equipment to metal-ion measurements.[3]

1.3 - Chemosensors based on macrocycle detection receptors.

Cyclic polydentate ligands are defined as macrocycles if they feature nine or more atoms (including heteroatoms) and at least three donor atoms.[19] As an example, three representative macrocyclic systems, a crown-ether (**3**), a polyamine ligand (**4**) and a poly thia-aza system (**5**) are shown in scheme 1.5.

As the definition of macrocycle is very broad, the number of possible systems that can be designed is unlimited. For example just by changing the donor atoms the synthetic possibilities are infinites. The donor atoms can be oxygen, nitrogen, phosphorous, sulphur, selenium, or arsenium. Depending of the homo or hetero type of atoms used crown-ethers (O), polyamine (N)[20,21,22], polythioethers (SO)[23,24], polythia-aza (SN)[25] can be designed.

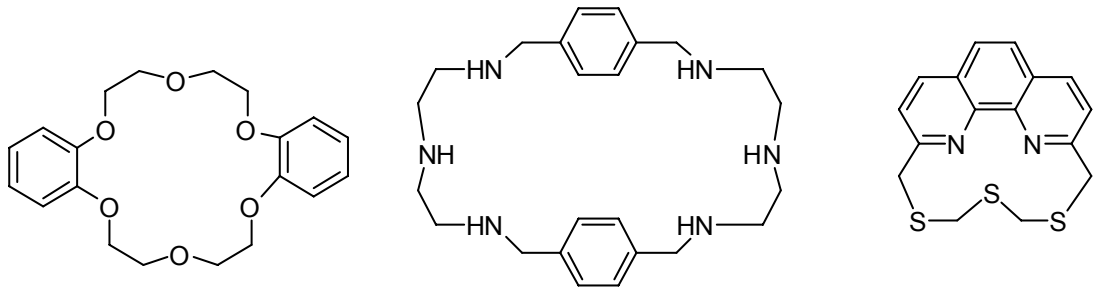

3 **4** **5**

Scheme 1.5 – Macrocyclic systems, **3** – crown ether macrocycle, **4** - Polyamine macrocycle, **5** - Polythiaza macrocycle

Apart from the type of donor atoms other parameters such as its cavity size, shape, conformation, topology and rigidity are important because they influence the thermodynamic and kinetics properties of the corresponding metal complexes.[19]

The uses of macrocyclic ligands are important in chemistry due to the higher thermodynamic and kinectic stability shown in comparison with the acyclic ligands, called the chelate and macrocycle effects.[26,27]

Polyamine macrocycle receptors provides versatility to the chemosensor applications, since its properties can be modulated in huge extension by the pH, the interaction with metal ions,

anions etc. For example, the protonation of the polyamine unit at acidic pH values renders an anion sensor while at basic pH the unprotonated forms are ideal to form stable metal complexes modulating the properties to sense protons and/or metal ions.

In systems containing of nitrogen donor-atoms, the electron transfer process from the lone pair of the aliphatic amino groups to the excited luminophore occurs when the lone pair is free, and this process is blocked after protonation or complexation. This phenomenon was observed in organic solvents and in water.

When in the skeleton of the receptor unit an aromatic heterocycle is included, such as a pyridine, bipyridine, terpyridine, antracene, naphthalene or phenanthroline unit, for example as in compound **6**, (see Scheme 1.6), their protonation leads to a photoinduced electron transfer from the π-π^* excited state of the hydrocarbon fluorophore to the protonated heterocycle. In some special cases, when a hydrocarbon fluorophore (anthracene, naphthalene, etc) is connected to a nitrogen containing aromatic heterocycles through a polyamine chain, both quenching effects can occur, defining a pH window where the fluorescence emission appears.[28]

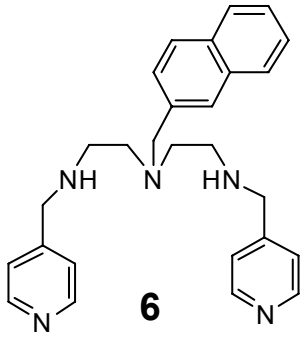

6

Scheme 1.6 – Structure of compound **6**.

Also, the use of crown ether as metal ion chemosensors, artificial membranes[29], smart material[30], actives components of molecular machines[31] and biomedical application[32] as potencial antitumor agents was reported by several authors.[33,34].

Replacement of the oxygen by nitrogen atoms, can changes their properties in metal sensing. For example, the aza-crowns (**7** and **8**) presented at Scheme 1.7 , were immobilized on an amino cellulose fibre substrate, for the detection of Na^+, K^+ levels in blood.[35,36]

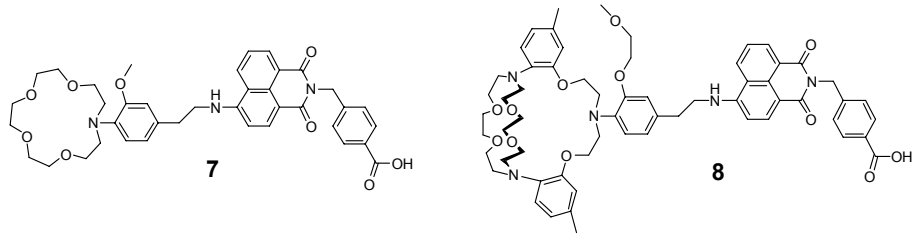

7 **8**

Scheme 1.7 – Structures of compounds **7** and **8**.

15-Crown-5 systems are usually used for the interaction with Na^{+},[37] whereas 15-crown-5 monoazacrown ethers show better results for Ca^{2+}.[38] In this case the size of the metal ion influenced notably the answer of the chemosensor.

In general, the addition of metal ions or protonation of the aza-crown ethers, "switches ON" the fluorescence emission, due the protection of the lone pair of electrons present in the nitrogen, preventing thus the PET process.

1.4 - Chemosensors containing bio-inspired units. From single amino acids to peptide chains as receptors.

A bio-inspired sensor has a similar structure of a classical chemosensor, but in this case, the receptor is formed by an amino acid (natural or synthetic) or by a peptide chain.[3]
The insertion of amino acids in the backbone of synthetic polymers can lead us to macromolecules containing biomimetic characteristics, with a specific structure and biological properties.
Their properties, as luminescence, conducting ability, higher thermal stability and metal ions or other analyte recognition can be modified with synthetic manipulation at the amino acids side chain.
Amino acids and peptides contain sites available for metal binding and recognition, making them good biosensors for metal detection in solution and in solid state. [39]

Ulijn and Smith[40] have described the design rules of peptide derivatives, and their applications in biotechnology and in the synthesis of nanomaterials. In Nature there are 20 amino acids available for peptide synthesis, they are chiral and exist in the L-form (except glycine).

An amino acid is formed by amine, and carboxylic terminals and a R-group at the side chain. Depending of the R-group, peptides can adopt different conformations, where a peptide can interact with other peptide by covalent linkage, and also by non-covalent linkage, *via* ionic, hydrophobic, hydrogen bonding and π - stacking interactions. The 20 amino acids, due to different characteristics of the R-groups, can be divided in hydrophobic, hydrophilic, charged or "other" (see Scheme 1.8).

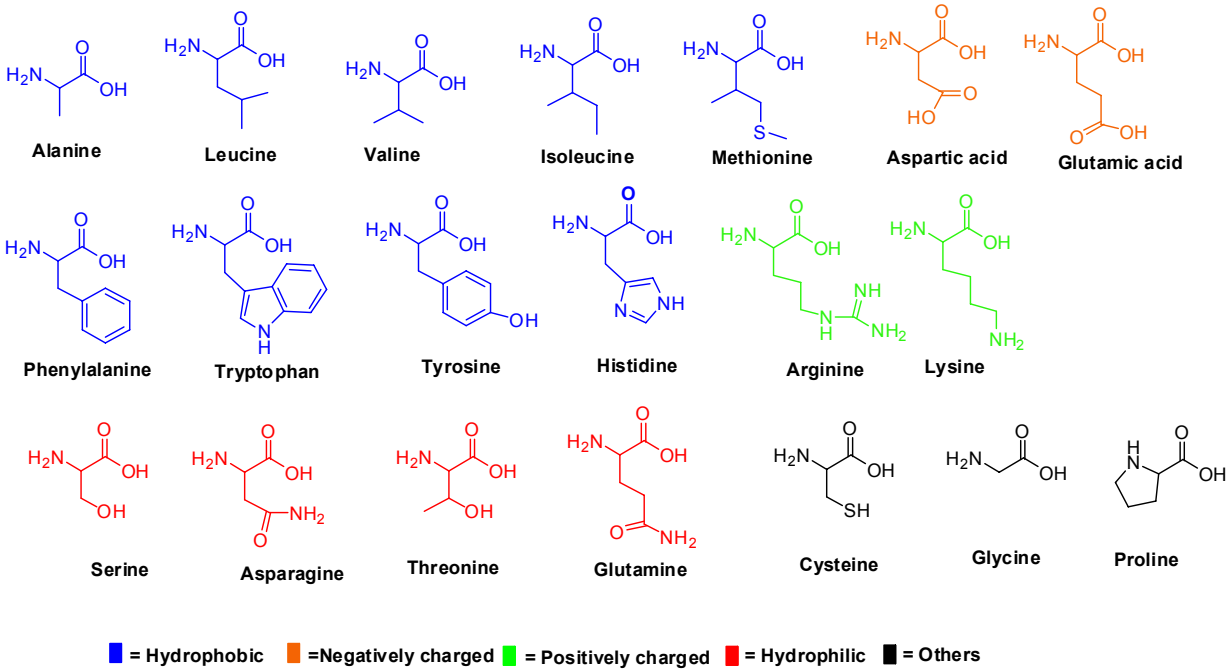

Scheme 1.8.- Amino acids structures.

In the hydrophobic aminoacids are included the aliphatic alanine, isoleucine, leucine, methionine and valine, the aromatic aminoacids are phenylalanine, tryptophan and tyrosine.

Aromatic residues can be very important in the interaction with proteins and peptides folding due to their π-π stacking characteristics. The hydrophilic residues are formed by serine, threonine, asparagine, and glutamine, and they can be involved in the hydrogen bonding interactions.

The charged amino acids are involved in specific charge-charge interactions, and they can be negatively charged as aspartic acid and glutamic acid, or positively charged as arginine and lysine. In the "other groups" are included the glicine, cysteine and proline.[40]

Taking into account, the peptide skeleton presented in this PhD dissertation, we are going to focus only on the properties of alanine, tryptophane and cysteine.
Alanine is a non-essencial amino acids, which means that the human body can produce it, being not necessary its inclusion through diet. It is present in food, particularly in meat, and Grosser et al. described their important anti-oxidant properties. [41]

Cysteine represents a unique chemical reactive, where due to the properties of its side chain, can be used as target for chemical modifications and interpeptide crosslinking. The presence of a sulfur atoms, gives it the ability for linkage at gold surfaces. [40]

Tryptophan is an essential amino acid in the human diet. This L- form amino acid is used in structural or enzyme proteins. The distinguishing structural characteristic of tryptophan is that it contains an indole functional group. It is an essential amino acid as defined by its growth effects on rats.[42]

Tryptophan can be found in health food stores, as a dietary supplement; and shows some effectiveness for the treatment of a variety of conditions associated with low serotonin levels in the brain, being a considerable promise as an antidepressant.[43,44,45]

The oxygen, nitrogen and sulfur atoms present in the alanine, tryptophan and cysteine amino acids, makes these compounds good candidates as molecular probes for metal detection. Many publications containing alanine derivatives for metal detection have been previously described. [46]

The synthesis of metal complexes containing amino acids and transition-metal ions are knowing a huge development due to their importance in biology, pharmacy and industry.[47] Properties, such as antibacterial, antitumour, and anticancer activities has made them the target of many studies.[48]

In biological processes, there are many classes of enzymes with a metal ion as cofactor, and with the purpose of understanding these biological process, as reactivity, the interaction of metal complexes containing alanine amino acids has been tested[49].

Transition metals could also be used in the future as cleavage reagent for peptides and proteins in Peptide Mass Mapping (Proteomics Approach). [50]

Anbalagan et al., published palladium (II) complexes with small peptides containing histidine and methionine amino acids, where their interaction promotes a hydrolytic cleavage of these amino acid residues.[51]

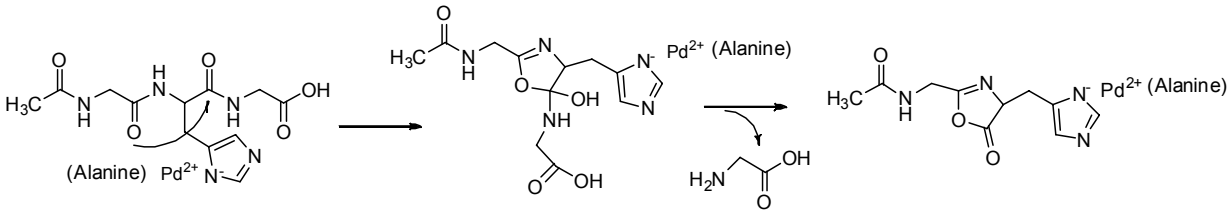

Scheme 1.9. – Cleavage mechanism of palladium (II) complex proposed by Anbalagan[51].

Concerning other metal ions studied with these bio-inspired probes, copper(II) can be found in some important biological process, such as oxidation transport and electron transfer, and also complexed with proteins containing hydrophobic sides[52]. For example *Marino et al.,* have published some interesting theoretical studies of the interaction of metal ions as Cu^{+} and Cu^{2+} with alanine amino acids, where Cu^{2+} ions, are preferentially bound to the C-terminal carboxylate group of alanine amino acids[53].

Mercury (II) as a soft metal ion has a strong affinity for sulfur-donor ligands, so the use of cysteine derivatives is very important for Hg^{2+} removal from waste waters. The complexation of mercury (II) with inorganic or natural organic ligands can change the speciation of Hg^{2+}, such as, its transport, transformation and bioavailability in natural water. There are many papers published on Hg^{2+}, demonstrating that it is normally linked to acid units, like, carboxylic acids, phenols, alcohols and thiols. [54,55,56]

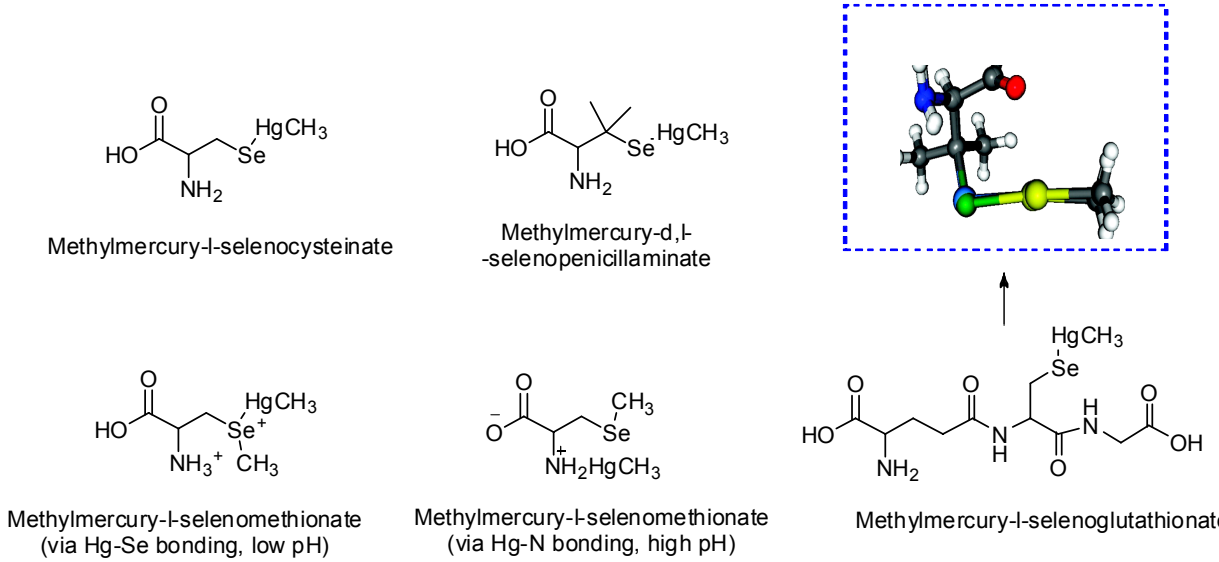

Scheme 1.10.- MeHg complexes with seleno amino acids.[55]

Finally, Belcastro et al. published the interaction of cysteine with Zn^{2+}, Cd^{2+} and Hg^{2+}, soft atoms coordination[57], and through theoretical studies they could conclude that these metals had different coordination sites in the amino acids. Zn^{2+} and Cd^{2+} link preferably to carbonyl oxygen, nitrogen and sulfur atoms, whereas, Hg^{2+} links at the sulphur atom of one the zwitterions forms of the amino acid residue.[58]

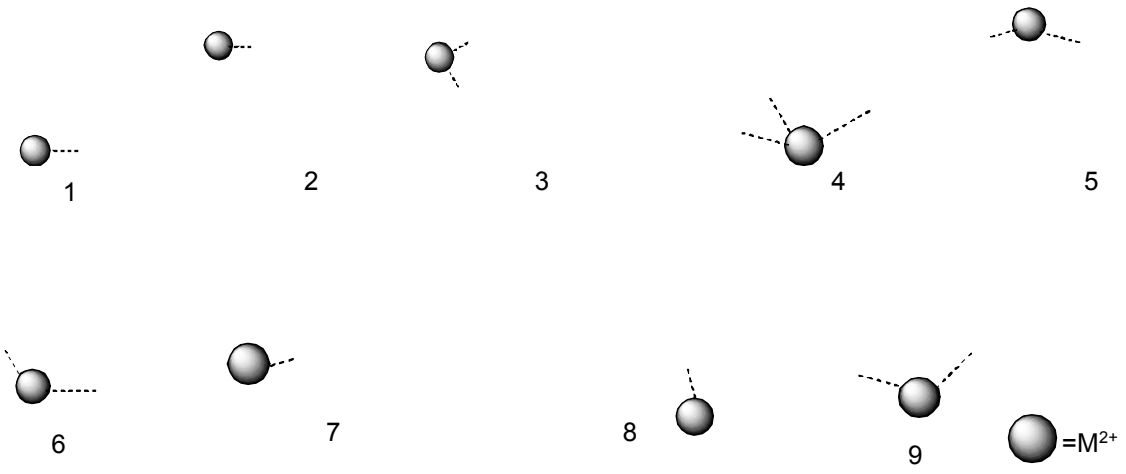

Scheme 1.11.- Theoretical structures of the complexes of cysteine with M^{2+} (= Cu^{2+}, Zn^{2+}, Cd^{2+} and Hg^{2+}). Depending on the metal ions, the distance in the molecule:metal ions changes.[58]

1.5 - Some aspects on the biological applications of emissive fluorophores

Peptides and proteins do not have fluorescent properties strong enough to be useful as intrinsic fluorescence chemosensor for sensing in the environment. So, their conjugation with emissive fluorophores can enhance their properties, for sensing and developing fluorescence peptide sensors.

Joshi et al. synthesized a fluorescent peptide containing a dansyl group as a fluorophore, with an amino acid sequence, and studied their interaction with metal ions. They showed that the peptide probe successfully exhibited a turn on and a ratiometric response for several metal ions, as Cd^{2+}, Pb^{2+}, Zn^{2+} and Ag^{+}. [59] (See Figure 1.12.)

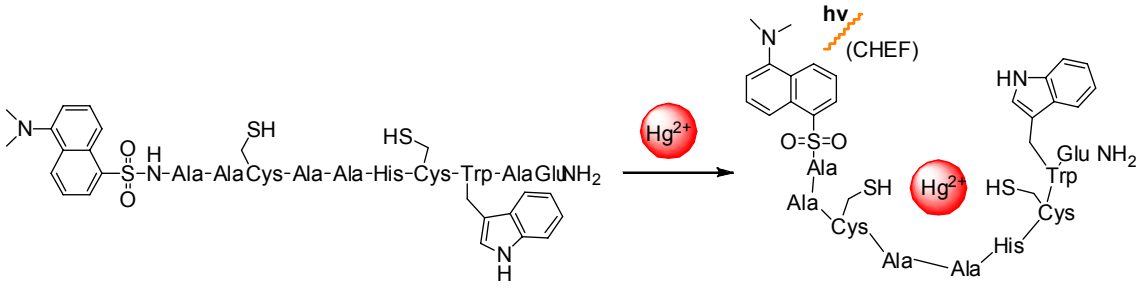

Scheme 1.12.- Possible mechanism for binding of Hg^{2+} metal ions in a fluorescent peptide containing dansyl as a fluorophore.[59]

Fluorescent molecular sensors based on conjugated aminoacids for *in vivo* applications, have to be soluble in aqueous media, penetrate in cell membranes, exhibit fluorescent changes with the pH variation and also for metal detection, the excitation wavelength must be located in the visible or near infrared, because UV radiation can damage cells and tissues.[60]

However, the majority of sensors developed until now have short-wavelength fluorophores, such as, coumarin, benzoxazol, anthracene or pyrene, which are suitable for abiotic analysis, but for in vivo applications they do not have optimal spectral conditions.

To improve the point, common fluorophores used for biological applications are fluorescein or rhodamine. They have long excitation wavelength (ca. 500 nm), high fluorescence quantum yields and extinction coefficients.[61],[62]

Other fluorophores, such as, BODIPY dyes, squaraines and cyanine are organic fluorescent emitting between 500 nm and at ca. 900 nm. Compounds containing Nile Red, Nile Blue are interesting for biological sensors, they are more photochemical stable than cyanine, but due to their structure, their solubility in aqueous solution is very limited. [63]

In our case, due to its biological properties, 2-Benzoxazol derivatives have been the target of many research and developments. They have high lipophilicity, a broad biological activity and they can act as antifungal, antimicrobial and anticancer agents. They also present good optical properties, as high molar coefficients and fluorescent quantum yields, and can be applied as fluorescent /colorimetric probes for metal or anionic detection.[39],[64]

Oligothiophenes derivatives have also biological activity and intrinsic fluorescence, where those properties can be synthetically modified; for example they can be applied in polymer science due to their electroluminescent properties, as fluorescent target for oligonucleotides; and they are stable under prolonged ultraviolet irradiation contrary to the fluorescein. Due to

their stability (oligo)thiophenes could be used for cellular imaging and fluorescence resonance energy transfer experiments.[63]

1.6 - The importance of metal ions. Recognition and Quantification.

As is well known, metal ions are present in nature, being essential to plants and animal life.[60] They can be grouped in different families, depending of their properties. In this dissertation we will discuss the following families, the alkaline, alkaline-earth and transition metal ions.

Alkaline Na^+, K^+ and alkaline earth, Mg^{2+}, Ca^{2+} are present in large quantities in the human body, contrary to the transition metal ions Cu^{2+}, Ni^{2+} and Pb^{2+}; and post-transition metals Zn^{2+}, Cd^{2+} and Hg^{2+}, (d-block elements) that are present in small quantities.[3]

Pearson's theory of hard and soft acids and bases states that "Hard Acids prefer to bind with hard bases, and soft acids to soft bases".[57] In this way, a compound containing oxygen atoms is considered hard; sulfur is soft and nitrogen is an intermediate, because it can link to soft or hard metal ions.
Alkaline, Li^+, Na^+, K^+, and alkaline earth, Mg^{2+}, Ca^{2+}, Sr^{2+} and Ba^{2+}; Cu^{2+}, Ni^{2+}, Zn^{2+}, Pb^{2+} under Pearson theory are considered hard metal ions; whereas Ag^+, Cu^+, Cd^{2+}, Hg^{2+} are considered soft metal ions.[57]

Metal ions have a very important role, such as, the stabilization and reactivity of proteins. However, for human and environmental welfare, they must exist in optimal quantities. Contrary, they can promote metabolic disorders, being easily absorbed and accumulated from the environment causing toxicity and diseases.[60]

Zinc (II) is the second most abundant metal ion in the human body, is an important structural or catalytic cofactor of many proteins (for example carbonic anhydrase and zinc finger proteins) and can chelate on brain, pancreas and spermatozoa.[65]

Copper (II) is the third in abundance in human bodies, is highly toxic for some bacteria and viruses, and is suspect of causing infant liver damage. The alteration of its level in cellular environmental can causes neurodegenerative diseases such as Alzheimer's disease.[66]

Cadmium (II), Lead(II), Mercury (II) are highly toxic and pollutant; present in water contaminations and are carcinogenic. Accumulation of methyl mercury through the food chain may lead to serious and permanent damage to the brain in humans. The maximum of

Hg^{2+} allowed in drinkable water is 10 nM, by the US Environmental Protection Agency (EPA). [67]

Nickel (II) is present in the environmental in small amounts, and it has many applications.[68] It can be used, as an ingredient of steal or other metals, is present in food, like chocolate, fats and vegetables, and in detergents. Their presence in small quantities is necessary, but large amounts can promote diseases such as cancer[69], heart disorders, birth deffects and respiratory failure.[7,53]

So, for these reasons, the metal ions detection and quantification is very important and it has been the target of increasing research.

Transition metal compounds can be colored due to their electronic transitions, such as charge transfer and d-d transitions. In a charge transfer transition, an electron of a ligand orbital interacts with other orbital from the metal, giving rise to a ligand-metal charge-transfer (LMCT) transition. These transitions can occur when the metal is in a high oxidation state. A metal-to ligand charge transfer (MLCT) transition occurs when the metal is in a low oxidation state and a ligand is easily reduced. [70]

In d-d transitions, the electrons move from one d-orbital to another, because in transition metal complexes the d orbitals do not have the same energy. All these transitions occur on metal ions that do not have the d shell completed; they are paramagnetic metal ions, for example Cu^{2+} ion. [3,15]

Copper(II) ions usually produce a chelation enhancement of quenching, because of its d shell is not completed, and an energy transfer quenching of the π^* emissive state through low-lying metal-centre unfilled d-orbitals.[9,71,39,64]

Zn^{2+}, Cd^{2+} and Hg^{2+} are metal ions with closed-shell nature, blain metals, making them good candidates for applications containing chemosensors based on PET. The interaction of chemosensors with d^{10} metal ions, normally produces a chelation enhancement of the fluorescence emission effect (CHEF), except for Hg^{2+}, which normally produces a chelation enhancement of quenching (CHEQ), because it is a “heavy” metal and increases the probability to occur a non-radiative process, the intersystem crossing, and decrease the emission intensity.[72, 73]

1.7 - On nanoparticle science. Gold or Silica nanoparticles.

Finally due to the interest in fluorescence and colorimetric chemosensors more sophisticated, efficient, sensible and selective for specific targets, and following the aims of supramolecular chemistry in self organization motifs, many research teams have been working during the last years in the design of a new generation of sensing materials based on soft aggregates[74], silica (SiNPs)[75,76], silver (AgNPs)[77,78,79] or gold (AuNPs) nanoparticles[80,81].
Fluorescent nanoparticles can be very appealing for the design of organized chemosensors due to their easy and cheaper pathway of synthesis.

In gold nanoparticles due to the presence of a metal core, can occur interesting processes such as electron and energy-transfer, which usually quenchs the natural luminescent of the conjugated fluorophores. Also, interesting colorimetric chemosensors can be developed with them.

On the other hand, transparent silica nanoparticles can be the best choice for sensing effects, because they can be modified at their surface using different alkoxysilane derivatives. In this case we could use different emissive dyes inert to the electron and energy-transfer processes. [82]

1.7.1 - Gold nanoparticles

In the last decade, more than one thousand papers and several patents had been published in the gold nanoparticles field.[83]

AuNPs have been investigated in many fields, such as, nano-biotecnology and bio-analytical chemistry[84]. They have been useful in applications like, imaging, catalysis, drug delivery, control of protein activity, in order to understand a local structure in protein folding, material science, physics, energy, design of nanosensors and biofuel cells. [85]

In bio-analytical chemistry, they have been explored as ionization enhancers in MALDI-MS (Matrix Assisted Laser Desorption Ionization-Mass Spectrometry) techniques, as substitutes of common matrices on peptide identification, and as probes that selectively trap and concentrated target species in sample solution.[84] Teng et al. have developed magnetic gold nanopaticles with negative charge, allowing different proteins to be separated by their isoelectric point (pI) turning their identification more quick and selective.[86]

AuNPs normally are synthesized by reduction of Gold(III) by borohydride/citrate.[87] In order to stabilized the nanoparticles, organic molecules or biomolecules containing thiol (-SH) groups are added to their surface *via* gold-thiol bond, preventing their irreversible aggregation (see Scheme 1.13.).

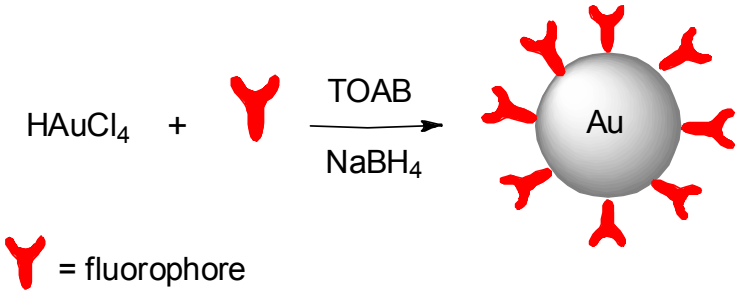

Scheme 1.13. – General pathway of gold nanoparticles decorated with fluorophores. (TOAB – tetraoctylammounium).

Unfortunately, direct interaction of the fluorophore to the gold surface could be quench the fluorescence properties and loss of specific functions. The introduction of a cross-linker between the gold surface and the fluorophore can be a good choice in order to stabilize the nanoparticles.[88]

AuNPs can be easily characterized by Uv-Vis, showing typical surface Plasmon band at *ca*. 520 nm; by dynamic light scattering, and transmission electronic microscopy (TEM). The colour of the AuNPs indicates the order of size obtained.

In the field of nano-biotecnology the conjugation of AuNPs with proteins has been used for many studies and developments, since the interface between the protein and the nanoparticle has always been tricky, and their characterization is very important.

M-E Aubin and K Hamad-Schifferli published four strategies for the approach between proteins and nanoparticles (NP) (see Scheme 1.14.). The approaches can occur by:

1.- *Direct conjugation to the NP surface by electrostatic adsorption.*

The direct reaction without a linker is used when the particle employed as biosensor shows FRET (fluorescence resonance energy transfer). This process is very sensitive to the distance, so the linkers that can help to adopt different conformations and their conjugation give rise to aggregates largers than the nanoparticles. This effect can cause cellular problems. For AuNPs this method is strongly favored, where the conjugation requires a protein with several cysteins, forming the stable Au-S bond.

2.- *Conjugation to the ligand on the NP surface.*

The nanoparticles are conjugated to a specific ligand that a protein can recognize, supramolecular approach. If the nanoparticles have multiple ligands, a number of proteins can distribute around the nanoparticle. In this case, varying the ratio of the reactants can influence the stoichiometry.

3.- *Conjugation to a small cofactor molecule that protein recognize and bind.*

This method is similar to the process mencioned in step 2, but the ligand used is a cofactor, a biolabel. Examples of bio-labeling are biotin-strepavidin binding, and when the NP is connected to an antibody, which is used by the protein, the protein binds.

4.- *Electrostatic adsorption*

This is the most simple techniques because it no requires chemical reaction. The interaction of the protein with the NP is made by charge interaction. Many variables such as the pH can modulate the charge of proteins (positive) and then, they can interact with the gold surface (negative).[85]

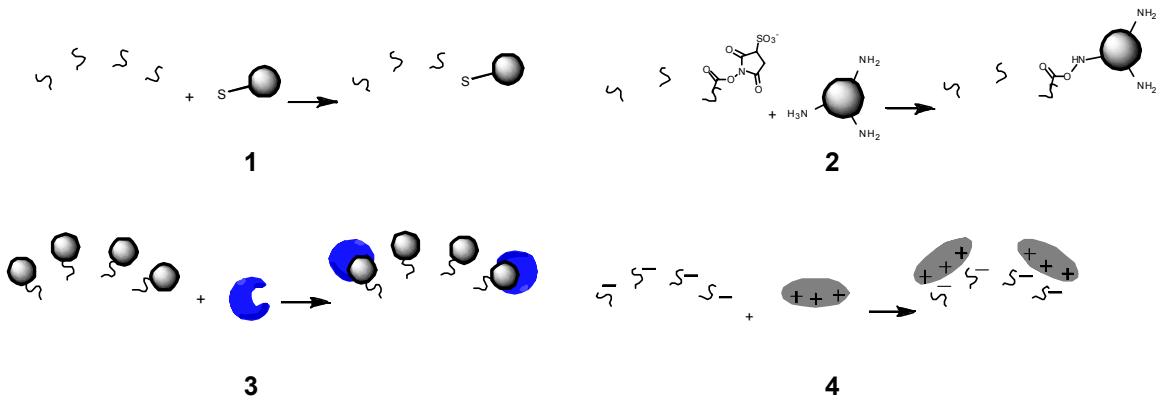

Scheme 1.14. – Nanoparticle-protein binding strategies.[85]

1.7.2 - Silica nanoparticles

Silica nanoparticles are transparent to the visible light, being used as labels in bioassays with optical detection. The silica polymerization is well studied; porosity and swelling changes do not occur at moderated pH and unfortunately they are not microbiologically degraded.

The most common precursors used on silica nanoparticles synthesis are tetramethoxysysilane (TMOS) and tetraethoxysilane (TEOS). [89]

Since 1969s pioneer work of Stöber, the synthetic procedure of monodisperse silica nanoparticles by condensation of tetralkoxysilane derivatives in ammonia, water and ethanol solutions is used.

Later Blaaderen, proposed some modifications on Stöber method, for the preparation of covalently linked dye-doped silica nanoparticles (DDNs). The DDNs have been explored and they can have bio-applications as label or sensors. Through this method, many fluorophores can be located around the NP, increasing highly their fluorescence emission.

Due to the strong emission enhancement they can be used as stain cells, drug delivery or immunoassays. However, the DDNs can have some disadvantages; such as their solubility in water can be modified depending on the different dyes incorporated.

Montalti et al. showed that the core and surface of DDNs, can be intrinsically different, even if they are labeled with the same dye, for example dansyl moieties. This effect can modify the properties (Scheme 1.15.). [90]

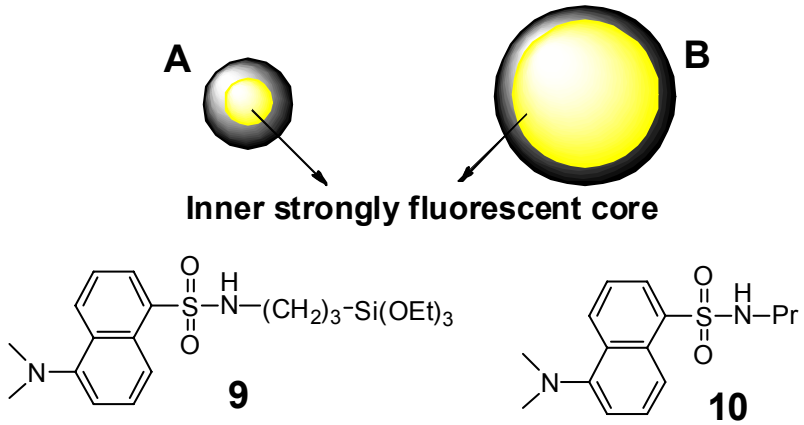

Scheme 1.15.- Proposed structure of Dye-Doped nanoparticles A and B, and dansyl derivatives (9 and 10).

DDNs nanoparticles have many advantages on the design of fluorescent labeling agents and chemosensors, due to their intense fluorescence and photostability. They are highly photophysical influenced by the polarity of the solvent, due to the influences of the energy of the electronic states. They are less polar than water and their mobility is strongly reduced. Preventing these problems by using the Stöber method, the SiNPs can encapsulate the fluorophore, protecting them from the environmental, preventing for example the diffusional quenching with other species, as molecular oxygen, giving highly emissive water soluble nanoparticles.[91] (See Scheme 1.16.).

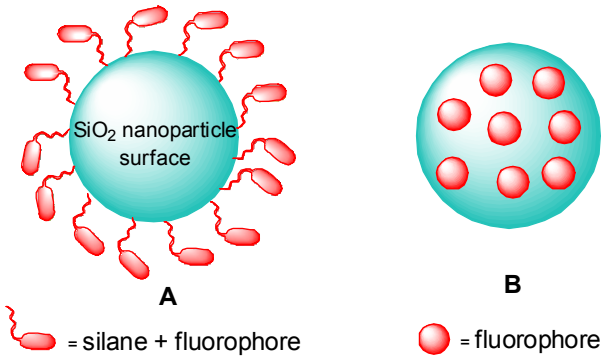

Scheme 1.16. –Schematic representation of dye-dopped silica nanoparticles (DDNs). Synthesis of DDNs on the silica surface (A) and inside the silica matrix (B).

Rampazzo et al. have published pyrene-doped silica nanoparticles *via* the Stöber-Van Blaaderen method. They observed that when the chromophore (pyrene) was encapsulated inside the silica nanoparticles, the fluorescence emission increased an order of magnitude, because of the absence of the quencher oxygen inside the nanoparticles. At low concentration, the pyrene was totally encapsulated in the silica core, being highly emissive; but at high concentrations some amount of compound still outside of the silica core, resulting in the appearance of the excimer emission. Growing of a secondary doped silica shell showed both species, the monomer and the excimer, but due to the protection of the oxygen their fluorescence emission is also increased.[92] (see Scheme 1.17).

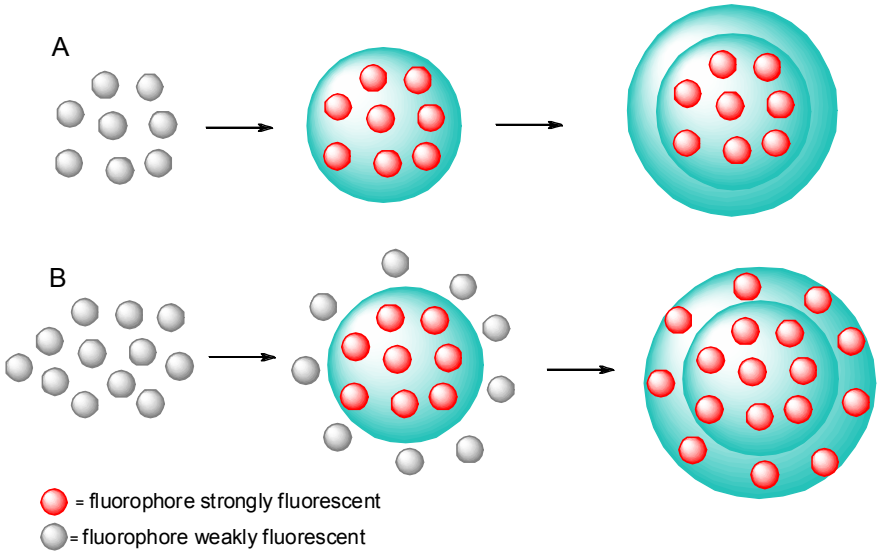

Scheme 1.17. – Schematic pathway of DDNs silica nanoparticles. A – Low concentration of fluorophore, (All molecules are totally encapsulated). B – High concentration of fluorophore, (Molecules are partially encapsulated, being necessary another silica shell to cover all the molecules). The fluorophores of the outside shell interact with those present in the inside shell. [92]

Alternatively there is also another synthetic method: the Reverse-micelle microemulsion method.

On reverse-micelle microemulsion (RMM) method a water-in oil emulsion is formed, by the addition of a small amount of water, an organic solvent and a surfactant. By the Stöber method hydrophobic and hydrophilic dyes can be encapsulated, whereas, the RMM method can be used for the synthesis of metal-chelate doped silica nanoparticles (NPs) and created more NPs with narrowed size distributions.[89]

The silica nanoparticles can be easily characterized by Uv-Vis, by dynamic light scattering, and transmission electronic microscopy (TEM).

1.8 - Aim of thesis

As was discussed in the previous introduction, macrocycles ligands are very good candidates for metal ion recognition. On the other hand, amino-acids and peptides have been also used extensively for metal ion detection and as new organic platforms for bio-science due to their versatile applications.

Considering both these aspects, the aim of this PhD dissertation is to explore several new flexible and rigid macrocyclic compounds as metal ion chemosensors for *in vitro* studies, in particular the biological important calcium, zinc and copper, and the environmental pollutant cadmium, mercury, aluminium and chromium.

In chapters 2 and 3 are summarized the results concerning the photophysical studies with a polyoxa-aza macrocycle ligand bearing an anthracene fluorescent unit (**L**, Figure 1.18), and the family of new aza crown-ether bearing two pendant arms (furyl, aryl or thienyl groups) linked through an imidazo moiety (**1**, **2** and **3**, Figure 1.18).

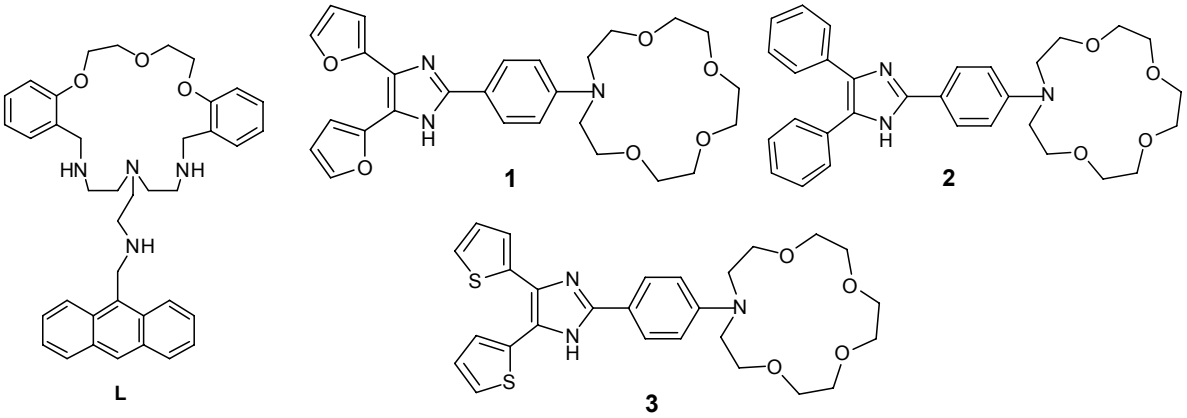

Scheme 1.18.- Macrocyclic **L** discussed in Chapter 2 and 15-aza-crown-5-imidazo crown ethers derivates (**1** to **3**) discussed in Chapter 3.

From the 20 natural aminoacids, alanine with hydrophobic character was selected for the synthesis of several luminescent new chemosensors. Chapter 4 and 5 summarized the photophysical and metal ion sensing using these compounds.

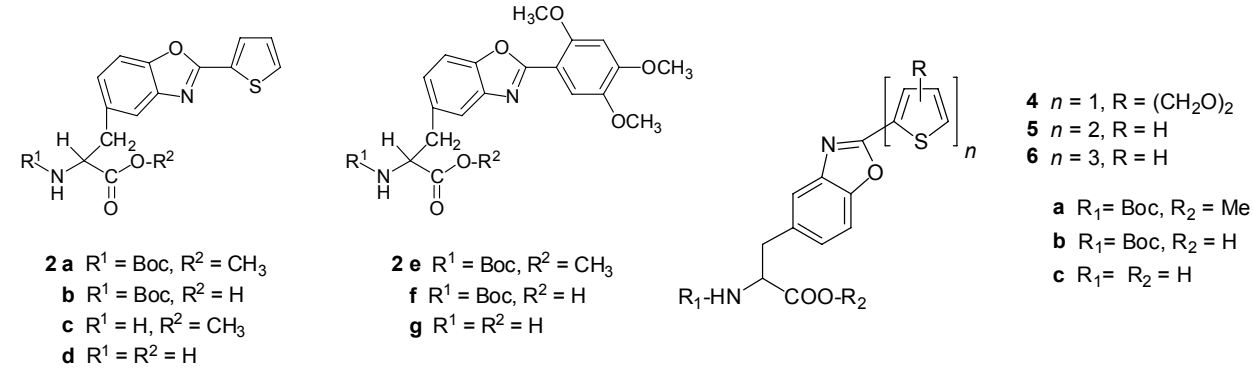

Scheme 1.19.- Alanine derivatives (**2a**-**g**) discussed in Chapter 4, and (Oligo)thienylbenzoxazolyl-alanine derivatives **4a-c** to **6a-c** discussed in Chapter 5.

Several mononuclear and dinuclear complexes were synthesized and characterized with compounds reported in chapters 4 and 5, and studied by DFT calculations. This research is summarized in Chapter 6.

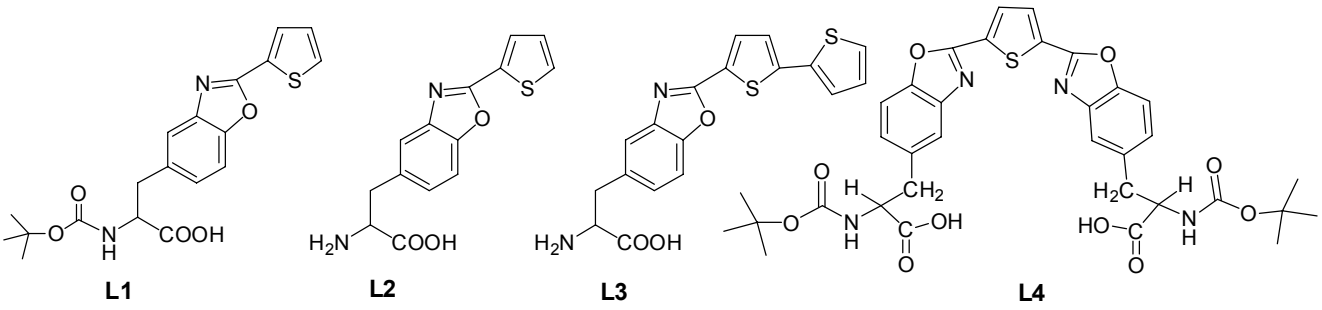

Scheme 1.20.- Alanine derivatives discussed in Chapter 6.

Using as precursors some amino acids reported in chapters 4 and 5, and incorporating cysteine and tryptophane as second and third amino acid residues, several new di and tri peptide compounds were synthesized and fully characterized. For all systems a deep study as fluorescence chemosensor was developed towards transition and post-transition metal ions. In order to add up to the application of these bio-inspired chemosensors, two groups of gold and silica emissive nanoparticles were synthesized. These results are summarized in Chapter 7.

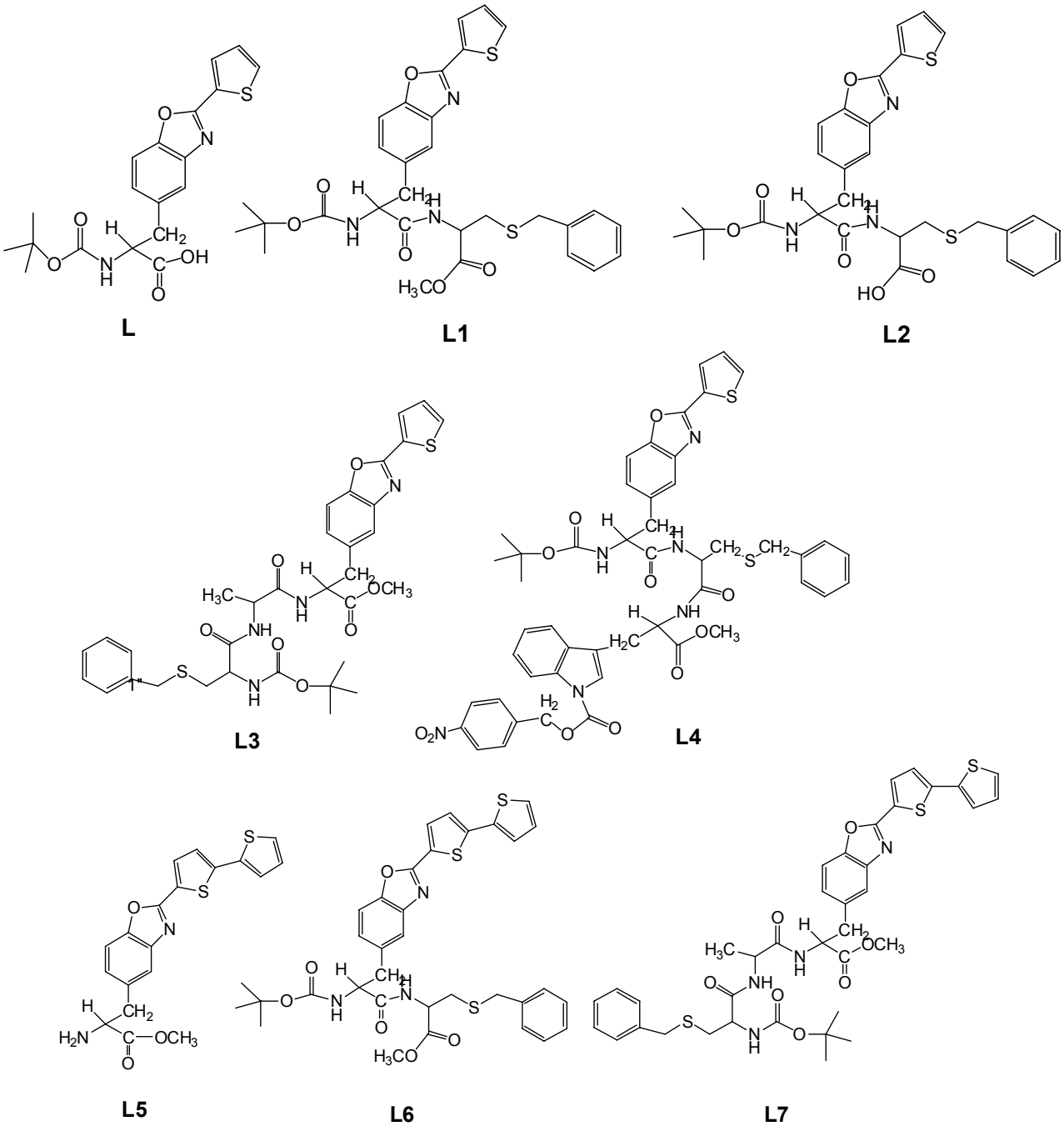

Scheme 1.21.- Amino acid and peptide sensors discussed in Chapter 7.

1.9 - References

[1] Stokes, G. G; *Philosophical Transactions of Royal Society London* A, **1852**, *142*, 463-562.

[2] Czarnik, A.W.; *Accounts of Chemical Res*earch, **1997**, *27*, 302-308.

[3] Lodeiro, C.; Capelo, J.L.; Mejuto J.C.; Oliveira, E.; Santos, H.M. ; Pedras, B.; Nuñez, C.; *Chemical Society Reviews,* **2010**, *39*, 1-29.

[4] Harvey, E. N.; *Science*, **1923**, *57*, 501-503.

[5] Sousa, L. R.; Larson, J. M.; *Journal of the American Chemical Soc*iety, **1977**, *99*, 307-310.

[6] Desvergne, J. P.; Czarnik, A. W; *Chemosensors of Ion and Molecule Recognition (NATO Science* Series, *Serie C:Mathematical and Physical Sciences*), Kluwer Academic,London, **1997**.

[7] Czarnik, A.W.; *Fluorescent Chemosensors for Ion and Molecule Recognition*, American Chemical Society, Washington DC, **1993**, vol. 538.

[8] Hulanicki, A.; Glab, S.; Ingman, F.; *Pure and Applied Chemistry*, **1991**, *63*, 1247-1250.

[9] Silva, de A. P.; Gunaratne, H. Q. N.; Gunnlaugsson, T.; Huxley, A. J. M.; Mccoy, C. P.; Rademacher, J. T.;. Rice, T. E; *Chemical Reviews*, **1997**, *97*, 1515–1566.

[10] Lodeiro, C.; Pina,F.; Parola AJ. Bencini A.; Bianchi A.; Bazzicalupi C.; Ciattini S.; Giorgi C.; Masotti A.; Valtancoli B.; Melo, J. S.; *Inorganic Chemistry*, **2001**, 40, 6813-6819.

[11] Basabe-Desmonts, L.; Reinhoudt, D.N.; Grego-Calama, M., *Chemical Society Reviews*, **2007**, *36*, 993-1017.

[12] Xu Z., Yoon J., Spring R.D., *Chemical Society Reviews*, **2010**, *39*, 1996-2006

[13] Akkaya, E. U.; Huston, M. E.; Czarnik, A. W.; *Journal of American Chemical Society*, **1990**, *112*, 3590–3593.

[14] Rurack, K.; *Spectrochimica Acta Part A*, **2001**, *57*, 2161-2195

[15] Valeur, Bernard; *Molecular Fluorescence: Principles and Applications*, Wiley-VCH Verlag GmbH, **2001**.

[16] Lodeiro, C.; Lima, JC.; Parola AJ., de Melo JSS., Capelo JL., Covelo B., Tamayo A., Pedras B., *Sensors and Actuators B-Chemical*, **2006**, *115*, 276-286.

[17] De Melo, JS.; Pina, J.; Pina, F.; Lodeiro, C.; Parola, AJ.; Lima, JC.; Albelda, MT.; Clares, MP.; Garcia-Espana, E.; Soriano, C.; *Journal of Physical Chemistry A*, **2003**, *51*, 11307-11318.

[18] Nunez, C.; Oliveira, E.; Giestas, L.; Valencia, L.; Macias, A.; Lima, JC.; Bastida, R.; Lodeiro, C.; *Inorganic Chimica Acta*, **2008**, *361*, 2183-2194.

[19] Lindoy, L.F.; *The coordination Chemistry of Macrocyclic Ligand Complexes*, Cambridge University Press, Cambridge, **1989**.

[20]Lehn, J.-M.; in *Structure and Bonding*, Springer, Berlin, **1973**, Vol.*16*, p.1

[21] Pedersen, C. J.; *Journal of American Chemical Society*, **1967**, *89*, 7071.

[22] Gokel, G. W.; *Crown Ethers and Cryptands*, *Royal Society of Chemis*try, Cambridge, **1991**.

[23] Curtis, N. F.; *Coordination Chemistry Reviews*, **1968**, 3, 3-47.

[24] Krakowiak, K. E.; Bradshaw, J. S.; Zamecka-Krakowiak, D. J.; *Chemical Reviews*, **1989**, 89, 929.

[25] Blake, A. J.; Schröder, M.; *Advanced Inorganic Chemistry*, **1990**, *35*, 1.

[26] Cotton, F.A; Wilkinson, G.; *Advanced Inorganic Chemistry* 5th Ed., Wiley, New York, **1988**, 735-738.

[27] Cabbiness, D.K.; Margerum, D.W.; *Journal of American Chemical Society,* **1969**, *91*, 6540-6541.

[28] Aucejo, R.; Alarcó, J.; García-España, E.; Llinares, J. M.; Marchin, K. L.; Soriano, C.; Lodeiro, C.; Bernando, M. A.; Pina, F.; Pina, J.; de Melo, J. S.; *European Journal of Inorganic Chemistry*, **2005**, 4301-4308.

[29] Biron, E.; Otis, F.; Meillon, J. C.; Robitaille, M.; Lamothe, J.; Hove, P. Van; Cormier, M. E.; Voyer, N.; *Bioorganic Medicinal Chemistry*, **2004**, *12*, 1279-1290.

[30] Yagai, S.; Kitamura, A.; *Chemical Society Reviews*, **2008**, *37*, 1520-1529.

[31] Kinbara, K.; Aida, T.; *Chemical Reviews*, **2005**, *105*, 1377-1400.

[32] Kralj, M.; Tusek-Bozic, L.; Frkanec, L.; *Chemical Medicinal Chemistry*, **2008**, *3*, 1478-1492.

[33] Lörh, H.G.; Vögtle, F.; *Accounts Chemical Research*, **1985**, *18*, 65-72.

[34] Okamoto, H.; Owari M.; Kimura, M.; Satake K.; *Tetrahedron Letters*, **2001**, *42*, 7453-7455.

[35] He, H. R.; Mortellaro, M. A.; Leiner, M. J. P.; Fraatz, R. J.; Tusa, J. K.; J*ournal of American Chemical Society*, **2003**, *125*, 1468–1469.

[36] He, H. R.; Mortellaro, M. A.; Leiner, M. J. P.; Young, S. T.; Fraatz, R. J.; Tusa, J. K.; *Analytical Chemistry*, **2003**, *75*, 549–555.

[37] Gokel, G. W.; Leevy, W. M.; Weber, M. E.; *Chemical Reviews*, **2004**, *104*, 2723-2750.

[38] Warmke, H.; Wiczk, W.; Ossowski, T. *Talanta*, **2000**, *52*, 449-456.

[39] Costa, S.P.G.; Oliveira, E.; Lodeiro, C.; Raposo, M.M.M.; *Tetrahedron Letters*, **2008**, *32*, 49, 5258-5261.

[40] Ulijn, R.V.; Smith, A. M.; *Chemical Society Reviews*, **2008**, *37*, 664-675.

[41] Grosser, N.; Oberle, S.; Berndt, G.; Erdmannk, K.; Hemmerle, A.; *Biochemical and Biophysical Research Communications*, **2004**, *314*, 351-355.

[42] Pallaghy, P.K.; Melnikova, A.P.; Jimenez, E.C.; Olivera, B.M.; Norton, R.S.; *Biochemistry*, **1999**, *38*, 35, 11553-11559.

[43] Levitan, R.D.; Shen, J.H.; Jindal, R.; Driver, H.S.; Kennedy, S.H.; Shapiro, C.M.; *Journal of Psychiatry & Neuroscience,* **2000***, 25*, 4, 337–46.

[44] Thomson, J.; Rankin, H.; Ashcroft, G.W.; Yates, C.M.; McQueen, J.K.; Cummings, S.W.; *Psychological medicine,* **1982***, 12***,** 4, 741–51.

[45] Kostowski, W.; Bidzinski A, Hauptmann M, Malinowski JE, Jerlicz M, Dymecki, J.; *Polish Journal Pharmacology Pharmacy,* **1978***, 30*, 1, 41–7.

[46] Guzow, K.; Szmigiel, D.; Wróblewski, D.; Milewska, M.; Karalczak, J.; Wiczk, W.; *Journal Photochemistry Photobiology A*, **2007**, *187*, 87-96.

[47] Pasini, A.; Casella, L.J.; *Inorganic Nuclear Chemistry*, **1979**, *36*, 2133.

[48] (a) Derose, V.J.; Burns, S.; Kim, N.K.; Vogt, M.; *Coordination Chemistry II*, **2004**, *8*, 787-813. (b) Lippard, S.J.; Berg, J.M.; *Principles of Bioinorganic Chemistry*, University Science Books, Sausalito, CA, **1994**. (c) Umezawa, H.; *Progress in Biochemistry Pharmacology*, **1976**, *11*, 18-27 (d) Chetana, P.R; Rao, R.; Roy, M.; Patra, A.K.; *Inorganic Chimica Acta*, **2009**, 362, *46*, 4692-4698.

[49] Hosny, M.N; *Transition Metal Chemistry*, **2007**, 32, 117-124.

[50] (a) Chin, J.; *Accounts Chemical Research,* **1991**, *24*, 144-145. (b) Suh, J.; *Accounts Chemical Research,* **1992**, *25*, 273-276. (c) Gallagher, J.; Zelenko, O.; Walts, AD.; Sigman, DS.; *Biochemistry,* **1998**, *37*, 2096-2104 (d) Hegg, EL.; Burstyn, JN.; *Journal of American Chemical Society,* **1995**, *117*, 7015-7016. (e) Rana, TM.; *Advanced Inorganic Biochemistry,* **1993**, *10*, 173,177.

[51] Anbalagan, V.; Stipdonk, V.M.J.; *Journal of Mass Spectrometry*, **2003**, *38*, 982-989.

[52] Yamashita, M.M.; Wesson, L.; Eisenman, G.; Eisenberg, D.; *Proceedings of the National Academy of Sciences. USA* **1990**, *87*, 5648-5652.

[53] Marine, T.; Russo, N.; Toscano, M.; *Journal of Mass Spectrometry,* **2002**, *37*, 786-791.

[54] Foti, C.; Giuffrè, O.; Lando, G.; Sammartano, S.; *Journal of Chemical Engineering Data*, **2009**, *54*, 893-903.

[55] Asaduzzaman, A. M.; Mohammad, A.K.K.; Schreckenbach, G.; Wang, F.; *Inorganic Chemistry*, **2010**, *49*,870-878.

[56] Jalilehvand, F.; Leung, B. O.; Izadifard, M.; Damian, E.; *Inorganic Chemistry*, **2006**, *45*, 66-73.

[57] Pearson, R. G.; *Journal of American Chemical Society*, **1962**, *84*, 16, 62-54.

[58] Belcastro, M.; Marino, T.; Russo, N.; Toscano, M.; *Journal of Mass Spectrometry*, **2005**, *40*, 300-306.

[59]Joshi, B. P.; Park, J.; Lee, W. I.; Lee, K.-H.; *Talanta*, **2009**, *78*, 903-909.

[60] Mameli, M.; Aragoni, M.C.; Arca, M.; Caltagirone, C.; Demartin, F.; Farruggia, G.; Filippo, G. D.; Devillanova, F. A.; Garau, A., Isaia, F.; Lippolis, V.; Murgia, S.; Prodi, L.; Pintus, A., Zaccheroni, N.; *Chemistry-A European Journal,* **2010**, *16*, 919-930.

[61] Clark, M. A.; Duffy, K.; Tribrewala, J.; Lippard, S. J.; *Organic Letters*, **2003**, *5*, 2051-2054.

[62] Choi, M. G.; Cha, S.; Park, J. E.; Lee, H.; Jeon, H. L.; Chang, S.-J., *Organic Letters*, **2010**, *12*, 1468-1471.

[63] Gonçalves, M.S.T.; *Chemical Reviews*, **2009**, *109*, 190-212.

[64] Costa, S.P.G; Oliveira, E.; Lodeiro, C.; Raposo, M.M.M.; *Sensors*, **2007**, *7*, 2096-2114.

[65] Hanaoka, K.; Muramatsu, Y.; Urano, Y.; Terai, T.; Nagano, T.; *Chemisty –A European Journal*, **2010**, *16*, 568-572.

[66] Zhao, Y.; Zhang, X.-B.; Han, Z.-X.; Qiao, L.; Li, C.-Y.; Jian, L.-X.; Shen, G.-L.; Yu, R.-Q.; *Analytical Chemistry*, **2009**, *81*, 7022-7030.

[67] Li, W.; Guo, Y.; McGill, K.; Zhang, P.; *New Journal of Chemistry*, **2010**, *34*, 1148-1152.

[68] McNeil, Ian. "*The Emergence of Nickel". An Encyclopaedia of the History of Technology*. Taylor & Francis. **1990**. pp. 96–100.

[69] Kasprzak; S. J, F. W.; Salnikow, K.; *Mutation research*, **2003**, *533* 1-2: 67–97

[70] Dunn, T.M.; Lewis, J.; Wilkins, R.G.; *Modern Coordination Chemistry*, New York: Interscience., Chapter 4, Section 4, "Charge Transfer Spectra", **1960**, pp. 268-273.

[71] Oliveira, E.; Vicente, M.; Valencia, L.; Macías, A.; Bértolo, E.; Bastida, R.; Lodeiro, C.; *Inorganic Chimica Acta*, **2007**, *360*, 2734-2743.

[72] Jensen, W. B.; *Journal of Chemical Education*, **2003**, *80*, 8, 952–961.

[73] Cotton, F. A.; Wilkinson, G.; Murillo, C. A.; *Advanced Inorganic Chemistry* (6th ed.). New York: Wiley, **1999**.

[74] Mancin, F.; Scrimin, P.; Tecilla, P.; Tonellato, U.; *Coordination Chemistry Reviews*; **2009**, *253*, 2150-2165.

[75] Montalti, M.; Prodi, L.; Zaccheroni, N.; *Journal of Materials Chemistry*, **2005**, *15*, 2810-2814

[76] Bonacchi, S.; Rampazzo, E.; Montalti, M.; Prodi, L.; Zaccheroni, N.; Mancin, F.; Teolato, P.; *Langmuir*, **2008**, *24*, 8387-8392.

[77] Xiong, D.; Chen, M.; Li, H.; *Chemical Communications*, **2008**, 880-882

[78] Han, C. P.; Zhang, L.; Li, H. B.; *Chemical Communications*, **2009**, 3545-3547.

[79] Li, H. B.; Bian, Y. H.; *Nanotechnology*, **2009**, *20*, 145502-145508

[80] Wang, Z.; Ma, L.; *Coordination Chemistry Reviews*, **2009**, *253*, 1607-1618.

[81] Buck, S. M.; Koo, Y. El. L.; Park, E.; Xu, H.; Brasuel, M.; Philbert, M. A.; Kopelman, R.; *Current Opinion in Chemical Biology*, **2004**, *8*, 540-546.

[82] Prodi, L.; *New Journal of Chemistry*, **2005**, *29*, 20-31.

[83] SCI Finder Scholar, American Chemical Society, **2010**, database search on the use of the keywords “gold” and “nanoparticle”, either “as entered” or “as concept”.

[84] Cioffi N.; Palo F.; Calvano C.; Werf D.I.; Palmisano F.; Zambonin G.P.; *Sensor Letters*, **2008**, *6*, 1-8.

[85] Tam, M-E.; Shifferli-H.K.; *Biomedical Materials*, **2008**, *3*, 034001

[86] Teng, C.-H.; Ho, C.-K.; Lin, S.-Y.; Chen, C.-Y; *Analytical Chemistry*, **2004**, *76*, 4337-4342.

[87] Satyabrata, S.; Mandal, T. K.; *Chemistry-A European Journal*, **2007**, *13*, 3160-3168.

[88] Montalti, M.; Prodi, L.; Zaccheroni, N.; Beltrame, M.; Morotti, T.; Quici, S.; *New Journal of Chemistry*, **2007**, *31*, 102-108.

[89] Navajas-Godoy, J.; Caballos-Aguilar, M-P.; *Journal of Fluorescence*, **2010**, *20*, 171-180.

[90] Montalti, M.; Prodi, L.; Zaccheroni, N.; Battistini, G.; Marcuz, S.; Fabrizio, M., Rampazzo, E; Tonellato, U.; *Langmuir*, **2006**, *22*, 5877-5881.

[91] Montalti, M.; Prodi, L.; Zaccheroni, N.; Falini, G.; *Journal of American Chemical Society*, **2002**, *124*, 13540-13546.

[92] Rampazzo, E.; Bonacchi, S.; Montalti, Marco; Prodi, Luca; Zaccheroni, N.; *Journal of American Chemical Society,* **2007**, *129*, 14251-14256.

Chapter 2

Metal ion interaction with a novel anthracene pendant-armed fluorescent molecular probe. Synthesis, Characterization, and fluorescent studies

Elisabete Oliveira, Manuel Vicente, L. Valencia, Alejandro Macías, Rufina Bastida, Carlos Lodeiro, *Inorganic Chimica Acta*, **2007**, 360, 2734-2743.

"Inspiration is a guest who is reluctant to visit the lazy"

Pjotr Tjajkovskij, 1840-1893

Index

2.1 - Graphical Abstract

A new scorpionate system (**L**) containing an emissive anthracene pendant arm has been synthesised and characterised. An increase in the fluorescence emission (CHEF effect) was observed in methanol and in methanol/water mixtures in the presence of Cd^{2+}, Zn^{2+}, Cr^{3+} and Al^{3+}. A CHEQ effect was observed for Cu^{2+} and Hg^{2+}.

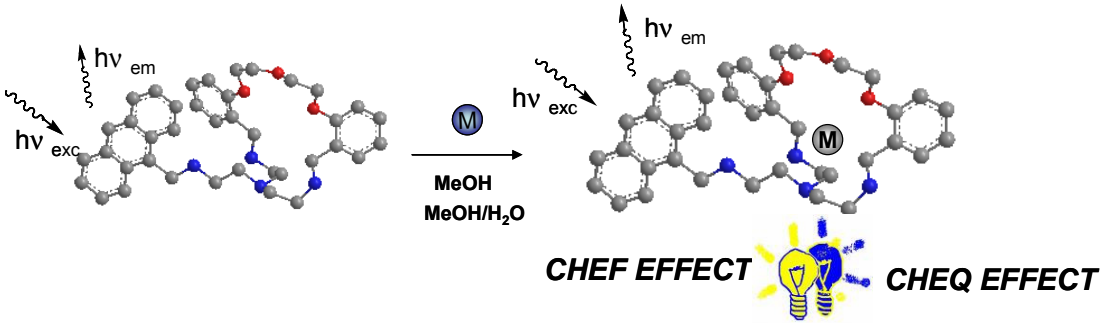

2.2 - Abstract

A new scorpionate system (**L**) containing an emissive anthracene pendant arm, derived of O^1,O^7-bis(2-formylphenyl)-1,4,7-trioxaheptane and tren, has been synthesized and characterized. The sensing capability of **L** towards a range of metal ions has been studied. Protonation and complexation studies, using UV–Vis and fluorescent emission measurements, have been performed with alkaline and alkaline earth metal ions (M = Na^+, K^+, Li^+, Ca^{2+}, Mg^{2+}), as well as transition and post-transition metal ions (M = Cr^{3+},Cu^{2+} and Zn^{2+}, Cd^{2+}, Hg^{2+} and Al^{3+}). An increase in the fluorescence emission (CHEF effect) was observed in methanol and in methanol/water mixtures in the presence of Cd^{2+} (5.0-fold), Zn^{2+} (4.5-fold), Cr^{3+} (2.0-fold) and Al^{3+} (1.8-fold); these results suggest a notable sensing ability of this new N_3O_4 ligand for these metals; these experiments were also performed in the presence of large amounts of alkaline and alkaline earth metal ions.

My contribution for this work was all photophysical studies, and their application as metal chemosensor.

2.3 - Resumo

Um novo sistema (L) contendo um antraceno emissivo como braço pendente, derivado do O1,O7- bi (2-formilfenil) -1,4,7-trioxaheptano e tren, foram sintetizados e caracterizados. A capacidade de sensibilidade de L na presença de iões metálicos foi também estudada. Os estudos de protonação e de complexação, com uso de medidas UV-Vis e de emissão de fluorescência, foram efectuadas com iões metálicos alcalinos e alcalino terrosos (M = Na^+, K^+, Li^+, Ca^{2+}, Mg^{2+}), assim como iões metálicos de transição e de pós-transição (M = Cr^{3+},Cu^{2+} and Zn^{2+}, Cd^{2+}, Hg^{2+} and Al^{3+}). Foi observado um aumento de intensidade de emissão de fluorescência (efeito CHEF), em metanol e em misturas metanol/água, na presença de Cd^{2+} (5.0 vezes), Zn^{2+} (4.5 vezes), Cr^{3+} (2.0 vezes) e Al^{3+} (1.8 vezes); estes resultados sugerem que o ligando N_3O_4 apresenta uma notável sensibilidade na presença destes metais; estas experiências foram também efectuadas na presença de metais alcalinos e alcalinos terrosos em elevada concentração.

A minha contribuição para este trabalho consistiu na realização de todos os estudos fotofísicos e a sua aplicação como sensor químico de metais.

2.4 - Introduction

A considerable number of papers have focused on the use of anthracene containing compounds as protein photo cleavers [1], organic light-emitting diodes and materials [2], crystal engineering [3], molecular imprinted polymers [4], sensors and chemosensors [5]. Anthracene is one of the most employed chromophore studied due to its ability to induce PET (Photoinduced Electron Transfer) processes. A. W. Czarnik and coworkers were among the pioneers in molecular probes containing anthracene [6]. These abiotic receptors can be synthesized by covalently linking a fluorophore to a receptor unit [7]. Following this synthetic strategy many related molecules appropriate for metal ion and anion detection have reported in the literature [8,10].

Scheme 2.1 depicts several scorpionate ligands containing anthracene which have been successfully used for metal ion chelation. The modification of the nature of the donor atoms in the macrocycle produces changes on the sensing capabilities of the ligands. In the polyaza phenanthroline ligand (I), A. Bencini and coworkers [11] have described a nice elementary molecular movement upon coordination with Zn^{2+}; this system coordinates also Cd^{2+} and Hg^{2+}, but no excimer formation between the phenanthroline and the anthracene moieties was observed. We have recently reported the interactions of Cu^{2+}, Co^{2+}, Ni^{2+}, Zn^{2+} and Pd^{2+} with the thiaza macrocycle II [12]; the presence of sulphur atoms increases the affinity for soft metal ions. The oxa-aza system III is an elegant example of on/off behavior in the presence of Cu^{2+} and Ni^{2+} [13]; the N containing macrocyclic ring is capable of incorporating the metal ion with simultaneous release of two amide protons, which provokes a photoinduced electron transfer process, resulting on the quenching of the fluorescence emission of the anthracene. When sufficient number of oxygen atoms are incorporated into the macrocycle skeleton, the interaction with alkaline and alkaline earth metal ions can be studied. A. P. de Silva and coworkers reported in the late eighties the system IV as fluorescent sensor for K^{+} [14]. In absence of the metal ion, the system is not emissive due to an electron transfer process from the tertiary amine nitrogen to the near excited anthracene fragment; complexation with K^{+} restore the fluorescence by the involvement of the nitrogen lone pair.

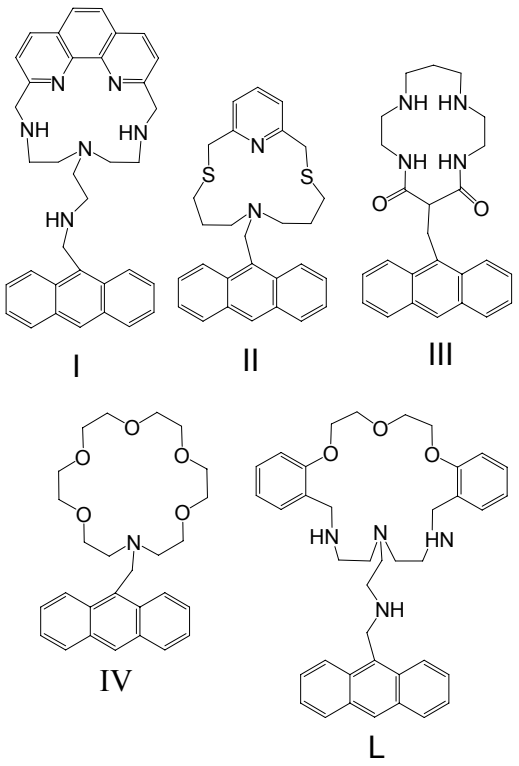

Scheme 2.1 - Several scorpionate ligands containing anthracene which have been successfully used for metal ion chelation

We have recently reported the macrocyclic ligand **2** (Scheme 2.2) derived from O^1,O^7-bis(2-formylphenyl)-1,4,7-trioxaheptane and tren containing an amine terminal pendant arm [15]. In the pH range 7-9, this ligand shows a 10-fold fluorescence emission increase in water solution in the presence of Zn^{2+}. This result suggests that, in water solution, **2** is as a good sensor for this metal ion of biological relevance. Fluorescence emission of system **2** complexed with Zn^{2+} was not affected in the presence of alkaline or alkaline earth metal ions. We have also reported the protonation and complexation reactions of **2** in the presence of Cd^{2+} and Cu^{2+} [15].

Herein we report the synthesis and characterization of a related new functionalised anthracene pendant armed macrocyclic ligand (**L**) and its protonation and complexation reactions. The interaction of **L** with alkaline and alkaline earth ions (M= Na^+, K^+, Li^+, Ca^{2+}, Mg^{2+}), and transition and post-transition ions (M= Cr^{3+}, Al^{3+}, Cu^{2+}, Zn^{2+}, Cd^{2+}, and Hg^{2+}) were studied by UV-vis and fluorescent emission measurements. The results obtained will be discussed in this paper.

2.5 - Experimental

2.5.1 - Physical measurements

Elemental analyses were carried out by the Universidade de Santiago de Compostela Microanalytical Service on Fisons Instruments EA1108 and Leco CNHS-932 micro-analysers, and in the REQUIMTE DQ, Universidade Nova de Lisboa Service on a Thermo Finnigan-CE Flash-EA 1112-CHNS Instrument. Infrared spectra were recorded as KBr discs using Mattson Cygnus 100 and Bio-Rad FTS 175-C spectrophotometers. Proton NMR spectra were recorded using a Bruker WM-500 spectrometer. Positive ion FAB mass spectra were recorded on a Kratos MS50TC spectrometer using a 3-nitrobenzyl alcohol (MNBA) matrix. Electronic Impact spectra were determined on a HP 5988-A spectrometer (University of Santiago de Compostela) and in a Micromass (GCT-TOF7000) (REQUIMTE, Chemistry Department, Universidade Nova de Lisboa).

2.5.2 - Spectrophotometric and spectrofluorimetric measurements

Absorption spectra were recorded on a Perkin–Elmer lambda 35 spectrophotometer and fluorescence emission on a Perkin–Elmer LS45. The linearity of the fluorescence emission versus concentration was checked in the concentration range used (10^{-4}–10^{-6} M). A correction for the absorbed light was performed when necessary. All spectrofluorimetric titrations were performed as follows: the stock solutions of the ligand (ca. 1×10^{-3} M) were prepared by dissolving an appropriate amount of the ligand in a 50mL volumetric flask and diluting to the mark with MeOH UVA-sol or mixtures MeOH/H2O 50/50 v/v. The titration solutions ([L] = 9.00×10^{-6}; 1.35×10^{-5} and 1.25×10^{-5} M,) were prepared by appropriate dilution of the stock solutions. Titrations of the ligand were carried out by addition of microliter amounts of standard solutions of the ions in methanol or absolute ethanol. HBF_4, triethylamine and tetrabutylamonium hydroxide were used to change the acidity conditions of the MeOH solutions. Luminescence quantum yields were measured using a solution of sublimated anthracene in cyclohexane as a standard [ϕ_F = 0.36].[16]

2.5.3 - Chemical and starting materials

O^1,O^7-Bis(2-formylphenyl)-*1,4,7*-trioxaheptane (**1**) [17] and *N,N*-bis(2-aminoethyl)-*N*-{2-[(9-anthrylmethyl)amino]ethyl}amine [18] were prepared according a literature method.

Tris(2-aminoethyl)amine, and the metal salts, $Cr(NO_3)_3$, $AlCl_3$, $Zn(NO_3)_2$, $Cd(NO_3)_2$, $Cu(CF_3SO_3)_2$, $Hg(CF_3SO_3)_2$, $LiClO_4$, $NaNO_3$, KNO_3, $Ca(NO_3)_2$, and $Mg(NO_3)_2$ were commercial products (from Alfa, Fluka and Aldrich) used without further purification. Solvents were of reagent grade purified by the usual methods.

2.5.4 - Synthesis of macrocycle L

The synthesis of macrocycle **L** was carried out according to a modification of a literature method [19].

N,N-Bis(2-aminoethyl)-*N*-{2-[(9-anthrylmethyl)amino]ethyl}amine (1.2 mmol, 0.41g) in methanol (25 mL) was added to a boiling solution of O^1,O^7-bis(2-formylphenyl)-*1,4,7*-trioxaheptane (1.2 mmol, 0.38g) in methanol (100 mL). The tetrahydrobromide amine precursor had to be firstly released by addition of excess of Na_2CO_3 to a water solution. The resulting mixture was refluxed for 2 h and cooled, and then solid $NaBH_4$ (8 mmol, 0.30 g) was carefully added portionwise with stirring. After 3 h, the solution was concentrated to approximately. 50 mL in a rotary evaporator and the volume was increased 2-fold by addition of crushed ice. Stirring was continued at room temperature overnight in an open beaker. The solution was extracted with chloroform (4 x 2 mL), and the organic layer was dried over anhydrous sodium sulphate and then taken to dryness in a rotary evaporator. The crude product was obtained as a yellow oil, air-stable and soluble in chloroform, acetonitrile, dimethyl sulfoxide, methanol and ethanol, moderately soluble in water, and insoluble in diethyl ether. Yield 76%. *Anal.* Calc. for $C_{39}H_{46}N_4O_3.5CH_3OH$: C, 67.8; N, 7.2; H, 8.5. Found: C, 67.5; N, 7.2; H, 7.6%. MS (FAB, MNBA, *m/z):* 191 (100%) [anthrylmethyl]$^+$, 619 [**L**+H]$^+$. IR (NaCl window, cm^{-1}): 3310 br, $\nu(CH_2)$ 3298, 2926, 2873; δ(NH) 1670. ^{1}H NMR ($CDCl_3$); δ(ppm): 8.41 (s, 1H, H_x), 8.32 (d, J=10.0 Hz, 2H, H_v), 8.01 (d, J=9.7 Hz, 2H, H_s), 7.54-7.43 (m, 4H, H_t, H_u), 7.18-7.08 (m, 4H, H_g, H_e), 6.88 (t, J=7.4 Hz, 2H, H_f), 6.54 (d, J=8.2 Hz, 2H, H_d), 4,65 (s, 2H, H_p), 3.87 (m, 4H, H_b), 3.72 (s, 4H, H_i), 3.65 (m, 4H, H_a), 2.81 (t, J=6.3 Hz, 2H, H_n), 2.59 (m, 4H, H_k), 2.50 (m, 4H, H_l), 2.40 (t, J=6.3 Hz, 2H, H_m). ^{13}C NMR ($CDCl_3$); δ(ppm): 70.1 (C_a), 68.0 (C_b), 157.0 (C_c), 116.1 (C_d), 130.7 (C_e), 120.7 (C_f), 128.4 (C_g), 49.3 (C_i), 46.4 (C_k), 54.2 (C_l), 54.8 (C_m), 48.1 (C_n), 45.9 (C_p), 132.0 (C_q), 131.5 (C_r), 129.0 (C_s), 125.0 (C_t), 126.0 (C_u), 124.4 (C_v), 130.3 (C_w), 127.0 (C_x).

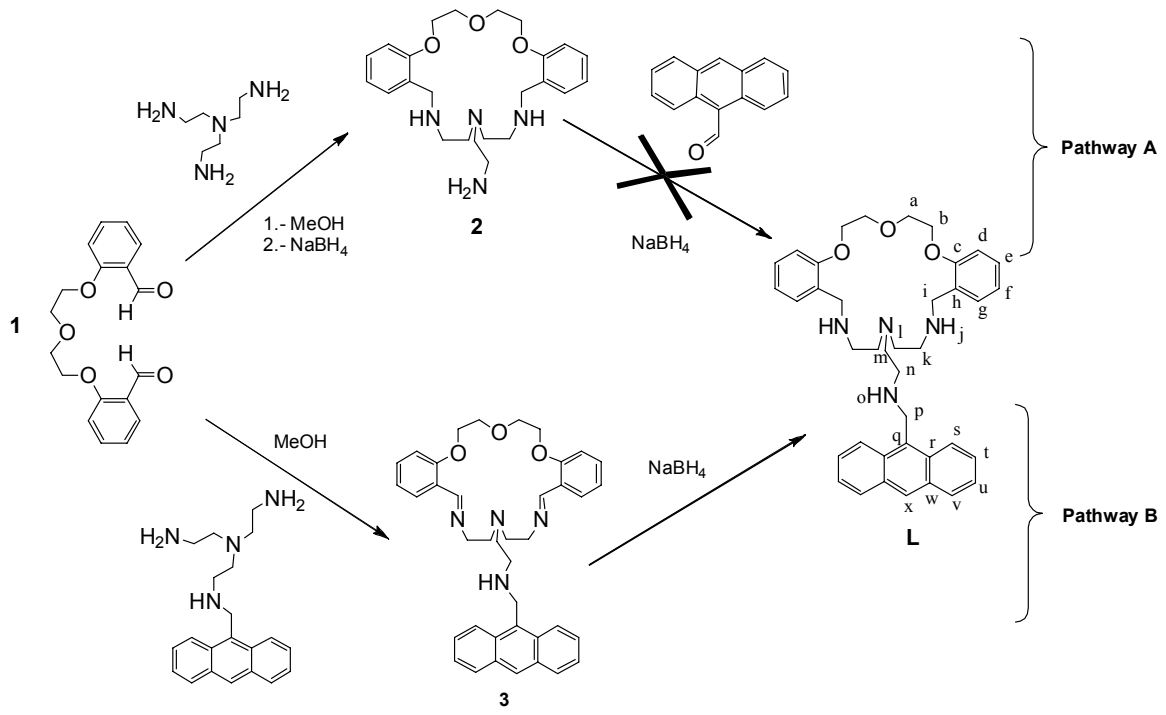

Scheme 2.2 – Synthetic pathways of ligand **L**.

2.6 - Results and discussion

2.6.1 - Synthesis and characterization of L

Ligand **L** was prepared by direct cyclocondensation between O^1,O^7-bis(2-formylphenyl)-*1,4,7*-trioxaheptane and *N,N*-Bis(2-aminoethyl)-*N*-{2-[(9-anthrylmethyl)amino]ethyl}amine in methanol, followed by an in situ reduction with $NaBH_4$. Attempts to prepare the ligand by direct reaction between the macrocycle precursor **2** [15] and 9-antrhaldehyde, followed by an in situ reduction with $NaBH_4$, were unsuccessful (see scheme 2.2). The FAB mass spectrum of L.5MeOH features the parent peak at *m/z* 619 assigned to the molecular ion $[\mathbf{L}+H]^+$ providing evidence that the macrocycle is the 1:1 condensation product. The IR spectrum of **L** (NaCl windows) shows no bands assignable to carbonyl or azometine groups. The presence of an intense broad band centred at *ca*. 3310 cm^{-1}, consistent with the presence of methanol (as suggested from the microanalytical data), prevents the observation of bands attributable to amine stretches.

2.6.2 - NMR Spectra of L

The ^{1}H and ^{13}C NMR spectra of **L**.5MeOH, recorded in $CDCl_3$, confirm the integrity of the ligand and its stability in solution. Spectral data are listed in the Experimental Section and in Table SI2.1 (Supporting information). The identification of the proton signals was based upon standard 2D homonuclear (COSY) and $^{1}H/^{13}C$ heteronuclear spectra (HMQC); the identification labels for each proton are given in Scheme 2.2. Both spectra can be found in the Supporting information (Figures SI2.1 and SI2.2). The spectra show that the two halves of the macrocyclic ring are chemically equivalent. Also, the ^{13}C spectrum exhibits only 10 resonances for the carbons of the macrocyclic backbone and 11 for the carbons of the pendant arm. In the proton NMR spectra the presence of the anthrylmethyl pendant is confirmed by the signals ascribed to the aromatic protons and the singlet at 4.65 ppm for the H_p proton.

2.6.3 - Spectrophotometric and spectrofluorimetric studies.

2.6.3.1 - Studies in organic media

The absorption, emission and excitation spectra of compound **L** in methanol solution are reported in Figure 2.1. The spectra show the characteristic band of the anthracene derivatives above 330 nm; the band has vibrational fine structure with maxima at 333, 350, 368 and 388 nm.

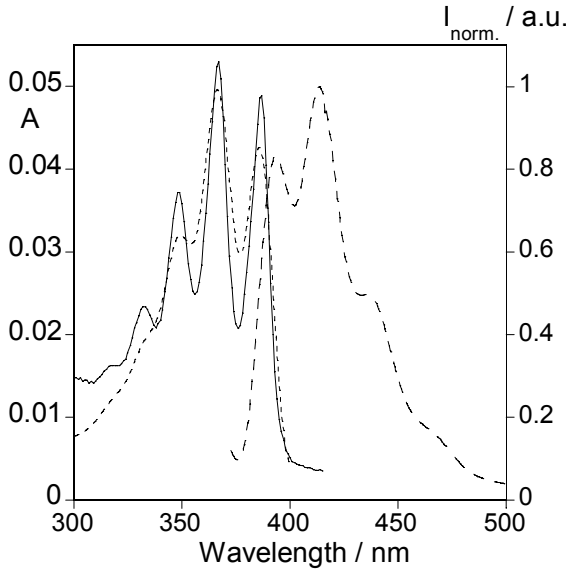

Figure 2.1- Absorption (full line), emission (broke line) and excitation (dotted line) spectra of **L** (λ_{exc} = 367 nm; λ_{em}= 413 nm, [L] =9.00×10^{-6} M) in methanol at room temperature.

The absorption spectrum of **L** is based on the anthracene moiety and is slightly dependent on the protonation state of the polyamine present on the macrocyclic skeleton (see Figure 2.2A). Inspection of Figure 2.2B shows that the first two protons added increase slightly the absorbance of **L**. Addition of more protons leads to a steady decrease; after the addition of the four proton equivalents, the absorbance remains constant. This result suggests the first N protonated is the one near the anthracene pendant arm. Protonation of the intracyclic amine groups could induce the formation of hydrogen bond with the oxygen present in the macrocycle, and thus the absorption for the high protonated species would be lowest; these results are similar to those previously reported for ligand **2** [15].

The emission spectra showed in figure 2.2C were obtained by titration with a freshly methanolic acid solution of HBF_4. Carefully inspection shows that upon four protons the fluorescence emission achieves a plateau, as it is shown in figure 2.2D). This suggests that all nitrogens are protonated at this point, preventing the PET phenomena observed in the free ligand. The presence of an electron rich anthracene moiety increases notably the basicity of the amine group included in the pendant arm. The initial equivalents of H^+ added are thus involved in the protonation of this amine group, which prevents the PET more efficiently than the intracyclic amines, because the long distance between these intracyclic amines and the anthracene ring [8b]. In order to elucidate this point, we have performed several experiments using alkaline methanol solutions to deprotonate completely the system. Addition of a freshly prepared triethylamine or tetramethylamonium hydroxide methanol solution affects both the absorption and the fluorescence emission spectra. Moreover, protonation studies of an alkaline methanol solution of **L** suggest that after four protons are added the fluorescence emission is totally restored.

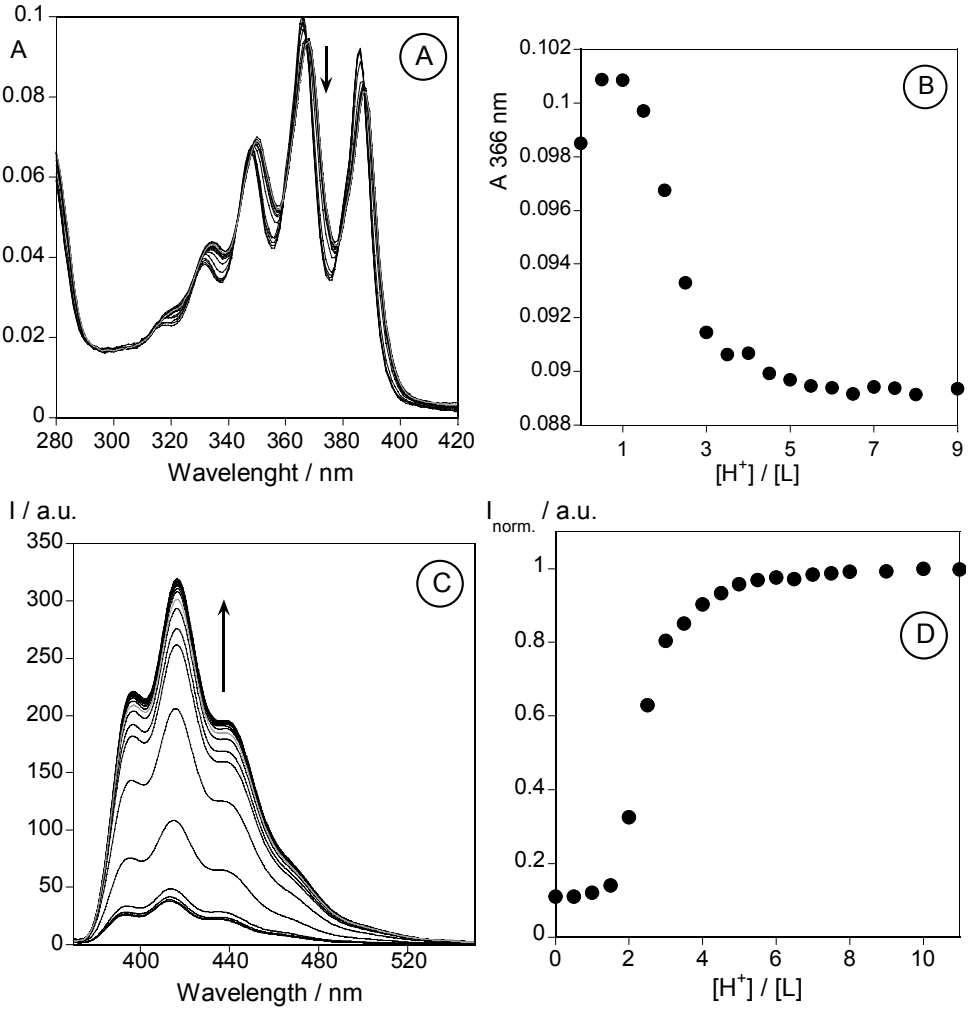

Figure 2.2.- Absorption (A) and emission (C) spectra of methanol solutions of **L** as a function of added HBF_4. Figures (B) and (D) show (respectively) the absorption at 366 nm and the normalized fluorescence intensity at 416 nm. ([L] = 9.0×10^{-6} M, λ_{exc} = 367 nm).

2.6.4 - Metal Complexes

The complexation capability of **L** towards alkaline and alkaline earths metal ions (M= Na^+, K^+, Li^+, Ca^{2+}, Mg^{2+}), as well as transition and post-transition metal ions (M= Cr^{3+}, Cu^{2+}, Zn^{2+}, Cd^{2+}, Hg^{2+} and Al^{3+}) was studied by UV-vis and fluorescence emission measurements.

The absorption spectra for all the metal ion titrations are very similar to that of the free ligand, showing the characteristic bands of the anthracene derivatives above 330 nm. In all cases a small red shift is observed upon complexation (see Figures 2.3A, 2.4A, 2.5A and 2.6A).

2.6.4.1 - Li^+, Na^+, K^+, Ca^+ and Mg^{2+} titrations

No significant effect can be observed upon complexation with the alkaline metals Li^+, Na^+, K^+, and alkaline earth metals Ca^{2+} and Mg^{2+}. The addition, in equimolar amounts, of methanolic solutions of these metal ions to a methanolic or water/methanol solution of **L** does not affect the intensity of emission.

Increasing the metal ion concentration to 50 equivalents causes only a slight decrease in the fluorescence intensity for Ca^{2+} and Mg^{2+}.

2.6.4.2 - Zn^{2+} and Cd^{2+} titrations

Zn^{2+} and Cd^{2+} coordinated to polyammonium ligands or, in our case, to an oxo-aza macrocyclic ligand are generally emissive species, leading to a CHEF effect (*Chelation Enhancement of the Fluorescence Emission*) [20]. The stronger the involvement of the nitrogen atoms in the complexation, the stronger the effect on the luminescence of the ligand. This was confirmed by the fluorescence emission titration curves reported in Figures 2.3B and 2.4B, insets.

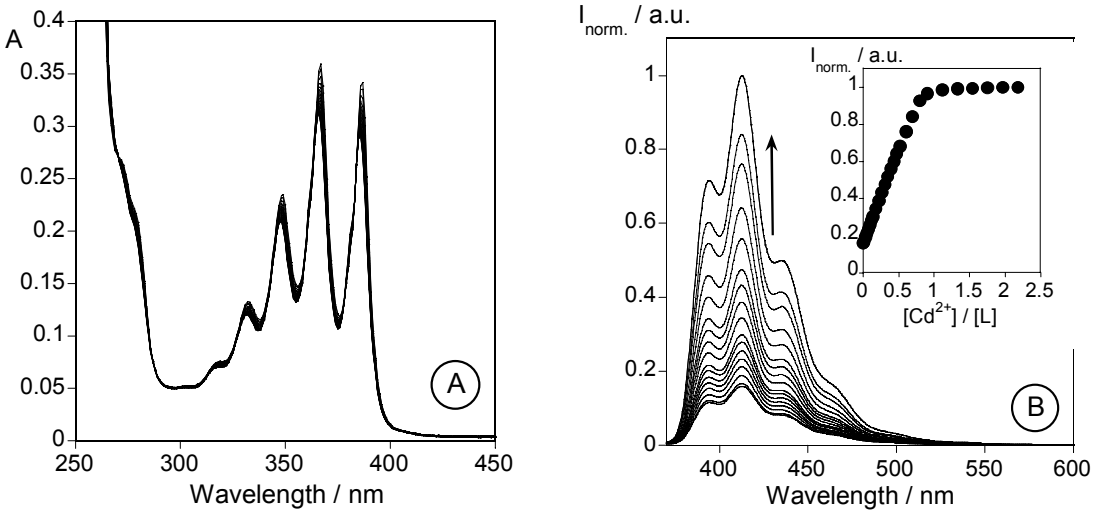

Figure 2.3.- Absorption (A) and emission (B) spectra of methanol solutions of **L** as a function of increasing amounts of $Cd(NO_3)_2$. The inset shows the normalized fluorescence intensity at 413 nm. ([L] = 1.35×10^{-5} M, λ_{exc} = 367 nm).

Similar CHEF intensity was observed for both ions, leading to a 4.5-fold increase for Zn^{2+} and 5-fold for Cd^{2+}. Insets of Figures 3 and 4 shows that these changes occur upon addition of

one equivalent of metal, achieving a plateau for higher metal/ligand ratios. These data suggest the formation of mononuclear complexes with both metals. This behavior is also reflected in the values of the quantum yield of the free, protonated and complexed species (see Table 2.1), and can be explained by assuming that the protonation of the aliphatic amine and complexation with Zn^{2+} and Cd^{2+} prevents the PET from its lone pair of electrons to the anthracene moiety.

Table 2.1. – Quantum yields in methanol at 298 K.

	ϕ
L	0.051
L + $4H^+$	0.415
L + Cd^{2+}	0.305
L + Zn^{2+}	0.283
L + Cr^{3+}	0.131
L + Al^{3+}	0.084
L+Hg^{2+}	0.021
L + Cu^{2+}	0.002

Previously, we have reported for ligand **2** a stronger CHEF effect for Zn^{2+} than for Cd^{2+} [15]. In that case, complexation with Zn^{2+} leads to a ten-fold fluorescence emission increase. Now, the introduction of a bulky anthracene moiety into the pendant-arm has reduced notably the fluorescence emission intensity observed for Zn^{2+}, and both Zn^{2+} and Cd^{2+} present a similar CHEF effect.

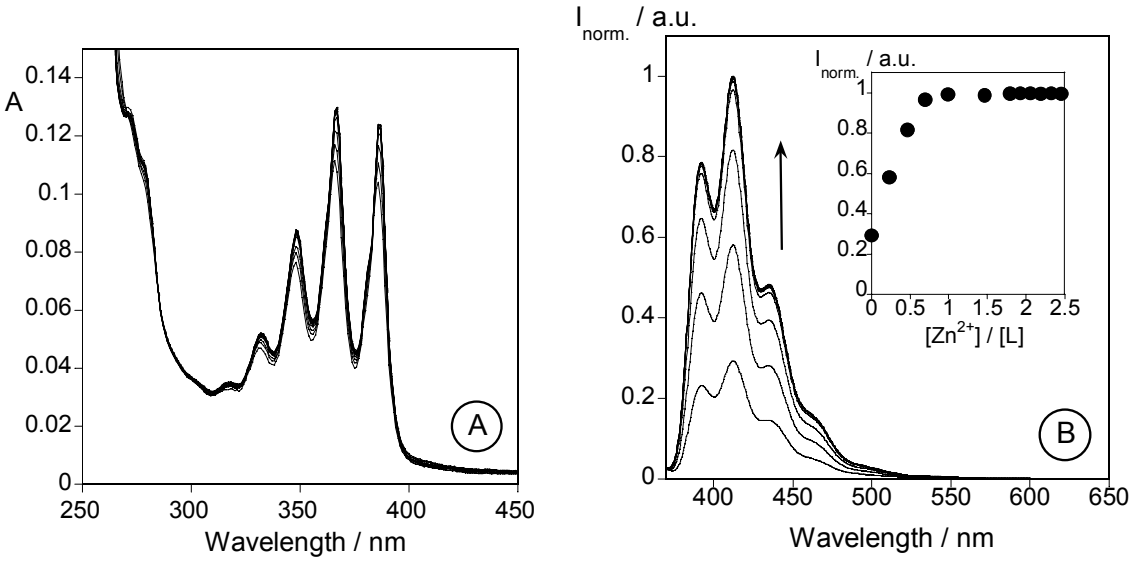

Figure 2.4.- Absorption (A) and emission (B) spectra of methanol solutions of **L** as a function of increasing amounts of $Zn(NO_3)_2$. The inset shows the normalized fluorescence intensity at 413 nm. ([L] = 1.25×10^{-5} M, λ_{exc} = 367 nm).

2.6.4.3 - Cu^{2+} and Hg^{2+} titrations

Concerning the Cu^{2+} and Hg^{2+} complexes, a strong CHEQ effect (*Chelation Enhancement of the Quenching*) can be observed upon metal ion complexation. This CHEQ effect is commonly observed in polyamine ligands containing aromatic fluorophores, and can be attributed to an energy transfer quenching of the π* emissive state though low-lying metal-centred unfilled d-orbitals for Cu^{2+}, and to an intersystem crossing mechanism due to the heavy atom effect for Hg^{2+} [20b].

In both cases a plateau was achieved upon one equivalent of metal added. The quantum yield after the complexation of Cu^{2+} generates a strong quenching due to photoinduce electron transfer or energy transfer to the excited anthracene moiety (See Table 1).[21. 20a]

2.6.4.4 - Trivalent metal ions: Al^{3+} and Cr^{3+}

A considerable amount of literature has focused on the detection of Aluminium [22] and Chromium, due to the high toxicity of their compounds and their widespread use. For instance, Al^{3+} is employed in water treatment, as food additives, in medicine, etc. Cr^{3+} is used to harden steel, in the manufacture stainless steel, in alloys, to prevent corrosion, and as catalyst. Many analytical techniques based on sample destructive methods can be used to detect these metals; in contrast, few examples of fluorescence chemosensors as non destructive method have been reported for the detection of Al^{3+} [23] and Cr^{3+} [24] in solution.

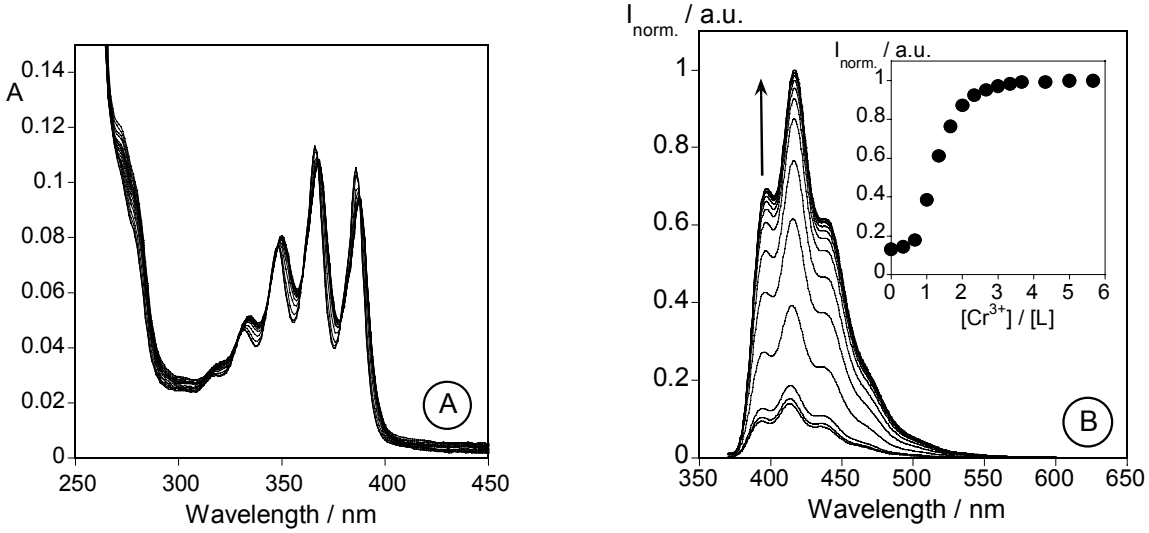

Figure 2.5.- Absorption (A) and emission (B) spectra of methanol solutions of **L** as a function of increasing amounts of $Cr(NO_3)_3$. The inset shows the normalized fluorescence intensity at 413 nm. ([L] = 1.35×10^{-5} M, λ_{exc} = 367 nm).

The interaction of ligand **L** with Al^{3+} and Cr^{3+} in methanol or water/methanol solutions gave a CHEF effect (*Chelation Enhancement of the Fluorescence*) in both cases upon metal ion complexation. Figures 2.5B and 2.6B show the fluorescence emission spectra for both metal ion titrations. The insets show that similar CHEF intensity was observed, leading an increase of 1.80-fold for Al^{3+} and 2.0-fold for Cr^{3+}; these changes occur upon addition of one equivalent of metal, achieving a plateau for two metal/ligand ratio. These results suggest the formation of dinuclear complexes with both metals. In absence of any crystal structures, decisive in order to elucidate the coordinative environment of the metal ion in the molecule, we must be extremely careful when attempting to explain the formation of di nuclear complexes, depending only on the metal ion employed. Taking into account the classification of Al^{3+} and Cr^{3+} as hard Lewis Acids [25], coordination could take place by the oxygen and nitrogen atoms in the ligand **L**, leading a dinuclear complexes.

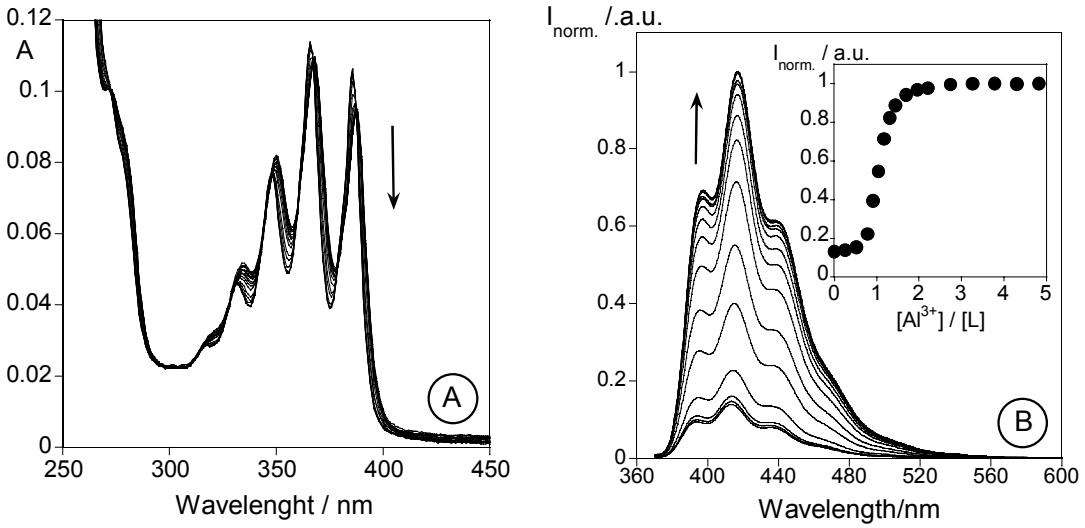

Figure 2.6.- Absorption (A) and emission (B) spectra of methanol solutions of **L** as a function of increasing amounts of $AlCl_3$. The inset shows the normalized fluorescence intensity at 413 nm. ([L] = 1.35×10^{-5} M, λ_{exc} = 367 nm).

2.6.5 - Studies in mixtures water-organic media

Any realistic studies of the potential ability of any compound to act as a chemosensor should be performed in water solution. Due to the low solubility of ligand **L** in water at neutral and basic pH, we have performed some experiments in 50/50 (v/v) MeOH/H_2O mixtures. The pH dependent emission spectra of compound **L** in MeOH/H_2O is shown in Figure 2.7. Inspection of this figure shows a decrease in intensity when the pH increases. This effect is due to the PET process from the lone pair of electrons of the free amine nitrogens to the excited anthracene chromophore. As it is shown in the inset, after pH 8 all the nitrogen atoms are deprotonated, and the ligand remains not emissive. Maximum emission is achieved in the pH interval 2-4; within this range, the ligand has at least three protons. This behaviour is similar to that of ligand **2**, reported previously [15].

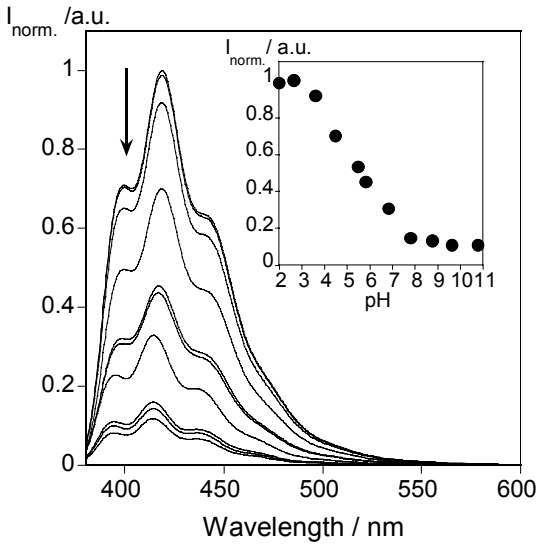

Figure 2.7.- Emission spectra of **L** in water/methanol solutions (50/50, v/v) as a function of pH. The inset shows the normalized fluorescence intensity at 419 nm. ([L] = 1.35×10^{-5} M, λ_{exc} = 367 nm). (pH =1.9; 2.7; 3.6; 4.5; 5.5; 5.8; 6.8; 7.8; 8.7; 9.7; 10.8)

In water/methanol mixtures the sensing effect for the metal ion studied was similar to that of pure methanol. Only for Al^{3+} and Cr^{3+} the plateau was achieved for more than one metal ion. Zn^{2+}, Cd^{2+}, Cu^{2+} and Hg^{2+} form mononuclear complexes and the effects observed in the intensity of fluorescence were the same described above.

Figure 2.8 compares the fluorescence emission spectra of **L** in the presence and absence of all the cations tested, in order to evaluate its chemosensor ability. For Cr^{3+}, Al^{3+}, Zn^{2+} and Cd^{2+} a CHEF effect was detected by an increase in fluorescence emission. On the contrary, a CHEQ effect was observed with by Cu^{2+} and Hg^{2+}, as discussed above. This quenching is stronger in the case of Cu^{2+} probably due to its higher affinity to nitrogen and oxygen atoms when compared Hg^{2+} ion. A schematic representation of the possible PET mechanism observed for all metals studied is given in Scheme 2.3.

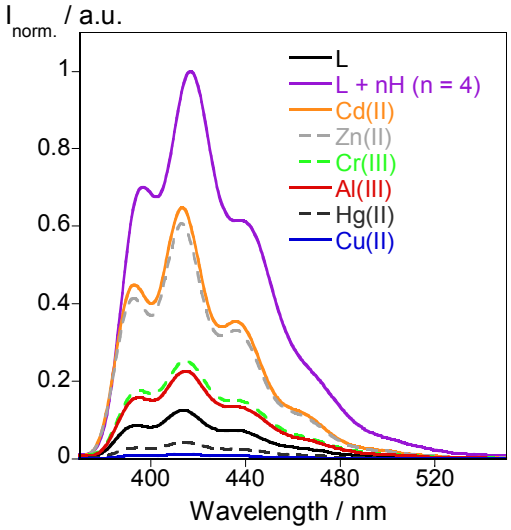

Figure 2.8.- Fluorescence emission spectra of methanol solutions of **L** in the presence of one equivalent of $Zn(NO_3)_2$, $Cd(NO_3)_2$, $Cr(NO_3)_3$, $AlCl_3$, $Hg(CF_3SO_3)_2$ and $Cu(CF_3SO_3)_2$. ([L] = 1.25×10^{-5} M, λ_{exc} = 367 nm).

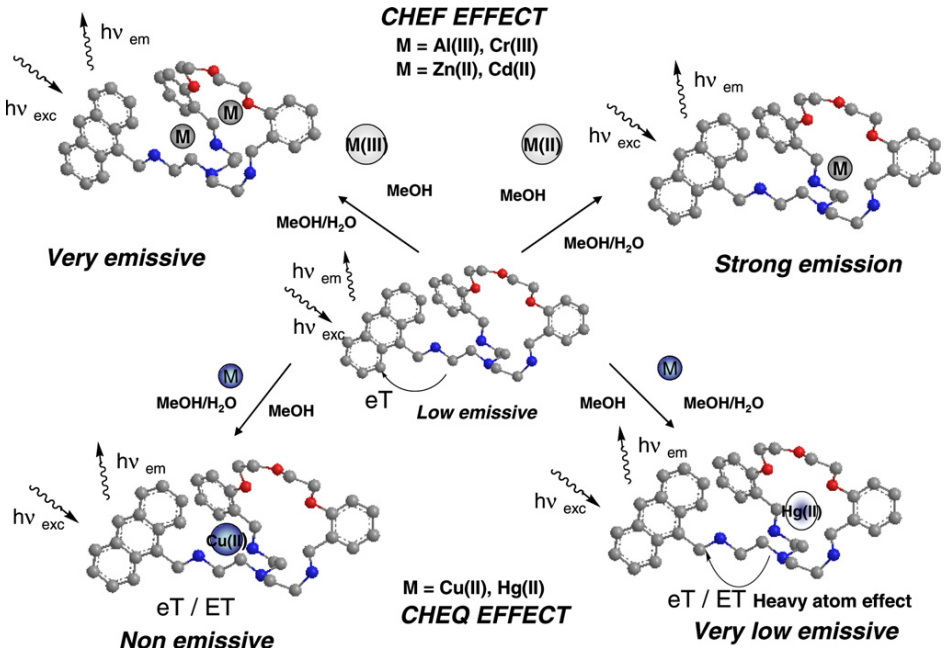

Scheme 2.3. Schematic representation of the photoinduced electron and energy transfer mechanism observed in system **L** upon complexation with Al^{3+}, Cr^{3+}, Zn^{2+}, Cd^{2+}, Hg^{2+} and Cu^{2+}.

The fluorescence response of **L** (1.25 E^{-5}M) towards Cr^{3+}, Cu^{2+}, Hg^{2+}, Zn^{2+}, Cd^{2+}, and Al^{3+}, and other metal ions of biological relevance, such as Li^{+}. Na^{+}, K^{+}, Ca^{2+} and Mg^{2+} are summarized in Figure SI3 Supplementary material.

A stronger CHEQ effect is observed in the case of Cu^{2+} with respect to Hg^{2+} in the conditions employed (methanol, room temperature, λ_{exc}=367 nm, λ_{em} = 413 nm).

The intensity observed for Zn^{2+} and Cd^{2+} is not affected by the presence of the alkaline metal ions studied (Li^+, Na^+ and K^+). However, for the alkaline earth metals tested (Ca^{2+} and Mg^{2+}), the presence of Zn^{2+} induced a small decrease in the fluorescence emission intensity. A similar result was discussed previously for the alkaline earth Ca^{2+} and Mg^{2+}.

2.7 - Conclusion

The cyclocondensation of *O*^{1},*O*^{7}-bis(2-formylphenyl)-*1,4,7*-trioxaheptane with *N,N*-Bis(2-aminoethyl)-*N*-{2-[(9-anthrylmethyl)amino]ethyl}amine in methanol followed by an in situ reduction with $NaBH_4$ yields the new macrocycle L containing an anthracene pendant arm. The studies conducted suggest that this ligand is an effective complexation molecular device for several divalent metal ions of biological importance as well as for Al^{3+} and Cr^{3+}, both metals of great revelance in medicine and environmental chemistry.

The introduction of an anthracene pendant arm into the macrocycle skeleton increases the quantum yield observed for the parent compound **2**. A strong quenching effect was observed for metal ions with semi fielded d orbital occupied (Cu^{2+}), as well as for Hg^{2+}, and a moderate fluorescence emission intensity was observed for Zn^{2+} and Cd^{2+}. A very promising result was observed for Al^{3+} and Cr^{3+}; the CHEF effect observed in both cases could be used as a starting point to developed a more efficiently fluorescence chemosensor based on macrocyclic ligands for these metals. The study of the interaction of the ZnL complex with biological anions and amino acids is currently in progress.

2.8 - Acknowledgements

We are indebted to Fundação para a Ciência e a Tecnologia / FEDER (Portugal/EU) (Project POCI/QUI/55519/2004 FCT-FEDER), Xunta de Galicia (Spain) (Project PGIDT04PXIB2091PR), and Canterbury Christ Church University Research Fund for financial support. E.B and C. L also thank bilateral program “Acçoes integradas Luso-Británicas 2006” for the bilateral agreement number B-16/06.

2.9 - Supporting Information

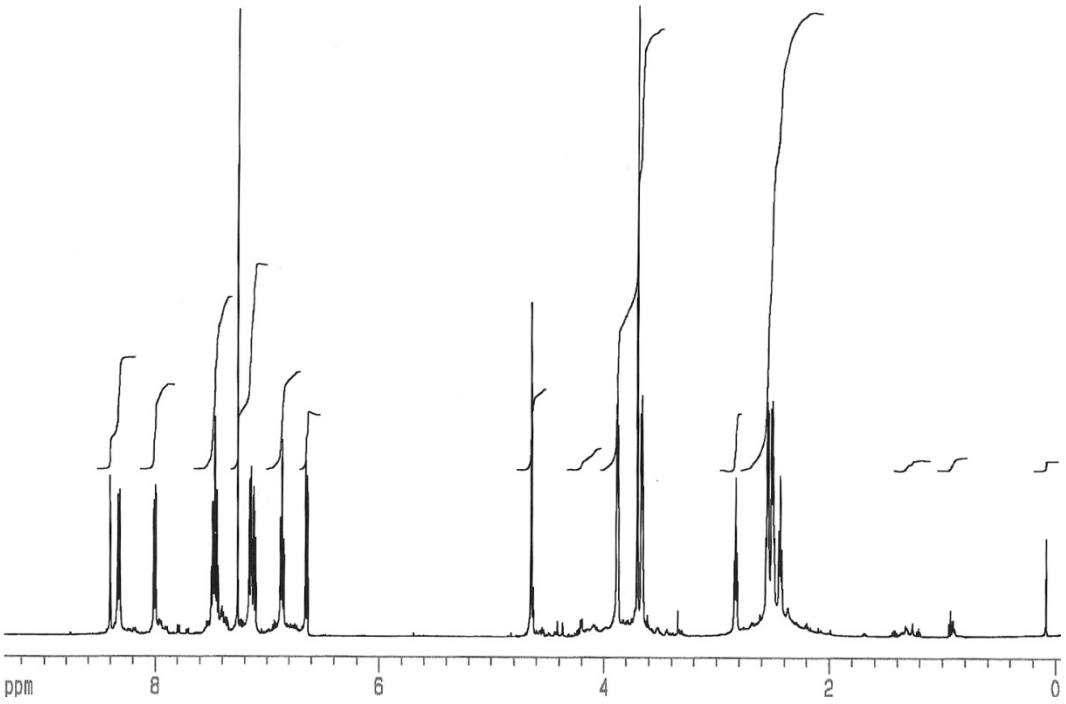

Figure SI2.1. 500 MHz ^{1}H NMR of **L** in $CDCl_3$.

Table SI2.1. ^{1}H NMR data at 500 MHz of **L** in $CDCl_3$

	Integration	Shift (ppm) δ
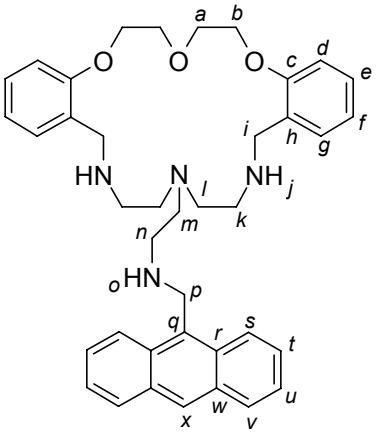	H_x	8.41 (s, 1H)
	H_v	8.32 (d, J =10.0 Hz, 2H)
	H_s	8.01 (d, J =9.70 Hz, 2H)
	H_t, H_u	7.54-7.43 (m, 4H)
	H_g,H_e	7.18-7.08 (m, 4H)
	H_f	6.88 (t, J =7.4 Hz, 2H)
	H_d	6.54 (d, J =8.2 Hz, 2H)
	H_p	4.65 (s, 2H)
	H_b	3.87 (m, 4H)
	H_i	3.72 (s, 4H)
	H_a	3.65 (m, 4H)
	H_n	2.81 (t, J =6.3 Hz, 2H)
	H_k	2.59 (m, 4H)
	H_l	2.50 (m, 4H)
	H_m	2.40 (t, J =6.3 Hz, 2H)

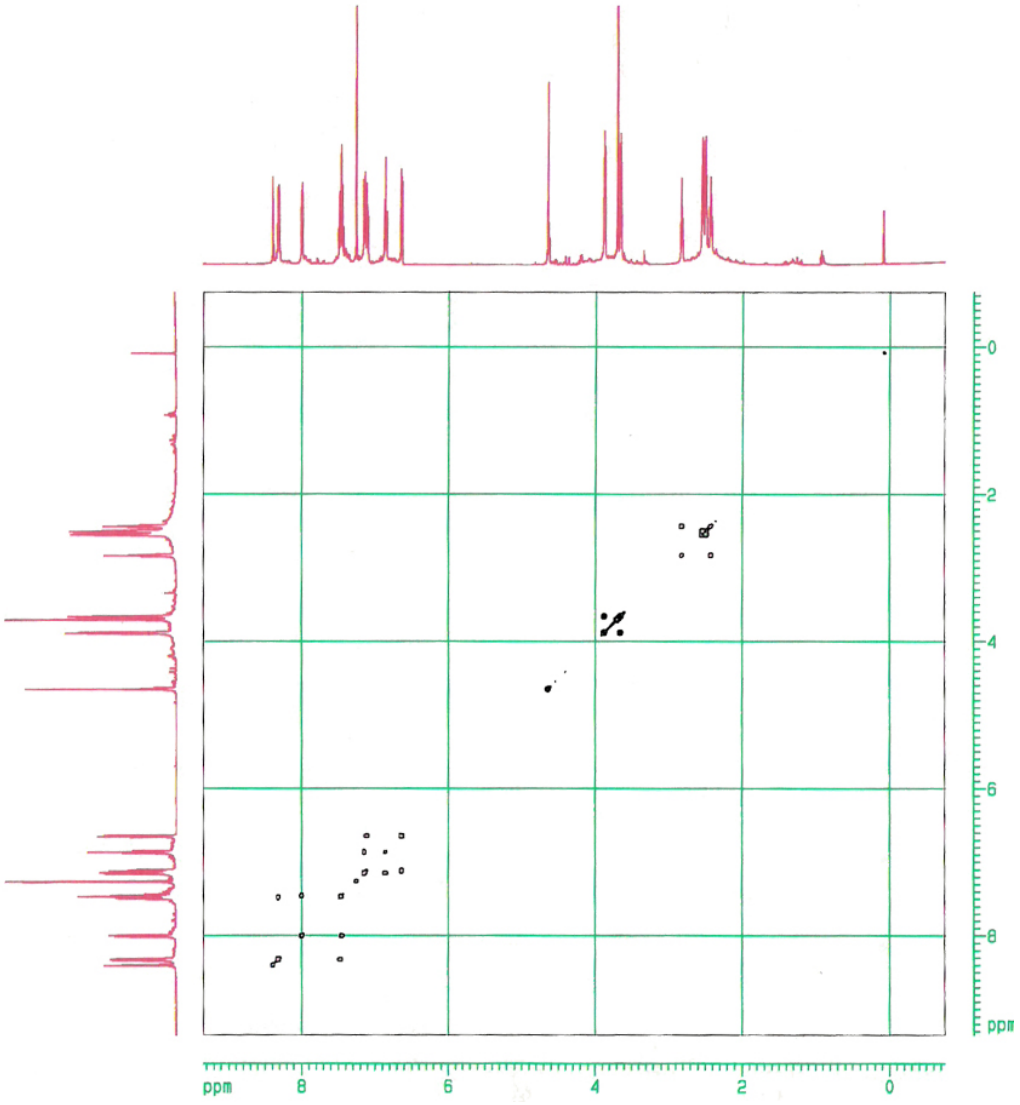

Figure SI2.2. 500 MHz ^{1}H-^{1}H (COSY 45) NMR of **L** in $CDCl_3$.

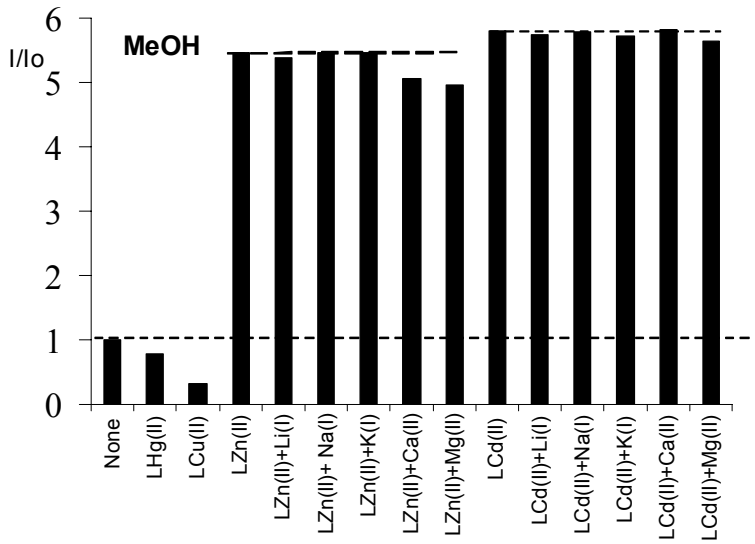

Figure SI2.3. Relative fluorescence intensity at 413 nm of **L** in methanol to 1 equiv. of metal ions ([L] = 1.25×10^{-5} M, λ_{exc} = 367 nm). Io is the emission at 413 nm of L ([L] = 1.25×10^{-5} M, λ_{exc} = 367 nm) in the absence of metal ions. The presence of an excess amount (up to 1:50) of Li^{+}, Na^{+}, K^{+}, Ca^{2+} and Mg^{2+} is represented in the nearest columns to Zn^{2+} and Cd^{2+}.

2.10 - References

[1] W. Hasewaga., A. Suzuki, S. Matsumura, K. Toshima, Sci. Tech. Avd. Mate, 7, (2006), 169.

[2] (a) J. H. Jou, S. Chiu, R. Y. Wang, H. C. Hu, C. P. Wang, H. W. Lin, Org. Electronics, 7, (2006), 8 (b) J. Li, Y. Duan, X. H. Li, C. N. Li, J. Y. Hou, S. Y. Liu, Semiconductor Sci. Tech., 21, (2006),148; (c) K. Yun-Hi, H-C, Jeong, S-H, Kim, K. Yang, S-K. Kwon, Adv. Func. Mat., 15, (2005), 1799; (d) M. T. Lee, C. H. Liao, C. H. Tsai, C. H. Chen, Adv. Mat., 17 (2005), 2493.

[3] T. L. Hu, J. R. Li. Y. B. Xie, X. H. Bu, X. Crystal Growth and Design, 2006, 6, 648.

[4] Y. C. Chen, J. J. Brazier, M. D. Yan, P. R. Bargo, S. A. Pral, Sensors. Act, B-Chem., 102, (2004), 107.

[5] (a) K. Schonefeld, A. Barann, K. Vogel, K. H. Feller, D. Kunze, D, P. Muller, E. Weber, Int. J. Environ. Anal. Chem., 85, (2005) 655; (b) S. C. Magri, J. F. Callan, A. Prasanna de Silva, D. B. Fox, N. D. McClenaghan, N. D.; K. R. A., Samankumara Sandanayake, J. Fluorescence, 15, (2005), 769. (c) L. Rodríguez, S. Alves, J. C. Lima, A. J. Parola, F. Pina, C. Soriano, M. T. Albelda, E. Garcia-España , J. Photochem. Photobiology, A: Chem., 159, (2003), 251.

[6] (a) A. E. Huston, K. W. Haider, A. W. Czanik, J. Am. Chem. Soc., 110, (1988), 4460, (b) M. Y. Chae, J. Y. Yoon, W. W. Czarnik, J. Mol. Recog., 9(4) (1996), 297.

[7] (a) A. W. Czarnik, Fluorescent Chemosensors for Ion and Molecule Recognition; American Chemical Society: Washington, DC, 1993. (b) a. P. de Silva, H. Q. N. Gunaratne, T. Gunnlaugsson, A. J. M. Huxley, C. P. McCoy, J. T. Rademacher, T. E. Rice, Chem. Rev., 97, (1997), 1515.

[8] (a) M. T. Albelda, P. Díaz, E. García-España, J. C. Lima, C. Lodeiro, J. S. de Melo, A. J. Parola, F. Pina, C. Soriano, Chem. Phys. Lett. 353, (2002), 63; (b) F. Pina, J. C. Lima, C. Lodeiro, J. S. de Melo, P. Díaz, M. T. Albelda, E. García-España, E. J. Phys. Chem. A , 106, (2002), 8207; (c) J. S. de Melo, J. Pina, F. Pina, C. Lodeiro, A. J. Parola, J. C. Lima, M. T. Albelda, M. P. Clares, E. García-España, C. Soriano, J. Phys. Chem. A, 107, (2003), 11307; (d) F. Pina, M. A. Bernardo, E. García-España, Eur. J. Inorg. Chem., 10, (2000), 2143; (e) A. Tamayo, L. Escriche, J. Casabo, B. Covelo, C. Lodeiro, Eur. J. Inorg. Chem., 15, (2006), 2997.

[9] (a) L. Fabbrizzi, M. Licchelli, G. Rabaioli, A. Taglietti, Coord. Chem. Rev., 205, (2000), 85; (b) L. Fabbrizzi, M. Licchelli, F. Mancin, M. Pizzeqhello, G. Rabaioli, A. Taglietti, P. Tecilla, U.

Tonellato, Chem. A. Eur. J., 8, (2002), 94; (c) L. Fabbrizzi, M. Licchelli, A. Perotti, A. Poggi, G. Rabaioli, S. Sacchi, A. Taglietti, J. Chem. Soc., Perkin Trans. 2., 11, (2001), 2108; (d) V. Amendola, L. Fabbrizzi, C. Mangano, P. Pallavicini, Structure and Bonding, 99, (2001), 79; (e) K. Ghoso, G. Masanta, Chem. Letters, 35, (2006),414; (f) E. G. Moore, P. V. Bernhardt, A. Furstenberg, M. J. Riley, E. Vauthey, J. Phys. Chem., A., 109, (2005), 11715.

[10] (a) D. C. Magri, J. F. Callan, A. P. de Silva, D. B. Fox, N. D. McClenaghan, K. R. A. S. Sandanayake, J. Fluorescence, 15, (2005), 769; (b) K. Kubo, A. Mori, J. Mat. Chem., 15, (2005), 2902; (c) T. Gunnlauqsson, H. D. P. Ali, M. Glynn, P. E. Kruger, G. M. Hussey, F. M. Pfeffer, C. M. G. dos Santos, J. Tierney., J. Fluorescence, 15, (2005), 287; (d) N. J. Youn, S. K. Chang, Tetrahedron Lett., 2005, 46, 125; (e) T. Gunnlauqsson, T. C. Lee, R. Parkesh, Org. Lett., 5, (2003), 4065; (f) K. Kubo, T. Sakurai, A. Mori, Talanta, 50, (1999), 73

[11] (a) A. Bencini, A. Bianchi, C. Lodeiro, A. Masotti, A.J. Parola, F. Pina, F. J. S. de Melo, B. Valtancoli, Chem. Commun., 17, (2000), 1639. (b) ; (g) A. Bencini, E. Berni, A. Bianchi, P. Fornasari, C. Giorgi, J. C. Lima, C. Lodeiro, M. J. Melo, J. S. de Melo, A. J. Parola, F. Pina, J. Pina, B. Valtancoli, Dalton Transations, 14, (2004), 2180.

[12] A. Tamayo, C. Lodeiro, L. Escriche, J. Casabo, B. Covelo, P. Gonzalez, Inorg. Chem., 44, (2005), 8105.

[13] G. DeSantis, L. Fabbrizzi, M. Licchelli, N.Sardone, A. H. Velders, Chem. A. Eur. J., 2, (1996), 1243.

[14] A. P. de Silva, S. A. de Silva, J. Chem. Soc., Chem. Commun., (1986), 1709.

[15] M. Vicente, R. Bastida, C. Lodeiro, A. Macías, A. J. Parola, L. Valencia, S. E. Spey, Inorg. Chem., 42, (2003), 6768.

[16] I. B. Berlan, Handbook of Fluorescence Spectra of Aromatic Molecules, 2nd ed.; Academic Press: New York, (1971).

[17] F. R. Adam, A. J. Leong, L. F. Lindoy, H. C. Lip, B. W. Skelton, A. H. White, J. Am. Chem. Soc. 105, (1983) , 4645.

[18] S. Alves, F. Pina, M. T. Alvelda, E. García-España, C. Soriano, S. V. Luís, Eur. J. Inorg. Chem., (2001), 405.

[19] C. A. Davis, P. A. Duckworth, L. F. Lindoy, W. E. Moody, Aust. J. Chem., 48, (1995) , 1819.

[20] a) B. Valeur, Molecular Fluorescence. Principles and Applications; Wiley-VCH: Weinheim, (2002); b) K. Rurack, Spect. Acta. A, 57, (2001), 1261.

[21] S. Alves, F. Pina, M. T. Albelda, E. García-España, C. Soriano, S. V. Luis, S. V.; Eur. J. Inorg. Chem., 2, (2001), 405.

[22] a) R. Doll, Age Ageing, 22, (1993), 138; (b) J. Burgess, Chem. Soc. Rev., 25, (1996), 85; R. B. Martin, Acc. Chem. Res., 27, (1994), 204.

[23] a) M. Arduini, F. Felluga, F. Mancin, P. Rossi, P. Tecilla, U. Tonellato, N. Valentinuzzi, Chem. Commun., (2003), 1606; (b) F. Launay, V. Alain, E, Destandau, N. Ramos, E. Bardez, P. Baret, J-L. Pierre, New. J. Chem., 25, (2001), 1269.

[24] a) M. Kimura, M. Tsunenaga, S. Takami, Y. Ohbayashi, Bull. Chem .Soc. Japan, 2005, 78, 929; b) F. de Rosa, X. Bu, K. Pohaku, P. C. Ford., Inorg. Chem., 44, (2005), 4166; c) F. de Rosa, X. Bu, P. C. Ford., Inorg. Chem., 44, (2005), 4157.

[25] R. G. Pearson, J. Am. Chem. Soc., 85, (1963), 3533.

Chapter 3

Exploring the Emissive Properties of New Azacrown Compounds Bearing Aryl, Furyl, or Thienyl Moieties: A Special Case of Chelation Enhancement of Fluorescence upon Interaction with Ca^{2+}, Cu^{2+}, or Ni^{2+}.

Elisabete Oliveira, Rosa M. F. Baptista, Susana P. G. Costa, M. Manuela M. Raposo, Carlos Lodeiro, *Inorganic Chemistry*, **2010**, *49*, 10847-10857.

"Creativity is awakened in the child's sense of wonder"

Georg Klein, b.1925

Index

3.1 - Abstract

Three new compounds bearing furyl, aryl, or thienyl moieties linked to an imidazo-crown ether system (**1**, **2**, and **3**) were synthesized and fully characterized by elemental analysis, infrared, UV-vis absorption, and emission spectroscopy, X-ray crystal diffraction, and MALDI-TOF-MS spectrometry. The interaction toward metal ions (Ca^{2+}, Cu^{2+}, Ni^{2+}, and Hg^{2+}) and F- has been explored in solution by absorption and fluorescence spectroscopy. Mononuclear and binuclear metal complexes using Cu^{2+} or Hg^{2+} as metal centers have been synthesized and characterized. Compounds **2** and **3** show a noticeable enhancement of the fluorescence intensity in the presence of Ca^{2+} and Cu^{2+} ions. Moreover compound **3** presents a dual sensory detection way by modification of the fluorimetric and colorimetric properties in the presence of Cu^{2+} or Hg^{2+}. EPR studies in frozen solution and in microcrystalline state of the dinuclear Cu(II)**3** complex revealed the presence of an unique Cu^{2+} type.

My contribution for this work was the synthesis of the metallic complexes, the obtaining of single crystal suitable for diffraction and all photophysical and fluorescence studies.

3.2 - Resumo

Três novos compostos, contendo unidades de furano, arilo e tiofeno, ligadas a um sistema éter coroa-imidazo (1, 2 e 3) foram sintetizados e totalmente caracterizados por análise elementar, infravermelhos, espectroscopia de absorção e de emissão de fluorescência, difracção cristal de raios X, e espectroscopia de MALDI-TOF-MS. A interacção com os iões metálicos (Ca^{2+}, Cu^{2+}, Ni^{2+} e Hg^{2+}) e F^{-}, foi explorada em solução por espectroscopia de absorção e de emissão de fluorescência. Foram sintetizados e caracterizados complexos metálicos mononucleares e binucleares contendo como centros metálicos Cu^{2+} e Hg^{2+}. Os compostos **2** e **3** apresentam na presença dos iões metálicos Ca^{2+} e Cu^{2+} um notável aumento da intensidade de emissão de fluorescência. Além disso, o composto **3** apresenta uma forma de detecção dupla sensorial, ou seja, pela alteração das propriedades fluorimétricas e colorimétricas na presença de Cu^{2+} ou Hg^{2+}. Os estudos de EPR, em solução congelada e em estados microcristalino do complexo dinuclear Cu(II)**2** revelaram a presença de um único tipo de Cu^{2+}.

A minha contribuição para este trabalho consistiu na síntese dos complexos metálicos, obtenção de mono cristais para difracção e a realização de todos os estudos fotofísicos e de fluorescência.

3.3 - Introduction

Classically a fluorescent chemosensor is a molecular device formed by an ionophore, a fluorophore, and a chemical spacer in between.[1] On the basis of this basic architectural premise, the field of fluorescence chemosensors has grown during recent years due to their importance in applications, such as in material sciences, biomedical, analytical chemistry, and environmental sciences.[2] Pioneering studies by H.G. Löhr and F. Vögtle on the properties of chromo and fluoroinophoric dyes,[3] and the studies by Okamoto on the chemiluminescent behaviors of several crown-ether-modified Iophine peroxide ionophore,[4] increased notably the knowledge on crown-ether derivatives as metal ion chemosensors. Incorporation of the imidazole group in abiotic systems has been extensively explored since the initial work of Debus in 1858[5] because of their interesting chemical and biochemical properties. These compounds have important pharmacological properties and play an important role in many biochemical processes, such as inhibitors of P38MAP kinase, fungicides or herbicides, and therapeutic agents.[6] Besides their classical applications in medicinal chemistry,[6] 2,4,5-triaryl(heteroaryl)-imidazoles play also important roles in materials science because of their optoelectronic properties.[7] Recently, triaryl(heteroaryl)-imidazole-based chromophores have received increasing attention because of their distinctive linear and nonlinear optical properties and also because of their excellent thermal stability in guest-host systems. Therefore, they have found application as nonlinear optical materials,[7a-j] fluorescent chemosensors,[7k-m] two-photon absorbing molecules,[7n] and thermally stable luminescent materials for several applications such as OLEDs.[7] Earlier studies on triaryl(heteroaryl)-imidazoles showed that the fluorescence properties of these derivatives could be tuned by substitution of the aryl group at the position 2 by a 5-membered heterocyclic ring such as thiophene or thiazole.[7n,o,q-r] It is expected that the use of five-membered heteroaromatics such as thiophenes and thiazoles in the conjugation pathway should minimize the distortion of conjugation between the imidazole ring and the aromatic ring at the position 2, thus enhancing conjugation and the charge transport properties along the oligomer backbone. [7o,q,r] Therefore, a comparative study of the fluorescence properties for several 2,4,5-triaryl(heteroaryl)-imidazoles showed that the substitution of the 2-phenyl ring in 2,4,5- triphenyl-imidazole by a thiophene or a thiazole improved the fluorescence quantum yields, from 0.48 to 0.86 in the case of thiophene or to 0.57 in the case of the thiazole, due to a more planar conformation of the heterocyclic imidazoles.[7r] In addition the study of the effect of N-alkylation of the imidazole ring on the fluorescent properties of 2,4,5-triaryl (hetero)aryl-imidazoles showed a significant fluorescence reduction for the 1-substituted derivatives. However, the fluorescence decrease is noticeably much

smaller for imidazoles having thiophene or thiazoles in position 2 because of the higher planarity of these conjugated systems.[7r]

Among other analytical techniques, fluorescence spectroscopy has been extensively applied for the study of the interaction of natural or artificial chemosensors with metal ions, mainly due to higher sensibility and sensitivity achieved and for being a nondestructive technique.[8,9] The general interest on the detection of bioinorganic metal ions, such as Ca^{2+}, Cu^{2+}, and even Ni^{2+} is the result of the difference in the electronic properties of these metals, which leads to different recognition mechanisms that can be followed by fluorimetry.[10] For example, Ca^{2+}, as an alkaline earth metal ion, is normally recognized by the enhancement in the fluorescence intensity (CHEF effect),[11] while paramagnetic transition metal ions or heavy metals, such as Cu^{2+}, Ni^{2+}, and Hg^{2+}, with unfilled d shells orbitals are usually recognized by a chelation enhancement of the quenching (CHEQ effect), *via* an electron- or an energy-transfer mechanism. Among these, Hg^{2+} as a diamagnetic d^{10} metal is an exception, for which the quenching could also be caused by the spin-orbit coupling, being the main route for the nonradiative deactivation k_{nr} process.[12] However, few examples are reported in the literature for the recognition of Cu^{2+}, Ni^{2+}, or Hg^{2+} by fluorescence enhancement,[13] and so, the development of new sensors for Cu^{2+}, Ni^{2+}, and Hg^{2+} by CHEF recognition is a key topic in chemosensor research. Following our current interests on colorimetric and fluorimetric chemosensors for metal ion detection provided with heterocyclic moieties bearing N, O, and S donor atoms,[14] and having in mind earlier studies concerning the optical properties of 2,4,5-tri(hetero)aryl-imizadole derivatives, we decided to synthesize and characterize three new imidazo-crown ether derivatives bearing a furyl (**1**), aryl (**2**), or thienyl (**3**) ring linked via the imidazo unit to the azacrown ether system, in order to tune their photophysical properties and evaluate their chemosensor ability. The interaction with Ca^{2+}, Cu^{2+}, Ni^{2+}, and Hg^{2+} in solution and in solid state was explored using absorption and fluorescence spectroscopy, electron paramagnetic resonance (EPR), and MALDI-TOF-MS spectrometry. To explore the acid-base behavior of these systems, interaction with H^+ and a basic anion, F-, were also studied. The X-ray crystallographic structure of compound **2** is also reported.

3.4 - Experimental Section

3.4.1 - Materials and Apparatus

Reaction progress was monitored by thin layer chromatography (0.25 mm thick precoated silica plates: Merck Fertigplatten Kieselgel 60 F254), while purification was performed by silica gel column chromatography (Merck Kieselgel 60; 230-400 mesh). NMR spectra of the ligands were obtained on a Varian Unity Plus Spectrometer at an

operating frequency of 300 MHz for ^{1}HNMR and 75.4 MHz for ^{13}C NMR or a Bruker Avance III 400 at an operating frequency of 400 MHz for ^{1}H NMR and 100.6 MHz for ^{13}C NMR using the solvent peak as internal reference. The solvents are indicated in parentheses before the chemical shift values (δ relative to tetramethylsilane and given in ppm). Melting points were determined on a Gallenkamp apparatus and are uncorrected. Infrared spectra were recorded on a BOMEM MB 104 or a JASCO IR spectrophotometer. Mass spectrometry analyses of the ligands were performed at the "C.A.C.T.I.; Unidad de Espectrometria de Masas" at the University of Vigo, Spain. Elemental analyses were carried out by the REQUIMTE DQ, Universidade Nova de Lisboa Service on a Thermo Finnigan- CE Flash-EA 1112-CHNS Instrument. Proton ^{1}H NMR of the complexes were recorded on a Bruker Avance III 400 at an operating frequency of 400 MHz .The MALDI analysis has been performed in a MALDI-TOF-MS model Voyager-DE 4700 Proteomics Analyzer, by positive reflector mode, at the REQUIMTE, Chemistry Department, Universidade Nova de Lisboa.

3.4.2 - Spectrofotometric and spectrofluorimetric measurements

Absorption spectra were recorded on a Perkin-Elmer lambda 45 spectrophotometer and fluorescence on a Perkin-Elmer L55. The linearity of the fluorescence *vs* concentration was checked in the concentration used (10^{-4}-10^{-6} M). A correction for the absorbed light was performed when necessary. Stock solutions of the compounds (~10^{-3} M) were prepared in absolute ethanol and acetonitrile for **1**, and in absolute ethanol, acetonitrile, and dichloromethane for **2** and **3**. Titrations of ligands **1**, **2**, and **3** (10^{-5}-10^{-6} M, prepared by dilution of the stock solutions) were carried out by the addition of microliter amounts of standard solutions of the ions in absolute ethanol or acetonitrile. All the measurements were performed at 298 K. The competition experiments were carried out on a JASCO 650 UV-vis spectrometer and on a Horiba-Jovin Ibon Fluoromax 4 spectrofluorimeter.

Luminescence quantum yields were measured using a solution of quinine sulfate in sulphuric acid (0.5M) as a standard[15] [φ]=0.54 and were corrected for different refraction indexes of solvents,[15b] for compounds **2** and **3**. For compound **1**, the relative quantum yield was measurement using an ethanol solution of anthracene as standard [φ] = 0.27.[15]

3.4.3 - EPR Measurements.

EPR measurements were performed in the REQUIMTE, Universidade NOVA de Lisboa at 70 K in both finely powdered and ethanol dissolved samples at 9.65 GHz with a Bruker EMX spectrometer using a rectangular cavity equipped with an Oxford

continuous helium flow cryostat. Modulation field: 5 Gpp, modulation frequency: 100 KHz, attenuation: 30 dB (200 microW).

3.4.4 - X-ray Crystal Structure Determinations

Single crystals of ligand **2** was analyzed by X-ray diffraction and a summary of the crystallographic data and the structure refinement parameters is reported in Table 3.1. Crystallographic data were collected on a Bruker Smart 1000 CCD diffractometer at CACTI (Universidade de Vigo) at 20 ºC using graphite monochromated MoKR radiation (λ=0.71073A °) and were corrected for Lorentz and polarization effects. The software SMART[16] was used for collecting frames of data, indexing reflections, and the determination of lattice parameters, SAINT[17] for integration of intensity of reflections and scaling, and SADABS[18] for empirical absorption correction. The structures were solved by direct methods using the program SHELXS97.[19]

All non-hydrogen atoms were refined with anisotropic thermal parameters by full-matrix least-squares calculations on F2 using the program SHELXL97.[20] Hydrogen atoms were inserted at calculated positions and constrained with isotropic thermal parameters. The contribution of the disordered solvent to the diffraction pattern that could not be rigorously included in the crystallographic calculations, were subtracted by the SQUEEZE procedure implemented in the PLATON software.[21] Drawings were produced with PLATON[6] software (ellipsoids and ball and stick). Crystallographic data have been deposited with the Cambridge Crystallographic Data Centre, CCDC 730341 for **2**. Copies of this information may be obtained free of charge from The Director, CCDC, 12 Union Road, Cambridge, CB2 1EZ, UK (fax: þ44-1233-336033; e-mail: deposit@ccdc.cam.ac.uk or http://www.ccdc.ac.uk).

Table 3.1. Crystal data and structure refinement of ligand **2**

	(2)
Empirical formula	$C_{31}H_{35}N_3O_4$
Formula weight	513.62
Temperature	293(2) K
Wavelength	0.71073 Å
Crystal system	Tetragonal
Space group	P4/ncc
Unit cell dimensions	a = 28.201(11) Å α= 90° b = 28.201(11) Å β= 90° c = 15.453(12) Å γ = 90°
Volume	12290.5(12) $Å^3$
Z	16
Density (calculated)	1.110 g/cm^3
Absorption coefficient	0.074 mm^{-1}
F(000)	4384
Crystal size	0.50 x 0.46 x 0.30 mm^3
Theta range for data collection	2.04 to 24.99º
Index ranges	$-33 \le h \le 32$, $-25 \le k \le 33$, $-18 \le l \le 18$
Reflections collected	40683
Independent reflections	5300 [R(int) = 0.0684]
Completeness to theta =	97.7% (24.99º)
Absorption correction	Empirical (Sadabs)
Refinement method	Full-matrix least-squares on F^2
Data / restraints / parameters	5300 / 0 / 343
Goodness-of-fit on F^2	1.069
Final R indices [I>2sigma(I)]	R1 = 0.0704, wR2 = 0.2291
R indices (all data)	R1 = 0.1441, wR2 = 0.2516
Largest diff. peak and hole	0.341 / -0.206 $eÅ^{-3}$

3.4.5 - Chemicals and starting materials

$Na(BF_4)$, $Ca(CF_3COO)_2$, $Cu(BF_4)_2$, $Ni(BF_4)_2$, $Hg(CF_3COO)_2$ metal salts, $F(NBu_4)$ and CH_3SO_3H have been purchased from Stream Chemicals, Sigma Aldrich or Solchemar. All solvents used were spectroscopic grade from Chromasolv or PANREAC without any further purification.

3.4.6 - Synthesis of ligands

3.5.6.1 - Synthesis of 4-(1,4,10,13-Tetraoxa-7-azacyclopentadecan-7-yl)benzaldehyde IV

$POCl_3$ (1.20 mmol) was added to DMF (1.20 mmol) at 0 ºC, and the mixture was stirred for 15 min at 0 ºC. 13-Phenyl-1,4,7,10-tetraoxa-13-azacyclopentadecane (1.03 mmol) dissolved in DMF (1 mL) was added dropwise with stirring. The reaction mixture was heated for 2 h at 60 ºC. The solution was then poured slowly into 5 mL saturated sodium acetate aqueous solution and stirred during 30 min. The organic layer was diluted with ether, washed with saturated $NaHCO_3$ aqueous solution, and dried with anhydrous $MgSO_4$. The organic extract was filtered and evaporated under reduced pressure giving the 4-(1,4,10,13-tetraoxa-7-azacyclopentadecan-7-yl)benzaldehyde **IV**[22] as an yellow solid in 90% yield.

^{1}HNMR (300 MHz, CDCl3): δ 3.61 (m, 16H, 8 × CH_2), 3.70 (m, 4H, 2×CH_2), 6.66 (d, 2H, J=9 Hz, 2 and 6-H), 7.66 (d, 2H, J = 9 Hz, 3 and 5-H), 9.67 (s, 1H, CHO).

2.4.5.2 - General Procedure for the Synthesis of 2,4,5-Tri(hetero)arylimidazo Crown Ether Ligands (**1**-**3**).

A mixture of the formyl azacrown ether **IV** (0.35 mmol), NH4OAc (10 equiv) and 1, 2-diones **I**-**III** (0.35 mmol) in glacial acetic acid (20 mL) (Method A) or in ethanol (20 mL) (Method B) was stirred and heated at reflux for 12 h. The mixture was then cooled to room temperature and the product precipitated during neutralization with NH_4OH 5 M. The crude product was purified through column chromatography on silica using chloroform/methanol (9:1) as eluent.

7-(4-(4,5-Di(furan-2-yl)-1H-imidazol-2-yl)phenyl)-1,4,10,13- tetraoxa-7 azacyclopenta-decane **1**.

Compound **1** was obtained as a brown solid (Method B, 58%). MP: (94.2-95.8) ºC. UV-vis (EtOH): λ_{exc}=328 nm, log $\varepsilon_{328\ nm}$=4.69. Emission (EtOH): λ_{em}=400nm, φ=0.87. IR (cm^{-1}; liquidfilm): v 3125, 3006, 2870, 1614, 1495, 1392, 1355, 1295, 1205, 1123, 1008, 885, 820, 753. ^{1}H NMR (300 MHz, acetone-d_6): δ 3.57 (m, 16H, 8 × CH_2), 3.73 (m, 4H, 2 × CH_2), 6.55 (m, 2H, 2 × 4'-H), 6.74 (d, 2H, J=7.2Hz, 2 and 6-H), 6.73 (dd, 2H, J=4 and 0.8 Hz, 2 × 3'-H), 7.60 (dd, 2H, J=2 and 0.8Hz, 2 × 5'-H), 7.98 (d, 2H, J=7.2, 3 and 5-H). ^{13}C NMR (75.4 MHz, acetone-d_6): δ 53.11 (CH_2), 69.17 (CH_2), 70.55 (CH_2), 70.79 (CH_2), 71.76 (CH_2), 107.86 (2 × $C_{3'}$), 112.06 (C_2 and C_6), 112.22 (2 × $C_{4'}$), 118.06 (C_4), 127.87 (C_3 and C_5), 148.35 (C_2), 148.70 (C_{3a} and C_{3b}), 149.23 (C_2). MS (FAB) m/z (%):

494 ([M + H]$^+$, 100), 234 (8). HRMS: m/z (FAB) for $C_{27}H_{31}N_3O_6$ calcd 494.22785; found 494.22856.

7-(4-(4,5-Diphenyl-1H-imidazol-2-yl)phenyl)-1,4,10,13-tetraoxa-7-azacyclopentadecane **2**.

Compound **2** was obtained as a yellow solid (45% method A; 64% method B). MP(178.4-179.2) ºC. UV-vis (EtOH): λ_{exc} = 320 nm, log $\varepsilon_{320\ nm}$= 4.64. Emission (EtOH): λ_{em} = 420 nm, φ = 0.35. IR (cm^{-1}; liquid film): v 3224, 3008, 2870, 1734, 1614, 1508, 1495, 1390, 1355, 1216, 1123, 821, 756, 697. IR (cm^{-1}; KBr pellet): v 3189, 1614, 1510-1495, 1122. ^{1}H NMR (300 MHz, acetone-d_6): δ 3.59 (m, 16H, 8 × CH_2), 3.75 (m, 4H, 2× CH_2), 6.77 (d, 2H, J=9Hz, 2 and 6-H), 7.26 (m, 2H,2× 40-H), 7.33 (m, 4H, 2 × (3' and 5'-H), 7.58 (m, 4H, 2 × (20 and 60-H), 7.94 (d, 2H, J = 9 Hz, 3 and 5-H). ^{13}C NMR (75.4 MHz, acetone-d_6): δ 53.16 (CH_2), 69.27 (CH_2), 70.62 (CH_2), 70.84 (CH_2), 71.84 (CH_2), 112.13 (C_2 and C_6), 119.14 (C_4), 127.41 (2 × (C_3 and C_5), 127.56 (2× $C_{4'}$), 128.62 (2× $C_{2'}$ and $C_{6'}$), 129.04 (2× ($C_{3'}$ and $C_{5'}$)), 147.79 (C_2), 148.91 (C_1). MS (FAB)m/z (%): 514 ([M+ H]$^+$, 100), 222 (8).HRMS m/z (FAB) for $C_{31}H_{35}N_3O_4$ calcd 514.26955; found 514.27003.

7-(4-(4,5-Di(thien-2-yl)-1H-imidazol-2-yl)phenyl)-1,4,10,13-tetraoxa-7 azacyclopentadecane **3**.

The compound was isolated as a yellow solid (20 % method A, 47% method B). MP (213.1-214.6) ºC. UV (EtOH): λ_{exc} = 320 nm, log ε_{320nm}= 4.55, λ_{em} = 440 nm, ϕ = 0.07. IR (cm^{-1}; liquid film): *v* 3101, 1615, 1508, 1392, 1353, 1297, 1251, 1212, 1121, 988, 934, 819, 689. IR (cm^{-1}; KBr pellet): *v* 3110, 1616, 15110-1495, 1122. ^{1}H NMR (300 MHz, $CDCl_3$): δ 3.56 (m, 16H, 8×C*H*$_2$), 3.76 (m, 4H, 2× C*H*$_2$), 6.78 (d, 2H, *J*=9.0 Hz, 2 and 6-*H*), 7.07 (m, 2*H*, 2×4'-H), 7.30 (dd, 2H, *J*=4 and 1.2 Hz, 2×3'-*H*), 7.43 (br d, 2H, *J*=4.8 Hz, 2×5'-*H*), 7.91 (d, 2H, *J*=9.0 Hz, 3 and 5-*H*). ^{13}C NMR (75.4 MHz, acetone-d_6): δ 53.20 (*C*H_2) 69.27 (*C*H_2), 70.65 (*C*H_2), 70.89 (*C*H_2), 71.87 (*C*H_2), 79.17 (*C*H_2) 112.18 (*C*$_2$+*C*$_6$), 118.37 (*C*$_4$), 126.09 (2×C$_{3'}$and 2×*C*$_{5'}$), 127.57 (*C*$_3$ and *C*$_5$), 127.96 (2×*C*$_{4'}$), 147.97 (*C*$_2$), 149.23 (*C*$_1$). MS (FAB) *m/z* (%): 526 ([M+H]$^+$, 100), 216 (7). HRMS *m/z* (FAB) for $C_{27}H_{31}N_3O_4S_2$; calcd 526.18255; found 526.18288.

3.4.7 - Synthesis of solid complexes. General method

The corresponding metal salt ($Cu(BF_4)_2$ or $Hg(CF_3COO)_2$) (0.2 mmol) was dissolved in abs. ethanol (5 mL) and added to a stirred solution of the respective ligand **2** (0.2 mmol) or **3** (0.1 mmol) in abs. ethanol. The resulting solution was stirred at reflux overnight. The color of the solution changes from colorless to deep red after the addition of the metal ion. The solvent was removed under reduced pressure and the solid was precipitated with the addition of diethyl ether. The solid was separated by centrifugation, washed several times with cold abs. ethanol and diethyl ether and dried under vacuum.

[Cu2]$(BF_4)_2$.$2H_2O$ (4). Colour: Red. Yield: 70%. $C_{37}H_{51}B_2CuF_8N_3O_6$, FW = 870.9. Elemental analysis: (Found: C, 47.1; H, 5.3; N, 5.0 % CHNS requires for $C_{37}H_{51}B_2CuF_8N_3O_6$: C, 47.5; H, 5.5; N, 4.5). IR (cm^{-1}; KBr pellet): *v* 3175, 1606, 1513-1495, 1124, 1183. UV-vis in ethanol (λ nm): Band at 336 nm, log ε ≈ 4.59. Emission spectra in ethanol (λ_{exc} = 336nm, λ_{em} = 410 nm), $\phi_{ethanol}$ = 0.65.
MALDI-TOF-MS calc. (found) = [**2**Cu]$^+$ 576.7 (576.2), [(**2**)$_2$Cu]$^+$ 1089.0 (1089.5).

[$Cu_2$3]$(BF_4)_4$].$4H_2O$ (5). Colour: Dark Red. Yield: 79%. $C_{25}H_{35}B_4Cu_2F_{16}N_3O_8S_2$, FW = 1044. Elemental analysis: (Found: C, 30.2; H, 4.2; N, 4.0; S, 5.0 % CHNS requires for $C_{25}H_{35}B_4Cu_2F_{16}N_3O_8S_2$: C, 30.2; H, 3.7; N, 3.9; S, 5.9). IR (cm^{-1}; KBr pellet): *v* 3087, 1604, 1500-1495, 1107, 1183. UV-vis in ethanol (λ nm): Band at 331 nm, log ε ≈ 4.43. Emission spectra in ethanol (λ_{exc} = 331nm, λ_{em} = 422 nm), $\phi_{ethanol}$ = 0.20.
MALDI-TOF-MS calc. (found) = [**3** Cu]$^+$ 588.6 (588.1), [(**3**)$_2$Cu]$^+$ 1113.8 (1113.4), [(**3**)$_2$$Cu_2$]$^+$ 1177.4 (1177.3).

[Hg3]$(CF_3COO)_2$].$5H_2O$ (6). Colour: Dark red. Yield: 77%. $C_{33}H_{35}F_{12}Hg_3N_3O_{14}S_2$, FW = 1391. Elemental analysis: (Found: C, 28.3; H, 2.6; N, 3.7; S, 5.5 % CHNS requires for $C_{33}H_{35}F_{12}Hg_3N_3O_{14}S_2$: C, 28.5; H, 2.5; N, 3.1; S, 4.7). IR (cm^{-1}; KBr pellet): *v* 3097, 1604, 1517-1495, 1107, 1183. UV-vis in DMSO (λ nm): Band at 342 nm, log ε ≈ 4.74. Emission spectra in DMSO (λ_{exc} = 342nm, λ_{em} = 434 nm), $\phi_{ethanol}$ = 0.01.

3.5 - Results and Discussion

3.5.1 - Synthesis and characterization of organic ligands

The aldehyde precursor **IV**[22] was synthesized in 90% yield through Vilsmeier formylation of 13-phenyl-1,4,7,10- tetraoxa-13-aza-cyclopentadecane. Heteroaromatic **I** and **III** and aromatic **II** diones with furyl, thienyl, and aryl groups were used as precursors of imidazo-crown ethers **1**-**3** to evaluate the effect of the electronic nature of the (hetero)aryl groups on the photophysical and sensory properties of these compounds. Therefore, compounds **1**-**3** with furyl, aryl, or thienyl moieties linked to the imidazo-crown ether system were synthesized through the condensation of commercially available diones **I**-**III** with the formyl crown ether derivative **IV** and ammonium acetate (see Scheme 3.1).[7i,j,q,23] After the reaction was performed using two different solvents (acetic acid: Method A; or ethanol: Method B) in refluxing conditions (12 h), ethanol gave the highest yields (47-64%) for the synthesis of compounds **1**-**3** compared to the classical Radziszewski conditions[7i,j,23] (20-45%). Application of Radziszewski conditions to the synthesis of furyl derivative **1** gave a very complex mixture with decomposition (TLC and 1H NMR) in which it was not possible to identify the target compound **1**. This compound was only synthesized through method B using mild reaction conditions (Scheme 3.1).

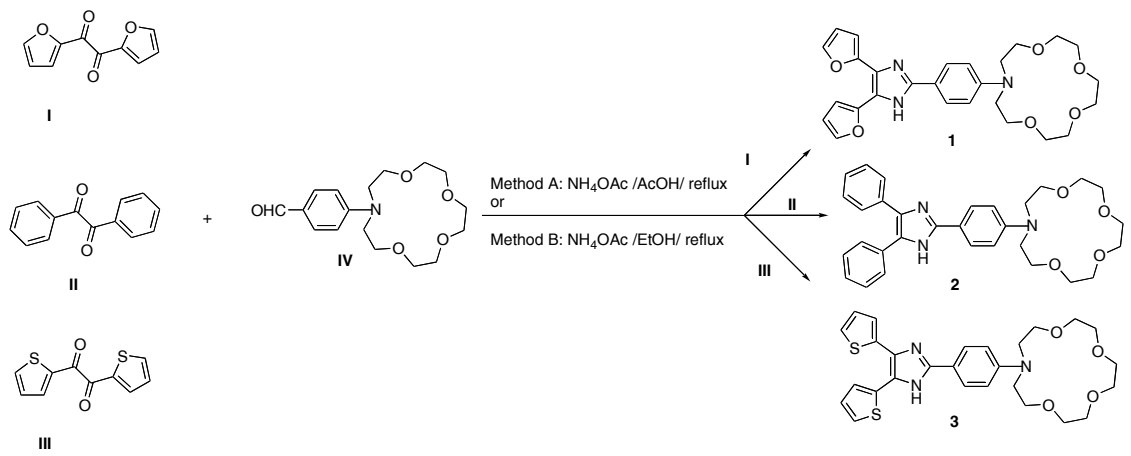

Scheme 3.1.- Synthesis of 2,4,5-Tri(hetero)aryl-imidazo-crown Ether Ligands **1**-**3**

Complexation reactions between ligands **2** and **3** with the metal salts $Cu(BF_4)_2$ and $Hg(CF_3COO)_2$ in refluxing ethanol and in a 1:2 L/M molar ratio for **3** and 1:1 for **2** were carried out to investigate the coordination capability of both ligands in the solid state. Analytically pure products were obtained and formulated as [Cu**2**]$(BF_4)_2 \cdot 2H_2O$ (**4**), [Cu_2**3**]$(BF_4)_4] \cdot 4H_2O$ (**5**), and [Hg**3**]$(CF_3COO)_2] \cdot 5H_2O$(**6**). All complexes were obtained in good yield of 70% for **4**, 79% for **5**, and 77% for **6**. The MALDI-TOF mass spectra of

the complexes feature peaks corresponding to the free ligand $[LH]^+$, and the fragments $[ML]^+$ (L = 2 or 3), $[M_2\mathbf{3}]^+$, and $[M_2\mathbf{3}_2]^+$. The IR spectra of the complexes were recorded using KBr discs, and all show similar features. After complexation to the metal ion, peaks attributable to the presence of absorption bands from vNH imidazole groups at ~3175 cm^{-1}, and the bands for vC=N groups shift to lower wavenumbers.[24] All spectra exhibit medium to strong bands at ~1600 and 1455 cm^{-1}, as expected for the two highest-energy benzene ring vibrations.[25] A broad absorption band in the region 3450-3385 cm^{-1} present in the majority of the complexes is probably due to the existence of lattice or coordinated water in the complexes. [24] A peak due to the BF_4 counterions appears at 1183 cm^{-1}.

3.5.2 - Photophysical Studies

The photophysical characterization of compound **1**, **2**, and **3** was performed in acetonitrile, absolute ethanol and dichloromethane. Table 3.2 summarizes the optical data for all ligands in these protic and aprotic solvents. The absorption and emission band were centered at 328, 320, 325 and 400, 420-440, 440-445 nm, respectively, for **1**, **2**, and **3**. The use of protic and aprotic solvent apparently does not affect the absorption spectra in all cases. However the steady-state luminescence spectra is quenched in aprotic solvents more strongly for compound **1** and **2**, being unaffected for compound **3**. As can be seen in Table 3.2, compounds **1**-**3** in the same solvent, absolute ethanol, exhibit quantum yields with values of 0.87 for **1**, 0.35 for **2**, and 0.09 for **3** being the thiophene derivative the less emissive system because of the strong quenching caused by the sulfur atom.[26] It is also noteworthy that the substitution of the furyl heterocycle at the 4 and 5 positions of the imidazo system on compound **1** by two aryl rings give rise to a dramatical reduction of the fluorescence probably due to lesser planarity of the aryl-imidazo conjugated system **2**.[7r] The same experiment in an aprotic solvent like acetonitrile, showed that all ligands are less emissive, being the fluorescence quantum yields of 0.65 for **1**, 0.07 for **2**, and 0.06 for **3**. The highest value obtained in protic solvents is probably due to protonation of the imidazole nitrogen atom preventing photoinduced electron transfer (PET) phenomena.[27]

Table 3.2. – Optical data of compounds **1** to **3** in protic and aprotic solvents.

Compounds	Solvents	UV-Vis			Fluorescence	
		λ_{exc} (nm)	Stokes's shift	Log ε ($M.cm^{-1}$)	λ_{em} (nm)	ϕ
1	CH_3CN	328	75	4.69	400	0.65
	EtOH	328	75	4.69	400	0.87
2	CH_3CN	320	120	4.64	440	0.07
	CH_2Cl_2	320	100	4.64	420	0.09
	EtOH	320	100	4.64	420	0.35
3	CH_3CN	325	130	4.55	455	0.06
	CH_2Cl_2	325	125	4.55	450	0.07
	EtOH	325	115	4.55	440	0.09

The absorption and emission spectra of compounds **1**, **2**, and **3** in acetonitrile solution are shown in Figure 3.1. The insertion of the furan, thiophene, and benzene units in the ligand structure poorly affect the absorption wavelength band. On the other hand, the emission bands showed a noticeable red shift from 400 (**1**) to 455 (**3**) nm, being the highest for the thiophene derivative.

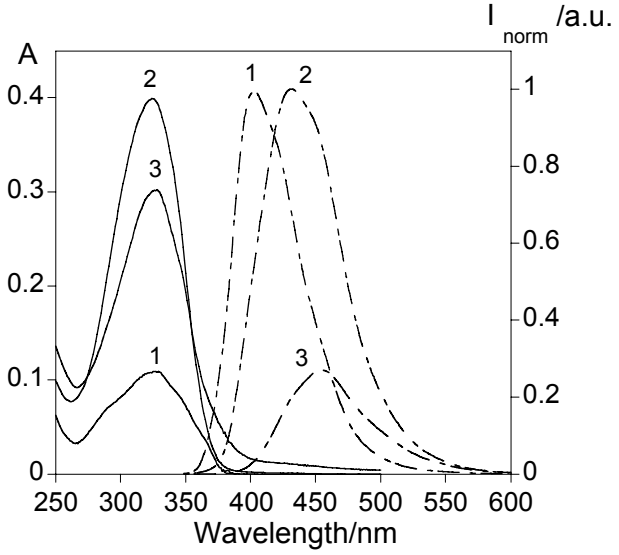

Figure 3.1. – Absorption (full line) and emission spectra (dotted line) of compounds **1** to **3** in acetronitrile solution. ([**1**] = 2.25×10^{-6} M, [**2**] = 9.05×10^{-6} M, [**3**] = 8.55×10^{-6} M, λ_{exc1} = 328 nm, λ_{exc2} = 320 nm, λ_{exc3} = 325 nm, T=298K).

To explore the sensory ability of systems **1**-**3** in solution toward H^+, F^-, Na^+, Ca^{2+}, Cu^{2+}, Ni^{2+}, and Hg^{2+}, several UV-vis and fluorescence titrations were performed. The acid-base behavior of compounds **1**-**3** was studied with the increasing addition of protons

using methanesulfonic acid, CH_3SO_3H, and fluoride ion as basic anion. The results obtained showed that protonation and deprotonation of the nitrogen present in the azacrown- ether and also at the imidazole nitrogen atom could modulate the fluorescence emission. As an example, in Figure 3.2 shows the absorption and fluorescence titration of compound **1** with the addition of increasing amount of acid. The fluorescence band was slightly red-shifted and quenched.[28] Protonation induced a similar behavior when the parent azacrown **IV** was used, suggesting that the observed quenching in the fluorescence emission is probably because of the formation of a hydrogen-bond interaction between the protonated nitrogen located in the azacrown and the oxygen atoms, as reported previously for a macrocyclic ligand based on a pseudocrown structure.[29]

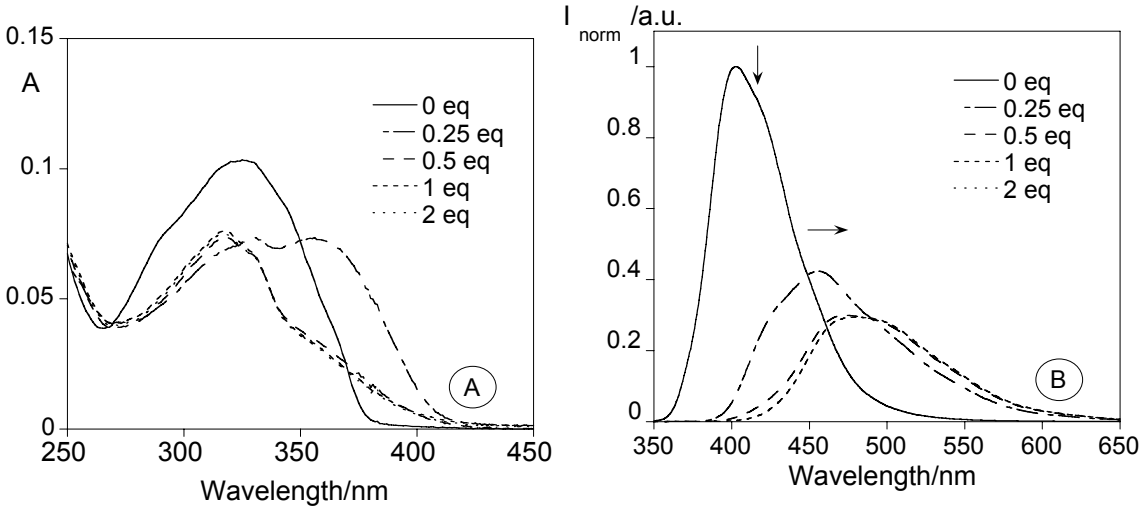

Figure 3.2.- Absorption (A) and emission (B) spectra of compound **1**, with the addition of 0, 0.25, 0.5, 1 and 2 equivalents of methanesulfonic acid (CH_3SO_3H) in CH_3CN. (T=298 K, [**1**] = 2.23×10^{-6} M, [CH_3SO_3H] = 1.00×10^{-2} M, λ_{exc} = 328 nm.

With the addition of the fluoride anion, a small red shift in the absorption spectra for all ligands was observed; at the same time the emission spectra was quenched and red shifted.

Figure 3.3 shows the fluorescence titrations of **1**-**3** with the addition of F^-. Taking into account the results observed previously for the protonation of the azacrown nitrogen, deprotonation of this nitrogen should induce a recovery of the fluorescence emission. However, the quenching observed with the addition of a base can be attributed to the deprotonation of the imidazole nitrogen, inducing a PET process from the lone pair of electrons located in this nitrogen atom to the excited chromophore. [30] This quenching is similar for imidazo-azacrown derivatives **1**-**3**. The interaction constants of ligands **2** and **3** with the various ions were calculated and are summarized in Table 3.3.

Table 3.3.- Stability Constants with Compounds **1**-**3** by Hypspec Program[a].
[a] (1:1) =LM. (1:2) = LM^2

Compounds	**1**	**2**	**3**
F^-	-	2.021±0.004 (1:1)	3.055±0.002 (1:1)
Ca^{2+}	4.236±0.004 (1:1)	4.745±0.002 (1:1)	4.155±0.001 (1:1)
Cu^{2+}	11.120±0.003 (1:2)	5.320±0.001 (1:1)	11.580±0.002 (1:2)
Ni^{2+}	-	4.288±0.003 (1:1)	3.906±0.001 (1:1) 6.364±0.004 (1:2)
Hg^{2+}	10.038±0.034 (1:2)	-	8.421±0.3 (1:1) 11.843 ±0.3 (1:2)

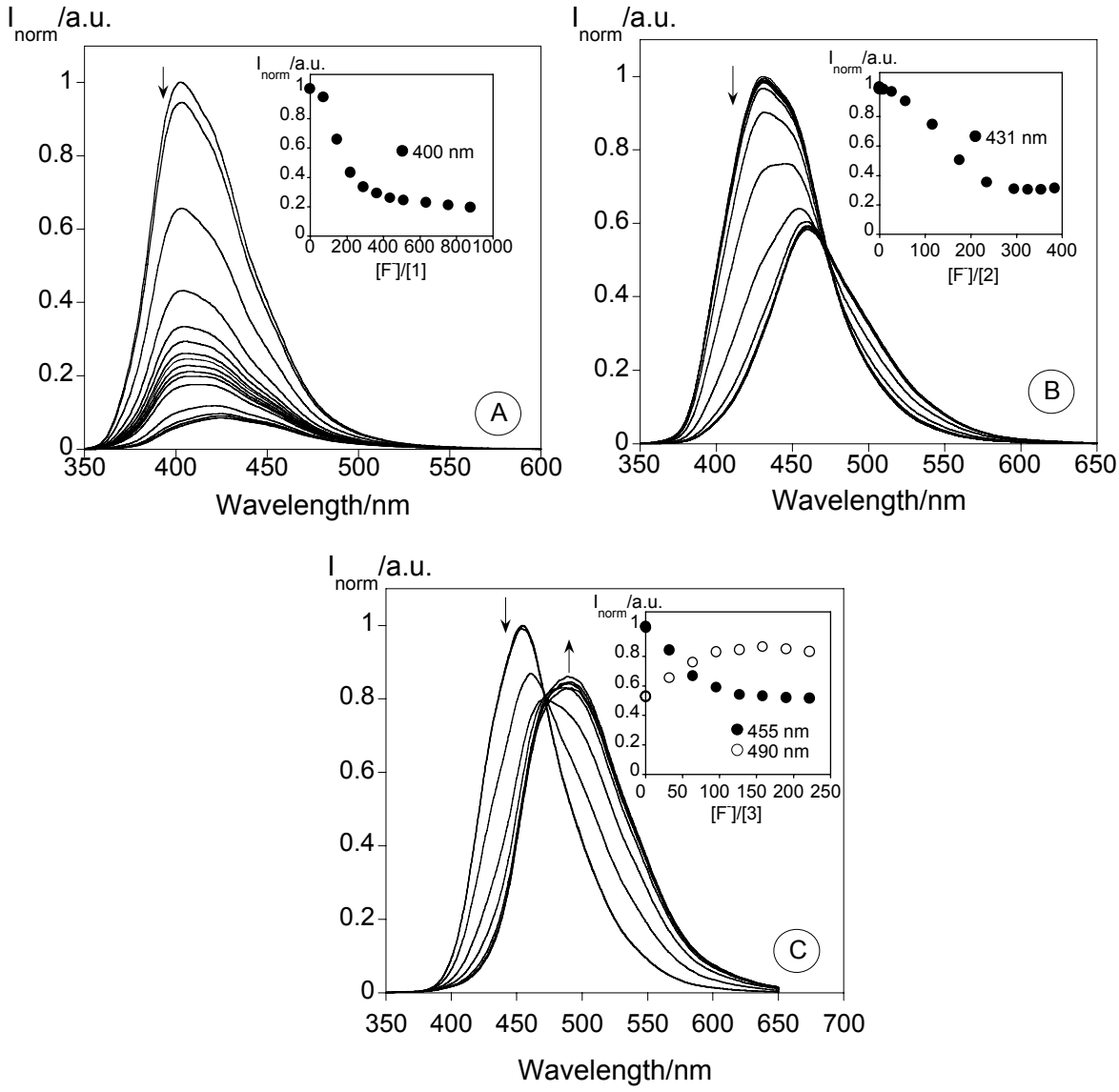

Figure 3.3.- Spectrofluorimetric titrations of compounds **1** (A), **2** (B) and **3** (C), in the presence of F^-, in acetonitrile. The inset represents the emission for **1** (A) at 400 nm, for **2** (B) at 431 nm and for **3** (C) at 455 nm and 490 nm.

15-Crown-5 systems are usually used for the interaction with Na^+,[31] whereas 15 crown-5 monoazacrown ethers show better results for Ca^{2+}.[32] In this case, compounds **1**-**3** did not show any changes in the ground state (absorption) and in the excited stated (emission) after addition of Na^+. However, in the presence of Ca^{2+} ligands **2** and **3** in acetonitrile or absolute ethanol, respectively, showed a blue shift in the absorption spectra and an enhancement of the fluorescence emission (see Figure 3.4).

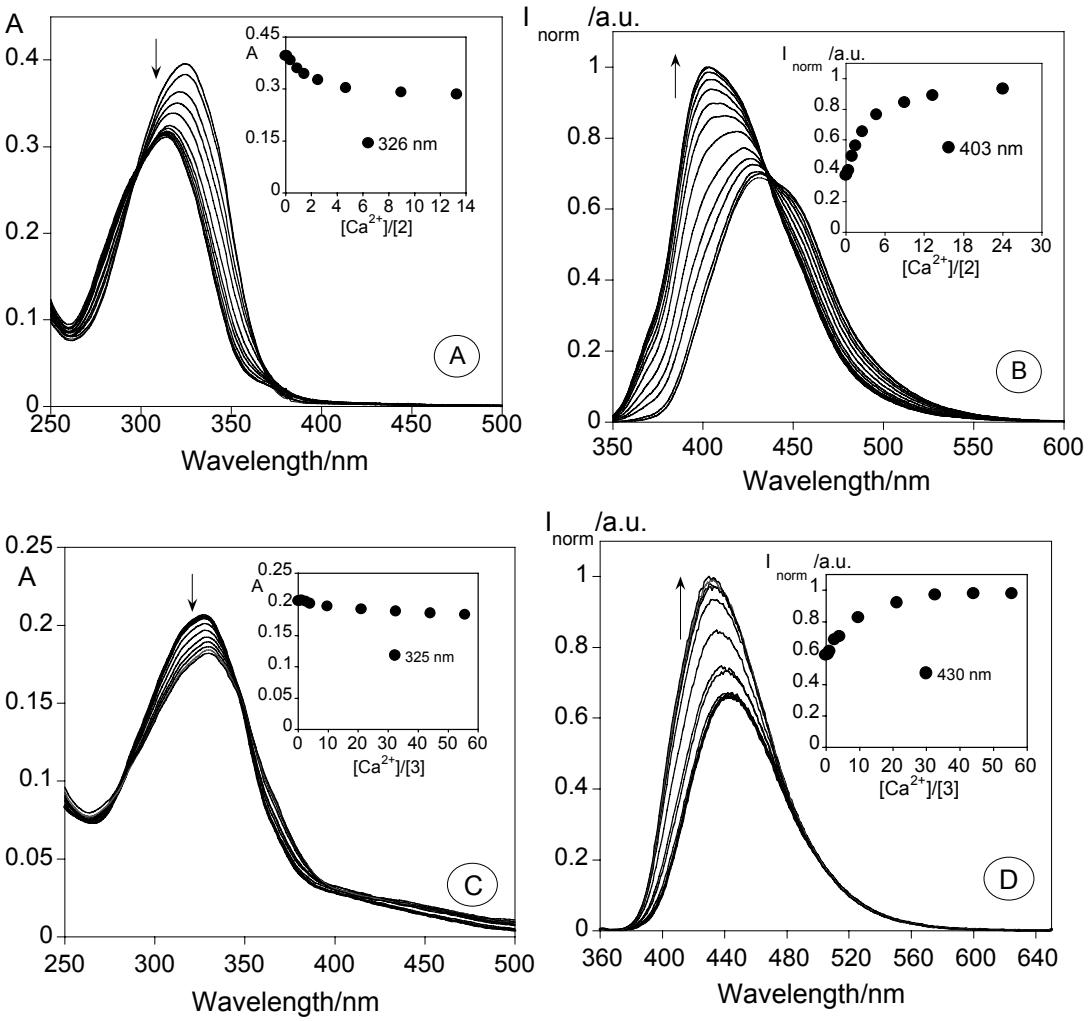

Figure 3.4. – Absorption (A and C) and emission titrations (B and D) of compounds **2** and **3** with the addition of increased amount of Ca^{2+} in acetronitrile (**2**) and absolute ethanol (**3**) solution. The inset represents the absorption at 326 nm (A) and 325 nm (C), and the emission at 403 nm (B), and 430 nm (D) as a function of [Ca^{2+}]/[**2**] or [Ca^{2+}]/[**3**]. ([2] = 9.06×10^{-6} M, [3] = 6.34×10^{-6} M, [$Ca(CF_3COO)_2$] = 1.46×10^{-2} M, λ_{exc2} = 320 nm nm, λ_{exc3} = 325 nm, T=298K).

The complexation constants with Ca^{2+} were calculated using the program HYPSPEC[33] and are summarized in Table 3.3. In all cases, the constants suggest the formation of a mononuclear complex with a value between log β 4.75(0.01 for **2** and log β 4.16(0.01 for **3**.

Following our exploration of the different coordination sites present in ligands **1**-**3**, the second site to be explored will be the nitrogen atom located at the imidazole ring. This imidazole nitrogen atom can form a chelate unit with the potential coordinative oxygen or sulfur atoms present in the furan **1** or thiophene **3** heterocycles. To explore the interaction of transition (Cu^{2+} and Ni^{2+}) and post-transition (Hg^{2+}) metal ions with this coordination site, several metal titrations were performed. With the addition of Ni^{2+}, only ligands **2** and **3** showed a red shift on the absorption spectra and an enhancement on the fluorescence emission intensity (Figure 3.5). The complexation constants fit to a mononuclear species for ligand **2** with a value of log β 4.29 (0.02, and to mononuclear and dinuclear species for compound **3** with values of log β 3.91(0.01 and 6.36(0.01, respectively. It is important to note that for compound **3** after formation of the dinuclear species, a colored band centered at ~550 nm was developed. This band could be attributable to a tetracoordinated Ni^{2+} complexes.[34]

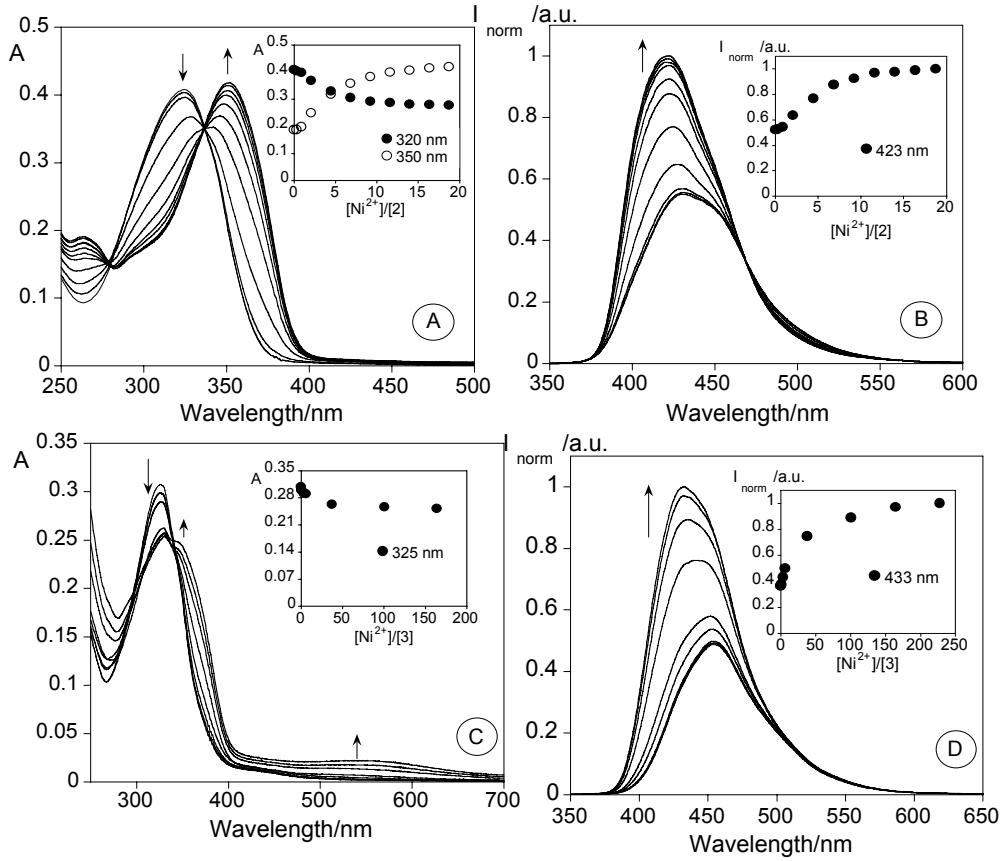

Figure 3.5 – Absorption (A and C) and emission titrations (B and D) of compounds **2** and **3** with the addition of increased amount of Ni^{2+} in acetronitrile. The inset represents the absorption at 320 nm, 350 nm (A) and 325 nm (C), and the emission at 423 nm (B),

and 433 nm (D) as a function of $[Ni^{2+}]/[\mathbf{2}]$ or $[Ni^{2+}]/[\mathbf{3}]$. ([**2**] = 9.06×10^{-6} M, [**3**] =8.55×10^{-6} M, $[Ni(BF_4)_2]$ = 1.62×10^{-2} M, λ_{exc2} = 320 nm nm, λ_{exc3} = 325 nm, T=298K).

Taking into account the presence of two thiophene rings in ligand **3**, addition of a soft-metal ion[35] could be used to explore the involvement of the sulphur atoms in the complex stabilization. Figure 3.6 represents the absorption and emission titrations of compound **3** with addition of Hg^{2+}. The absorption spectra showed a remarkable red shift and the formation of band centered at ~510 nm, with the color of the final solution turning pale pink. At the same time the fluorescence increased with the addition of one metal ion equivalent, followed by an intense decrease with further metal addition. This final quenching could be attributed to a partial reabsorption of the emitted light by the colored complex and by the heavy atom effect via the enhancement of spin-orbit coupling.[36] The complexation constants are summarized in Table 3.3.

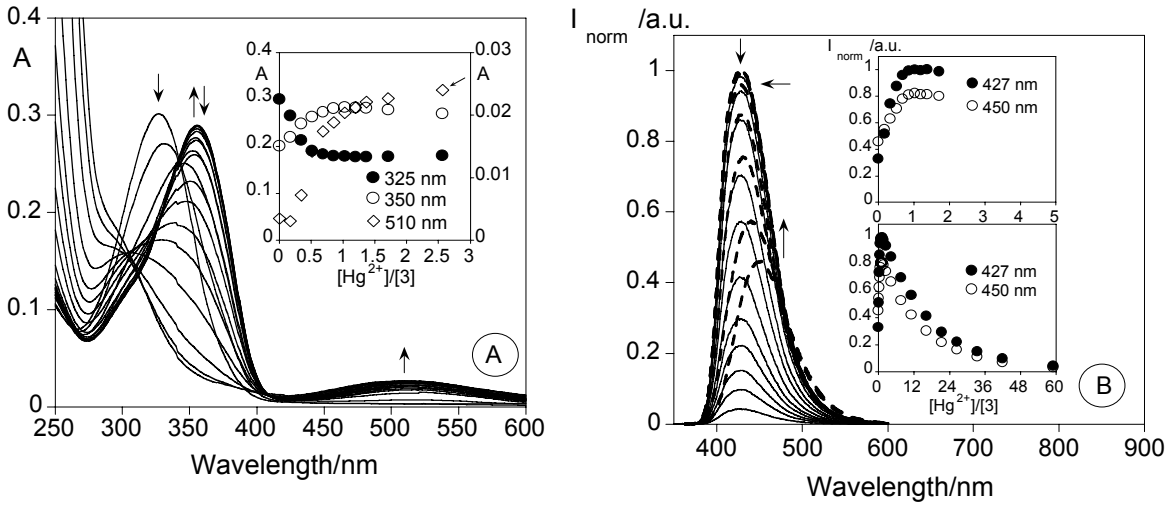

Figure 3.6 –Spectrofotometric (A) and spectrofluorimetric (B) titration of **3** in the presence of Hg^{2+}, in an acetonitrile solution. The inset represents the absorption (A) at 325, 350 and 510 nm, and the emission (B) at 427 nm and 450 nm, as a function of $[Hg^{2+}]/[\mathbf{3}]$. ([**3**] = 6.66×10^{-6} M, [Hg $(CF_3COO)_2$] = 1.7×10^{-2} M, λ_{exc3} = 325 nm, T=298K).

The most interesting results arise from the interaction with Cu^{2+}. All ligands were explored in the presence of Cu^{2+} in an absolute ethanol solution to prevent the self reduction to Cu^{+} sometimes observed in acetonitrile.[37] For all cases, an enhancement of the fluorescence emission at 430 nm was observed (see Figure 3.7). The absorption spectrum showed a red shift with the formation of well-defined isosbestic points at 333, 334, and 336 nm, for **1**-**3** respectively. This result indicates that the stoichiometry of the reaction remains unchanged during the chemical reaction and no secondary reactions occur during the considered time range. For compound **3** a visible band centered at 510 nm was observed. Nevertheless, as previously discussed for the Hg^{2+} complex, this fact did not influence the fluorescence emission, and the final complex formed was

highly emissive with a fluorescence quantum yield of 0.48. The complexation constants for all cases are summarized in Table 3.3. The highest values were obtained for compounds **1** and **3**, and agree with the formation of dinuclear species. However due to the instability observed in the complex with compound **1** bearing furyl substituent, further studies with this complex were prevented.

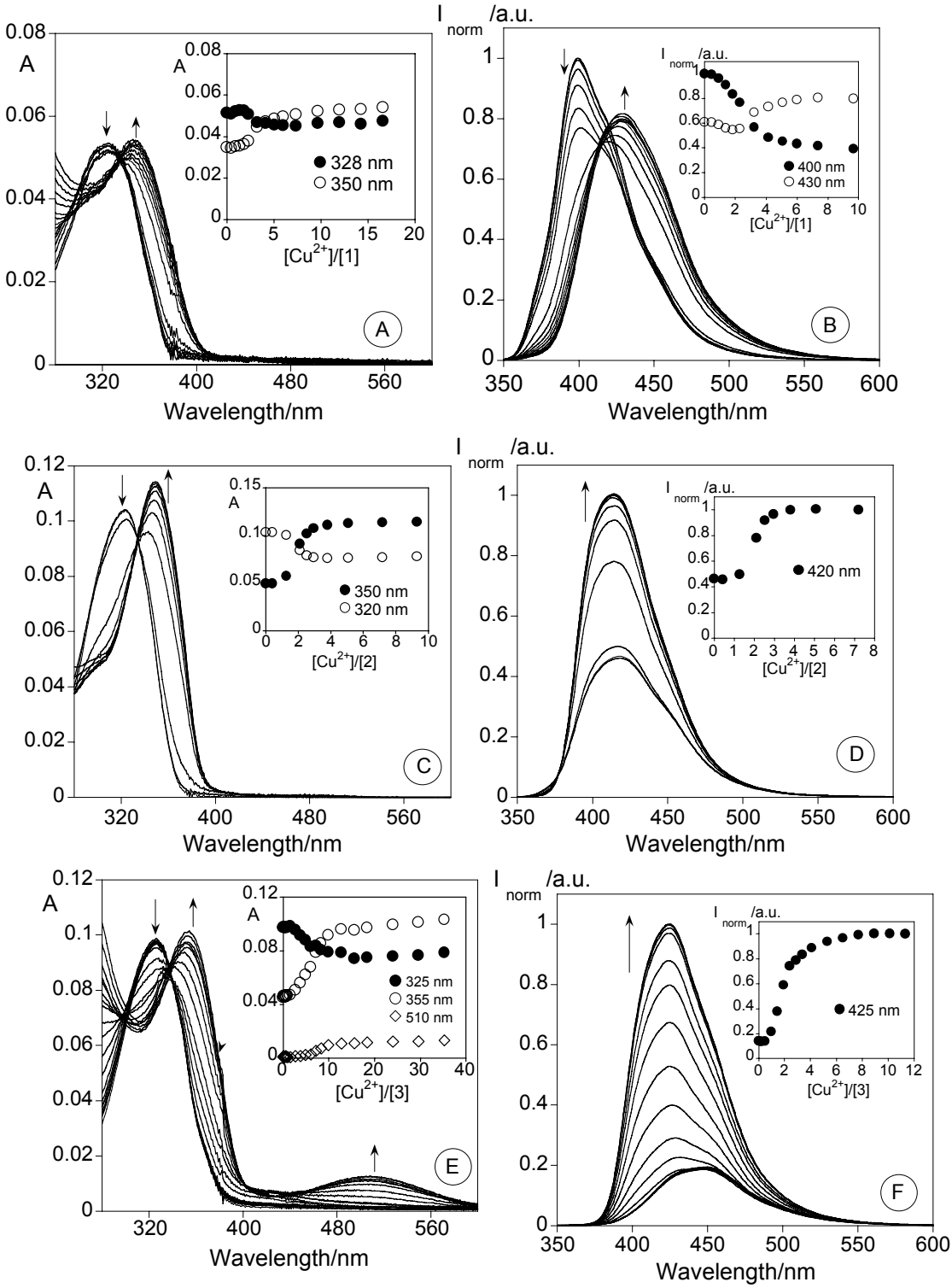

Figure 3.7 – Absorption (A, C and E) and emission titrations (B, D and F) of compounds **1** to **3** with the addition of increased amount of Cu^{2+} in absolute ethanol.

The inset represents the absorption at 328 nm, 350 nm for (A), 320 nm, 350 nm for (C) and 325 nm, 355 nm, 510 nm for (E); and the emission at 400, 430 nm (B), 420 nm (D) and 425 nm for (F) as a function of $[Cu^{2+}]/[\mathbf{1}]$, $(Cu^{2+}]/[\mathbf{2}]$, $[Cu^{2+}]/[\mathbf{3}]$ respectively. ([**1**] = 1.49×10^{-6} [**2**] = 1.62×10^{-6} M, [**3**] =2.05×10^{-6} M, $[Cu(BF_4)_2]$ = 1.62×10^{-2} M, λ_{exc1} = 328 nm, λ_{exc2} = 320 nm, λ_{exc3} = 325 nm, T=298K).

As is well-known, copper complexes with brown-red color can be understood as complexes with Cu^{+}.[38] Because of the deep dark red color observed in the complex with ligand **3** (see Figure 3.8), additional studies concerning the oxidation state of the metal centers was performed by NMR and EPR spectroscopy. The NMR spectra in acetonitrile-d_3 revealed a group of very broad signals, suggesting the presence of Cu^{2+} paramagnetic centers.

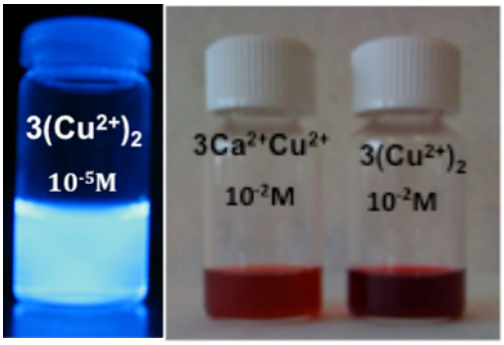

Figure 3.8**.** (Right) Ethanol solutions of compound **3** in the presence of one equivalent of Cu^{2+} and Ca^{2+}, and in the presence of two equivalents of Cu^{2+}. (Left) Emission under irradiation at 365 nm of an ethanolic solution of compound **3** in the presence of 2 equiv of Cu^{2+}.

The EPR solution spectra (see Figure 3.9) showed the same behavior for all Cu^{2+} paramagnetic complexes. Simulation of the solution spectrum yielded the EPR parameters: g_1= 2.435, g_2= 2.097, g_3= 2.074, A_1= 110 G in all cases. These results suggest that the two metal centers present in the complex with ligand **3** are in similar environment coordination sites. It can be postulated that one metal could be located in the azacrown unit, coordinated to the nitrogen atom and at least four oxygen atoms, and the second metal center could be located in the imidazole ring, coordinated to the imidazole nitrogen completing the coordination sphere with several water molecules. The presence of these water molecules was proved also by the infrared spectra in KBr pellets.

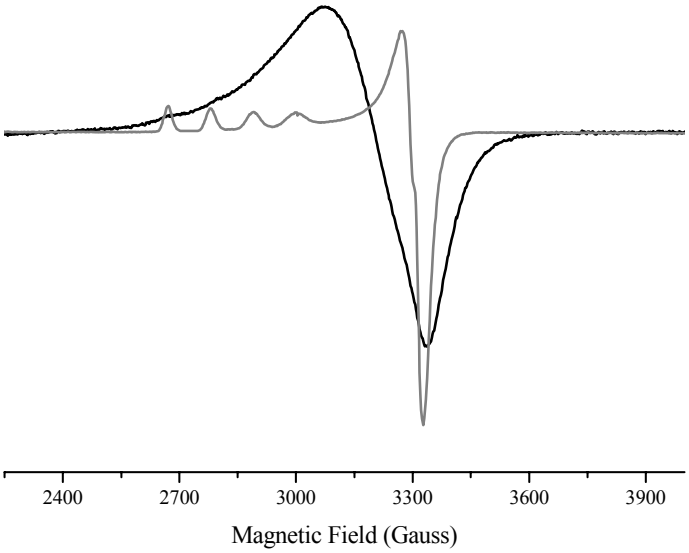

Figure 3.9. - EPR spectra of compound $[Cu_2\mathbf{3}](BF_4)_4].4H_2O$ **(5)** recorded in a polycrystalline powdered sample (black) and dissolved in acetonitrile (grey). Simulation of the solution spectrum yields the EPR parameters: g_1= 2.435, g_2= 2.097, g_3= 2.074, A_1= 110 Gauss. Simulation was performed using Simfonia v1.25 (Bruker, Inc.).

As ligand **3** can be coordinated by two metal ions, the formation of heterodinuclear species by the addition of Ca^{2+} followed by one Cu^{2+} equivalent was explored. The color of the complex changes from deep dark red to orange. The fluorescence quantum yield for the dinuclear Cu^{2+} complex synthesized with **3** was 0.48; for comparison purposes, the addition of 1 equiv of Cu^{2+}, followed by the addition of Ca^{2+} lead to a more emissive species with fluorescence quantum yield of 0.79 (table 3.4). Taking into account that Ca^{2+} will be coordinated to the azacrown, the Cu^{2+} center must be now located at the imidazole ring. To explore the effect of simultaneous coordination on the fluorescence emission of ligands **2** and **3**, several competitive experiments were performed in absolute ethanol. As was discussed previously, in ethanol the imidazole nitrogen is partially or totally protonated preventing the PET effect.

Table 3.4 – Luminescence quantum yield of compound **3** in the presence of Ca^{2+} and Cu^{2+}.

Species	**Quantum Yield, ϕ**
3	0.07
3 + Cu^{2+}	0.48
3 + Ca^{2+}	0.30
3+ Cu^{2+} + Ca^{2+}	0.79

Careful inspection of Figure 3.10A shows that addition of Cu^{2+}, Ni^{2+}, and Ca^{2+} to ligand **2** induced an one-fold increase of the fluorescence intensity (observed previously in the metal titrations) and after addition of pairs Cu^{2+}/Ca^{2+} and Cu^{2+}/Ni^{2+} a small decrease of the intensity was observed. Finally, as expected, addition of Hg^{2+} and the pair Cu^{2+}/Hg^{2+} quenched the fluorescence emission.

In Figure 3.10B are shown the results of the same experiments for ligand **3**. An enhancement of the fluorescence emission was observed after coordination by two equivalent of Cu^{2+} with similar intensity as observed for the pair Cu^{2+}/Ni^{2+}. This CHEF effect was also observed for the addition of Ca^{2+}, being more intense when the pair Cu^{2+}/ Ca^{2+} was used.

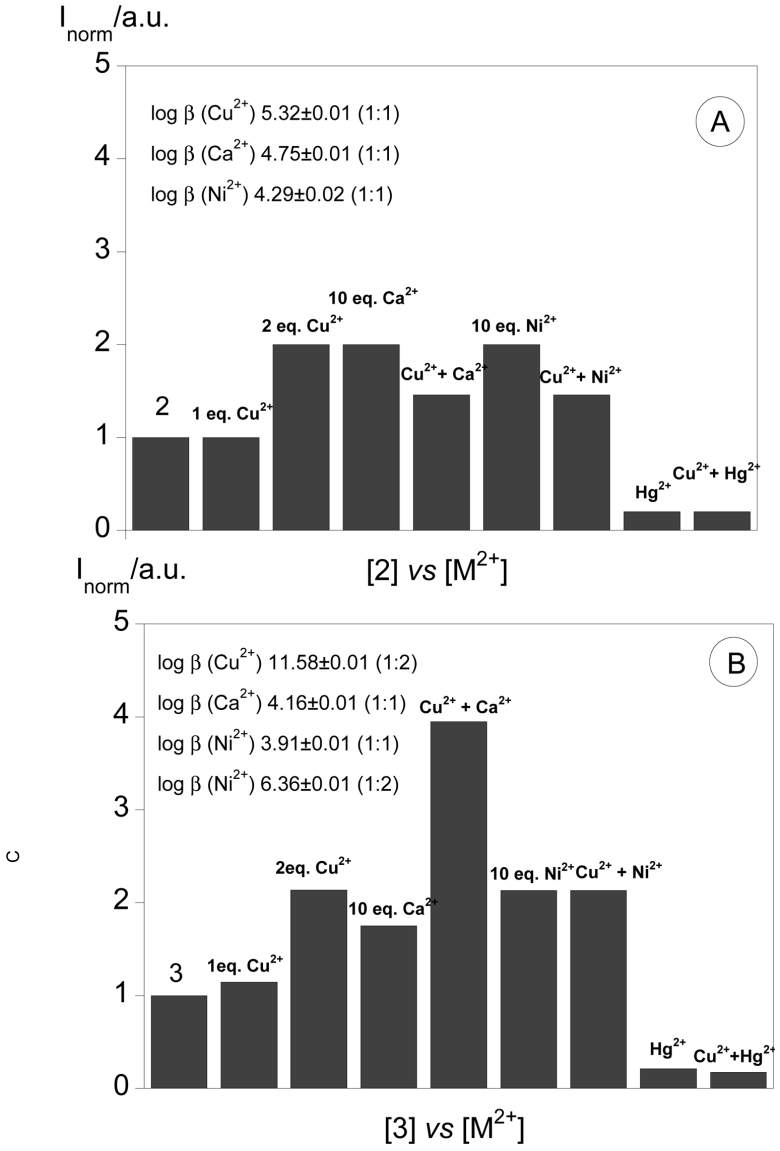

Figure 3.10 - Normalized fluorescence of compounds **2** (A) and **3** (B) in the presence of $Cu^{2+,}$ Ca^{2+}, Ni^{2+} and Hg^{2+}, in absolute ethanol.

To use compound **3** as fluorescent chemosensor for Cu^{2+} in solution, the detection (DL) and quantification (QL) limits were determined in absolute ethanol. The values obtained at 510 nm, where the visible band was formed, was of 0.003(0.001 (DL) and 0.007 (0.002 (QL). Taking into account these results, the minimal amount of Cu^{2+} that could be determined in absolute ethanol is 1.60 ppm.

3.6 - Crystallography data

Crystals of compound **2** (Figure 3.11) suitable for X-ray diffraction were obtained by slow evaporation of an ethanolic solution. Bond distances and angles are all within the normal ranges. The modified azacrown ethers adopt a nearly planar conformation, with the four oxygen and the nitrogen atoms of the molecule describing a slightly distorted plane. The dihedral angle between the planes containing the phenyl and the imidazolyl units are 121º, while between the planes containing the phenyl and the crown-ether units are 122º.

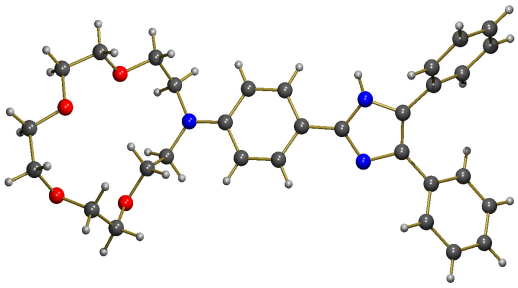

Figure 3.11. X-Ray crystallographic structures of compound **3.**

Note:

3: Selected bond lengths (Å) and angles (º): S(2)-C(24) 1.714(4), S(2)-C(21) 1.735(4), S(1)-C(11) 1.707(4), S(1)-C(14) 1.784(4), O(1)-C(39) 1.403(4), O(1)-C(38) 1.465(4),N(2)-C(3) 1.372(5), N(2)-C(2) 1.428(5), C(1)-N(1) 1.427(5), O(2)-C(41) 1.344(4), O(2)-C(40) 1.413(4), C(3)-N(1) 1.357(4), N(3)-C(34) 1.413(5), N(3)-C(46) 1.466(5), N(3)-C(37) 1.546(4), C(24)-S(2)-C(21) 90.43(2), C(11)-S(1)-C(14) 94.57(19), C(39)-O(1)-C(38) 113.09(3), C(3)-N(2)-C2 108.81(3), C(41)-O(2)-C(40) 114.70(3), C(22)-C(21)-S(2) 112.07(3), C(2)-C(21)-S(2) 117.08(3), C(31)-C(3)-N(1) 126.43(4), C(31)-C(3)-N(2) 127.72(4), N(1)-C(3)-N(2) 105.85(3), C(1)-C(2)-N(2) 108.33(4), N(2)-C(2)-C(21) 114.37(3), C(34)-N(3)-C(46) 119.01(3), C(34)-N(3)-C(37) 125.09(3), C(46)-N(3)-C(37) 113.55(3), C(42)-O(3)-C(43) 117.87(3), O(1)-C(39)-C(40) 109.99(3), C(45)-O(4)-C(44) 107.93(3), O(4)-C(45)-C(46) 100.51(3), C(3)-N(1)-C(1) 110.55(3), C(1)-C(11)-S(1) 122.80(3), C(12)-C(11)-S(1) 115.41(3), C(13)-C(14)-S(1) 108.51(3), C(23)-C(24)-S(2) 110.73(4).

3.7 - Conclusions

A new family of emissive molecular probes **1**-**3**, derived from 15-crown-5 monoaza macrocyclic ligands bearing a furyl, aryl or thienyl 4,5-disubstituted imidazole system have been synthesized in good to excellent yields by a simple reaction, and their photophysical properties have been evaluated in solution and in solid state by absorption and fluorescence emission spectroscopy and by MALDI-TOFMS spectrometry in the gas phase. Their capacity to act as potential sensors for divalent

metal ions Ca^{2+}, Cu^{2+}, Ni^{2+} and Hg^{2+} was explored in solution and in solid state. Interesting results were found for compound **3** bearing the thiophene rings being an example of enhancement of fluorescent emission upon coordination to Cu^{2+}, Ni^{2+} or Ca^{2+}. The complex $(CuCa\mathbf{3})^{4+}$ in solution was the most emissive with a fluorescence quantum yield of 0.79.

3.8 - Acknowledgment

We are indebted to InOU Uvigo by project K914 122P 64702 (Spain) and FCT-Portugal by project PTDC/QUI/66250/2006 for financial support. The NMR spectrometers are part of the National NMR Network and were purchased in the framework of the National Programme for Scientific Re-equipment, contract REDE/1517/RMN/2005, with funds from POCI 2010 (FEDER) and FCT-Portugal. C.L. thanks Xunta de Galicia, Spain, for the Isidro Parga Pondal Research Program. E.O. and R.B. thank FCT-MCTES (Portugal) by their PhD grants SFRH/BD/35905/2007 and SFRH/BD/36396/2007, respectively. We are gratefull to Dr. Cristina Nuñez and Dr. Pablo González from the REQUIMTE, Universidade NOVA de Lisboa, Portugal, for their important help with the crystallographic and EPR data, respectively, and Dr. Jose Luis Capelo from the University of Vigo, Spain, for the help with the MALDI-TOFMS spectra.

3.9 - Supporting Information Available

X-ray crystallographic data of **2** in CIF format and Job's plot for compound **3** in the presence of Cu^{2+}. This material is available free of charge via the Internet at http://pubs.acs.org.

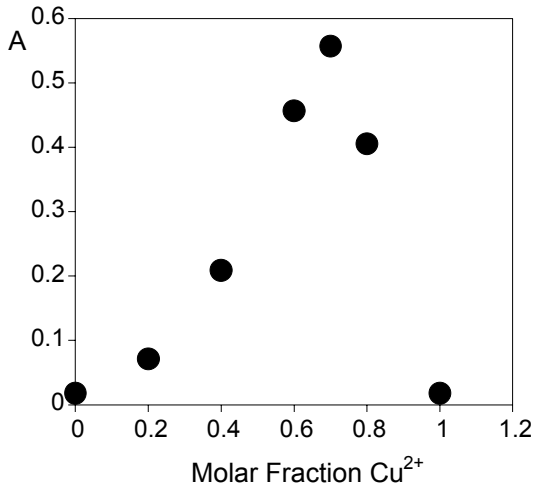

Figure SI 3.1.- Job´s plot for compound **3** in the presence of Cu^{2+}.

3.10 - References

(1) (a) Czarnik, A. W. *Acc. Chem. Res*. **1994**, *27*, 302–308. (b) Czarnik, A. W. *Acc. Chem. Res*. **1998**, *31*, 201–207.

(2) (a) Ulijn, R. V.; Smith, A. M. *Chem. Soc. Rev*. **2008**, *37*, 664–675. (b) Cavalli, S.; Albericio, F.; Kros, A. *Chem. Soc. Rev*. **2010**, *39*, 241–263. (c) Sawada, T.; Takahashi, T.; Mihara, H. *J. Am. Chem. Soc*. **2009**, *131* (40), 14434–14441. (d) Lodeiro, C.; Pina., F. *Coord. Chem. Rev*. **2009**, *253*, 1353–1383. (e) Prodi, L; Bolleta, F.; Montalti, M.; Zaccheroni, N. *Coord. Chem. Rev.* **2000**, *205*, 59–83. (f) Martínez-Ma~nez, M.; Sanceno, F. *Chem. Rev*. **2003**, *103*, 4419–4476. (g) Jiang, P. J.; Guo, Z. J. *Coord. Chem. Rev*. **2004**, *248*, 205–229. (h) Finney, N. S. Current *Opp. Chem. Biol.* **2006**, *10*, 238–245.

(3) Lörh, H. G.; Vögtle, F. *Acc. Chem. Res*. **1985**, *18*, 65–72.

(4) Okamoto, H.; Owari, M.; Kimura, M.; Satake, K. *Tetrahedron Lett.* **2001**, *42*, 7453 - 7455.

(5) Debus, H. Liebigs *Ann. Chem*. **1858**, *107*, 199–208.

(6) (a) Siddiqui, S. A.; Narkhede, U. C.; Palimkar, S. S.; Daniel, T.; Rajgopal, J. L.; Srinivasan, K. V. *Tetrahedron* **2005**, *61*, 3539–3546 and references therein. (b) Bellina, F.; Cauteruccio, S.; Rossi, R. *Tetrahedron* **2007**, *63*, 4571–4624 and references therein.

(7) (a) Moylan, C. R.; Miller, R. D.; Twieg, R. J.; Betterton, K. M.; Lee, V. Y.; Matray, T. J.; Nguyen, *C. Chem. Mat*. **1993**, *5*, 1499. (b) Bu, X. R.; Li, H. Y.;VanDerveer, D.; Mintz, E. A. *Tetrahedron Lett*. **1996**, *37*, 7331. (c) Santos, J.; Mintz, E. A.; Zehnder, O.; Bosshard, C.; Bu, X. R.; Gunter, P. *Tetrahedron Lett.* **2001**, *42*, 805. (d) Wang, S.; Zhao, L.; Xu, Z.; Wu, C.; Cheng, S. *Mater. Letters* **2002**, *56*, 1035. (e) Wu, W.; Ye, C.; Wang, D. *Arkivoc* **2003**, *59*. (f) Wu, W.; Zhang, Z.; Zhang, X. *J. Chem. Res*. **2004**, *9*, 617. (g) Wu, W.; Zhang, Z. L.; Zhang, X. Y. *J. Nonlinear Opt. Phys. Mater*. **2005**, *14*, 61. (h) Ren, J.; Wang, S. M.;Wu, L. F.; Xu, Z. X.; Dong, B. H. *Dyes Pigments* **2008**, *76*, 310. (i) Batista, R. M. F.; Costa, S. P. G.; Belsley, M.; Lodeiro, C.; Raposo, M. M. M. *Tetrahedron* **2008**, *64*, 9230. (j) Batista, R. M. F.; Costa, S. P. G.; Belsley, M.; Raposo, M. M. M. *Dyes Pigments* **2009**, *80*, 329. (k) Feng, K.; Hsu, F. L.; Bota, K.; Bu, X. R. *Microchem J*. **2005**, *81*, 23. (l) Zhang, M.; Li, M.; Zhao, Q.; Li, F.; Zhang, D.; Zhang, J.; Yi, T.; Huang, C. *Tetrahedron Lett.* **2007**, *48*, 2329. (m) Zhang, M.; Li, M. Y.; Li, F. Y.; Cheng, Y. F.; Zhang, J. P.; Yi, T.; Huang, C. H. *Dyes Pigments* **2008**, *77*, 408. (n) Feng, K.; De Boni, L.; Misoguti, L.; Mendonca, C. R.; Meador, M.; Hsu, F. L.; Bu, X. R.

Chem. Commun. **2004**, *1178*. (o) Zhao, L.; Li, S. B.; Wen, G. A.; Peng, B.; Huang,W. *Mater. Chem. Phys*. **2006**, *100*, 460. (p) Fang, Z.;Wang, S.; Zhao, L.; Xu, Z.; Ren, J.;Wang, X.; Yang, Q. *Mater. Chem. Phys*. **2008,** *107*, 305. (q) Pina, J.; Seixas de Melo, J.; Batista, R. M. F.; Costa, S. P. G.; Raposo, M. M. M. *J. Phys. Chem. B* **2010**, *114*, 4964. (r) Feng, K.; Hsu, F. L.; Van DerVeer, D.; Bota, K.; Bu, X. R. *J. Photochem. Photobiol. A-Chem*. **2004**, *165*, 223.

(8) De Silva, A. P.; Gunaratne, H. Q. N.; Gunnlaugsson, T.; Huxley, A. J. M.; McCoy, C. P.; Rademacher, J. T.; Rice, T. E. *Chem. Rev*. **1997**, *97*, 1515–1566.

(9) (a) Bolletta, F.; Costa, I.; Fabbrizzi, L.; Licchelli, M.; Montalti, M.; Pallavicini, P.; Prodi, L.; Zaccheroni, N. *J. Chem. Soc.*, *Dalton Trans*. **1999**, 1381–1386. (b) Goldsmith, C. R.; Lippard, S. *J. Inorg. Chem*. **2006**, *45*, 6474–6478. (c)Wu, D.; Huang,W.; Duan, C.; Zhihua, L.; Meng, Q. *Inorg. Chem*. **2007**, *46*, 1538–1540. (d) Alarcon, J.; Albelda, M. T.; Belda, R.; Clares, M. R.; Delgado-Pinar, E.; Frias, J. C.; García-España, E.; González, J.; Soriano, C. *Dalton Trans*. **2008**, *46*, 6530–6538. (e) Mameli, M.; Aragoni, M. C.; Arca, M.; Caltagirone, C.; Demartin, F.; Farrugia, G.; De Filippo, G.; Devillanova, F. A.; Garau, A.; Isaia, F.; Lippolis, V.; Murgia, S.; Prodi, L.; Pintus, A.; Zaccheroni, N. *Chem.;Eur. J*. **2010**, *16*, 919–930.

(10) Rurack, K. *Spectrochim. Acta A* **2001**, *57*, 2161–2195.

(11) (a) Kim, J.; Morozumi, T.; Nakamura, H. *Org. Lett*. **2007**, *9*, 4419– 4422. (b) Magri, D. C.; Callan, J. F.; de Silva, A. P.; Fox, D. B.; McClenaghan, N. D.; Sandanayake, K. R. A. S. *J. Fluoresc*. **2005**, *15*, 769–775. (c) Vysotski, E. S.; Lee, *J. Acc. Chem. Res.* **2004**, *37*, 405–415. (d) Parkers, R.; Mohsin, S.; Lee, T. C.; Gunnlaugsson, T. *Chem. Mater.* **2007**, *19*, 1656–1663. (e) Gerencser, A. A.; Adam-Vizi, V. *Cell Calcium* **2001**, *30*, 311–321.

(12) (a) Boiocchi, M.; Fabbrizzi, L.; Licchelli, M.; Sacchi, D.; V_azquez, M.; Zampa, C. *Chem. Commun.* **2003**, 1812–1813. (b) Anda, C.; Bazzicalupi, C.; Bencini, A.; Bianchi, A.; Fornasari, P.; Giorgi, C.; Valtancoli, B.; Lodeiro, C.; Parola, A. J.; Pina., F. *Dalton Trans*. **2003**, 1299–1307. (c) Nuñez, C.; Bastida, R.; Macias, A.; Bértolo, E.; Fernandes, L.; Capelo, J. L.; Lodeiro, C. *Tetrahedron* **2009**, *65*, 6179–6188. (d) Tamayo, A.; Lodeiro, C.; Escriche, L.; Casabo, J.; Covelo, B.; González, P. *Inorg. Chem*. **2005**, *44*, 8105–8115. (e) Fernandes, L.; Boucher, M.; Fernández-Lodeiro, J.; Oliveira, E.; Nuñez, C.; Santos, H. M.; Capelo, J. L.; Faza, O. N.; Bértolo, E.; Lodeiro, C. *Inorg. Chem. Commun*. **2009**, *12*, 905–912. (f) Aragoni, M. C.; Arca, M.; Bencini, A.; Blake, A. J.; Caltagirone, C.; Decortes, A.; Demartin, F.; Devillanova, F. A.; Faggi, E;

Dolci, L. S.; Garau, A.; Isaia, F.; Lipplis, V.; Prodi, L.; Valtancoli, B.; Zaccheroni, N. *Dalton Trans*. **2005**, 2994–3004.

(13) (a) Yu, M.; Shi, M.; Chen, Z.; Li, F.; Li, X.; Gao, Y.; Xu, J.; Yang, H.; Zhou, Z.; Yi, T.; Huang, C. *Chem.;Eur. J*. **2008**, *14*, 6892–6900. (b) Xu, Z.; Xiao, Y.; Qian, X.; Cui, J.; Cui, D. *Org. Lett*. **2005**, *7*, 889–892. (c) Chem, X. Q.; Jia, J.; Ma, H. M.;Wang, S. J.;Wang, X. C. *Anal. Chim. Acta* **2009**, *1*, 9–14. (d) Wang, H. X.; Wang, D. L.; Wang, Q.; Li, X. Y.; Schalley, C. A. *Org. Biomol. Chem*. **2010**, *8*, 1017–1026. (e) Yang, Y. K.; Yook, K. J.; Tae, J. *J. Am. Chem. Soc*. **2005**, *127*, 16760–16761. (f) Zhang, G.; Zhang, D.; Yin, S.; Yang, X.; Shuai, Z.; Zhu, D. *Chem. Commun*. **2005**, *16*, 2161–2163. (g) Guo, X.; Qian, X.; Jia, L. *J. Am. Chem. Soc*. **2004**, *126*, 2272–2273. (h) Nolan, E. M.; Lippard, S. J. *J. Am. Chem. Soc.* **2003**, *125*, 14270–14721. (i) Hennrich, G.;Walther,W.; Resch-Genger, U.; Sonnenshein, H. *Inorg. Chem*. **2001**, *40*, 641–644. (j) Zhao, Y.; Lin, Z.; He, C.; Wu, H.; Duan, C. *Inorg. Chem*. **2006**, *45*, 10013–10015. (k) Shamsipur, M.; Hosseini, M.; Alixadeh, K.; Alizadeh, N.; Yari, A.; Caltagirone, C.; Lippolis, V. *Anal. Chim. Acta* **2005**, *353*, 17–24. (l) Goretzki, G.; Bonnesen, P. V.; Dabestain, R.; Brown, G. M. *ACS Symp. Ser*. **2008**, *943*, 13–33. (m) Al-Kady, A. S.; Gaber, M.; Hussein, M. M.; Ebeid, E. Z.M. *J. Phys. Chem. A*. **2009**, *34*, 9474–9478. (n) Lee, Y. J.; Seo, D.; Kwom, J. Y.; Son, G.; Park, M. S.; Choi, Y.-H.; Soh, J. H.; Lee, H. N.; Lee, K. D.; Yoon, J. *Tetrahedron* **2006**, *62*,12340–12344. (o) Chandrasekhar, V.; Bag, P.; Pandey, M. D. *Tetrahedron* **2009**, *65*, 9876–9883.

(14) (a) Batista, R. M. F.; Oliveira, E.; Nuñez, C.; Costa, S. P. G.; Lodeiro, C.; Raposo, M. M. M. *J. Phys. Org. Chem*. **2009**, *22*, 362–366. (b) Pedras, B.; Fernandes, L.; Oliveira, E.; Rodriguez, L.; Raposo, M. M. M.; Capelo, J. L.; Lodeiro, C. *Inorg. Chem. Commun*. **2009**, *12*, 79–85. (c) Batista, R. M. F.; Oliveira, E.; Costa, S. P. G.; Lodeiro, C.; Raposo, M. M. M. *Org. Lett*. **2007**, *9*, 3201–3204. (d) Costa, S. P. G.; Oliveira, E.; Lodeiro, C.; Raposo, M. M. M. *Sensors* **2007**, *7*, 2096–2114. (e) Lodeiro, C.; Capelo, J. L.; Mejuto, J. C.; Oliveira, E.; Santos, H. M.; Pedras, B.; Nuñez, C. *Chem. Soc. Rev*. **2010**, *39*, 2948–2976. (f) Raposo, M. M. M.; García-Acosta, B.; Ábalos, T.; Martínez-Manez, R.; Ros-Lis, J. V.; Soto, J. *J. Org. Chem*. **2010**, *75*, 2922–2933.

(15) (a) Berlman, I. B. *Handbook of Fluorescence Spectra of Aromatic Molecules*, 2nd ed.; Academic Press: New York, 1971. (b) Montalti, L.; Credi, A.; Prodi, T.; Gandolfi, M. T.; Handbook of Photochemistry, 3rd ed.; Taylor and Francis Group: Boca Rat_on, FL, 2006.

(16) *SMART: Instrument Control and Data Collection Software*, version 5.054; Bruker Analytical X-ray Systems Inc.: Madison, WI, 1997.

(17) *SAINT: Data Integration software package*, version 6.01; Bruker Analytical X-ray Systems Inc.: Madison, WI, 1997.

(18) Sheldrick, G. M. *SADABS. A Computer Program for Absorption Corrections*; University of G€ottingen: G€ottingen, Germany, 1996.

(19) Sheldrick, G. M. *SHELXS97. A Computer Program for the Solution of Crystal Structures from X-ray Data*; University of Göttingen: Göttingen, Germany, 1997.

(20) Sheldrick, G. M. *SHELXL97. A Computer Program for the Refinement of Crystal Structures from X-ray Data*; University of Göttingen: Göttingen, Germany, 1997.

(21) Spek, A. L. *PLATON. A Multipurpose Crystallographic Tool*; Utrecht University; Utrecht, The Netherlands, 2001.

(22) Qin, W.; Baruah, M.; Silwa, M.; Van der Auweraer, M.; De Borggraeve, W. M.; Beljonne, D.; Averbeke, B. V.; Boens, N. *J. Phys. Chem. A* **2008**, *112*, 6104–6114.

(23) Davidson, D.; Weiss, M.; Jelling, M. J. *J. Org. Chem*. **1937**, *2*, 319– 327.

(24) Nakamoto, K. *Infrared and Raman Spectra of Inorganic and Coordination Compounds*, 3rd ed.; Wiley-Interscience: New York, 1978.

(25) Peng, S. M.; Gordon, G. C.; Goedken, V. L. *Inorg. Chem*. **1978**, *17*, 119–126.

(26) (a) Costa, S. P. G.; Oliveira, E.; Lodeiro, C.; Raposo, M. M. M. *Tetrahedron Lett*. **2008**, *49*, 5258–5261. (b) Batista, R. M. F.; Oliveira, E.; Costa, S. P. G.; Lodeiro, C.; Raposo, M. M. M. *Tetrahedron Lett.* **2008**, *49*, 6575–6578.

(27) Saleh, A.; Al-Soud, Y. A.; Nau, W. M. *Spectrochim. Acta, Part A* **2008**, *71*, 818 - 822.

(28) (a) Lodeiro, C.; Parola, A. J.; Pina, F.; Bazzicalupi, C.; Bencini, A.; Bianchi, A.; Giorgi, C.; Masotti, A.; Valtancoli, B. *Inorg. Chem*. **2001**, *40*, 2968–2975. (b) Bazzicalupi, C.; Bencini, A.; Berni, E.; Bianchi, A.; Danesi, A.; Giorgi, C.; Valtancoli, B.; Lodeiro, C.; Lima, J. C.; Pina, F.; Bernardo, M. A. *Inorg. Chem*. **2004**, *43*, 5134–5146. (c) Pina, J.; Seixas de Melo, J.; Pina, F.; Lodeiro, C.; Lima, J. C.; Parola, A. J.; Soriano, C.; Clares, M. P.; Albelda, M. T.; Aucejo, R.; Garcia-España, E. *Inorg. Chem*. **2005**, *44*, 7449–7458. (d) Pedras, B.; Oliveira, E.; Santos, H.; Rodríguez, L.; Crehuet, R.; Avilés, T.; Capelo, J. L.; Lodeiro, C. *Inorg. Chim. Acta* **2009**, *362*, 2627–2635.

(29) (a) NMR titration experiments were carried out in deuterated DMSO, due to the low solubility of 1 in ethanol at NMR concentration, and showed two protonation steps:

a first step involving the azacrown nitrogen and a second step involving the imidazole nitrogen. After protonation, both set of signals were broadned and difficult to differentiate. In this case, the signals attributed to the protonated azacrown nitrogen at 3.9-3.4 ppm were stabilized by increasing addition of protons before the signals attributed to the protonated imidazole nitrogen. (b) Vicente, M.; Bastida, R.; Lodeiro, C.; Macias, A.; Parola, A. J.; Valência, L.; Spey, S. E. *Inorg. Chem*. **2003**, *42*, 6768–6779.

(30) (a) Yang, T.; Gao, M.; Qin, W.; Yang, J. *Ind. J. Chem. A*. **2010**, *49*, 45–48. (b) Li, R.-J.; Chang, I.-J. *J. Chin. Chem. Soc*. **2002**, *49*, 161–164.

(31) Gokel, G. W.; Leevy, W. M.; Weber, M. E. *Chem. Rev*. **2004**, *104*, 2723–2750.

(32) Warmke, H.; Wiczk, W.; Ossowski, T. *Talanta* **2000**, *52*, 449–456.

(33) Gans, P.; Sabatini, A.; Vacca, A. *Talanta* **1996**, *43*, 1739–1753.

(34) Lever, A. B. P. *Inorganic Electronic Spectroscopy*; Elsevier: Amsterdam, 1968.

(35) Pearson, R. G. *J. Am. Chem. Soc*. **1963**, *22*, 3533–3539.

(36) (a) McClure, D. S. *J. Chem. Phys.* **1952**, *20*, 682–686. (b) Burress, C. N.; Bodine, M. I.; Elbjeirami, O.; Reibenspies, J. H.; Omary, M. A.; Gabbaie, F. P. *Inorg. Chem.* **2007**, *46*, 1388–1395. (c) Mameli, M.; Lippolis, V.; Caltagirone, C.; Capelo, J. L.; Nieto-Faza, O.; Lodeiro, C. *Inorg. Chem.* **2010**, *49*(18), 8276–828610.1021/ic1007439. (d) Tamayo, A.; Pedras, B.; Lodeiro, C.; Escriche, L.; Casabó, L.; Capelo, J. L.; Covelo, B.; Kivekäs, R.; Sillanpäa, R. *Inorg. Chem.* **2007**, *46*, 7818–7826.

(37) (a) Beloglazkina, E. Z.; Shimorsky, A. V.; Mazhuga, A. G.; Shilova, O. V.; Tafeenko, V. A.; Zyk, N. V. *Rus. J. Gen. Chem*. **2009**, *79*, 1504–1508. (b) Milne, J. B. *Can. J. Chem*. **1970**, *48*, 75–79.

(38) (a) Strange, A. F.; Klein, A.; Klinkhammer, K.-W.; Kaim, W. *Inorg. Chim. Acta* **2001**, *324*, 336–341. (b) Rapenne, G.; Dietrich-Buchecker, C.; Sauvage, J.-P. *J. Am. Chem. Soc*. **1999**, *121*, 994–1001.

Chapter 4

Synthesis, Characterization and Metal Ion Detection of Novel Fluoroionophores Based on Heterocyclic Substituted Alanines

Susana P. G. Costa, Elisabete Oliveira, M. Manuela M. Raposo, Carlos Lodeiro, *Sensors,* **2007**, 7, 2096-2114.

"We haven´t the money so we have got to think"

Sir Ernest Rutherford, 1871-1937

Nobel Prize in Chemistry, 1908.

Index

4.1 - Abstract

The synthesis of new fluorescent probes containing the thiophene and benzoxazole moieties combined with an alanine residue is described. The resulting highly fluorescent heterocyclic alanine derivatives respond via a quenching effect, with paramagnetic Cu^{2+} and Ni^{2+} metal ions and with diamagnetic Hg^{2+}, as shown by the absorption and steady-state fluorescence spectroscopy studies. The formation of mononuclear or dinuclear metal complexes was postulated based on the presence of the free carboxylic acid as binding site and also with the interaction with the donor atoms in the chromophore. Interaction with other important biological metal ions such as Zn^{2+}, Ca^{2+} and Na^{+} was also explored.

My contribution for this work was all photophysical studies and applications as chemosensors.

4.2 - Resumo

Neste trabalho é descrita a síntese de novas sondas fluorescentes contendo unidades de tiofeno e benzoxazole combinadas com um resíduo alanina. Os derivados heterocíclicos alaninas altamente fluorescentes respondem *via* efeito supressão de emissão, com os iões metálicos paramagnéticos Cu^{2+} e Ni^{2+}, e comoo diamagnético Hg^{2+}, sendo monitorizado por estudos de espectroscopias absorção e de emissão de fluorescência. A formação de complexos metálicos mononucleares e dinucleares foi postulado, com base na presença de um grupo carboxílico como um local de ligação e também na interacção dos átomos doadores do cromóforo. A interacção com outros iões metálicos biologicamente importantes, como o Zn^{2+}, Ca^{2+} e o Na^{+} foi também explorada.

A minha contribuição para este trabalho consistiu na realização de todos os estudos fotofísicos e aplicações como sensores químicos.

4.3 - Introduction

In the last few years various 2-substituted benzoxazole derivatives were studied extensively for their antitumor, antiviral, antimicrobial activities as non-nucleoside topoisomerase 1 poison, HIV-1 reverse transcriptase and/or DNA gyrase inhibitors [1]. Other applications include *in vivo* probes for positron emission tomography (PET) and single-photon emission computed tomography for early detection of amyloid plaque formation and for visualization of brain dopamine D_3 receptors [2-4]. Derivatives containing the benzoxazole or the thiophene nucleus combined with amino acid moieties have also important biological applications such as potent inhibitors of human cystein proteases, as ligands of the NMDA receptor, in molecular recognition, as biomarkers or biosensors [5-8]. Owing to their excellent optical properties and high lipophilicity, it is possible for benzoxazole compounds to be used as sensing materials. Therefore, several authors described recently the application of benzoxazole derivatives as fluorescent and/or colorimetric sensors for metals, anionic species and pharmaceutical analysis [9-17].

The interesting biological activity and photophysical properties of thiophene and benzazole derivatives lead us to the synthesis of alanine derivatives containing these heterocyclic nuclei [18-24]. The thienyl-benzoxazole amino acid derivatives can be incorporated into peptide chains and as such used as energy donors in conformational studies of peptides by means of fluorescence or be used as fluorescence markers. To our knowledge this is the first time that a fluorescent sensor containing the thiophene and benzoxazole fluorophores combined with the alanine residue selectively deprotected is described.

As a part of our ongoing research, in the present work we have combined the ability of amino acids for metal ion chelation with the strong fluorescence properties of the 2-substituted benzoxazole moiety. Thus, we were interested in studying the influence of both potential chelating units incorporated: *i)* the amino acid residue, bearing an amino and carboxylic acid terminal groups, partially or totally deprotected and *ii)* the aromatic chelating unit in the chromophore, with two possibilities for chelation: a NS or OS donor sets. The presence of two or more coordination centres in these compounds can lead to the design of interesting supramolecular structures for biological and environmental applications.

4.4 - Results and Discussion

4.4.1 - Synthesis

Starting from commercially available 3-nitro-L-tyrosine, reaction with thionyl chloride in methanol yielded the corresponding methyl ester **1a**. Subsequent reaction with *t*-butyl pyrocarbonate resulted in the *N*-Boc protected derivative **1b**. The nitro group in this compound was reduced to the amino group, by catalytic hydrogenation, yielding compound **1c** [25], which was condensed with 2-formylthiophene, in order to obtain the imino derivative **1d**. By reaction with lead tetraacetate (LTA) in DMSO [26], compound **1d** was oxidised to the [2-(2'-thienyl)benzoxazol-5-yl] alanine derivative **2a**.

Compound **2a** was then selectively deprotected at its C- and N-terminus, yielding the corresponding *N*-Boc protected compound **2b** and the methyl ester derivative **2c**, as well as the fully deprotected alanine derivative **2d**. By using similar procedures, compound **1c** was reacted with 2,4,5-trimethoxybenzaldehyde, yielding imine **1e**. Oxidation of this compound yielded [2-(2',4',5'-trimethoxyphenyl)benzoxazol-5-yl] alanine derivative **2e** [27]. Selective removal of the protecting groups resulted in the corresponding *N*-Boc protected **2f** and the fully deprotected **2g** alanine derivatives (Scheme 1). Compounds **2e-g** based on trimethoxyphenyl were prepared in order to confirm the involvement of the sulphur atom at the thiophene ring in the coordination process. All the compounds were obtained in good to excellent yields (Table 1) and were completely characterised by the usual techniques (MS, IR, UV-vis, ^{1}H and ^{13}C NMR spectroscopy).

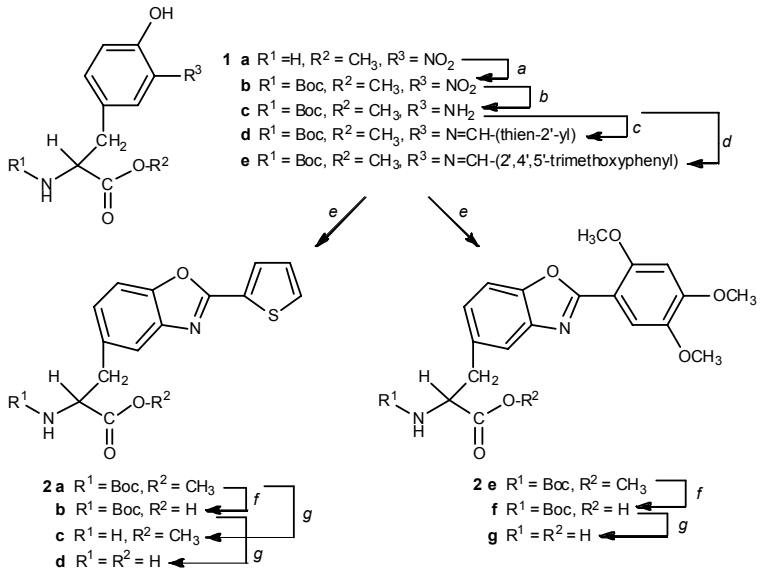

Scheme 4.1. - Synthesis of tyrosine derivatives **1a**-**e** and alanine derivatives **2a**-**g**. *Reagents and conditions: a)* $(Boc)_2O$, NaOH 1 M aq solution, rt, 2 days; *b)* 1,4-cyclohexadiene, Pd/C, MeOH, reflux, 24h; *c)* 2-formylthiophene, EtOH, rt, 5 days; *d)* 2,4,5-trimethoxybenzaldehyde,

EtOH, rt, 3 days; *e)* **1d** or **1e**, LTA, DMSO, rt, 3 days; *f)* NaOH 1 M aq solution, dioxane, rt, 3h; *g)* trifluoacetic acid/dichloromethane, 1:1, rt, 2h.

Table 4.1**. -** Synthesis data of tyrosine derivatives **1d**-**e** and alanine derivatives **2a**-**g**.

Compound	Yield (%)	IR (cm^{-1})	^{1}H NMR (δ, ppm)
1d	98	3375, 1754	8.76 (N=CH)
			6.90-6.95 (H-2), 7.05 (H-5)
1e	97	3430, 1741	9.01 (N=CH)
			6.88-6.94 (H-2), 6.99 (H-5)
2a	56	3358, 1734	7.48 (H-4), 7.45 (H-7)
2b	84	3357, 1752	7.63 (H-4), 7.48 (H-7)
2c	74	3310, 1741	7.56-7.59 (H-4), 7.49 (H-7)
2d	54	3413, 1620	7.93-7.96 (H-4), 7.62-7.67 (H-7)
2e	65	---	7.50 (H-4), 7.45 (H-7)
2f	82	3340, 1761	7.66 (H-4), 7.50 (H-7)
2g	44	3400, 1618	7.95(H-4), 7.60 (H-7)

4.4.2 - Photophysical study

The absorption and emission spectra of benzoxazolyl-alanines **2a-d** bearing a thiophene heterocycle and trimethoxy-phenyl alanine derivatives **2e-g** in absolute ethanol solution at 298 K were performed. The absorption and emission bands of the 2-substituted benzoxazole derivatives were centered at 315-336 and 393-398 nm, respectively. The fluorescence quantum yields for compounds **2a-g** were determined and the derivatives **2a-d** with a thiophene moiety were found to be strongly emissive ($0.66 < \Phi_F < 0.80$) while compounds **2e-g** displayed much lower quantum yields ($0.26 < \Phi_F < 0.47$) (Table 2). As can be seen by the results, the selective deprotection at the amino and carboxylic groups of the amino acid residue had only a minor influence on the fluorescence quantum yields. No solvatochromic effect in the absorption spectra was observed in absolute ethanol/water (1:1), absolute ethanol, acetonitrile, dioxane and cyclohexane for all compounds studied.

Table 4.2. - UV-vis and fluorescence data for alanine derivatives **2a**-**g**.

Compound	UV-vis	Fluorescence		
	λ_{max} (nm)	λ_{em} (nm)		Stokes' shift (nm)
2a	315	394	0.80	79
2b	316	393	0.66	77
2c	315	394	0.77	79
2d	315	393	0.76	78
2e	334	396	0.47	62
2f	334	395	0.44	61
2g	336	398	0.26	62

Compounds **2a-g** are amino acid derivatives, which in solution are present in zwitterionic form, and during our studies their zwitterionic nature was taken into account. All of our studies were performed in absolute ethanol and/or in water-absolute ethanol mixtures and the measured pH value was always between 5-6, at which the zwitterionic form predominates. At this pH value, the amine group in alanine derivatives is protonated and the carboxylic group is deprotonated, being available for coordination with the metal ions studied, Cu^{2+}, Hg^{2+} and Ni^{2+}, in these conditions.

4.4.2.1 - Spectrofluorimetric titrations and metal sensing effect

In order to evaluate the sensor ability of systems **2a-g** in solution towards Zn^{2+}, Hg^{2+}, Cu^{2+}, Ni^{2+}, Ca^{2+} and Na^{+} in low acidic or neutral conditions, UV-vis and fluorescence studies were performed.

4.4.2.2 - Protonation effects

In the presence of increasing amount of HBF_4, only compounds **2a** and **2f,** in acetonitrile or absolute ethanol were slightly affected. The maximum of absorption at 315 nm (**2a**) and 334 nm (**2f**), showed a 4 nm red shift upon acid addition. For compound **2f**, a new band centered at 380 nm was observed when a larger amount of acid was added (30 to 190 equivalents). As previously reported for related quinoxalinyl derivatives [15], compounds **2b**-**d** and **2e,g** did not reveal any significant change in the absorption spectrum upon acid addition in absolute ethanol and absolute ethanol/water (1:1). With further addition of acid, a decrease in the intensity of the fluorescence emission was observed. This quenching may be a result of protonation on the benzoxazole nitrogen atom.

4.4.2.3 - Deprotonation effects

Addition of bases such as potassium hydroxide, triethylamine and tetramethylammonium hydroxide solutions to ligands **2b, 2d, 2f** and **2g** in ethanolic solutions (with a free carboxylic acid group) was performed.

The maximum of absorption at 315 nm for **2a**, and 334 nm for **2f**, was slightly affected upon addition of 100 equivalents of tetrabutylammonium hydroxide solution. With further addition of base (more than 500 equivalents), a 50% quenching effect in fluorescence emission was observed. This effect can be attributed to a photoinduced electron transfer (PET) process from the NH_2 deprotonated group to chromophore. At this point, the pH value was 10-11 and addition of Hg(II) ions to a basic solution of ligand **2d** led to the precipitation of a solid (hydroxide complex), thus preventing complexation studies in basic conditions.

4.4.2.4 - Metal sensing effects

Compounds **2a** and **2e**, protected at amino and carboxylic terminals, did not show any change in the ground (absorption) and excited (emission) states after the addition of Na^+, Ca^{2+}, Zn^{2+}, Cu^{2+} and Ni^{2+} cations. In the titration of **2a** with a $Hg(CF_3SO_2)_2$ ethanolic solution, the intensity of fluorescence was reduced in 30% after the addition of 30 equivalents of metal ion, while the spectrum of trimethoxy-phenyl alanine derivative **2e** was not affected by Hg^{2+} addition. This result can be due to the involvement of the S atom in complexation.

Selective deprotection of the carboxylic terminal in **2a** and **2e**, gave compounds **2b** and **2f**. Both systems responded to the presence of Cu^{2+}, Ni^{2+} and Hg^{2+}, while addition of increasing amounts of Na^+ and Ca^{2+} did not change either the absorption and emission spectra. A rising CHEQ effect (Chelation Enhancement of the Quenching) [28-29] was observed in the cases of Cu^{2+}, Ni^{2+} and Hg^{2+}. This CHEQ effect is commonly observed in polyamine ligands containing aromatic fluorophores, and can be attributed to an energy transfer quenching of the π* emissive state through low-lying metal-centre unfilled d-orbitals for Cu^{2+}, and to an intersystem crossing mechanism due to the heavy atom effect for Hg^{2+} [29]. While the quenching of fluorescence is predominantly connected with the nature of metal ion, the ligand fluorescence enhancement could be result from changes of the geometry between the steady and excited states, or be also induced by the ligand. A very small CHEF effect (Chelation enhancement of the Fluorescence Emission) was observed only when compound **2b** was titrated with Zn^{2+} [30-31].

Although Cu^{2+} and Ni^{2+} affected only the excited state of the chromophore in both aforementioned ligands **2b** and **2f**, Hg^{2+} affected the ground and excited states when ligand **2b**, bearing a thiophene unit, was used. This result suggests that the metal ion interacts with both chelating units present in the compound: the carboxylic acid group of the amino acid

residue and the S atom of the thiophene heterocycle [32]. For ligand **2b**, complexation constants using the SPECFIT/32 program [33] were obtained only for the interaction with Hg^{2+}. The results suggested that two metal ions are coordinated to the ligand. In the case of ligand **2f** all metal complexation studies showed values that agree with 2:1 metal to ligand molar ratio for Hg^{2+} and 1:1 metal to ligand ratio for Cu^{2+} and Ni^{2+} (Table 4.3).

Table 4.3. - Complexation constants for alanine derivatives **2b**-**d** and **2f-g** with Cu^{2+}, Ni^{2+} and Hg^{2+} in absolute ethanol.

Compound	Metal complex	Log K	M.L.H[a]
2b	2bHg	5.01 ± 4.0E-02	1.1.0
		9.37 ± 7.0E-02	2.1.0
2d	2dHg	7.78 ± 2.0E-02	2.1.0
2d	2dCu	9.77 ± 2.0E-02	2.1.0
2f	2fHg	7.09 ± 8.0E-02	2.1.0
2f	2fCu	6.22 ± 2.0E-02	1.1.0
2f	2fNi	6.67 ± 6.0E-02	1.1.0
2g	2gCu	6.10 ± 6.0E-02	1.1.0
2g	2gNi	10.26 ± 8.0E-02	2.1.0

[a]M.L.H means Metal. Ligand. proton ratio

In Figure 4.1 is represented the absorption (A) and emission (B) spectra of compound **2b** in the presence of increasing amount of Hg^{2+}. The increase of Hg^{2+} ion concentration in absolute ethanol solution caused the decrease in the absorbance in the range of 280-340 nm, and increase in absorption between 340-390 nm. A sharp isosbestic point at λ= 330 nm was detected (Fig. 4.1A). After the addition of small molar ratio equivalents of metal ions (0.25 to 1 equivalent) a small effect in absorption and emission was observed. By increasing the metal-ligand molar ratio, strong changes in absorption and emission were observed (inset Figure 4.1B).

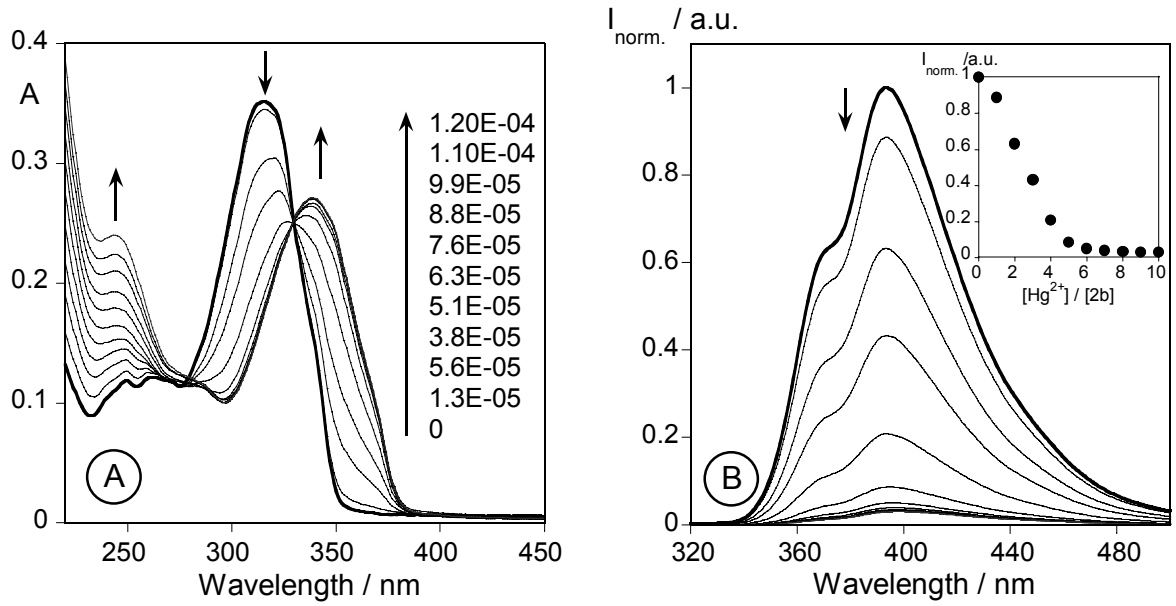

Figure 4.1. - Spectrophotometric titration (A) and fluorimetric titration (B) of an ethanolic solution of **2b** with a standard solution of $Hg(CF_3SO_2)_2$ in absolute ethanol ([**2b**] = 1.30E-5 M, T = 298 K, λ_{exc} = 316 nm. Inset: normalized emission at 394 nm).

The absorption and emission spectra of compound **2b** with increasing amount of Cu^{2+} is represented in figure 4.2. It can be seen that while the emission was strongly affected by metal ion complexation, no major changes were seen in the absorption. These results did not allow us to calculate the stoichiometry of complexes with Cu^{2+} and Ni^{2+}, formed in the ground state. Probably the formation of the 1:1 M:L metal complexes has relatively low values for the binding constants. Increasing the metal ion concentration forces the formation of dinuclear species. Due to the spectral response, complexation probably takes place firstly at the carboxylic acid group of the aminoacid residue, farther from the chromophore, and the second metal ion complexation occurs at the donor atoms present in the chromophore unit. As observed before, interaction of ligand **2b** with Hg^{2+}, Ni^{2+} and Cu^{2+} also caused a strong CHEQ effect, suggesting the interaction with these metal ions with the chromophore.

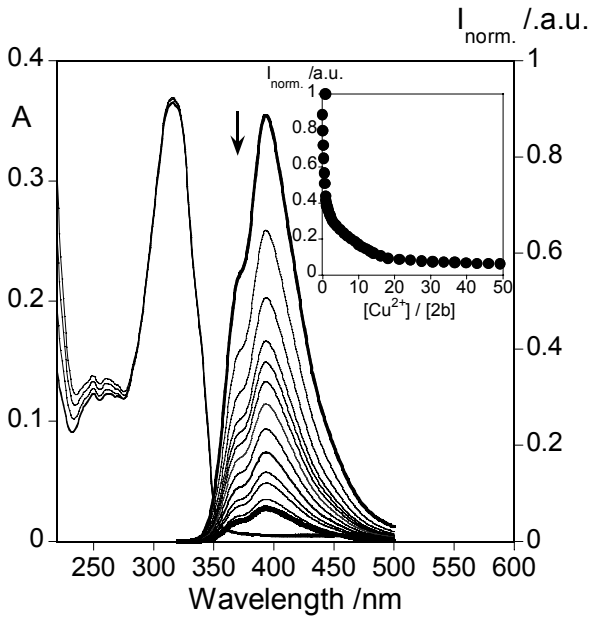

Figure 4.2**. -** Spectrophotometric titration and fluorimetric titration of an ethanolic solution of **2b** with a standard solution of $Cu(CF_3SO_2)_2$ in absolute ethanol. ([**2b**] = 1.30E-5 M, T = 298 K, λ_{exc} = 316 nm. Inset: normalized emission at 394 nm).

The complexation of ligand **2f** with Hg^{2+}, Cu^{2+} and Ni^{2+} in absolute ethanol can be seen in Figures 4.3 and 4.4, respectively. The amount of metal ion necessary to quench the fluorescence emission was higher than that used for the thiophenic ligand **2b**. In the case of compound **2f**, fifty equivalents were used, in contrast with the six equivalents of Hg^{2+} needed to quench ligand **2b**. These results suggest lower complexation constants for compound **2f**. In the cases of Ni^{2+} and Cu^{2+}, 5 equivalents of metal ion were enough in all cases to reduce the intensity of emission in 80%.

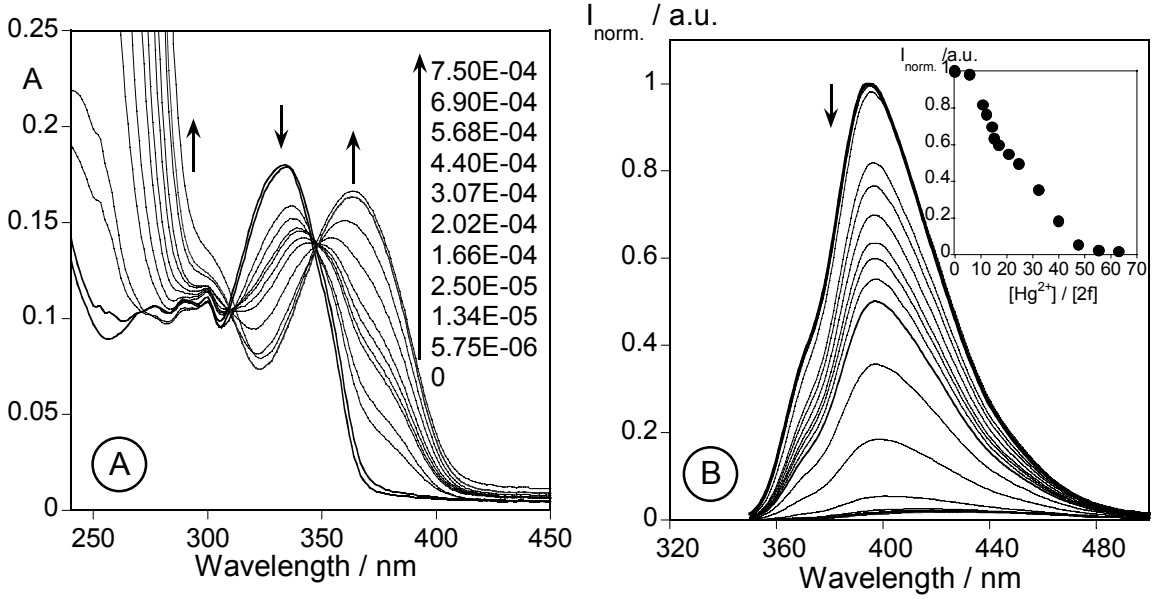

Figure 4.3. - Spectrophotometric titration (A) and fluorimetric titration (B) of an ethanolic solution of **2f** with a standard solution of $Hg(CF_3SO_2)_2$ in absolute ethanol. ([**2f**] = 1.00E-5 M, T = 298 K, λ_{exc} = 334 nm. Inset: normalized emission at 395 nm).

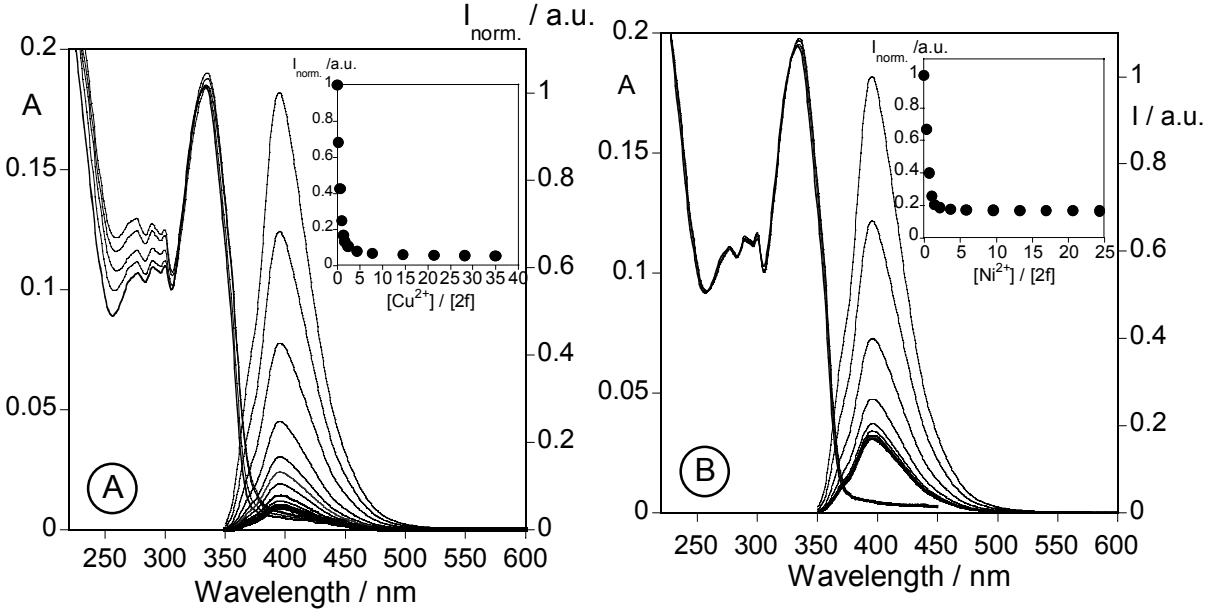

Figure 4.4.- Spectrophotometric titration and fluorimetric titration of an ethanolic solution of **2f** with a standard solution of $Cu(CF_3SO_2)_2$ (A) and $Ni(BF_4)_2$ (B) in absolute ethanol. ([**2f**] = 1.00E-5 M, T = 298 K, λ_{exc} = 334 nm. Insets: normalized emission at 396 nm in both cases).

Selective deprotection at the amino terminal of the amino acid gave compound **2c** with a free NH_2 group. The compound **2c** studied (pH = 5-6) in which the amine group is protonated,

NH_3^+, a strong decrease in the coordination ability in absolute ethanol and absolute ethanol/water (1:1) was observed when compared with ligand **2b**, with a free carboxylic acid group. After addition of Na^+, Ca^{2+}, Zn^{2+}, and Ni^{2+}, only minor changes were observed in the absorption and emission spectra. In the case of Hg^{2+} and Cu^{2+} a decrease in the intensity of the fluorescence emission in 40% and 30%, respectively, was observed when a metal to ligand molar ratio of 30:1 was achieved.

Total deprotection of both amino and carboxylic acid terminals in alanines **2a** and **2e** gave compounds **2d** and **2g** in the form of free amino acid residues. In our conditions, the zwiterionic form was present in solution. Although higher solubility in water would be expected, ligands **2d** and **2g** were sparingly soluble in water probably due to the heteroaromatic moiety present at the ligands. Therefore, the complexation studies were carried out in acetonitrile, absolute ethanol and/or water-absolute ethanol mixtures, in order to compare the results for all ligands studied. Once again, no interaction was observed upon complexation with Na^+, Ca^{2+} and Zn^{2+} for both ligands, **2d** and **2g**, in the absorption and emission spectra.

In figure 4.5 is represented the Hg^{2+} titration with ligand **2d**, showing that both, ground and excited states, are affected by the complexation and an isosbestic point at 325 nm is observed. In contrast, interaction of Hg^{2+} with compound **2g** affected only the excited state, and in this case the intensity of the emission was reduced in 30%. This result is comparable with the results obtained for compounds **2a** and **2b**, suggesting the importance of the sulphur atom for the sensing of this metal ion, due to its role on the complexation. The values for the complexation constants were calculated and are presented in Table 4.3.

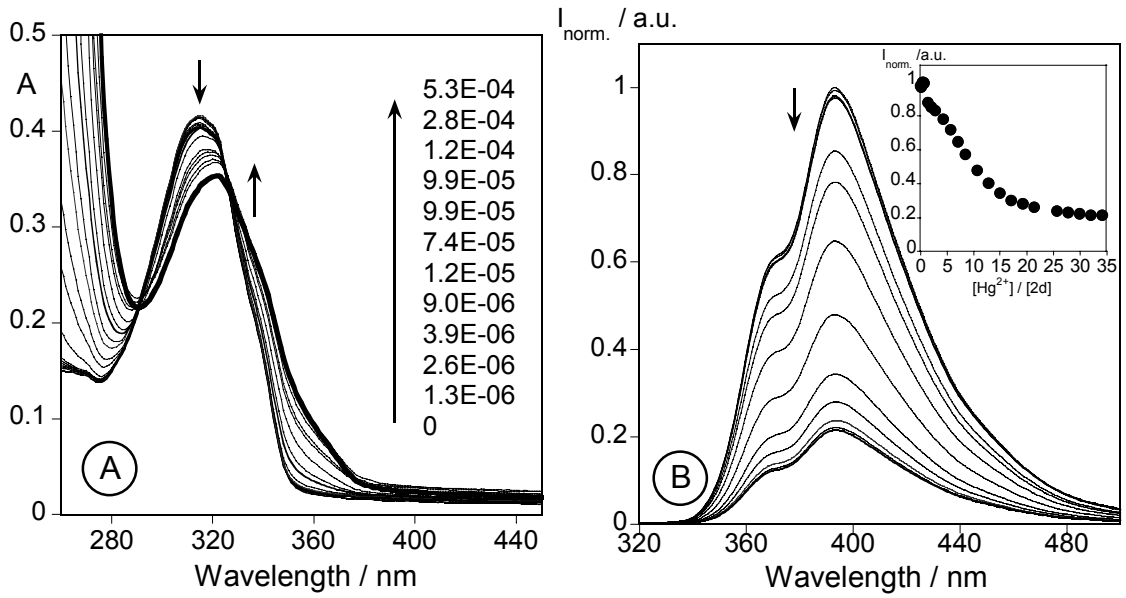

Figure 4.5.- Spectrophotometric titration (A) and fluorimetric titration (B) of an ethanolic solution of **2d** with a standard solution of $Hg(CF_3SO_2)_2$ in absolute ethanol. ([**2d**] = 1.00E-5 M, T = 298 K, λ_{exc} = 315 nm. Inset: normalized emission at 393 nm).

Cu^{2+} and Ni^{2+} complexation are represented in figure 4.6A and 4.6B for ligand **2d**, and in figures 4.7A and 4.7B for ligand **2g.** Stronger interaction with Cu^{2+} was observed in both ligands. Five and two Cu^{2+} equivalents were enough to totally quench the fluorescence emission of **2d** and **2g**, while 40 and 10 equivalents of Ni^{2+}, respectively, were necessary to quench the fluorescence emission to 90%. A dinuclear complex could be postulated by the global log K calculated using the SPECFIT32 programme in the case of Ni^{2+}, and a mononuclear species was postulated for Cu^{2+} (see table 4.3). A schematic drawing of the proposed coordination process is displayed in Scheme 4.2. Firstly, the metal ion binds through the carboxylic acid at the alanine residue with small change in the fluorescence emission, followed by another metal ion interaction at the coordinative site present in the chromophore, which strongly affects the emission spectrum.

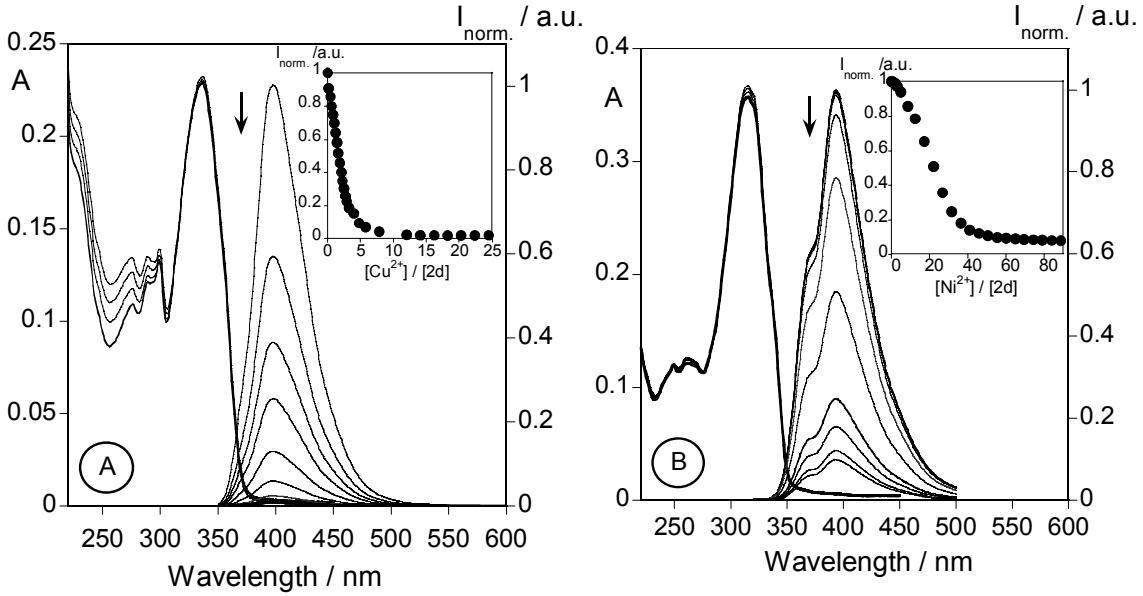

Figure 4.6.- Spectrophotometric titration and fluorimetric titration of an ethanolic solution of **2d** with a standard solution of $Cu(CF_3SO_2)_2$ (A) and $Ni(BF_4)_2$ (B) in absolute ethanol. ([**2d**] = 1.80E-5 M, T = 298 K, λ_{exc} = 315 nm. Insets: normalized emission at 394 nm in both cases).

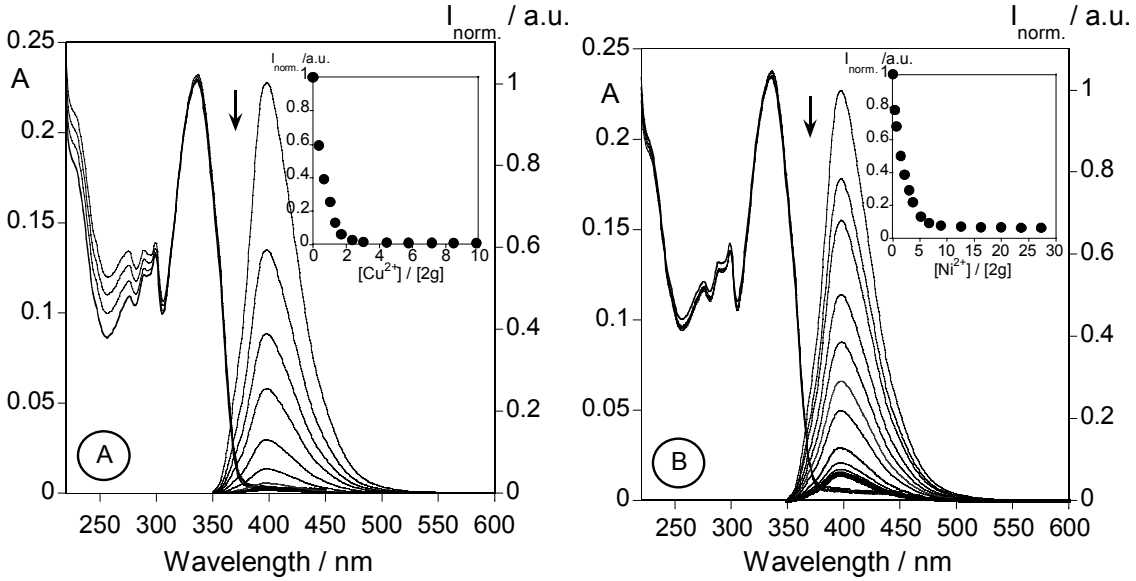

Figure 4.7. - Spectrophotometric titration and fluorimetric titration of an ethanolic solution of **2g** with a standard solution of $Cu(CF_3SO_2)_2$ (A) and $Ni(BF_4)_2$ (B) in absolute ethanol. ([**2g**] = 1.00E-5 M, T = 298 K, λ_{exc} = 336 nm. Inset: normalized emission at 397 and 398 nm, respectively).

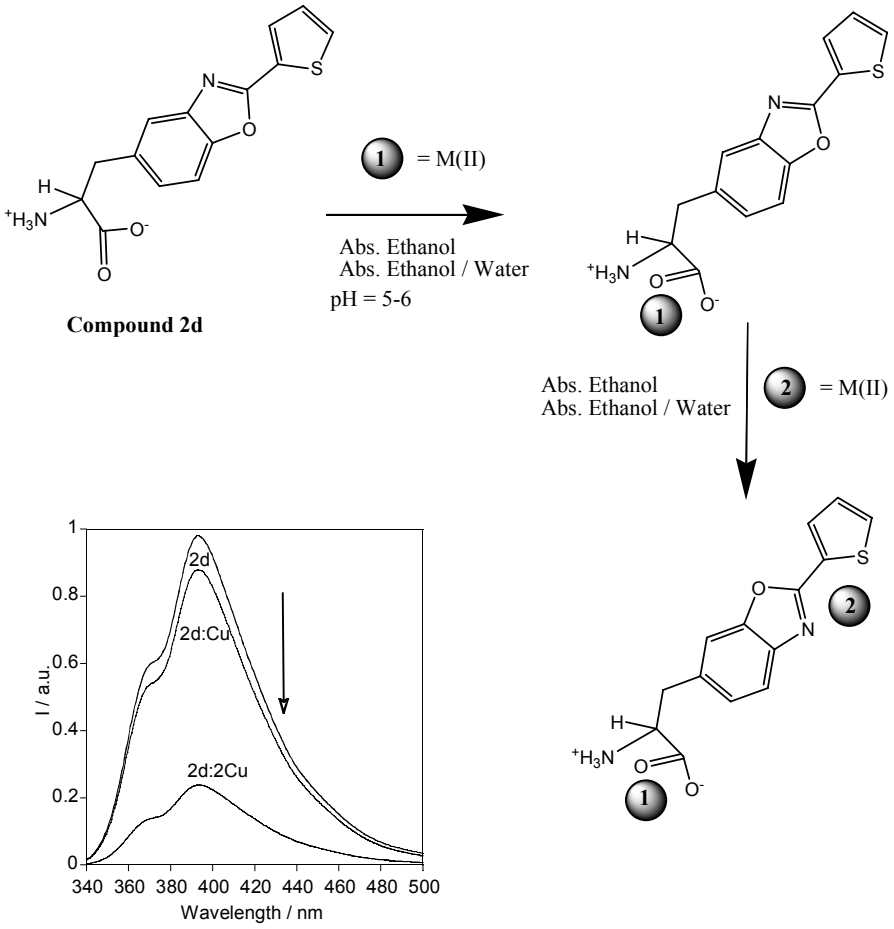

Scheme 4.2. - Schematic representation of the complexation mechanism proposed for alanine **2d** upon complexation with Cu^{2+}, Ni^{2+} and Hg^{2+}. Fluorescence spectra of **2d** in the presence of one and two equivalents of Cu^{2+} in absolute ethanol.

4.5 - Experimental Section

4.5.1 - Synthesis general

All melting points were measured on a Gallenkamp melting point apparatus and are uncorrected. TLC analyses were carried out on 0.25 mm thick precoated silica plates (Merck Fertigplatten Kieselgel $60F_{254}$) and spots were visualised under UV light. Chromatography on silica gel was carried out on Merck Kieselgel (230-240 mesh). IR spectra were determined on a Perkin Elmer FTIR-1600 using KBr discs. UV/visible spectra were run on a Shimadzu UV/2501PC or a Perkin Elmer lamda-35 spectrophotometers. ^{1}H NMR spectra were recorded on a Varian 300 spectrometer in $CDCl_3$ or DMSO-d_6 at 300 MHz at 25 ºC. All chemical shifts are given in ppm using δ_H Me_4Si = 0 ppm as reference and *J* values are given in Hz. ^{13}C NMR spectra were run in the same instrument at 75.4 MHz using the solvent peak as internal reference. Assignments were made by comparison of chemical shifts, peak multiplicities and *J* values and were supported by spin decoupling-double resonance and bidimensional heteronuclear HMBC and HMQC correlation techniques. Mass spectrometry analyses were performed at the "C.A.C.T.I. -Unidad de Espectrometria de Masas", University of Vigo, Spain. Elemental analyses were carried out on a Leco CHNS 932 instrument. Fluorescence spectra were collected using a Perkin Elmer LS45.

3-Nitro-L-tyrosine methyl ester hydrochloride (1a): Thionyl chloride (0.65 mL, 8.85 × 10^{-3} mol) was added drop wise with stirring to methanol (10 mL), cooled in an ice bath, followed by the addition of 3-nitrotyrosine (2.00 g, 8.85 × 10^{-3} mol). The solution was heated at 40 ºC for 5 h. The solvent was evaporated under reduced pressure, yielding a yellowish green solid (2.44 g, quant.). M.p. > 300 ºC [lit. [25] data not quoted]. ^{1}H NMR (DMSO-d_6): δ = 3.11 (d, *J* = 6.3 Hz, 2H, β CH_2), 3.71 (s, 3H, CH_3), 4.30 (t, *J* = 6.6 Hz, 1H, αH), 7.15 (d, *J* = 8.4 Hz, 1H, H-5), 7.38 (dd, *J* = 2.1 and 8.4 Hz, 1H, H-6), 7.78 (d, *J* = 2.1 Hz, 1H, H-2), 8.55 (br s, 3H, $^+NH_3$), 11.08 (br s, 1H, OH) ppm. ^{13}C NMR (DMSO-d_6): δ = 34.26 (β CH_2), 52.75 (CH_3), 52.94 (αC), 119.36 (C5), 125.46 (C1), 126.15 (C2), 136.30 (C3), 136.59 (C6), 151.51 (C4), 169.24 (C=O) ppm. IR (KBr): v = 3388 (br), 3204, 2856, 1746, 1635, 1589, 1544, 1493, 1445, 1390, 1318, 1241, 1064, 990 cm^{-1}.

***N-tert*-Butyloxycarbonyl-3-nitro-L-tyrosine methyl ester (1b)**: Compound **1a** (1.52 g, 5.5 × 10^{-3} mol) was added to 1,4-dioxane (11 mL), water (5.5 mL) and sodium hydroxide 1 M aqueous solution (5.5 mL), with stirring in an ice bath. *t*-Butyl pyrocarbonate (1.36 g, 1.1 eq, 6.05 × 10^{-3} mol) was added and the mixture stirred at room temperature for 2 days. The volume was reduced by half in a rotary evaporator under reduced pressure and ethyl acetate was added to cover the aqueous layer. The mixture was acidified by addition of $KHSO_4$ 1 M

aqueous solution, until acidic pH with congo red paper, and extracted with ethyl acetate (3 × 10 mL), followed by washing of the organic layer with water (3 × 10 mL). The organic layer was dried with anhydrous magnesium sulphate and evaporated under reduced pressure, resulting a yellow solid (1.68 g, 90%). M.p. 97.3-98.4 ºC [lit. [25] 90-91ºC]. ^{1}H NMR ($CDCl_3$): δ = 1.43 (s, 9H, $C(CH_3)_3$), 2.95-3.04 (m, 1H, β CH_2), 3.12-3.22 (m, 1H, β CH_2), 3.76 (s, 3H, CH_3), 4.54-4.60 (m, 1H, αH), 5.07 (d, *J* = 6.6 Hz, 1H, NH), 7.10 (d, *J* = 8.4 Hz, 1H, H-5), 7.37 (dd, *J* = 1.8 and 8.4 Hz, 1H, H-6), 7.87 (d, *J* = 1.8 Hz, 1H, H-2), 10.50 (s, 1H, OH) ppm. ^{13}C NMR ($CDCl_3$) δ = 28.21 ($C(\underline{C}H_3)_3$), 37.23 (β CH_2), 52.51 (CH_3), 54.18 (αC), 80.27 ($\underline{C}(CH_3)_3$), 120.09 (C5), 125.25 (C2), 128.62 (C1), 133.28 (C3), 138.65 (C6), 154.13 (C4 and C=O Boc), 171.69 (C=O ester) ppm. IR (KBr): v = 3335, 3023, 3007, 2984, 2955, 2936, 1732, 1685, 1629, 1578, 1536, 1439, 1324, 1221, 1162, 1061, 994, 838 cm^{-1}.

***N-tert*-Butyloxycarbonyl-3-amino-L-tyrosine methyl ester (1c)**: Compound **1b** (1.00 g, 2.94 × 10^{-3} mol), 1,4-cyclohexadiene (0.5 mL, 1.8 eq, 5.29 × 10^{-3} mol) and Pd/C (147 mg) were dissolved in methanol (15 mL) and refluxed for 24h. The solvent was evaporated and the residue submitted to column chromatography with silica gel (eluent: $CHCl_3$/MeOH, 98:2). The fractions were combined and the product was obtained as a light brown solid (0.92 g, 98%). M.p. 52.0-52.9 ºC [lit. [25] data not quoted]. ^{1}H NMR ($CDCl_3$): δ = 1.43 (s, 9H, $C(CH_3)_3$), 2.92 (d, *J* = 4.8 Hz, 2H, β CH_2), 3.74 (s, 3H, CH_3), 4.47-4.54 (m, 1H, αH), 5.05 (d, *J* = 8.4 Hz, 1H, NH), 6.37 (dd, *J* = 2.1 and 8.1 Hz, 1H, H-6), 6.53 (d, *J* = 2.1 Hz, 1H, H-2), 6.64 (d, *J* = 8.1 Hz, 1H, H-5) ppm. ^{13}C NMR ($CDCl_3$) δ = 28.27 ($C(\underline{C}H_3)_3$), 37.64 (β CH_2), 52.21 (CH_3), 54.57 (αC), 80.11 ($\underline{C}(CH_3)_3$), 115.30 (C5), 117.33 (C2), 119.89 (C6), 128.32 (C1), 134.65 (C3), 143.33 (C4), 155.36 (C=O Boc), 172.78 (C=O ester) ppm. IR (KBr): v = 3376, 3005, 2955, 1738, 1694, 1615, 1520, 1505, 1454, 1441, 1393, 1368, 1288, 1251, 1217, 1164, 1059, 1022, 912, 861, 799, 758 cm^{-1}. MS (FAB): *m/z* (%) = 311 (M^+ + H, 41), 310 (M^+, 100), 307 (20), 255 (59), 254 (47), 211 (57), 193 (27) 155 (24), 154 (83). HRMS (FAB): calcd. for $C_{15}H_{23}N_2O_5$ 311.1607, found 311.1568.

***N-tert*-Butyloxycarbonyl-3-[(thien-2'-ylmethylene)amino]-L-tyrosine methyl ester (1d)**: Compound **1c** (0.54 g, 1.74 × 10^{-3} mol) was stirred with 2-formylthiophene (0.16 mL, 1.76 × 10^{-3} mol) in absolute ethanol (5 mL) for 5 days. The solvent was evaporated and the crude residue was used in the next step without further purification, as light yellow oil (0.68 g, 98%). ^{1}H NMR ($CDCl_3$): δ = 1.42 (s, 9H, $C(CH_3)_3$), 2.98-3.10 (m, 2H, β CH_2), 3.72 (s, 3H, CH_3), 4.52-4.60 (m, 1H, αH), 5.02 (d, *J* = 7.80 Hz, 1H, NH), 6.90-6.95 (m, 2H, H-2 + H-6), 7.05 (br s, 1H, H-5), 7.14-7.17 (m, 1H, H-4'), 7.51-7.55 (m, 2H, H-3' + H-5'), 8.76 (s, 1H, N=CH) ppm. ^{13}C NMR ($CDCl_3$) δ = 28.28 ($C(\underline{C}H_3)_3$), 37.84 (β CH_2), 52.23 (CH_3), 54.55 (αC), 79.99 ($\underline{C}(CH_3)_3$), 114.99 (C2), 116.54 (C5), 127.56 (C1), 127.99 (C4'), 129.46 (C6), 130.82 (C3' or C5'), 132.59 (C3' or C5'), 134.98 (C3), 142.73 (C2'), 149.88 (CH), 151.15 (C4),

155.09 (C=O Boc), 172.41 (C=O ester) ppm. IR (KBr): v = 3375, 2981, 2930, 1754, 1682, 1617, 1602, 1513, 1500, 1430, 1392, 1367, 1295, 1253, 1217, 1165, 1047, 1025, 855, 814 cm^{-1}. MS (FAB): *m/z* (%) = 405 (M^+ + H, 40), 350 (22), 349 (100), 216 (33). HRMS (FAB): calcd. for $C_{20}H_{25}N_2O_5S$ 405.1484, found 405.1488.

***N-tert*-Butyloxycarbonyl-3-[(2',4',5'-trimethoxyphenylmethylene)amino]-L-tyrosine methyl ester (1e)**: Compound **1c** (0.365 g, 1.18 × 10^{-3} mol) was stirred with 2,4,5-trimethoxybenzaldehyde (0.231 g, 1.18 × 10^{-3} mol) in absolute ethanol (5 mL) for 3 days. The solvent was evaporated and the residue was used in the next step without further purification as brown oil (0.56 g, 97%). ^{1}H NMR ($CDCl_3$): δ = 1.52 (s, 9H, $C(CH_3)_3$), 2.97-3.05 (m, 2H, β CH_2), 3.88 (s, 3H, OCH_3), 3.93 (s, 3H, OCH_3), 3.97 (s, 3H, OCH_3), 4.50-4.58 (m, 1H, α-H), 5.00 (d, *J* = 8.4 Hz, 1H, NH), 6.53 (s, 1H, H-3'), 6.88-6.94 (m, 2H, H-2 + H-6), 6.99 (br s, 1H, H-5), 7.63 (s, 1H, H-6'), 9.01 (s, 1H, N=CH) ppm. ^{13}C NMR ($CDCl_3$) δ = 28.40 ($C(\underline{C}H_3)_3$), 38.02 (β CH_2), 52.27 (CH_3), 54.65 (αC), 80.06 ($\underline{C}(CH_3)_3$), 100.12 (C3'), 106.33 (C1'), 115.11 (C2), 115.71 (C6'), 116.33 (C5), 127.71 (C1), 129.76 (C6), 135.12 (C3), 135.79 (C5'), 144.76 (C4'), 149.79 (CH), 151.18 (C4), 152.06 (C2'), 155.01 (C=O Boc), 172.23 (C=O ester) ppm. IR (KBr): v = 3430 (br), 2956, 2927, 2854, 1741, 1708, 1611, 1596, 1510, 1466, 1439, 1412, 1366, 1340, 1280, 1210, 1165, 029, 811 cm^{-1}. MS (FAB): *m/z* (%) = 489 (M^+ + H, 53), 434 (31), 349 (100). HRMS (FAB): calcd. for $C_{25}H_{33}N_2O_8$ 489.2238, found 489.2252.

***N-tert*-Butyloxycarbonyl [2-(thien-2'-yl)benzoxazol-5-yl]-L-alanine methyl ester (2a)**: The crude imine **1d** (0.70 g 1.74 × 10^{-3} mol) and lead tetraacetate (1.17 g, 2.64 × 10^{-3} mol) were stirred at room temperature in DMSO (5 mL) for 3 days. The mixture was poured over water and extracted with ethyl acetate (3 × 10 mL). After drying with anhydrous magnesium sulphate and evaporation of the solvent, the resulting brown oil was submitted to column chromatography with silica gel (eluent: dichloromethane). The product was isolated as a light yellow solid (0.39 g, 56%). M.p. 106.6-107.8 ºC. ^{1}H NMR ($CDCl_3$): δ = 1.42 (s, 9H, $C(CH_3)_3$), 3.15-3.28 (m, 2H, β CH_2), 3.73 (s, 3H, CH_3), 4.61-4.67 (m, 1H, αH), 5.04 (d, *J* = 7.8 Hz, 1H, NH), 7.10 (dd, *J* = 1.8 and 8.4 Hz, 1H, H-6), 7.17-7.20 (m, 1H, H-4'), 7.45 (d, *J* = 8.4 Hz, 1H, H-7), 7.48 (d, *J* = 1.8 Hz, 1H, H-4), 7.56 (dd, *J* = 1.2 and 5.1 Hz, 1H, H-5'), 7.90 (dd, *J* = 1.2 and 3.9 Hz, 1H, H-3') ppm. ^{13}C NMR ($CDCl_3$) δ = 28.24 ($C(\underline{C}H_3)_3$), 38.27 (β CH_2), 52.29 (CH_3), 54.57 (αC), 80.00 ($\underline{C}(CH_3)_3$), 110.26 (C7), 120.31 (C4), 126.32 (C6), 128.24 (C4'), 129.50 (C2), 129.97 (C3'), 130.31 (C5'), 132.79 (C5), 142.28 (C3a), 149.59 (C7a), 155.04 (C=O Boc), 159.41 (C2'), 172.08 (C=O ester) ppm. IR (KBr): v = 3358, 2982, 2928, 1734, 1693, 1573, 1526, 1475, 1438, 1369, 1289, 1244, 1172, 1052, 1021, 857 cm^{-1}. UV/Vis (ethanol, nm): λ_{max} (ε) = 315 (2.13 × 10^4). MS (FAB): *m/z* (%) = 403 (M^+ + H, 73), 348 (23), 347 (100), 243 (29), 215 (27), 185 (21). HRMS (FAB): calcd. for $C_{20}H_{23}N_2O_5S$ 403.1328,

found 403.1324. $C_{20}H_{22}N_2O_5S$: calcd. C 59.69, H 5.51, N 6.96, S 7.97; found C 59.44, H 5.63, N 6.69, S 7.66.

***N-tert*-Butyloxycarbonyl [2-(thien-2'-yl)benzoxazol-5-yl]-L-alanine (2b)**: Compound **2a** (0.062 g, 1.54 × 10^{-4} mol) was dissolved in 1,4-dioxane (1 mL), in an ice bath, and sodium hydroxide 1 M aqueous solution (0.23 mL, 2.3 × 10^{-4} mol, 1.5 eq) was added drop wise. The mixture was stirred at room temperature for 3h. The pH was adjusted to 2-3 by addition of $KHSO_4$ 1 M aqueous solution and extracted with ethyl acetate (3 × 10 mL). After drying with anhydrous magnesium sulphate and evaporation of the solvent, the residue was triturated with diethyl ether and a off-white solid was obtained (0.050 g, 84%). M.p. 153.5-154.0 ºC. ^{1}H NMR ($CDCl_3$): δ = 1.46 (s, 9H, $C(CH_3)_3$), 3.30-3.36 (m, 2H, β CH_2), 4.68-4.73 (m, 1H, αH), 5.17 (d, *J* = 7.5 Hz, 1H, NH), 7.16-7.22 (m, 2H, H-6 + H-4'), 7.48 (d, *J* = 8.4 Hz, 1H, H-7), 7.57 (dd, *J* = 1.2 and 5.1 Hz, 1H, H-5'), 7.63 (d, *J* = 2.1 Hz, 1H, H-4), 7.93 (dd, *J* = 1.2 and 3.9 Hz, 1H, H-3') ppm. ^{13}C NMR ($CDCl_3$) δ = 28.31 ($C(\underline{C}H_3)_3$), 37.63 (β CH_2), 54.46 (αC), 80.14 ($\underline{C}(CH_3)_3$), 110.34 (C7), 120.03 (C4), 127.05 (C6), 128.43 (C4'), 128.67 (C2), 130.73 (C3'), 130.84 (C5'), 133.24 (C5), 141.26 (C3a), 149.35 (C7a), 155.31 (C=O Boc), 159.49 (C2'), 174.66 (COOH) ppm. IR (KBr): ν = 3357, 3113, 2998, 2929, 1752, 1691, 1569, 1527, 1479, 1418, 1371, 1327, 1281, 1252, 1213, 1168, 1051, 856 cm^{-1}. UV/Vis (ethanol, nm): λ_{max} (ε) = 316 (2.73 × 10^4). MS (FAB): *m/z* (%) = 389 (M^+ + H, 57), 333 (45), 185 (100). HRMS (FAB): calcd. for $C_{19}H_{21}N_2O_5S$ 389.1171, found 389.1173.

[2-(Thien-2'-yl)benzoxazol-5-yl]-L-alanine methyl ester (2c): Compound **2a** (0.103 g, 2.56 × 10^{-4} mol) was stirred in a trifluoroacetic acid/dichloromethane solution (1:1, 1 mL) at room temperature for 2h. The solvent was evaporated, the solid residue dissolved in pH 8 aqueous buffer solution and extracted with ethyl acetate (3 × 10 mL). After drying with anhydrous magnesium sulphate and evaporation of the solvent, the product was isolated as a light yellow solid (0.054 g, 74%). M.p. 80.7-81.4 ºC. ^{1}H NMR ($CDCl_3$): δ = 1.46 (s, 9H, $C(CH_3)_3$), 2.98-3.06 (m, 1H, β CH_2), 3.17-3.24 (m, 1H, β CH_2), 3.74 (s, 3H, CH_3), 3.77-3.82 (m, 1H, αH), 7.17-7.22 (m, 2H, H-6 + H-4'), 7.49 (d, *J* = 8.4 Hz, 1H, H-7), 7.56-7.59 (m, 2H, H-5' + H-4), 7.91 (dd, *J* = 1.5 and 3.9 Hz, 1H, H-3') ppm. ^{13}C NMR ($CDCl_3$) δ = 40.77 (β CH_2), 52.07 (CH_3), 55.92 (αC), 110.25 (C7), 120.18 (C4), 126.33 (C6), 128.24 (C4'), 129.51 (C2), 129.97 (C3'), 130.31 (C5'), 133.85 (C5), 142.33 (C3a), 149.49 (C7a), 159.41 (C2'), 175.12 (C=O ester) ppm. IR (KBr): ν = 3310, 2925, 1741, 1590, 1478, 1415, 1325, 1260, 1063, 855 cm^{-1}. UV/Vis (ethanol, nm): λ_{max} (ε) = 315 (3.07 × 10^4). MS (FAB): *m/z* (%) = 303 (M^+ + H, 100), 215 (20). HRMS (FAB): calcd. for $C_{15}H_{15}N_2O_3S$ 303.0803, found 303.0803.

[2-(Thien-2'-yl)benzoxazol-5-yl]-L-alanine (2d): Compound **2b** (0.100 g, 2.58 × 10^{-4} mol) was stirred in a trifluoroacetic acid/dichloromethane solution (1:1, 1 mL) at room temperature

for 2h. The solvent was evaporated, the solid residue dissolved in pH 8 aqueous buffer solution and extracted with ethyl acetate (3 × 10 mL). After drying with anhydrous magnesium sulphate and evaporation of the solvent, the product was isolated as a light brown solid (0.040 g, 54%). M.p. 238.9-239.9 ºC. ^{1}H NMR (DMSO-d_6): δ = 2.94-3.02 (m, 1H, β CH_2), 3.23-3.30 (m, 1H, β CH_2), 3.46-3.51 (m, 1H, αH), 7.28-7.31 (m, 2H, H-6 + H-4'), 7.62-7.67 (m, 2H, H-7 + H-5'), 7.93-7.96 (m, 2H, H-3' + H-4) ppm. ^{13}C NMR (DMSO-d_6) δ = 30.40 (β CH_2), 53.01 (αC), 109.92 (C5'), 119.40 (C7), 126.57 (C6), 128.50 (C4'), 129.72 (C2), 130.03 (C4), 131.38 (C3'), 132.34 (C5), 141.36 (C3a), 151.70 (C7a), 159.50 (C2'), 180.83 (C=O) ppm. IR (KBr): ν = 3413, 3072, 2940, 1620, 1572, 1548, 1479, 1407, 1346, 1312, 1287, 1269, 1217, 1195, 1160, 1049, 1024, 1005, 872, 853 cm^{-1}. UV/Vis (ethanol, nm): λ_{max} (ε) = 315 (2.17 × 10^4). MS (FAB): *m/z* (%) = 289 (M^+ + H, 30), 278 (22), 277 (21), 186 (71). HRMS (FAB): calcd. for $C_{14}H_{13}N_2O_3S$ 289.0646, found 289.0647.

***N-tert*-Butyloxycarbonyl-3-[2-(2',4',5'-trimethoxyphenyl)benzoxazol-5-yl]-L-alanine methyl ester (2e)**: The crude imine **1e** (0.470 g, 9.63 × 10^{-4} mol) and lead tetraacetate (0.640 g, 1.44 × 10^{-3} mol, 1.5 eq.) were stirred at room temperature in DMSO (5 mL) for 3 days. The mixture was poured over water and extracted with ethyl acetate (3 × 10 mL). After drying with anhydrous magnesium sulphate and evaporation of the solvent, the resulting brown oil was submitted to column chromatography with silica gel (eluent: chloroform). The product was isolated as light brown oil (0.304 g, 65%) [lit. [27] M.p. 137-140 ºC]. ^{1}H NMR ($CDCl_3$): δ = 1.43 (s, 9H, $C(CH_3)_3$), 3.22 (d, *J* = 4.2 Hz, 2H, β CH_2), 3.74 (s, 3H, CH_3), 3.97 (s, 3H, OCH_3), 4.00 (s, 3H, OCH_3), 4.02 (s, 3H, OCH_3), 4.62-4.66 (m, 1H, α-H), 5.01 (d, *J* = 8.1 Hz, 1H, NH), 6.66 (s, 1H, H-3'), 7.08 (dd, *J* = 1.8 and 8.4 Hz, 1H, H-6), 7.45 (d, *J* = 8.4 Hz, 1H, H-7), 7.50 (d, *J* = 1.8 Hz, 1H, H-4) 7.65 (s, 1H, H-6') ppm. UV/Vis (ethanol, nm): λ_{max} (ε) = 334 (1.41 × 10^4). MS (FAB): *m/z* (%) = 489 (M^+ + H, 100), 488 (21), 433 (14), 300 (38), 154 (14). HRMS (FAB): calcd. for $C_{25}H_{33}N_2O_8$ 489.2237, found 489.2238.

***N-tert*-Butyloxycarbonyl-3-[2-(2',4',5'-trimethoxyphenyl)benzoxazol-5-yl]-L-alanine (2f)**: Compound **2e** (0.060 g, 1.23 × 10^{-4} mol) was dissolved in 1,4-dioxane (1 mL), in an ice bath, and sodium hydroxide 1 M aqueous solution (0.19 mL, 1.9 × 10^{-4} mol, 1.5 eq) was added drop wise. The mixture was stirred at room temperature for 3h. The pH was adjusted to 2-3 by addition of $KHSO_4$ 1 M aqueous solution and extracted with ethyl acetate (3 × 10 mL). After drying with anhydrous magnesium sulphate and evaporation of the solvent, the residue was triturated with diethyl ether and a brown solid was obtained (0.048 g, 82%). M.p. 135.5-137.0 ºC. ^{1}H NMR ($CDCl_3$): δ = 1.45 (s, 9H, $C(CH_3)_3$), 3.30-3.34 (m, 2H, β CH_2), 3.94 (s, 3H, OCH_3), 3.97 (s, 3H, OCH_3), 3.98 (s, 3H, OCH_3), 4.64-4.68 (m, 1H, α-H), 5.12 (d, *J* = 8.4 Hz, 1H, NH), 6.62 (s, 1H, H-3'), 7.18 (dd, *J* = 1.5 and 8.4 Hz, 1H, H-6), 7.50 (d, *J* = 8.4 Hz, 1H, H-7), 7.60 (s, 1H, H-6'), 7.66 (s, 1H, H-4) ppm. ^{13}C NMR ($CDCl_3$) δ = 28.36

(C($\underline{C}H_3)_3$), 37.67 (β CH_2), 54.46 (αC), 80.20 ($\underline{C}(CH_3)_3$), 100.35 (C3'), 106.43 (C1'), 110.35 (C7), 114.95 (C6'), 120.15 (C4), 126.96 (C6), 128.90 (C2), 133.34 (C5), 135.93 (C5'), 141.18 (C3a), 145.02 (C4'), 149.54 (C7a), 152.26 (C2'), 155.40 (C=O Boc), 174.48 (COOH) ppm. IR (KBr): v = 3340, 3108, 2988, 2930, 1761, 1684, 1569, 1527, 1420, 1377, 1343, 1265, 1250, 1178, 1049, 850 cm^{-1}. UV/Vis (ethanol, nm): λ_{max} (ε) = 334 (1.75 × 10^4). MS (FAB): *m/z* (%) = 473 (M^+ + H, 34), 472 (M^+, 16), 417 (16), 307 (17), 195 (21), 155 (27), 154 (100). HRMS (FAB): calcd. for $C_{24}H_{29}N_2O_8$ 473.1924, found 473.1935.

3-[2-(2',4',5'-Trimethoxyphenyl)benzoxazol-5-yl]-L-alanine (2g): Compound **2f** (0.035 g, 7.41 × 10^{-5} mol) was stirred in a trifluoroacetic acid/dichloromethane solution (1:1, 1 mL) at room temperature for 2h. The solvent was evaporated, the solid residue dissolved in pH 8 aqueous buffer solution and extracted with ethyl acetate (3 × 10 mL). After drying with anhydrous magnesium sulphate and evaporation of the solvent, the product was isolated as an off-white solid (0.012 g, 44%). M.p. 251.6-253.3 ºC. ^{1}H NMR (DMSO-d_6): δ = 2.94-3.02 (m, 1H, β CH_2), 3.23-3.30 (m, 1H, β CH_2), 3.46-3.51 (m, 1H, αH), 4.05 (s, 3H, OCH_3), 4.11 (s, 3H, OCH_3), 4.14 (s, 3H, OCH_3), 7.28-7.31 (m, 2H, H-6 + H-3'), 7.60 (d, *J* = 8.4 Hz, 1H, H-7), 7.65 (s, 1H, H-6'), 7.95 (br s, 1H, H-4) ppm. ^{13}C NMR (DMSO-d_6) δ = 30.28 (β CH_2), 53.11 (αC), 101.30 (C3'), 105.99 (C1'), 115.34 (C6'), 119.43 (C7), 126.35 (C6), 129.82 (C2), 130.06 (C4), 132.55 (C5), 135.41 (C5'), 141.34 (C3a), 145.13 (C4'), 151.57 (C7a), 152.25 (C2'), 180.88 (C=O) ppm. IR (KBr): v = 3400, 3052, 2954, 1618, 1570, 1490, 1350, 1325, 1307, 1250, 1198, 1163, 1057, 1030, 1001, 853 cm^{-1}. UV/Vis (ethanol, nm): λ_{max} (ε) = 336 (2.29 × 10^4). MS (FAB): *m/z* (%) = 373 (M^+ + H, 30), 372 (M^+, 43), 278 (100), 186 (51). HRMS (FAB): calcd. for $C_{19}H_{21}N_2O_6$ 373.1401, found 372.1395.

4.5.2 - Spectrofluorimetric titrations

The linearity of the fluorescence emission *vs.* concentration was checked in the concentration range used (10^{-4}-10^{-6} M). A correction for the absorbed light was performed when necessary. All spectrofluorimetric titrations were performed as follows: stock solutions of compounds **2a-g** (*ca.* 10^{-3} M) were prepared in the corresponding solvents (absolute ethanol, acetonitrile, dioxane or cyclohexane, all of UVA-sol or HPLC grade) and used in the preparation of titration solutions by appropriate dilution. Titration of compounds **2a-g** was carried out by addition of microliter amounts of standard solutions of the ions in acetonitrile or absolute ethanol. Protonation and deprotonation studies were performed by addition of HBF_4, methanesulphonic acid, triethylamine and tetrabutylammonium hydroxide. $Cu(CF_3SO_3)_2$, $Ni(BF_4)_2$, $Zn(CF_3SO_3)_2$, $Hg(CF_3SO_3)_2$, $Ca(ClO_4)_2$ and $NaNO_3$ were purchased from Alfa Aesar and used as received. Luminescence quantum yields were measured using as standard a solution of 1-naphthylamine in cyclohexane (0.1 M) (Φ_F = 0.46) [34], and were corrected for

different refractive indexes of solvents. In all fluorimetric measurements the optical density did not exceed 0.1 [35].

4.6 - Acknowledgements

Thanks are due to Foundation for Science and Technology (Portugal) for financial support through Centro de Química (UM) and REQUIMTE (UNL) through project PTDC/QUI/66250/2006.

4.7 - References

1. Rida, S. M.; Ashour, F. A.; El-Hawash, S. A. M.; ElSemary, M. M.; Badr, M. H.; Shalaby, M. A. Synthesis of some novel benzoxazole derivatives as anticancer, anti-HIV-1 and antimicrobial agents. *Eur. J. Med. Chem*. **2005**, *40*, 949 and references cited therein.
2. Okamura, N.; Suemoto, T.; Shimazu, H.; Suzuki, M.; Shiomitsu, T.; Akatsu, H.; Yamamoto, T.; Staufenbiel, M.; Yanai, K.; Arai, H.; Sasaki, H.; Kudo, Y.; Sawada, T. Styrylbenzoxazole Derivatives for *In Vivo* Imaging of Amyloid Plaques in the Brain. *J. Neurosci.* **2004**, *24*, 2535.
3. Allagile, D.; Baldwin, R. M.; Tamagnan, G. D. One-step synthesis of 2-arylbenzothiazole ('BTA') and -benzoxazole precursors for in vivo imaging of β-amyloid plaques. *Tetrahedron Lett.* **2005**, *46*, 1349.
4. Leopoldo, M.; Lacivita, E.; De Giorgio, P.; Colabufo, N. A.; Niso, M.; Berardi, F.; Perrone, R. Design, Synthesis, and Binding Affinities of Potential Positron Emission Tomography (PET) Ligands for Visualization of Brain Dopamine D_3 Receptors. *J. Med. Chem.* **2006**, *49*, 358.
5. Aquilina, J. A.; Carver, J. A.; Truscott, R. J. W. Polypeptide Modification and Cross-Linking by Oxidized 3-Hydroxykynurenine. *Biochemistry* **2000**, *39*, 16176.
6. McGrath, M. E.; Sprengeler, P. A.; Hill, C. M.; Martichonok, V.; Cheung, H.; Somoza, J. R.; Palmer, J. T.; Janc, J. W. Peptide Ketobenzoxazole Inhibitors Bound to Cathepsin K. *Biochemistry* **2003**, *42*, 15018.
7. Lima, P. G.; Caruso, R. R. B.; Alves, S. O.; Pessôa, R. F.; Mendonça-Silva, D. L.; Nunes, R. J.; Nöel, F.; Castro, N. G.; Costa, P. R. R. Stereoselective synthesis and preliminary evaluation of new D-3-heteroarylcarbonylalanines as ligands of the NMDA receptor. *Bioorg. Med. Chem. Lett.* **2004**, *14*, 4399.
8. Cagnoli, R.; Lanzi, M.; Mucci, A.; Parenti, F.; Schenetti, L. Polymerization of cysteine functionalized thiophenes. *Polymer*, **2005**, *46*, 3588 and references cited therein.
9. Wang, Y.; Wang, K.; Liu, W.; Shen, G.; Yu, R. Optical Chemical Sensors for Pharmaceutical Analysis Using 1,4-Bis(1,3-benzoxazol-2-yl)benzene as Sensing Material. *Analyst* **1997**, *122*, 69 and references cited therein.

10. Taki, M.; Wolford, J. L.; O´Halloran, T. V. Emission Ratiometric Imaging of Intracellular Zinc: Design of a Benzoxazole Fluorescent Sensor and Its Application in Two-Photon Microscopy. *J. Am. Chem. Soc*. **2003**, *126*, 712.
11. Shamsipur, M.; Poursaberi, T.; Karami, A. R.; Hosseini, M.; Momeni, A.; Alizadeh, N.; Yousefi, M.; Ganjali, M. R. Development of a new fluorimetric bulk optode membrane based on 2,5-thiophenylbis(5-tert-butyl-1,3-benzexazole) for nickel(II) ions. *Anal. Chim. Acta* **2004**, *501*, 55.
12. Ohshima, A.; Momotake, A.; Arai, T. A new fluorescent metal sensor with two binding moieties. *Tetrahedron Lett*. **2004**, *45*, 9377.
13. Lee, J. K.; Na, J.; Kim, T. H.; Kim, Y.-S.; Park, W. H.; Lee, T. S. Synthesis of polyhydroxybenzoxazole-based colorimetric chemosensor for anionic species. *Mat. Sci. Eng. C- Bio S* **2004**, *24*, 261.
14. Guzow, K.; Milewska, M.; Wróblewski, D.; Gieldón, A.; Wiczk, W. 3-[2-(8-Quinolinyl)benzoxazol-5-yl]alanine derivative - a specific fluorophore for transition and rare-earth metal ion detection. *Tetrahedron* **2004**, *60*, 11889.
15. Milewska, M.; Skwierawska, A.; Guzow, K.; Szmigiel, D.; Wiczk, W. 3-[2-(2-Quinoxalinyl)benzoxazol-5-yl]alanine derivative – A specific fluoroionophore for Ni(II). *Inorg. Chem. Commun.* **2005**, *8*, 947.
16. Ohshima, A.; Momotake, A.; Arai, T. Photochemical and complexation studies for new fluorescent and colored chelator. *Sci. Tech. Adv. Mat.* **2005**, *6*, 633.
17. Zang, X.-B.; Peng, J.; He, C.-L.; Shen, G.-L.; Yu, R.-Q. A highly selective fluorescent sensor for Cu^{2+} based on 2-(2′-hydroxyphenyl)benzoxazole in a poly(vinyl chloride) matrix. *Anal. Chim. Acta* **2006**, *567*, 189.
18. Batista, R. M. F.; Costa, S. P. G.; Raposo, M. M. M. Synthesis of new fluorescent 2-(2',2''-bithienyl)-1,3-benzothiazoles. *Tetrahedron Lett*. 2004, 45(13), 2825.
19. Costa, S. P. G.; Batista, R. M. F.; Cardoso, P.; Belsley, M.; Raposo, M. M. M. 2-Arylthienyl-substituted 1,3-benzothiazoles as new nonlinear optical chromophores. *Eur. J. Org. Chem.* **2006**, *17*, 3938.
20. Costa, S. P. G.; Batista, R. M. F.; Sousa, A. M. R. C.; Raposo, M. M. M. New fluorescent heterocyclic materials: synthesis, solvatochromic and fluorescence properties. *Mater. Sci. Forum* **2006**, *514-516*, 147.
21. Batista, R. M. F.; Costa, S. P. G.; Malheiro, E. L.; Belsley, M.; Raposo, M. M. M. Synthesis and characterization of new thienylpyrrolyl-benzothiazoles as efficient and thermally stable nonlinear optical chromophores. *Tetrahedron* **2007**, *63*(20), 4258-4265.
22. Pina, J.; Seixas de Melo, J.; Burrows, H. D.; Batista, R. M. F.; Costa, S. P. G.; Raposo, M. M. M. Spectral and photophysical characterization of donor-π-acceptor arylthienyl- and bithienyl-benzothiazole derivatives in solution and solid state. *J. Phys. Chem. A*, **2007**, *111*, 8574-8578.
23. Batista, R. M. F.; Costa, S. P. G.; Belsley, M.; Raposo, M. M. M. Synthesis and second-order nonlinear optical properties of new chromophores containing benzimidazole, thiophene and pyrrole heterocycles. *Tetrahedron*, **2007**, *63* (39), 9842-9849.

24. Batista, R. M. F.; Oliveira, E.; Costa, S. P. G.; Lodeiro, C.; Raposo, M. M. M. Synthesis and ion sensing properties of new colorimetric and fluorimetric chemosensors based on bithienyl-imidazo-anthraquinone chromophores. *Org. Lett*., **2007**, *9* (17), 3201-3204.
25. Guzow, K.; Szabelski, M.; Malicka, J.; Wiczk, W. Synthesis of a new, highly fluorescent amino acid derivative: N-[(tert-butoxy)carbonyl]-3-[2-(1H-indol-3-yl)benzoxazol-5-yl]-l-alanine methyl ester. *Helv. Chim. Acta* **2001**, *84*, 1086 and references cited therein.
26. Stephens, F. F.; Bower, J. D. The preparation of benziminazoles and benzoxazoles from Schiff's bases. Part I. *J. Chem. Soc*. **1949**, 2971.
27. Guzow, K.; Zielińska, J.; Mazurkiewicz, K.; Karolczak, J.; Wiczk, W. Influence of substituents in the phenyl ring on photophysical properties of 3-[2-(phenyl)benzoxazol-5-yl]alanine derivatives. *J. Photochem. Photobiol. A* **2005**, *175*, 57.
28. Czarnik, A. W. *Fluorescent Chemosensors for Ion and Molecule Recognition*; American Chemical Society: Washington, DC, 1993.
29. de Silva, A. P.; Gunaratne, H. Q. N.; Gunnlaugsson, T.; Huxley, A. J. M.; McCoy, C. P.; Rademacher, J. T.; Rice, T. E. Signaling Recognition Events with Fluorescent Sensors and Switches. *Chem. Rev.* **1997**, *97*, 1515.
30. Valeur, B. *Molecular Fluorescence. Principles and Applications*; Wiley-VCH: Weinheim, 2002.
31. Rurack, K. Flipping the light switch 'ON' – the design of sensor molecules that show cation-induced fluorescence enhancement with heavy and transition metal ions. *Spect. Acta A* **2001**, *57*, 2161.
32. Pearson, R. G. Hard and Soft Acids and Bases. *J. Am. Chem. Soc*. **1963**, *85*, 3533.
33. SPECFIT/32 Global Analysis System, v. 3.0 Spectrum Software Associates, Malborough, MA, USA.
34. Berlman, B. *Handbook of Fluorescence Spectra of Aromatic Molecules*, 2nd ed., Academic Press: New York, 1971.
35. Lakowicz, J. R. *Principles of Fluorescence Spectroscopy*, 2nd ed., Kluwer Academic/Plenum Publisher: New York, 1999.

Chapter 5

Heteroaromatic alanine derivatives bearing (oligo)thiophene units: synthesis and photophysical properties

Susana P. G. Costa, Elisabete Oliveira, M. Manuela M. Raposo, Carlos Lodeiro, *Tetrahedron Letters,* **2008**, 49, 5258-5261.

"Success is the ability to go from one failure to another with no loss of enthusiasm"
Sir Winston Churchill, 1874-1965
Nobel Prize in Literature, 1953.

Index

5.1 - Graphical Abstract

New fluorescent benzoxazolylalanine derivatives bearing (oligo)thiophene units at the side chain were synthesized in good yields. Evaluation of the photophysical properties of the syntethized amino acids revealed that some of the derivatives display high fluorescent quantum yields, making them good candidates for application as fluorescent probes.

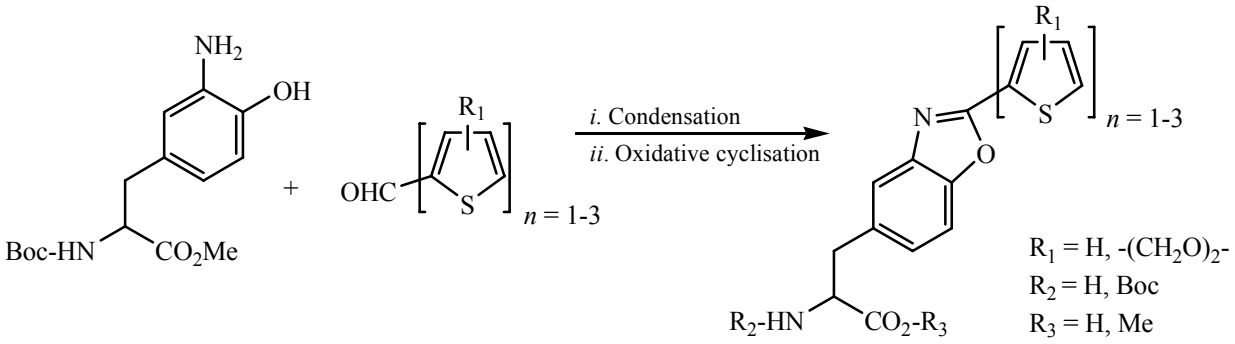

5.2 - Abstract

A series of new benzoxazolylalanine derivatives bearing (oligo)thiophene units at the side chain were synthesized in good yields. The photophysical characterization of these amino acids was performed by UV-vis absorption and fluorescence emission studies and revealed that some of the compounds display high fluorescent quantum yields, making them good candidates for application as fluorescent probes.

My contribution for this work was all photophysical studies.

5.3 - Resumo

Foram sintetizados, com um bom rendimento, uma série de novos derivados de benzoxazolilalanina contendo na cadeia lateral unidades de oligo(tiofenos). A caracterização fotofísica destes aminoácidos foi efectuada por estudos de absorção UV-vis e emissão de fluorescência e revelaram que alguns compostos têm um elevado rendimentos quântico de fluorescência, tornando-os portanto, bons candidatos para a aplicação como sondas fluorescentes.

A minha contribuição para este trabalho consistiu na realização de todos os estudos fotofísicos.

5.4 - Introduction

The insertion of coded and unnatural amino acids into the backbone of both natural and synthetic polymers is a very appealing area of research since it can lead to the development of macromolecules possessing biomimetic characteristics, with unique structural and biological properties. By synthetic manipulation at the side chain of the coded amino acids, new functions and functional relationships can be generated as well as altered physicochemical properties, such as luminescence, conducting ability, higher thermal stability and metal ion and other analytes recognition ability, among other properties. Furthermore, the chirality of the amino acid should make these polymers suitable for chiral recognition and induce chain helicity in aggregated phases.[1] The fact that amino acids and peptides are known to bind a variety of metal ions as they contain a large number of potential donor atoms through the peptide backbone and amino acid side chains has encouraged their application to the solution based detection of metals[2] and as solid-state metal-ion biosensors.[3]

2-Benzoxazole derivatives have long been recognized as very interesting biologically active compounds as they display high lipophilicity and broad range biological activity. In recent reports, several derivatives have been presented as antifungal, antimicrobial and anticancer agents.[4] Moreover, benzoxazoles also have excellent optical properties (broad spectral windows, high molar absorption coefficients and fluorescence quantum yields) and they have been described as fluorescent probes and sensing materials, namely as fluorescent and/or colorimetric sensors for metals, anionic species and pharmaceutical analysis.[2c,5] Thiophene and its derivatives also display interesting biological activity and important electroluminescent properties with wide application in polymer science, which has prompted their application as energy transfer and light-harvesting systems, for optical and electronic devices,[6] as sensors and as fluorescent markers.[7] Furthermore, the combination of amino acid building blocks and thiophene derivatives has resulted in several examples of heteroaromatic amino acids with application as ligands of the NMDA receptor, monomers for conducting polymers with complexing ability, paramagnetic amino acids for probing protein dynamics, as UV- and pharmaceutically active amino acids for incorporation into mutant proteins with changed optical and thermodynamic properties.[8]

The importance of the several above mentioned applications of thiophene, benzaxole and amino acid derivatives reveals that there is a practical interest on the synthesis of new and more complex systems that combine these units. Therefore, in order to contribute and expand the body of work published in this area in the last years, we decided to design new

amino acid-based systems consisting on functionalized alanines containing these heterocyclic nuclei. The (oligo)thienyl-benzoxazole amino acid derivatives, because of the presence of amino and carboxyl groups, can be incorporated into peptide chains and as such used as an energy donor in conformational studies of peptides by means of fluorescence or be used as fluorescence markers. Following our previous research in the synthesis and characterization of unnatural amino acids,[9] benz-X-azole derivatives with interesting optical properties[10] and heterocyclic colorimetric/fluorescent chemosensors containing (oligo)thiophene, benzoxazole and amino acid moieties,[2c,11] we now report the synthesis and characterization of a series of benzoxazolyl alanine derivatives bearing (oligo)thiophene units at the side chain. With the study of these new (oligo)thienyl-benzoxazolyl-alanines we intend to evaluate the effect of the length of the (oligo)thienyl group at the 2-position of the benzoxazole moiety in the photophysical properties of the resulting compounds.

5.5 - Results and Discussion

5.5.1 - Synthesis

The new (oligo)thienyl-benzoxazolyl-alanines **4-6** with ethylenedioxythiophene, bithiophene and terthiophene units linked to the benzoxazolyl alanine system were synthesized in good yields, by a multistep synthesis, in order to compare the photophysical properties of compounds **4-6** with our recently reported system with thiophene.[2c] Several (oligo)thiophene moieties were used in order to study the influence of the structure modification (e.g. the rigidification of the thiophene derivative by adding a ethylenedioxy bridge in compound **4a** and increase of the π-conjugated system in compounds **5a** and **6a**) on the overall optical properties of compounds **4-6**.

Starting from commercially available 3-nitro-L-tyrosine, *N*-Boc-3-amino-L-tyrosine methyl ester **1** was obtained by using simple synthetic procedures.[2c] The synthesis of 2-formyl-(oligo)thiophenes **2a**[12] and **2c**[13] has been previously reported by us. Condensation of compounds **1** and **2a-c** in ethanol afforded the corresponding imino derivatives **3a**-**c**, as stable solids which allowed their characterization. By reaction with lead tetraacetate (LTA) in DMSO, the imino compounds were oxidised to the [2-(oligothienyl)benzoxazol-5-yl] alanine derivatives **4a-6a**, in 56 to 74% yield (Scheme 5.1, Table 5.1).

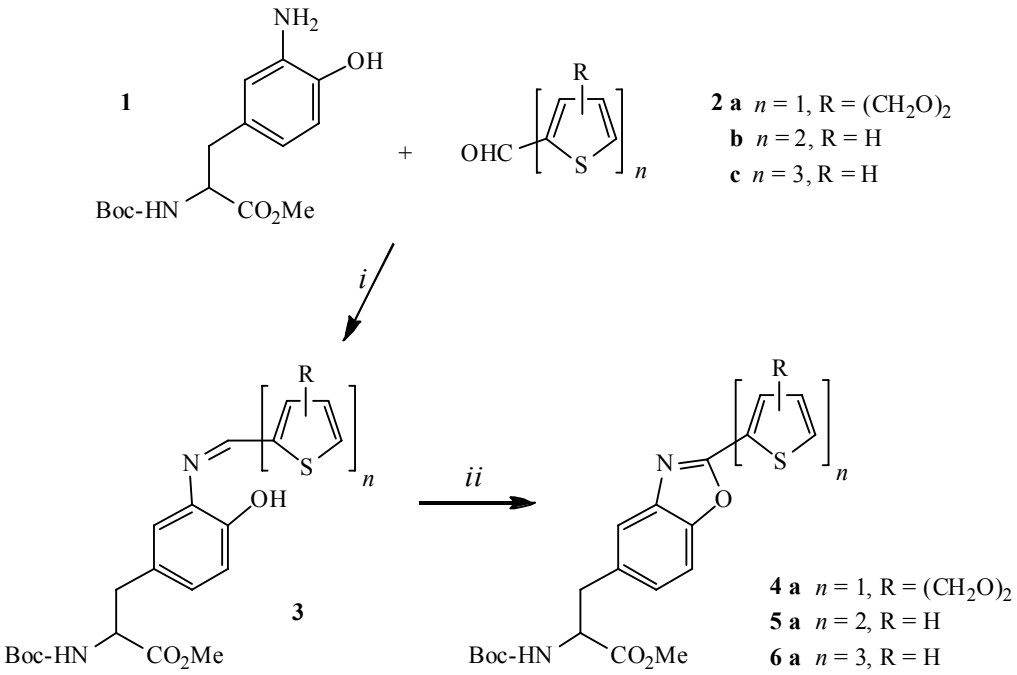

Scheme 5.1. - Synthesis of fully protected (oligo)thienylbenzoxazolyl-alanine derivatives **4a** to **6a**.

In order to study the effect of the *N*- and *C*-terminal protecting group of these amino acids in the photophysical properties, compound **4a** was then selectively deprotected at its *C*- and *N*-*terminus*, yielding the corresponding *N*-Boc protected compound **4b** and the fully deprotected ethylenodioxythienyl-benzoxazolyl-alanine derivative **4c**. By a similar procedure, compounds **5a**-**6a** were selectively deprotected, resulting in the corresponding *N*-Boc protected **5b**-**6b** and the fully deprotected alanine derivatives **5c-6c** (Scheme 5.2, Table 5.1). The structures of the new (oligo)thienyl-benzoxazolyl-alanines **4**-**6** were unambiguously confirmed by their analytical and spectral data.

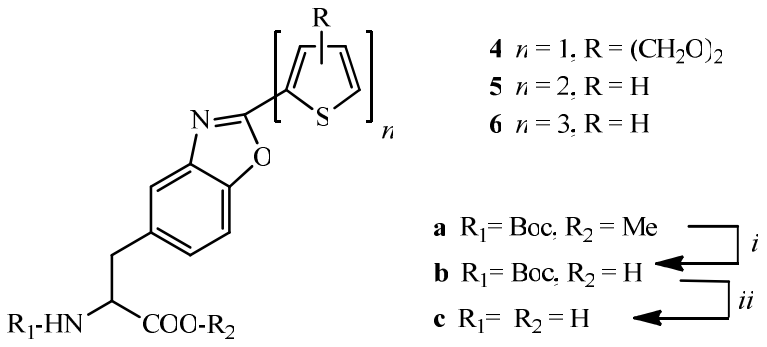

Scheme 5.2. - Synthesis of *N*- and *C*-terminal deprotected (oligo)thienylbenzoxazolyl-alanine derivatives **4a-c** to **6a-c**.

Table 5.1. - Yields, UV-visible absorption and emission data for (oligo)thienylbenzoxazolyl-alanines **4-6** in absolute ethanol.

Entry	Compd.	Yield (%)	Absorption λ_{max} (nm) (log ε)	Emission λ_{max} (nm)	Stokes' shift (nm)	Quantum yield Φ_F
1	**4a**	56	314 (4.37)	398	84	0.03
2	**4b**	84	320 (4.12)	400	80	0.03
3	**4c**	54	320 (4.28)	386	66	0.05
4	**5a**	74	365 (4.32)	445	80	0.46
5	**5b**	95	365 (4.39)	442	77	0.37
6	**5c**	55	365 (4.29)	448	83	0.55
7	**6a**	72	400 (4.57)	490	90	0.10
8	**6b**	96	400 (4.49)	480	80	0.13
9	**6c**	60	---[a]	---[a]	---[a]	---[a]

[a] The evaluation of the photophysical properties of compound **6c** was not possible due to insobility

5.5.2 - Photophysical study

The absorption and emission spectra of (oligo)thienylbenzoxazolyl-alanines **4-6** were measured in absolute ethanol (1 to 2 × 10^{-5} M solution) (Table 5.1). The nature of the thiophenic substituent at position 2 of the benzoxazole had a clear influence on the absorption and emission bands of compounds **4-6**. The wavelength of maximum absorption was shifted to longer wavelengths as the number of thiophene units increased, *ca.* 50 nm for each added thiophene (Table 5.1, entries 1, 4 and 7). The same trend was observed in the emission spectra as the position of the wavelength of maximum emission was red-shifted with the increase of the number of thiophene units, which varied from λ_{em}= 398 nm for **4a** to λ_{em}= 490 nm for **6a** (Figure 5.1).

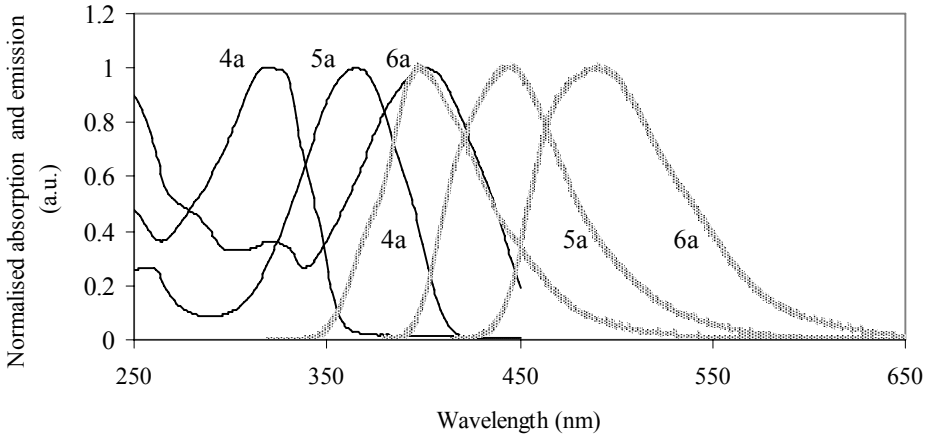

Figure 5.1. - Normalized UV-visible absorption and emission spectra of compounds **4a**, **5a** and **6a** in absolute ethanol at T = 298 K (**4a**, λ_{exc} = 314 nm; **5a**, λ_{exc} = 365 nm; **6a**, λ_{exc} = 400 nm) (absorption, full line; emission, dotted line).

The fluorescence quantum yields were determined using a 0.1 M solution of 1-naphthylamine in cyclohexane as standard (Φ_F = 0.46)[14] and (oligo)thienylbenzoxazolyl-alanines **4-6** exhibited good to excellent relative fluorescence quantum yields. Alanines **5a-c**, with a bithiophene at position 2 of the benzoxazole, were found to be strongly emissive (0.37 < Φ_F < 0.55) while compounds **6a-c**, with a terthiophene substituent, displayed much lower quantum yields (0.10 < Φ_F < 0.13). The ethylenedioxythienylbenzoxazolyl-alanines **4a-c** displayed residual fluorescence (Table 5.1, entries 1 to 3). For this compound it was found that the rigidity introduced by the ethylenedioxy bridge on the thiophene ring had practically no effect on the wavelengths of maximum absorption and emission, although a strongly deleterious effect on the fluorescence quantum yield was observed, when compared to 2-thienylbenzoxazolyl-alanine which was reported to have a fluorescence quantum yield of

0.79.[2c] A related alanine derivative containing a benzoxazole bearing a methylthiophene was reported by other authors,[15] with the wavelength of maximum emission at 354 nm and a relative fluorescente quantum yield of 0.64.

The fluorescence quantum yield of non substituted (oligo)thiophenes is expected to increase as the oligothiophene chain length increases, due to a further extension of the conjugated π-system. On the other hand, the heavy atom induced spin-orbit coupling by the sulphur atoms can give raise to a very efficient intersystem crossing mechanism, thus lowering the emission.[16] Moreover, azomethine nitrogens contribute to the heavy atom effect concomitant with the increased degree of conjugation.[16c] Also, the different chains (thiophene, bithiophene and terthiophene) should exihibt different degrees of torsion between the thiophene units, which leads to variations in the effectivity conjugation length, affecting the planarity of the whole heteroaromatic system.[16d] In our case, we believe that a combination of the above mentioned effects could be responsible for the trend observed in our results.

Keeping in mind further applications of these amino acids as emissive probes for energy transfer or FRET (Fluorescence Resonance Energy Transfer) studies in more complex structures as peptides chains, in Figure 5.1 can also be seen the good superposition of some absorption and emission spectra (for example compounds **6a** and **4a)**, which opens up a very wide range of potential interesting applications to be explored.

As can be seen by the results, the presence of *C*- and *N*-terminal protecting groups does not affect the position of the absorption and emission bands, nor the fluorescence quantum yield, which does not vary significantly, within the same series of compounds (for example, compare entries 1 to 3 in Table 5.1). In order to assess the influence of the solvent polarity in the photophysical properties of alanines **4-6**, spectra were run in cyclohexane, dioxane, acetonitrile and ethanol/water (1:1) and the obtained results showed that no solvatochromic effect was observed, suggesting that these compounds are solvent polarity independent.

5.6 - Conclusions

In summary, we have achieved the synthesis of new fluorescent heteroaromatic amino acid derivatives **4-6** containing (oligo)thiophene and benzoxazole moieties combined with an alanine residue by simple procedures in good yields and their photophysical properties were evaluated. Due to their interesting photophysical properties these heterocyclic alanine derivatives could find application as useful building blocks for peptide-based fluorimetric chemosensors, as fluorescent markers and probes for FRET studies in peptides. Studies on the application of these new derivatives as chemosensors are currently ongoing and it is

expected that their metal ion sensing ability can be comparable to that of 2-thienylbenzoxazolylalanine, which has been found to respond via a fluorescence quenching effect to the presence of Cu^{2+}, Ni^{2+} and Hg^{2+} in a very efficient manner.[2c]

5.7 - Experimental Section

5.7.1 - Synthesis general

General procedure for the synthesis of alanines **4a**-**6a**: compound **1** (1 equiv.) was stirred with the corresponding 2-formyl (oligo)thiophene **2** (1 equiv.) and heated in ethanol at reflux (5 mL/equiv.) for 3h. The solvent was evaporated and the crude imine **3** used in the next step without further purification.

N-tert-Butyloxycarbonyl 3-(bithien-2'-yl)imino-L-tyrosine methyl ester **3b** (crude): yellow solid. Mp. 162.5-163.6 ºC. ^{1}H NMR ($CDCl_3$) δ = 1.43 (s, 9H, $C(CH_3)_3$), 2.96-3.12 (m, 2H, β CH_2), 3.73 (s, 3H, CH_3), 4.52-4.60 (m, 1H, α-H), 5.01 (d, *J* = 7.8 Hz, 1H, NH), 6.92-6.95 (m, 2H, H-2 + H-5), 7.06-7.10 (m, 2H, H-6 + H-4''), 7.22 (d, *J* = 4.2 Hz, 1H, H-3'), 7.31-7.34 (m, 2H, H-3'' + H-5''), 7.41 (d, *J* = 3.9 Hz, 1H, H-4'), 8.70 (s, 1H, N=CH) ppm. ^{13}C NMR ($CDCl_3$) δ = 28.31 ($C(\underline{C}H_3)_3$), 37.90 (β CH_2), 52.26 (CH_3), 54.46 (αC), 80.01 ($\underline{C}(CH_3)_3$), 115.03 (C2), 116.45 (C6), 124.18 (C3'), 125.18 (C3''), 126.02 (C5''), 127.61 (C1), 128.21 (C4''), 129.49 (C5), 133.51 (C4'), 134.95 (C3), 136.86 (C2' or C2''), 141.09 (C5'), 142.88 (C2' or C2''), 149.37 (N=CH), 151.25 (C4), 155.12 (C=O Boc), 172.46 (C=O ester) ppm. MS (FAB) *m/z* (%): 487 ($[M + H]^+$, 63), 486 (28), 431 (26), 307 (38), 298 (36), 155 (30), 154 (100). HRMS: (FAB) *m/z* for $C_{24}H_{27}N_2O_5S_2$; calcd. 487.1361, found 487.1368. $C_{24}H_{26}N_2O_5S_2$: calcd. C 59.24, H 5.39, N 5.76, S, 13.18; found C 59.41, H 5.48, N 5.76, S 13.23.

The corresponding crude imine **3** (1 equiv.) and lead tetraacetate (1.5 equiv.) were stirred at room temperature in DMSO (5 mL/equiv.) for 3 days. The mixture was poured over water and extracted with ethyl acetate (3 × 10 mL). After drying with anhydrous magnesium sulphate and evaporation of the solvent under reduced pressure, the crude compound was submitted to column chromatography with silica gel by elution with dichloromethane.

N-tert-Butyloxycarbonyl [2-(bithien-2'-yl)benzoxazol-5-yl]-L-alanine methyl ester **5a**: yellow solid (0.198 g, 74%). Mp. 107.0-108.7 ºC. UV (ethanol): λ_{max} nm (log ε) 365.0 (4.53). ^{1}H NMR ($CDCl_3$) δ = 1.43 (s, 9H, $C(CH_3)_3$), 3.16-3.29 (m, 2H, β CH_2), 3.74 (s, 3H, CH_3), 4.63-4.66 (m, 1H, α-H), 5.03 (d, *J* = 8.1 Hz, 1H, NH), 7.06-7.09 (m, 1H, H-4''), 7.11 (dd, *J* = 1.2 and 8.4 Hz, 1H, H-6), 7.24 (d, *J* = 4.2 Hz, 1H, H-4'), 7.31-7.34 (m, 2H, H-7 and H-3'' or 5''), 7.44-7.46 (m, 1H, H-3'' or 5''), 7.48 (s, 1H, H-4), 7.80 (d, *J* = 4.2 Hz, 1H, H-3') ppm. ^{13}C NMR ($CDCl_3$) δ = 28.24 ($C(\underline{C}H_3)_3$), 38.26 (β CH_2), 52.29 (CH_3), 54.57 (αC), 79.99 ($\underline{C}(CH_3)_3$), 110.20 (C7),

120.23 (C4), 124.43 (C4'), 125.07 (C5''), 125.90 (C3''), 126.31 (C6), 127.38 (C2'), 128.14 (C4''), 130.66 (C3'), 132.85 (C5), 136.19 (C2''), 142.30 (C5'), 142.35 (C3a), 149.62 (C7a), 155.05 (C=O Boc), 159.01 (C2), 172.08 (C=O ester) ppm. MS (FAB) *m/z* (%): 486 ($[M + 2H]^+$, 34), 485 ($[M + H]^+$, 87), 430 (32), 429 (100), 325 (37), 297 (38), 296 (31), 293 (58), 193 (28), 185 (71), 171 (34). HRMS: (FAB) *m/z* for $C_{24}H_{25}N_2O_5S_2$; calcd. 485.1205, found 485.1212.

General procedure for the synthesis of alanines **4b**-**6b**: the corresponding alanine methyl ester (1 equiv.) was dissolved in 1,4-dioxane (1 mL/equiv.), in an ice bath, and sodium hydroxide 1 M aqueous solution (1.5 eq) was added drop wise. The mixture was stirred at room temperature for 3h. The pH was adjusted to 2-3 by addition of $KHSO_4$ 1 M aqueous solution and extracted with ethyl acetate (3 × 10 mL). After drying with anhydrous magnesium sulphate and evaporation of the solvent, the residue was triturated with diethyl ether and the pure compound was obtained as a solid.

N-tert-Butyloxycarbonyl [2-(bithien-2'-yl)benzoxazol-5-yl]-L-alanine **5b**: yellow solid (0.064 g, 95%). Mp. 183.5-185.0 ºC. UV (ethanol): λ_{max} nm (log ε) 365.0 (4.53). ^{1}H NMR ($CDCl_3$) δ = 1.46 (s, 9H, $C(CH_3)_3$), 3.34 (d, *J* = 4.5 Hz, 2H, β CH_2), 4.65-4.72 (m, 1H, α-H), 5.15 (d, *J* = 7.5 Hz, 1H, NH), 7.05-7.08 (m, 1H, H-4''), 7.18-7.22 (m, 2H, H-6 + H-4'), 7.29-7.33 (m, 2H, H-3'' + H-5''), 7.47 (d, *J* = 8.4 Hz, 1H, H-7), 7.61 (d, *J* = 1.2 Hz, 1H, H-4), 7.81 (d, *J* = 3.9 Hz, 1H, H-3') ppm. ^{13}C NMR ($CDCl_3$) δ = 28.30 ($C(\underline{C}H_3)_3$), 37.96 (β CH_2), 54.50 (αC), 80.10 ($\underline{C}(CH_3)_3$), 110.22 (C7), 120.18 (C4), 124.47 (C4'), 125.13 (C5''), 125.79 (C3''), 126.58 (C6), 127.35 (C2'), 128.25 (C4''), 130.43 (C3'), 133.01 (C5), 136.10 (C2''), 142.20 (C5'), 142.03 (C3a), 149.42 (C7a), 155.05 (C=O Boc), 159.01 (C2), 174.65 (CO_2H) ppm. MS (FAB) *m/z* (%): 472 ($[M + 2H]^+$, 6), 471 ($[M + H]^+$, 18), 470 (M^+, 10), 415 (11), 307 (32), 289 (16), 166 (11), 155 (30), 154 (100). HRMS: (FAB) *m/z* for $C_{23}H_{23}N_2O_5S_2$; calcd. 471.1048, found 471.1054.

16. General procedure for the synthesis of alanines **4c-6c**: the corresponding *N*-Boc protected alanine was stirred in a trifluoroacetic acid/dichloromethane solution (1:1, 4 mL/mmol) at room temperature for 2h. The solvent was evaporated, the solid residue dissolved in pH 8 aqueous buffer solution and extracted with ethyl acetate (3 × 10 mL). After drying with anhydrous magnesium sulphate and evaporation of the solvent, the product was isolated as a solid.

[2-(Bithien-2'-yl)benzoxazol-5-yl]-L-alanine **5c**: light yellow solid (0.031 g, 55%). Mp. 248.6-250.2 ºC. UV (ethanol): λ_{max} nm (log ε) 365.0 (4.04). ^{1}H NMR (DMSO-d_6) δ = 3.05-3.15 (m, 2H, β CH_2), 4.10-4.17 (m, 1H, α-H), 7.15-7.19 (m, 1H, H-4''), 7.30 (dd, *J* = 1.2 and 8.4 Hz, 1H, H-6), 7.48 (d, *J* = 3.9 Hz, 1H, H-4'), 7.54 (dd, *J* = 1.2 and 3.6 Hz, 1H, H-3'' or H-5''), 7.65 (d, *J* = 1.2 Hz, 1H, H-4), 7.66 (dd, *J* = 1.8 and 5.4 Hz, 1H, H-3'' or H-5''), 7.72 (d, *J* = 8.4 Hz, 1H, H-7), 7.91 (d, *J* = 3.9 Hz, 1H, H-3') ppm. ^{13}C NMR (DMSO-d_6) δ = 30.52 (β CH_2), 53.11 (αC), 118.92 (C7), 124.41 (C4'), 125.24 (C5''), 125.80 (C3''), 126.57 (C6), 127.33

(C2'), 128.10 (C4''), 130.18 (C4), 130.30 (C2), 130.45 (C3'), 132.41 (C5), 136.35 (C2''), 141.03 (C3a), 142.33 (C5'), 151.62 (C7a), 180.65 (CO_2H) ppm. MS (FAB) *m/z* (%): 372 ([M + 2H]$^+$, 11), 371 ([M + H]$^+$, 32), 278 (19), 186 (70), 154 (100). HRMS: (FAB) *m/z* for $C_{18}H_{15}N_2O_3S_2$; calcd. 371.0524, found 371.0522.

5.8 - Acknowledgments

Thanks are due to *Fundação para a Ciência e Tecnologia* (Portugal) for financial support through project PTDC/QUI/66250/2006 and a PhD grant to E. Oliveira SFRH/BD/35905/2007).

Supplementary data: Characterization data (^{1}H and ^{13}C NMR, MS and HRMS and UV-vis) for derivatives **4a**-**c** and **6a**-**c**.

5.9 - References

[1] (a) Nilsson, K. P. R.; Andersson, M. R.; Inganäs, O. *J. Phys.: Condens. Matter.* **2002**, *14*, 10011-10020. (b) Mucci, A.; Parenti, F.; Schenetti, L. *Macromol. Rapid Commun.* **2003**, *24*, 547-550.

[2] (a) Zheng, Y.; Gattás-Asfura, K. M.; Konka, V.; Leblanc, R. M. *Chem. Commun*. **2002**, 2350-2351. (b) Zheng, Y.; Cao, X.; Orbulescu, J.; Konka, V.; Andreopoulos, F. M.; Pham, S. M.; Leblanc, R. M. *Anal. Chem*. **2003**, *75*, 1706-1712. (c) Costa, S. P. G.; Oliveira, E.; Lodeiro, C.; Raposo, M. M. M. *Sensors* **2007**, *7*, 2096-2114.

[3] (a) Gooding; J. J.; Hibbert, D. B.; Yang, W. *Sensors,* **2001**, *1*, 75-90. (b) Yang, W.; Gooding; J. J.; Hibbert, D. B. *J. Electroanal. Chem.,* **2001**, *516*, 10-16.

[4] (a) Vinsova, J.; Cermakova, K.; Tomeckova, A.; Ceckova, M.; Jampilek, J.; Cermak, P.; Kunes, J.; Dolezal, M.; Staud, F. *Bioorg. Med. Chem.* **2006***, 14*, 5850-5865. (c) McKee, M. L.; Kerwin, S. M. *Bioorg. Med. Chem.* **2008**, *16*, 1775-1783.

[5] (a) Taki, M.; Wolford, J. L.; O´Halloran, T. V. *J. Am. Chem. Soc*. **2003**, *126*, 712-713. (b) Shamsipur, M.; Poursaberi, T.; Karami, A. R.; Hosseini, M.; Momeni, A.; Alizadeh, N.; Yousefi, M.; Ganjali, M. R. *Anal. Chim. Acta,* **2004**, *501*, 55-60. (c) Milewska, M.; Skwierawska, A.; Guzow, K.; Szmigiel, D.; Wiczk, W. *Inorg. Chem. Commun.,* **2005**, *8*, 947-950. (d) Zang, X.-B.; Peng, J.; He, C.-L.; Shen, G.-L.; Yu, R.-Q. *Anal. Chim. Acta,* **2006**, *567*, 189-195.

[6] (a) Roncali, J. *Chem. Rev.,* **1997**, *97*, 173-206. (b) Steybe, F.; Effenberger, F.; Beckman, S.; Gluber, U.; Bosshard, C.; Gunter, P. *Tetrahedron,* **1998**, *54*, 8469-8480. (c) Van Mullekom, H. A. M.; Vekemans, J. A. J. M.; Havinga, E. E.; Meijer, E. W. *Mat. Sci. Eng*., **2001**, *32*, 1-40.

[7] (a) Yu, J.; Shirota, Y. *Chem. Lett*. **2002**, *31*, 984-985. (b) Lin, S.-C.; Sun, S.-S. *Chem. Mater.* **2002**, *14*, 1884-1890. (c) Destri, S.; Pasini, M.; Botta, C.; Porzio, W.; Bertini, F.; Marchio, L. *J. Mater. Chem.* **2002**, *12*, 924. (d) Béra-Abérem, M.; Ho, H.-A.; Leclerc, M. *Tetrahedron* **2004**, *60*, 11169-11173. (e) Barbarella, G.; Melucci, M.; Sotgiu, G. *Adv. Mater.* **2005**, *17*, 1581-1593.

[8] (a) Budisa, N.; Alefelder, S.; Bae, J. H.; Golbik, R.; Minks, C.; Huber, R.; Moroder, L. *Protein Sci.* **2001**, *10*, 1281-1292. (b) Lima, P. G.; Caruso, R. R. B.; Alves, S. O.; Pessoa, R. F.; Mendonça-Silva, D. L.; Nunes, R. J.; Noël, F.; Castro, N. G.; Costa, P. R. R. *Bioorg. Med. Chem. Lett*. **2004**, *14*, 4399-4403. (c) Brembilla, A.; Collard, A.; Henry, B.; Jadamiec, M.; Lapkowski, M.; Matlengiewicz, M.; Rodehüser, L. *Phosphorus, Sulfur and Silicon* **2007**, *182*, 723-734. (d) Kálai, T.; Schindler, J.; Balog, M.; Fogassy, E.; Hideg, K. *Tetrahedron* **2008**, *64*, 1094-1100.

[9] (a) Costa, S. P. G.; Maia, H. L. S.; Pereira-Lima, S. M. M. A. *Org. Biomol. Chem.* **2003**, *1*, 1475-1479. (b) Jiang, W.-Q.; Costa, S. P. G.; Maia, H. L. S. *Org. Biomol. Chem.* **2003**, *1*, 3804-3810.

[10] (a) Batista, R. M. F.; Costa, S. P. G.; Raposo, M. M. M. *Tetrahedron Lett.* **2004**, *45*, 2825-2828. (b) Costa, S. P. G.; Batista, R. M. F.; Sousa, A. M. R. C.; Raposo, M. M. M. *Mater. Sci. Forum* **2006**, 514-516, 147-151. (c) Costa, S. P. G.; Batista, R. M. F.; Cardoso, P.; Belsey, M.; Raposo, M. M. M. *Eur. J. Org. Chem.* **2006**, *17*, 3938-3946. (d) Batista, R. M. F.; Costa, S. P. G.; Malheiro, E. L.; Belsey, M.; Raposo, M. M. M. *Tetrahedron* **2007**, *63*, 4258-4265. (e) Batista, R. M. F.; Costa, S. P. G.; Belsley, M.; Raposo, M. M. M. *Tetrahedron* **2007**, *63*, 9842-9849. (f) Pina, J.; Seixas de Melo, J.; Burrows, H. D.; Batista, R. M. F.; Costa, S. P. G.; Raposo, M. M. M. *J. Phys. Chem. A* **2007**, *111*, 8574-8578.

[11] Batista, R. M. F.; Oliveira, E.; Costa, S. P. G.; Lodeiro, C.; Raposo, M. M. M. *Org. Lett*. **2007**, *9*, 3201-3204.

[12] Costa, F.; Silva; C. J. R.; Raposo, M. M. M.; Fonseca, A. M.; Neves, I. C.; Carvalho, A. P.; Pires, J. *Microporous Mesoporous Mater*. **2004**, *72*, 111-118.

[13] Batista, R. M. F.; Costa, S. P. G.; Belsley, M.; Lodeiro, C.; Raposo, M. M. M. *Tetrahedron* **2008**, 64, 9230-9238.

[14] Berlman B. in *Handbook of Fluorescence Spectra of Organic Molecules*, 2nd Ed., Academic Press, New York, **1971**.

[15] Guzow, K.; Szmigiel, D.; Wróblewski, D.; Milewska, M.; Karolczak, J.; Wiczk, W. *J. Photochem. Photobiol. A: Chem.* **2007**, *187*, 87-96.

[16] (a) Becker, R. S.; Seixas de Melo, J.; Maçanita, A. L.; Elisei, F. *J. Phys. Chem*. **1996**, *100*, 18683-18695. (b) Seixas de Melo, J.; Silva, L. M.; Arnaut, L. G.; Becker, R. S. *J. Chem*. *Phys.* **1999**, *111*, 5427-5433. (c) Dufresne, S.; Bourgeaux, M.; Skene, W. G. *J. Mater. Chem*. **2007**, *17*, 1166-1177. (d) Seixas de Melo, J.; Burrows, H. D.; Svensson, M.; Andreson, M. R.; Monkman, A. P. *J. Chem*. *Phys.* **2003**, *118*, 1550-1556.

Chapter 6

Synthesis, characterization, fluorescence and computational studies of new Cu^{2+}, Ni^{2+} and Hg^{2+} complexes with emissive thienylbenzoxazolyl-alanine ligands.

Elisabete Oliveira, S. P. G. Costa, M. M. M. Raposo, Olalla Nieto Faza, Carlos Lodeiro, accepted in *Inorganica Chimica Acta*, **2010**.

"I never think about the future. It will come soon enough"

Albert Einstein, 1879-1955

Index

6.1 - Abstract

The interaction of four fluorescent compounds containing thiophene and benzoxazole moieties combined with an alanine residue with alkaline, alkaline-earth, transition and post-transition metal ions was explored. The highly fluorescent heterocyclic alanine derivatives are strongly quenched in the solid state after complexation with the paramagnetic metal ions Cu^{2+} and Ni^{2+}, and with the diamagnetic Hg^{2+}. Absorption and steady-state fluorescence titrations reveal a selective interaction with Cu^{2+}, Ni^{2+} and Hg^{2+}. In all cases the formation of mononuclear or dinuclear metal complexes in solid state and in solution are postulated. DFT calculations on the mercury(II) complexes confirm the formation of dinuclear species. Our results suggest that one metal ion is coordinated by the chelate group formed by the amine and the protonated carboxylic groups present in the amino acid residue while a second metal ion is directly linked to the chromophore. As parent compound, L4 shows no interaction with Cu^{2+} and Ni^{2+} salts. However, the interaction with Hg^{2+} induces a strong quenching and a red shift of the fluorescence emission.

My contribution for this work was the synthesis of the metallic complexes and all photophysical studies in solution and in solid state.

6.2 - Resumo

Foi explorada a interacção com iões metálicos alcalinos, alcalino-terrosos, transição e pós-transição, de quatro compostos fluorescentes contendo as unidades tiofeno e benzoxazol combinados com o resíduo alanina. Os derivados de alanina altamente fluorescentes apresentaram uma intensa supressão da intensidade de emissão, em solução e em estado sólido, após a complexação com os iões metálicos paramagnéticos Cu^{2+} e Ni^{2+}, e o diamagnético Hg^{2+}. As titulações por absorção e emissão de fluorescência revelaram uma interacção selectiva para Cu^{2+}, Ni^{2+} e Hg^{2+}. Em todos os casos foi postulado a formação de complexos metálicos mono- ou dinuclear em estado sólido e em solução. Os cálculos por DFT nos complexos de mercúrio (II) confirmam a formação de espécies dinucleares. Os resultados sugerem que um metal está coordenado pelo grupo quelato formado pela amina e o grupo carboxílico protonado presente no resíduo aminoácido, enquanto, o secundo ião metálico está directamente ligado ao cromóforo. Como parente, L4 não apresenta qualquer alteração na presença dos sais Cu^{2+} e Hg^{2+}. No entanto, a interacção com o Hg^{2+} induz a uma forte supressão e um desvio para o vermelho da emissão de fluorescência.

A minha contribuição para este trabalho consistiu na síntese dos complexos metálicos e a realização de todos os estudos fotofísicos em solução e em estado sólido.

6.3 - Introduction

The interactions of amino acids or peptides with transition metals have been extensively investigated due to their importance as multifunctional materials in biology, pharmacy and industry [1]. Many of these metal complexes show versatile properties including antibacterial, antitumor, or anticancer activities [2-5]. As is well known, many types of enzymes contain metal ions as cofactors, and in order to understand some of these biological processes, the interaction of metal complexes containing amino acids have been studied [6]. In this set of applications, Grosser et al. have recently concluded that the alanine residue has an anti-oxidant action [7].

In the field of peptide mass mapping (Proteomics approach), transition metal complexes can be used as cleavage reagents for peptides and proteins [8-12]. With this aim, several Pd^{2+} complexes with small peptides containing histidine and methionine as amino acids have been recently shown to promote a hydrolytic cleavage of these residues [13]. Copper(II) is one of the most interesting transition metal ions in biologic fields due to the participation in electron transfer processes in proteins containing hydrophobic sites [14]. In this way, Marine *et al.,* have published some interesting theoretical studies on the interaction of Cu^{2+} with alanine amino acids, their results showing that Cu^{2+} ions are preferentially linked to the C-terminal carboxylate group of the alanine residue [15].

In the present work we have combined the design of new fluorescent materials based on bio-inspired ligands with transition and pollutant heavy metal ions such as Cu^{2+}, Ni^{2+} and Hg^{2+} as potential proteomics platforms in the broader context of our research lines on fluorescence and colorimetric chemosensors [16 -19].

These compounds show selectivity towards Cu^{2+}, Ni^{2+} and Hg^{2+} over other metals including Zn^{2+}, Ca^{2+}, Na^{+} in solution [17]. Here we report the synthesis of eight new Cu^{2+}, Ni^{2+} and Hg^{2+} metal complexes with ligands L1, L2 and L3 (Scheme 6.1), their characterization, and spectroscopic and DFT studies. For comparative purposes, we also present the photophysical studies with metal ions using the *bis*-alanine L4, which contains two moieties of benzoxazolylalanine linked through a thiophene spacer (Scheme 6.1).

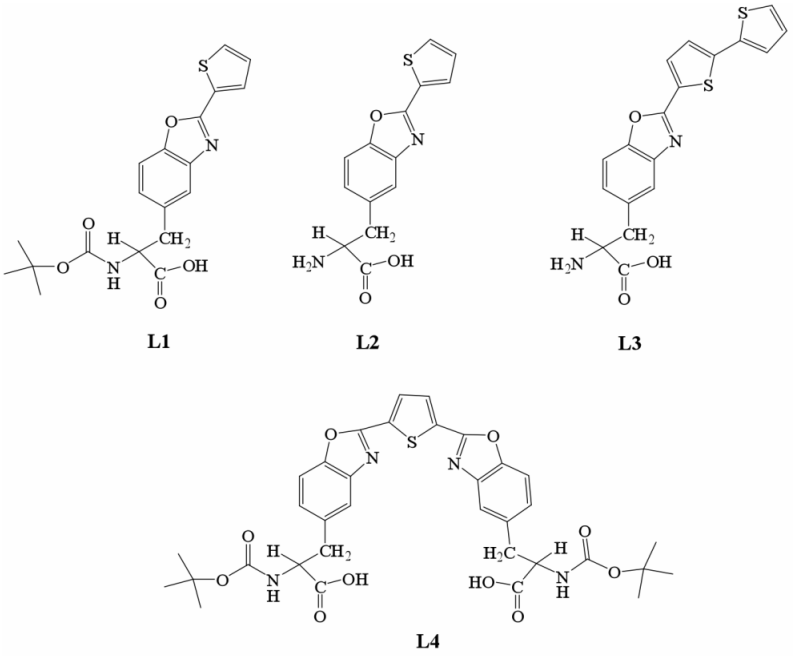

Scheme 6.1 – Structure of benzoxazolyl-alanine derivatives studied.

6.4 - Results and Discussion

6.4.1 - Synthesis and Characterization, Complexation studies

The synthesis of L1, L2 and L3 was previously reported by us [17,18], while L4 was obtained by a standard deprotection procedure from the methyl ester parent compound [19].

The synthesis of the metal complexes of L1, L2 and L3 with the hydrated metal salts [M= Cu^{2+}, Ni^{2+} and Hg^{2+} X= CF_3SO_3 or BF_4] was studied in absolute ethanol by direct reactions, leading to the formation of complexes with 1:1 or 2:1 metal-to-ligand ratio. The pure analytical complexes gave formula: $[Cu_2L1](CF_3SO_3)_4.2CH_3CN.\ 2H_2O$ **(1),** $[Ni_2L1](BF_4)_4.7H_2O$ **(2),** $[Hg_2L1](CF_3SO_3)_4.4H_20$ **(3),** $[Cu_2L2](CF_3SO_3)_4\ .3H_2O$ **(4),** $[Ni_2L2](BF_4)_4.6H_2O$ **(5),** $[Hg_2L2](CF_3SO_3)_4.2CH_3CN.2H_2O$ **(6),** $[Ni_2L3](BF_4)_4.4H_2O$ **(7)** and $[Cu_2L3]\ (CF_3SO_3)_4.3H_2O$ **(8).**

All colored solid complexes are air-stable and soluble in absolute ethanol, acetonitrile, DMSO, dichloromethane and chloroform.

All complexes were characterized by elemental analysis, IR, ^{1}H-NMR, UV-vis, fluorescence and matrix-assisted laser desorption ionization time-of-flight (MALDI-TOF-MS) spectroscopy.

To confirm the number of metal ions in each complex the amount of metal was determined by atomic absorption spectrometry following several methods previously reported [20].

The IR spectra registered in KBr pellets show similar bands attributed to the ν(C=N) and ν(C=C) stretching modes of the aromatic rings appear at 1619-1925 and at 1574-1579 respectively. As far as the counter ions are concerned, in all the BF_4 complexes four bands were observed at 777, 360, 1070 and 533 cm^{-1} and assigned to the four actives ν1, ν2, ν3, and ν4 vibrational modes respectively [22]. In the triflate complexes the intense band at 1280 cm^{-1}, associated with the vibrational tension band ν_{as}(S-O) corroborated the ionic presence of these anions [21]. These results suggest that both kinds of counterions are not involved in coordination to the metal ions. The appearance of a broad band at around 3400 cm^{-1} in all complexes indicates the presence of coordinated and/or hydrated water molecules [21]. This result is in agreement with the DFT studies where the metal ions are stabilized by completing the coordination sphere with water.

MALDI-TOF-MS spectra of the complexes (see experimental section) display peaks corresponding to $[M\mathbf{L}]^+$, $[M\mathbf{L}X]^+$, $[M\mathbf{L}X_2]^+$, $[M_2\mathbf{L}X]^+$ and $[M_2\mathbf{L}X_3]^+$ fragments, which indicates the integrity of the alanine derivatives and the presence of the metal ions in the complexes.

As was pointed above the ^{1}H-NMR spectra of the mercury(II) complexes were registered in DMSO-d_6 at room temperature. The signals observed were broad in comparison with those in the free ligand due to the complexation effect. However, all-important peaks attributed to the amino-acid moiety were observed confirming the integrity of the ligand in the metal complex. The most affected peaks were assigned to the aromatic chromophores.

All free ligands are very emissive in the solid state (See Figure 6.1). The strong emission band is centered at *ca*. 400, 430 and 485 nm for L1, L2 and L3 respectively. In the particular case of L1, the emission band showed a long tail centred at 500 nm that could be assigned to some intermolecular interactions between ligands in the ground state.

The fluorescence spectra of the solid complexes **1-8** were obtained exciting the samples at 315 nm. With respect to those of the ligands these spectra are in general highly quenched, with the exception of the Cu^{2+} and Ni^{2+} complexes with L2 and L3 (See Figure 6.1 panels B and C).

This quenching confirms the formation of the metal complexes. It is due to the energy transfer from the π* emissive state of the ligand though low-lying metal-centre, and the heavy metal effect in the case of Hg^{2+} inducing an effective intersystem crossing mechanism [23-25] which suggests that the metal interacts with the chromophore units. This observation was later confirmed by DFT studies.

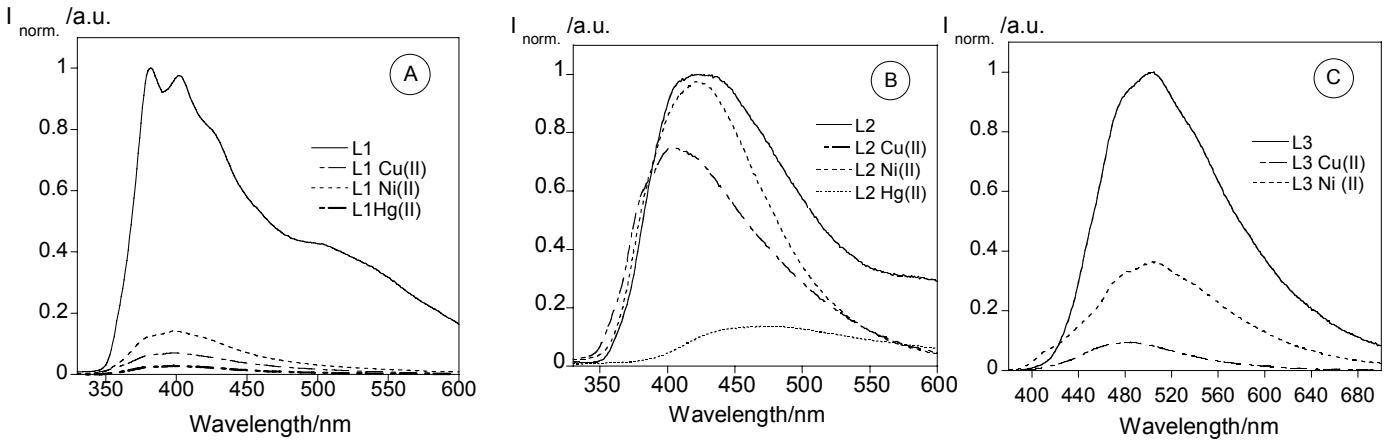

Figure 6.1. – Solid-state emission spectra of L1(A), L2(B) and L3(C) and its corresponding metal complexes with Cu^{2+}, Ni^{2+} and Hg^{2+} ($\lambda_{excL1,L2}$ = 315 nm, λ_{excL3} = 366 nm, T=298K).

6.4.2 - Computational Methods

DFT was used to optimize the geometries of L2 and the L2:Hg^{2+} and L2:Hg_2^{2+} complexes (See Figure 6.2). Since different coordination spheres can surround mercury, one to three explicit water molecules were included as co-ligands in the preliminar work. The following energetic discussion, however, only refers to the species with one water molecule, since only the tri-coordinate species were found to be stable with water (other water molecules leave the coordination site along the optimization). In order to stabilize a four-coordinated mercury complex it was necessary to use other co-ligands such as an acetonitrile molecule (See Figure 6.2).

The 1:1 (ML) complex is stabilized by 33 kcal/mol with respect to the free ligand and the $Hg(H_2O)_2^{2+}$ cation. The first metal cation is coordinated to both the deprotonated carboxylate and the amine of the alanine group, as expected. The coordination of this first cation to the sulfur and nitrogen on the aromatic part of L2 would only be favored by 7.5 kcal/mol when compared to the free species, and even by less when the coordination site is formed by S and O (see Table 6.1).

Coordination of two metal units is favoured by 33 kcal/mol with respect to the free fragments, and by about 1 kcal/mol with respect to the L2:$Hg(H_2O)$ complex, water and a further $Hg(H_2O)_2$ complex. In this case, there is a strong preference for S,N coordination, rather than the alternative complexation to S,O, that results in a energy difference between the L2:$[Hg(H_2O)]_2$_SN and L2:$[Hg(H_2O)]_2$_SO complexes of about 17 kcal/mol. The coordination

to the heteroatoms in the aromatic part of the ligand is not always symmetric. In the structures where L2 is chelating mercury through sulphur and nitrogen, the interaction is much stronger with the nitrogen atom, both in terms of bond distances (Hg-N distance of 2.20 A and Hg-S distance of 3.65 A) and the NBO bond orders (0.31 and 0.02 respectively). In the case of S,O coordination, there are two structures within a 1 kcal/mol energy region. In one of them (L2:[Hg(H_2O)]$_2$_SO), the metal is bonded to the sulphur atom (3.07 A, bond order of 0.14) with only electrostatic contributions to the O-Hg bonding (3.40 A and 0.02 bond order). In the other structure (L2:[Hg(H_2O)]$_2$_SO_2), the metal center displays a stronger interaction with the oxygen (Hg-S distance of 3.65 A and Hg-O distance of 2.99 A, with bond orders, respectively).

Although not common, other examples of tricoordinate mercury can be found in the literature [26], usually with sulphur and two halogens as ligands. In exploratory gas phase calculations, protonation of the aminoacid carboxilate is needed to achieve a stable L2:Hg(H_2O)$_2$ complex with a distorted trigonal pyramid geometry. As was pointed above, this increase in the allowed coordination number of mercury as a result of the lesser basicity of the ligands, is also found when a water molecule is replaced by acetonitrile on the second mercury cation, coordinated to the heterocyclic region of L2 (See Figure 6.2). Thus, a structure could be optimized where Hg^{2+} coordinates to the sulphur and nitrogen atoms on L2, completing its coordination sphere with one water and one acetonitrile molecule, also arrayed in a distorted trigonal pyramid, while this same fourth coordination site would not accept a water molecule. In this case, with a non-deprotonated alanine coordinating a Hg^{2+} center with two attached water molecules, a second Hg^{2+} cation with one water and one acetonitrile as ligands also prefers to coordinate to the chromophore through its N,S atoms instead of doing it through O,S. This preferece for nitrogen over oxygen coordination in this system has a value of about 8 kcal/mol and, in fact, Hg^{2+} with two ligands doesn´t bind to the heterocyclic oxygen, resulting in a new tricoordinate T-shaped moiety in contrast to the pyramidal S,N complex.

Thus, independently of the exact model chosen for the ligand (protonated or deprotonated aminoacid residue) or for the exact coordination sphere of the metal, these theoretical studies support the coordination proposed by resorting to UV-vis and Fluorescence spectroscopy: i) The first metal center coordinates to the alanine moiety, and ii) interaction with the aromatic chromophore is observed at larger metal concentrations.

Table 6.1 - DFT (CAM-B3LYP/def2-svp (PCM, ethanol)) electronic and free energies in kcal/mol for the mercury-L2 complexes studied. The relative values have been calculated

Structure	Electronic Energy	ΔG	Rel. Electronic Energy	Rel. DG
H_2O	-47901.77	-47899.46		
$Hg(H_2O)_2$	-191907.38	-191894.45		
L2_1	-798476.02	-798359.04		
L2_2	-798476.50	-798359.31		
L2:$Hg(H_2O)$	-942514.77	-942383.09	-32.66	-28.80
L2:$Hg(H_2O)$_SN	-942492.62	-942361.83	-10.50	-7.54
L2:$Hg(H_2O)$_SO	-942473.18	-942344.47	8.93	9.82
L2:$[Hg(H_2O)]_2$_SN	-1086522.80	-1086377.38	-35.07	-36.09
L2:$[Hg(H_2O)]_2$_SO	-1086505.26	-1086360.35	-17.53	-19.30
L2:$[Hg(H_2O)]_2$_SO_2	-1086505.13	-1086358.87	-17.40	-18.63

with respect to $Hg(H_2O)_2^{2+}$, the free ligand L2, and H_2O.

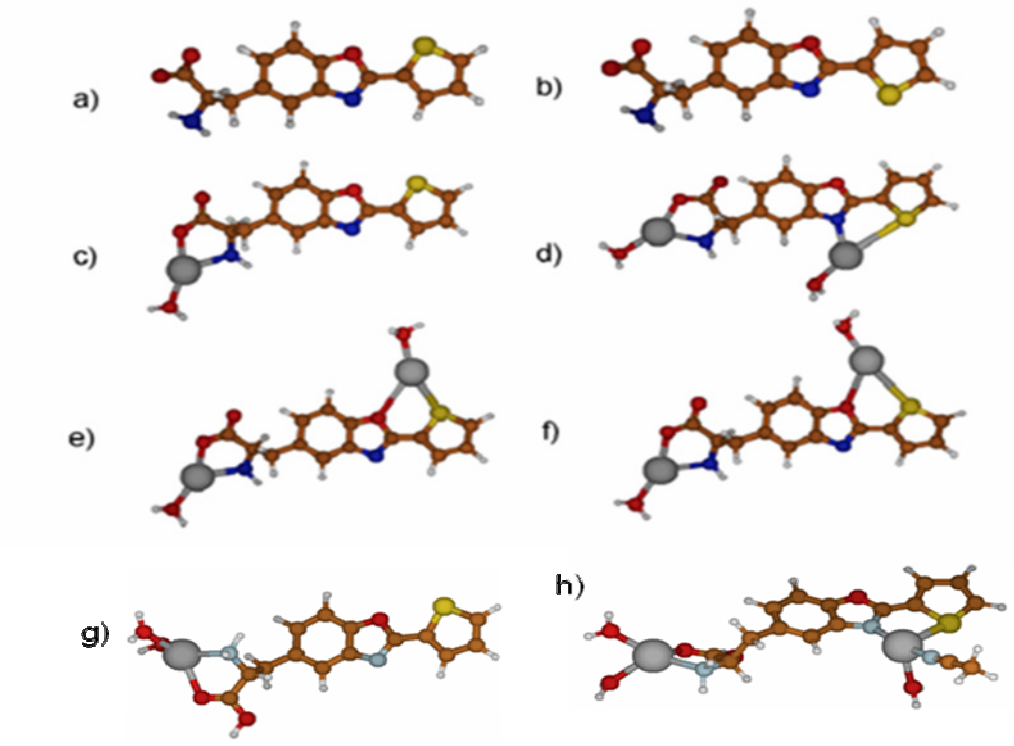

Figure 6.2. DFT structures of ligand L2 in the presence of one and two equivalents of Hg(II).

6.4.3 - Spectroscopyc Studies

In our previous study we have reported using ligands L1 and L2 as fluorescent probes in solution, for the detection of Na^{+}, Ca^{2+}, Zn^{2+}, Hg^{2+}, Cu^{2+} and Ni^{2+} [17]. In these cases only a selective interaction with Hg^{2+}, Cu^{2+} and Ni^{2+} was observed. Based on these results, now, we have evaluated the sensor capability of ligands L3 and L4 towards the same metal ions by UV-vis and fluorescence metal titrations using absolute ethanol or dichloromethane as solvents.

As can be seen in Scheme 6.1, compounds L1 and L4 have a protecting group at the N-terminal position of the amino residue, thus preventing the metal complexation by the amino group. These compounds were selected as model systems for L2 and L3 in order to better understand the coordination reactions by the carboxyl group and the chromophore.

During the titration of L3 with an ethanolic Hg^{2+} solution, the intensity of fluorescence was dramatically reduced. However, after the first metal additions a white precipitate appears immediately preventing further studies in solution. It is interesting to note that ligand L3 also does not produce good analytical results for the mercury(II) solid complex.

On the other hand as can be seen in Figure 6.3, even if the ground state was not affected after metal addition, (spectra do not show), a progressive quenching reaction could be observed in the presence of copper(II) (Figure 6.3, panel A) and nickel(II) (Figure 6.3, panel B).

The strongest quenching effect was observed for Cu^{2+}; half molar equivalent of metal ion was enough to totally quench the fluorescence emission. This result is unique among all the ligands reported, suggesting the formation in solution of a sandwich complex between two ligands and one metal center. Studies using the Hypspec program [27] confirmed this hypothesis and suggest a complex with log *K* of 12.81±0.05. Taking into account the strong effect observed in the emission band, we could postulate that the metal center also affects the chromophores of both ligands.

Table 6.2.- Complexation constants (log*K*) for benzoxazolyl-alanine ligands L1 to L4 with Cu^{2+}, Ni^{2+} and Hg^{2+} in absolute ethanol calculated with Hypspec program.

Compound	Complex [a] Ref.27	Log K	M:L
L1	L1Cu	3.75±0.05	1:1
	L1Hg [a]	5.01±0.04	1:1
		9.37±0.07	2:1
L2	L2Cu[a]	9.77±0.02	2:1
	L2Hg[a]	7.78±0.02	2:1
L3	L3Cu	12.81±0.05	1:2
	L3Ni	4.62±0.01	1:1
L4	L4Hg	6.50±0.03	1:1

In the titration with nickel(II) the complex obtained shows a ligand-metal stoichiometry of 1:1 with an association constant of 4.62±0.01 (see table 6.2), one of the smallest values obtained for these compounds. As can be seen in figure 2 the quenching achieved was not complete. In comparison with the previous published complexation constants with ligands L1 and L2 [17], the values obtained for L3 are higher, specially for copper(II).

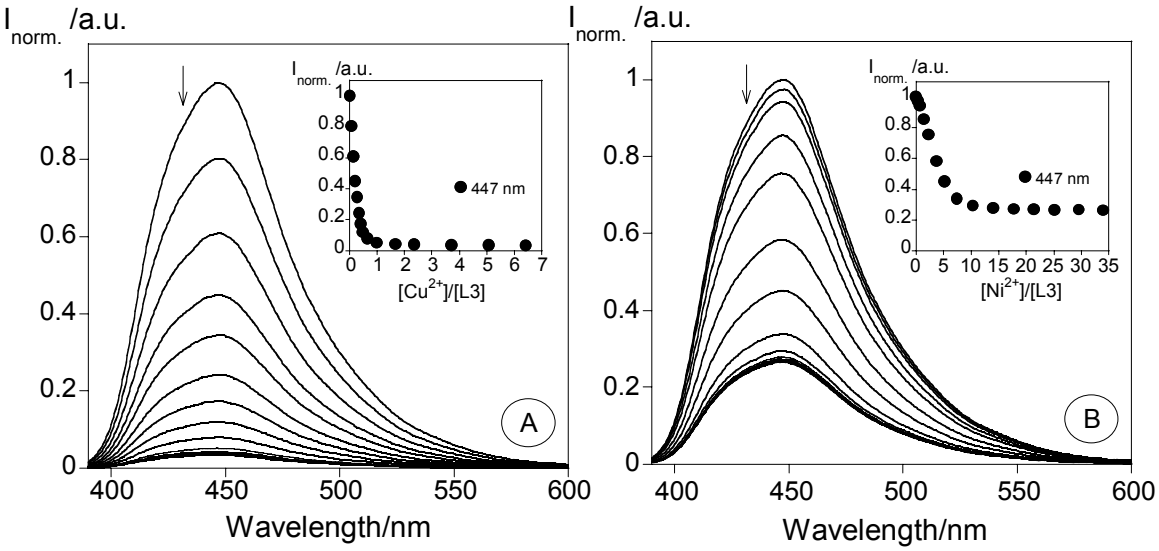

Figure 6.3. - Spectrofluorimetric titrations (A and B) of ligand L3 in the presence of $Cu(CF_3SO_2)_2$ (A) and $Ni(BF_4)_2$ (B) in absolute ethanol. ([**L3**] = 1.00 $\times 10^{-5}$ M, $[Cu(CF_3SO_2)_2]$ =1.02$\times 10^{-2}$M, $[Ni(BF_4)_2]$ =1.00$\times 10^{-2}$M, T = 298 K, λ_{exc} = 366 nm. (insets: normalized emission at 447 nm).

Ligand L4 results of the combination of a second benzoxazolylalanine moiety with ligand L1. L4 was obtained from a selective C-terminal deprotection of the methyl ester precursor reported previously by us [19]. The sensing ability of L4 towards the same transition metals was explored in order to evaluate the influence of the additional benzoxazolylalanine moiety. The corresponding photophysical characterization is reported in Figure 6.4 panel A.

Addition of Cu^{2+} or Ni^{2+} to a dichloromethane solution containing L4, does not modify the absorption and emission spectra. However a strong interaction resulting in a quenching effect was observed for mercury(II), see Figures 6.4 panel B and C, affecting both, ground and excited states. In this case, one metal center was enough to totally quench the strong fluorescence emission shown by the free ligand (Φ=0.77) [19]. The JOB plot experiments confirm the formation of a mononuclear complex (Figure 6.4 panel d). After complexation the emission band centered at 440 nm was red shifted to 480 nm and calculations by the Hypspec program gave a value for the complexation constant with a log β of 6.50±0.03.

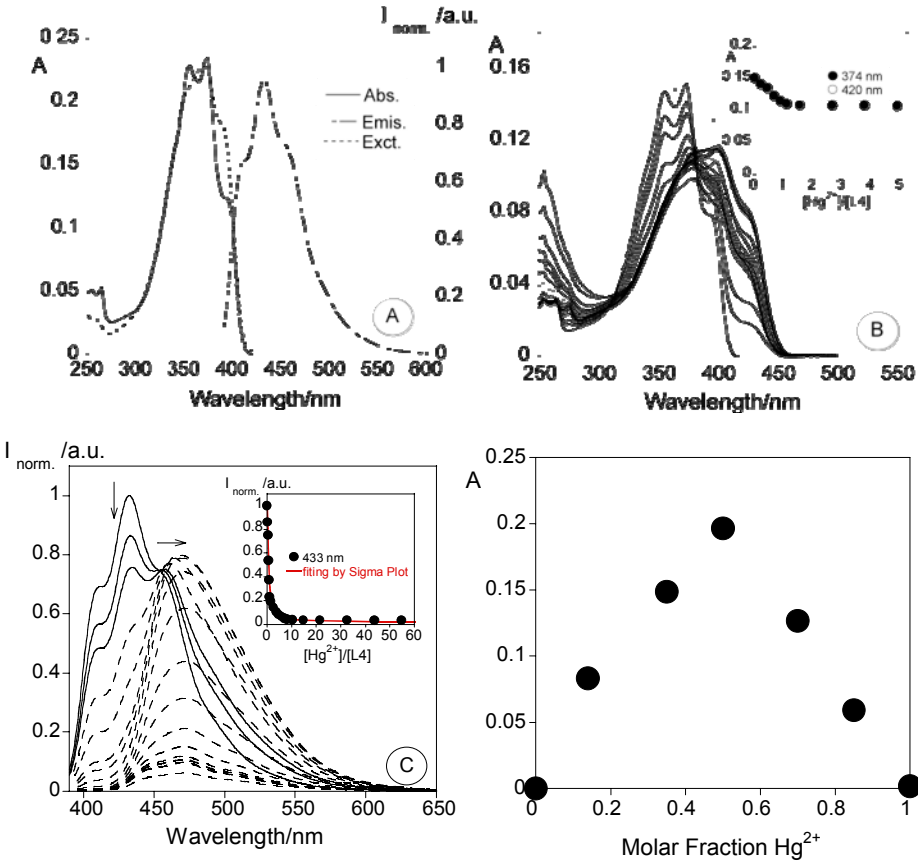

Figure 6.4 – Absorption, emission and excitation spectra of ligand L4 (T=298 K, [L4] = 1.40 $\times$ 10^{-6} M, λ_{exc} = 374 nm) (A) and spectrophotometric (B) and spectrofluorimetric titration (C) of

L4 with a standard solution of $Hg(CF_3SO_3)_2$ in dichloromethane, ([L4] = 1.40×10^{-6} M, λ_{exc} = 434 nm, the inset shows the normalized emission at 433 nm, and the fitting by Sigma Plot). Panel D shows the JOB plot for L4/Hg^{2+} interaction.

6.5 - Experimental

6.5.1 - Physical measurements

Elemental analyses were performed on a Fisons Instruments EA1108 microanalyser at the Universidade de Vigo. Infra-red spectra were recorded as KBr discs on a JASCO FT-IR 410 spectrophotometer.

MALDI-TOF-MS data were obtained using a MALDI-TOF-MS model Voyager DE-PRO Biospectrometry Workstation equipped with a nitrogen laser irradiating at 337 nm (Applied Biosystems, Foster City, United States) from the MALDI-TOF-MS Service of the REQUIMTE, Chemistry Department, Universidade Nova de Lisboa. The acceleration voltage was $2.0*10^4$ kV with a delayed extraction (DE) time of 200 ns. The spectra represent accumulations of 5*100 laser shots. The reflection mode was used. The ion source and flight tube pressures were less than $1.80*10^{-7}$ and $5.60*10^{-8}$ Torr, respectively.

The MALDI mass spectra of the soluble samples (1 or 2 mg/mL) such as the ligand and metal complexes were recorded using the conventional sample preparation method for MALDI-MS. In the metal ion titrations by MALDI the metal sample (1 mL) was put on the sample holder on which the chelating ligand **L** had been previously spotted. The sample holder was inserted into the ion source. Chemical reaction between the ligand and metal salts occurred in the holder and complex species were produced.

6.5.2 - Spectrophotometric and spectrofluorimetric measurements

Absorption spectra were recorded on a JASCO 650 spectrophotometer and fluorescence emission on a Horiba-Jovin Ibon Fluoromax 4. The linearity of the fluorescence emission vs. concentration was checked in the concentration used (10^{-4} – 10^{-6} M). A correction for the absorbed light was performed when necessary. The spectrometric characterizations and titrations were performed as follows: the stock solutions of the compounds (*ca*. 10^{-3} M) were prepared by dissolving an appropriated amount of the ligand in a 10 ml volumetric flask and diluting to the mark with the solvent. The titrated solutions were prepared by appropriate dilution of the stock solutions still 10^{-5} – 10^{-6} M. Titrations of the ligand L4 were carried out by the addition of microliter amounts of standard solutions of the ions in dichloromethane (1.40×10^{-6} M).

Fluorescence spectra of solid samples were recorded using a fiber optic system connected to the Horiba-Jovin Ybon Fluoromax 4 spectrofluorimetric exciting at appropriated λ (nm) the

solid compounds. All the measurements were performed at 298 K. Luminescence quantum yields were measured using a solution of quinine sulphate in sulphuric acid (0.5M) as a standard [ϕ] = 0.54 and were corrected for different refraction indexes of solvents [28].

6.5.3 - Computational Methods

Density Functional Theory (DFT) in the Kohn-Sham approximation was used to optimize the geometry of all the species modeled. The hybrid exchange-correlation functional with a long range correction, CAM-B3LYP [29] was used through all the calculations with the def2-svp basis set [30] for every atom and the ecp-60-mwb electron core potential for mercury [31]. The stability of the wave function and the hessian were calculated on the optimized geometries at the same level to establish that both the optimized geometry and the optimized wave function correspond to a minimum. Non-specific solvent effects were partially taken into account using a continuum model, PCM, with ethanol as the chosen dielectric. All the calculations have been performed using the Gaussian09 suite of programs [32].

6.5.4 - Chemicals and starting materials

$Cu(CF_3SO_3)_2$, $Ni(BF_4)_2$, $Hg(CF_3SO_3)_2$, $Zn(CF_3SO_3)_2$, $Ca(ClO_4)_2$ and $NaNO_3$ were purchased from Alfa Aesar and Sigma-Aldrich. All were used without further purification. All solvents used were from PANREAC and Riedel-de Häen without further purification.

The synthesis of organic ligands **L1** to **L3** was published recently [17,18].

6.5.5 - Synthesis of ligand L4

The starting compound *bis*-[*N*-*t*-butyloxycarbonyl [2-(thien-2'-yl)benzoxazol-5-yl]-L-alanine methyl ester] [19] (0.080 g, 1.54×10^{-4} mol) was dissolved in 1,4-dioxane (1 mL), in an ice bath, and sodium hydroxide 1M aqueous solution (0.23 mL, 2.3×10^{-4} mol, 1.5 eq) was added drop wise. The mixture was stirred at room temperature for 3h. The pH was adjusted to 2-3 by addition of $KHSO_4$ 1 M aqueous solution and extracted with ethyl acetate (3 × 10 mL). After drying with anhydrous magnesium sulphate and evaporation of the solvent, the residue was triturated with diethyl ether and a yellow solid was obtained

Colour: Yellow powder, melting point = 98ºC, Anal.Calc. for $C_{34}H_{36}N_4O_{10}S_2$. (MW= 692.2): C, 58.95; H, 5.25; N, 8.10; S, 4.65. Found: C, 59.15; H, 5.45; N, 8.15; S, 4.70 % CHNS. IR (NaCl windows): v (NH st) (cm^{-1})= 3310; v (COO^- st) (cm^{-1})= 1745, v (C=O) (cm^{-1})= 1698; v (C=C benzene) (cm^{-1})= 1660; v ($-CH_2$ δ) (cm^{-1})= 1452; v ($-CH_3$ δ) (cm^{-1})= 1372; v (C-O-C cyclic ethers) (cm^{-1})= 1260,1229; v (thiophene) (cm^{-1})= 3065 (CH st), 1538 (CH γ), 751 (CH δoop).

MS (MALDI-TOF-MS) *m/z* without matrix : 693.56 $[L4H]^+$.

6.5.6 - Synthesis of metal complexes – general procedure

Two equivalents of the appropriate metal salt of copper(II), nickel(II) or mercury(II) (0.26 mmol, 0,34 mmol, 0.26 mmol) were dissolved in abs. ethanol (5 mL) and added dropwise to a stirred solution of the ligand (0.13 mmol L_1, 0.17 mmol L_2, 0.13 mmol L_3) in absolute ethanol. The solution was gently heated and stirred over-nigth. The solvent was evaporated under vacuum until *ca.* 2 mL. Diethyl ether was added to the solution and the resulting solid products were isolated by filtration, washed with cold absolute ethanol, diethyl ether, and dried under vacuum. All complexes appear to be air stable soluble in DMSO, DMF, CH_3CN, $CHCl_3$, absolute CH_3OH but insoluble in water.

$[Cu_2L1](CF_3SO_3)_4.2CH_3CN.\ 2H_2O$ **(1)**

Colour: green. Yield: 27%. Anal.Calc. for $C_{27}H_{30}Cu_2F_{12}N_4O_{19}S_5$ (MW: 1227.85): C, 26.35; H, 2.45; Cu, 10.33; N, 4.55; S, 13.04. Found: C, 26.33; H, 2.50; Cu, 10.70; N, 4.55; S, 12.95. IR (KBr, cm^{-1}): 1619 [ν(C=O)], 1574 [ν(C=C)], 1480, 1418 [ν(C=N)], 1253 [ν(C-O) $_{benzoxazol}$]. MS (MALDI-TOF-MS) *m/z*: 451.03 $[L1Cu]^+$; 510.08 $[L1Cu.CH_3CN.H_2O]^+$; 1150.80 $[L1(Cu_2(CF_3SO_3)_4).CH_3CN]^+$. UV-Vis in abs. ethanol (λ nm): 315 nm, ($\varepsilon \approx 4.58$). Fluorescence emission band in abs. ethanol (λ_{exc} =315 nm) ; λ_{emis} = 384 nm.

$[Ni_2L1]\ (BF_4)_4\ .7H_2O$ **(2)**

Colour: brown. Yield: 51%. Anal.Calc. for $C_{19}H_{34}B_4F_{16}Ni_2N_2O_{12}S$ (MW: 978.07): C, 23.30; H, 3.50; N, 2.85; Ni, 11.99; S, 3.25. Found: C, 23.35; H, 3.60; N, 3.10; Ni, 12.25; S, 3.25. IR (KBr, cm^{-1}): 1619 [ν(C=O)], 1577 [ν(C=C)], 1415 [ν(C=N)], 1259 [ν(C-O) $_{benzoxazol}$]. MS (MALDI-TOF-MS) *m/z:* 446.05 $[L1Ni]^+$; 678.05 $[L1Ni_2(BF_4)_2]^+$ UV-Vis in abs. ethanol (λ nm): 316 nm, ($\varepsilon \approx 4.40$). Fluorescence emission band in abs. ethanol (λ_{exc} =315 nm) ; λ_{emis} = 384 nm.

$[Hg_2L1]\ (CF_3SO_3)_4\ .4H_20$ **(3)**

Colour: brown. Yield: 35%. Anal.Calc. for $C_{23}H_{28}F_{12}\ Hg_2N_2O_{21}S_5$ (MW: 1459.90): C, 18.95; H, 1.95; Hg, 27.50; N, 1.90; S, 11.00. Found: C, 18.65; H, 1.75; Hg, 27.75; N, 2.10; S, 11.20. IR (KBr, cm^{-1}): 1625 [ν(C=O)], 1579 [ν(C=C)], 1439 [ν(C=N)], 1256 [ν(C-O) $_{benzoxazol}$]. MS (MALDI-TOF-MS) *m/z:* 590.07 $[L1Hg]^+$; 843.65 $[L1Hg_2.3H_2O]^+$. UV-Vis in abs. ethanol (λ nm): 320 nm, ($\varepsilon \approx 4.39$). Fluorescence emission band in abs. ethanol (λ_{exc} =320 nm); λ_{emis} = 386 nm.

$[Cu_2L2](CF_3SO_3)_4\ .3H_2O$ **(4)**

Colour: green. Yield: 37%. Anal.Calc. for $C_{18}H_{18}Cu_2F_{12}N_2O_{18}S_5$ (MW: 1063.76): C, 20.30; H, 1.70; Cu, 11.93; N, 2.63; S, 15.04. Found: C, 20.25; H, 1.15; Cu, 12.03; N, 2.85; S, 15.00. IR (KBr, cm^{-1}): 1605 [ν(C=O)], 1573 [ν(C=C)], 1439 [ν(C=N)], 1256 [ν(C-O) $_{benzoxazol}$]. MS (MALDI-TOF-MS) *m/z:* 518.95 $[L2Cu(CF_3SO_3).H_2O]^+$; 862.65 $[L2Cu_2(CF_3SO_3)_3]^+$. UV-Vis bands in abs. ethanol (λ nm): 315 nm, (ε ≈ 4.30). Fluorescence emission band in abs. ethanol (λ_{exc} =315 nm); λ_{emis} = 384 nm.

$[Ni_2L2](BF_4)_4 .6\ H_2O$. **(5)**

Colour: green. Yield: 61%. Anal.Calc. for $C_{14}H_{23}B_4F_{16}Ni_2N_2O_9S$ (MW: 860.01): C, 19.55; H, 2.80; N, 3.25; Ni, 13.65; S, 3.70. Found: C, 20.15; H, 2.45; N, 3.60; Ni, 13.45; S, 3.45. IR (KBr, cm^{-1}): 1605 [ν(C=O)], 1579 [ν(C=C)], 1439 [ν(C=N)], 1256 [$\nu(C\text{-}O)_{benzoxazol}$]. MS (MALDI-TOF-MS) *m/z:* 347.00 $[L2Ni]^+$; 490.95 $[L2Ni_2(BF_4)]^{+\cdot}$ UV-Vis band in abs. ethanol (λ nm): 315 nm, (ε ≈ 4.24). Fluorescence emission band in abs. ethanol (λ_{exc} =315 nm); λ_{emis} = 384 nm.

$[Hg_2L2](CF_3SO_3)_4 .2CH_3CN.2H_2O$ **(6)**

Colour: yellow. Yield: 25%. Anal.Calc. for $C_{22}H_{22}F_{12}Hg_2N_4O_{17}S_5$ (MW: 1405.88): C, 18.85; H, 1.60; Hg, 28.58; N, 3.99; S, 11.45. Found: C, 19.05; H, 1.45; Hg, 28.65; N, 4.15; S, 11.35. IR (KBr, cm^{-1}): 1614 [ν(C=O)], 1576 [ν(C=C)], 1438 [ν(C=N)], 1256 [$\nu(C\text{-}O)_{benzoxazol}$]. MS (MALDI-TOF-MS) *m/z:* 638.90 $[L2Hg(CF_3SO_3)]^+$; 828.95 $[L2Hg(CF_3SO_3)_2.CH_3CN]^+$; 1136.75 $[L2Hg_2(CF_3SO_3)_3]^+$. UV-Vis bands in abs. ethanol (λ nm): 315 nm, log ε ≈ 4.24. Fluorescence emission band in abs. ethanol (λ_{exc} =315 nm); λ_{emis} = 384 nm.

$[Ni_2L3]\ (BF_4)_4 .4H_2O$ **(7)**

Colour: yellow-green. Yield: 23%. Anal.Calc. for $C_{18}H_{22}B_4F_{16}N_2Ni_2O_7S_2$ (MW: 905.96): C, 23.83; H, 2.45; N, 3.10; Ni, 12.95; S, 7.10. Found: C, 23.60; H, 2.90; N, 3.15; Ni, 13.25; S, 7.55. IR (KBr, cm^{-1}): 1605 [ν(C=O)], 1573 [ν(C=C)], 1439 [ν(C=N)], 1256 [$\nu(C\text{-}O)_{benzoxazol}$]. MS (MALDI-TOF-MS) *m/z:* 602.74 $[L3Ni(BF_4)_2]^+$; 697.45 $[L3Ni_2(BF_4)_2.2H_2O]^+$. UV-Vis bands in abs. ethanol (λ nm): 316 nm, log ε ≈ 4.35. Fluorescence emission band in abs. ethanol (λ_{exc} =316 nm); λ_{emis} = 386 nm.

$[Cu_2L3]\ (CF_3SO_3)_4.3H_2O$ **(8)**

Colour: green. Yield: 22%. Anal.Calc. for $C22H20Cu_2F12N_2O_{18}S_6$ (MW: 1145.74): C, 23.05; H, 1.75; N, 2.45; Cu, 11.07; S, 16.76. Found: C, 23.20; H, 1.90; N, 2.35; Cu, 11.25; S, 17.05. IR (KBr, cm^{-1}): 1602 [ν(C=O)], 1575 [ν(C=C)], 1439 [ν(C=N)], 1255 [ν(C-O) $_{benzoxazol}$]. MS (MALDI-TOF-MS) *m/z:* 732.38 $[L3Cu(CF_3SO_3)_2]^+$; 831.70 $[L3Cu_2(CF_3SO_3)_2 2H_2O]^+$. UV-Vis

bands in abs. ethanol (λ nm): 315 nm, log $\varepsilon \approx 4.45$. Fluorescence emission band in abs. ethanol (λ_{exc} =315 nm); λ_{emis} = 386 nm.

6.6 - Acknowledgments

We are indebted to *InOU Uvigo* by project K914 122P 64702 (Spain) and FCT- Portugal by project PTDC/QUI/66250/2006 for financial support. C. L. thanks Xunta de Galicia, Spain, for the Isidro Parga Pondal Research Program. E.O. thanks to FC-MCTES (Portugal) by her PhD grant SFRH/BD/35905/2007, and to Fundação Calouste Gulbenkian (Portugal), for the National Prize in creativity and quality in research activity, 2008. We also thank the CESGA (Centro de Supercomputación de Galicia) for generous allocation of computational resources. We are grateful to Dr. José Luis Capelo from the University of Vigo, Spain for the help with the MALDI-TOF-MS spectra.

6.7 - References

[1] A. Pasini, L.J. Casella, *Inorg. Nucl. Chem.*, 36 (1979) 2133.

[2] V.J. Derose, S. Burns, N.K. Kim, M. Vogt, *Compr. Coord. Chem*. II 8 (2004) 787.

[3] S J. Lippard, J.M. Berg, Principles of Bioinorganic Chemistry, University Science Books, Sausalito, CA, 1994.

[4] H. Umezawa, *Prog. Biochem. Pharmacol*. 11 (1976) 18.

[5] P.R. Chetana, R, Rao, M. Roy, A.K. Patra, *Inorg.Chim.Acta*, 362 (2009) 46 4692.

[6] M.N. Hosny, *Trans. Metal Chem.*, 32 (2007) 117.

[7] N. Grosser, S. Oberle, G. Berndt, K. Erdmannk, A. Hemmerle, *Biochem. Biophys. Res. Commun*., 314 (2004) 351.

[8] J. Chin, *Acc. Chem. Res.* 24 (1991) 145.

[9] J. Suh, *Acc. Chem. Res.* 25 (1992) 273.

[10] J. Gallagher, O. Zelenko, A. D. Walts, D. S. Sigman, *Biochemistry* 37 (1998) 2096.

[11] E. L. Hegg, J. N. Burstyn, *J. Am. Chem. Soc.* 117 (1995) 7015

[12] T. M. Rana, *Adv. Inorg. Biochem. 10* (1993) 177.

[13] V. Anbalagan, V. M. J. Stipdonk, *J. Mass Spectrom.*, 38 (2003) 982.

[14] M. M. Yamashita, L. Wesson, G. Eisenman, D. Eisenberg, *Proc. Natl. Acad. Sci. USA* 87 (1990) 5648.

[15] T. Marine, N. Russo, M. Toscano, *J. Mass Spectrom.,* 37 (2002) 786.

[16] (a) C. Lodeiro, J. L. Capelo, J. C. Mejuto, E. Oliveira, H. M. Santos, B. Pedras, C. Nuñez, *Chem. Soc. Rev.,* 39 (2010) 2948.

(b) C. Lodeiro, F. Pina, *Coord. Chem. Rev*., 253 (2009) 1353.

(c) L. Rodriguez, C. Lodeiro, J. C. Lima, R. Crehuet, Inorg. Chem., 47 (2008) 4952.

(d) R. M. F. Batista, E. Oliveira, S. P. G. Costa, C. Lodeiro, M. M. M. Raposo, Org. Letters, 9 (2007) 3201.

[17] S. P. G. Costa, E. Oliveira, C. Lodeiro, . M. M. M. Raposo, *Sensors* , 7 (2007) 2096.

[18] S. P. G. Costa, E. Oliveira, C. Lodeiro, M. M M. Raposo, *Tetrahedron Letters*, 49 (2008) 5258.

[19] S. P. G. Costa, R. M. F. Batista, M. M. M. Raposo, *Tetrahedron*, 64 (2008) 9733.

[20] (a) J.L. Capelo, A.V. Filgueiras, I. Lavilla, C. Bendicho, Talanta 50 (1999) 905;

(b) C. Fernandez, A.C.L. Conceição, R. Rial-Otero, C. Vaz, J.L. Capelo, Anal. Chem. 78 (2006) 2494;

(c) A. Tamayo, B. Pedras, C. Lodeiro, L. Escriche, J. Casabó, J.L. Capelo, B. Covelo, R. Sillanpää, R. Kivekäs, Inorg. Chem. 46 (2007) 7818.

[21] R. M. Silverstein, G. C. Bassler, T. C. Morrill, “Spectrometric identification of organic compounds”, 4th Ed. John Wiley & Sons, New York, 1981.

[22] C. Núñez, R. Bastida, A. Macías, E. Bértolo, L. Fernandes, J. L. Capelo, C. Lodeiro, *Tetrahedron*, 65, (2009), 6179.

[23] K. Ruckak, Spectrochim. Acta. A., 57 (2001) 2161.

[24] A. W. Czarnik, *Fluorescent Chemosensors for Ion and Molecule Recognition*; American Chemical Society: Washington, DC, 1993.

[25] de Silva, A. P.; Gunaratne, H. Q. N.; Gunnlaugsson, T.; Huxley, A. J. M.; McCoy, C. P.; Rademacher, J. T.; . Rice, T. E., *Chem. Rev.,* 97 (1997) 1515.

[26] (a) J. S. Casas, M. S. García-Tasende, J. Sordo, Coord. Chem. Rev., 209 2000 197. (b)

.G. Kuzmina, Yu. T. Struchkov, E. M. Rokhlina, D. N. Kravtsov *J. Struct. Chem.,* 24 1983 130. (c) Z. Popovic, D. Matkovic-Calogovic, Z.Soldin, G. Pavlovic, N. Davidovic, D.Vikic-Topic *Inorg.Chim.Acta ,* 294 1999 35. (d) S. S. Lemos, D. U. Martins, V. M. Deflon, J. Elena *J. Organomet. Chem.,* 694 2009 253. (e) M. Kato, K. Kojima, T. Okamura, H. Yamamoto, T. Yamamura, N. Ueyama, *Inorg. Chem.,* 44 2005 4037. (f) P.Fernandez, A.Sousa-Pedrares, J.Romero, J.A.Garcia-Vazquez, A.Sousa, P.Perez-Lourido, *Inorg.Chem.,* 47 2008 2121.

[27] P. Gans, A. Sabatini, A. Vacca, *Talanta*, 43 1996 1739.

[28] I. B. Berlman, *Handbook of Fluorescence Spectra of Aromatic Molecules*, 2nd ed.; Academic Press: New York, 1971.

[29] T. Yanai, D. P. Tew, N. C. Handy, *Chem. Phys. Lett*. 393 2004 51.

[30] F. Weigend, R. Ahlrichs, *J. Phys. Chem. Chem. Phys*. 7 2005 3297.

[31] D. Andrae, U. Haussermann, M. Dolg, H. Stoll, H. Preuss, *Theor. Chim. Acta*., 77 1990 123.

[32] Gaussian 09, Revision A.1, M. J. Frisch, G. W. Trucks, H. B. Schlegel, G. E. Scuseria, M. A. Robb, J. R. Cheeseman, G. Scalmani, V. Barone, B. Mennucci, G. A. Petersson, H. Nakatsuji, M. Caricato, X. Li, H. P. Hratchian, A. F. Izmaylov, J. Bloino, G. Zheng, J. L. Sonnenberg, M. Hada, M. Ehara, K. Toyota, R. Fukuda, J. Hasegawa, M. Ishida, T. Nakajima, Y. Honda, O. Kitao, H. Nakai, T. Vreven, J. A. Montgomery, Jr., J. E. Peralta, F. Ogliaro, M. Bearpark, J. J. Heyd, E. Brothers, K. N. Kudin, V. N. Staroverov, R. Kobayashi, J. Normand, K. Raghavachari, A. Rendell, J. C. Burant, S. S. Iyengar, J. Tomasi, M. Cossi, N. Rega, J. M. Millam, M. Klene, J. E. Knox, J. B. Cross, V. Bakken, C. Adamo, J. Jaramillo, R. Gomperts, R. E. Stratmann, O. Yazyev, A. J. Austin, R. Cammi, C. Pomelli, J. W. Ochterski, R. L. Martin, K. Morokuma, V. G. Zakrzewski, G. A. Voth, P. Salvador, J. J. Dannenberg, S. Dapprich, A. D. Daniels, Ö. Farkas, J. B. Foresman, J. V. Ortiz, J. Cioslowski, and D. J. Fox, Gaussian, Inc., Wallingford CT, 2009.

Chapter 7

Bio-inspired systems for Metal Ion Sensing: New Emissive Peptide Probes Based on Benzo[*d*]oxazole Derivatives and Their Gold and Silica Nanoparticles

Elisabete Oliveira, Daminao Genovesse, Riccardo Juris, Nelsi Zaccheroni, José Luis Capelo, M. Manuela M. Raposo, Susana P.G. Costa, Luca Prodi, Carlos Lodeiro, Submited **2010**.

"There is more to life than increasing its speed"

Mahatma Gandhi, 1869-1948

Index

7.1 - Abstract

Seven new bio-inspired chemosensors (**L1**-**L7**) based on fluorescent peptides were synthesized and characterized by elemental analysis, ^{1}H-NMR, ^{13}C-NMR, melting point, matrix assisted laser desorption-ionization time-of-flight mass spectrometry (MALDI-TOF-MS), Infrared, UV-Vis absorption and emission spectroscopy. The interaction with transition and post-transition metal ions (Cu^{2+}, Ni^{2+}, Ag^{+}, Zn^{2+}, Cd^{2+}, Hg^{2+} and Pb^{2+}) has been explored by absorption and fluorescence emission spectroscopy, and MALDI-TOF mass spectrometry. Gold and silica nanoparticles functionalized with these peptides were also obtained. All nanoparticles were characterized by dynamic light-scattering (DLS), transmission electron microscopy (TEM), UV-vis absorption and fluorescence emission spectroscopy. Non fluorescent gold(0) nanoparticles (diameter 2-10 nm) bearing ligands **L** and **L3** were obtained by common reductive synthesis. Commercial silica nanoparticles were decorated at their surface using compounds **L5** to **L7**, linked through a silane spacer. The same chemosensors were also taken into aqueous solutions through their dispersion in the outer layer of silica core/PEG shell nanoparticles. In both cases, these complex nanoarchitectures behaved as new sensitive materials for Ag^{+} and Hg^{2+} in solution.

My contribution for this work was the synthesis of the organic peptide compounds, all photophysical studies, lifetime measurements, gold and silica nanoparticles synthesis, its characterization by dynamic light scattering, the photophysical characterization and the application as metal ions chemosensors.

7.2 - Resumo

Sete novos sensores químicos bio-inspirados baseados em péptidos fluorescentes foram sintetizados e caracterizados por análise elementar, ^{1}H-NMR, ^{13}C-NMR, ponto de fusão, Infravermelho, MALDI-TOF-MS, espectroscopias de absorção e de emissão de fluorescência.

A interação com iões metálicos de transição e pós-transição (Cu^{2+}; Ni^{2+}; Ag^{+}; Zn^{2+}; Cd^{2+}; Hg^{2+} and Pb^{2+}) foi explorada por espectrocopia de absorção e de emissão de fluorescência, e espectrometria de MALDI-TOF-Ms.

Nanopartículas de ouro e sílica funcionalizadas como estes péptidos foram também obtidas. Todas as nanopartículas foram caracterizadas por “dymanic light-scattering” (DLS) e por microscopia de transmissão electrónica. Nanopartículas de ouro não emissivas contendo os ligandos L e L3 foram obtidas pelo método redutivo. Nanopartículas comerciais foram decoradas na sua superfície com os compostos **L5** e **L7**, ligandos através de um espaçador silano. Os mesmos sensores químicos foram também estudados em soluções aquosas através da sua dispersão para interior das nanopartículas de sílica/camada de nanopartículas PEG. Em ambos os casos, estas nano-arquitecturas complexas tornaram-se materiais sensíveis para Ag^{+} e Hg^{2+} em solução.

A minha contribuição para este trabalho consistiu na síntese dos compostos orgânicos peptidicos, todos os estudo fotofísicos, medidas de tempos de vida, síntese das nanopartículas, a sua caracterização por “dynamic light scattering”, caracterização fotofísica e aplicação como sensores químicos de metais.

7.3 - Introduction

Fluorescent chemosensors have experienced a great development in the last decades due to their important applications in many different areas, in particular in medical diagnostics, environmental and material sciences.[1] In a conjugate chemosensor, three main structural components can be distinguished: i) the receptor, ii) the fluorophore and, in some cases, iii) the spacer. In this framework, bio-inspired systems, i.e. chemosensors in which the binding moiety is a natural or synthetic amino acid or a peptide chain, are particularly valuable and suitable for applications both in biotechnology and in nano-electronics. [2] Wiczk and co-workers have presented several examples of alanine derivatives for metal ion detection [3] in which the introduction of a peptide chain is fundamental for the recognition event. Histidine, glutamine and cysteine are known to be the specific binding residues for Zn^{2+} in enzymes, while proline and glycine induce the bending of the structure ensuring the preorganization of the system. Lee and co-workers have merged these two aspects synthesizing a short peptide probe bound to a dansyl fluorophore to yield a selective chemosensor for extracellular and environmental zinc.[4] Andreopoulos, Leblanc and collaborators [5] have in turn shown that the selectivity of short peptidyl sequences toward metal cations and, in particular, toward Cu^{2+} ions, was greatly influenced by the reciprocal spatial alignment of the fluorophore and the amino acidic binding chain. The different arrangement of the various units in the chemosensor induced different transduction mechanisms between the receptor and the signalling dansyl group, which resulted in a different sensing performance.[5] On the other hand, Yang and Li investigated the possibilities offered by a long and flexible architecture by preparing a luminescent chemosensor for metal ions in aqueous solution based on the conjugation of amino acids with multidentate aminocarboxylate ligands.[6] In this case the system presented an EDTA derivative functionalized with two tryptophan units, whose indole moiety represented the signalling units, being also involved in the recognition event. This species revealed a remarkable selectivity for Ca^{2+} over other mono- and divalent cations in water, as shown by an important enhancement of the fluorescence intensity.

Peptide derivatives containing benzoxazole units as chromophores are also known and benzoxazoles have important biological applications as inhibitors of human cysteine proteases, as ligands of the NMDA receptor, and as biomarkers or biosensors.[7]

Recently, however, research is moving towards more complex and sophisticated structures trying to push further their limits of sensitivity and selectivity. Many different solutions have been proposed but, among them, sensing systems based on nanoparticles are certainly one of the most interesting and promising.[8] The impressive huge range of

interests and applications of nanoparticles arises from the incredible versatility and modulation of their properties. A great number of materials can be used to engineer nanoparticles such as carbon (fullerenes, carbon-dots, etc.), metals (silver, gold, copper, platinum), metal oxides (zinc, iron, titanium, copper oxides), semiconductors (e.g., CdSe/ZnS, PbS, InGaP, called quantum dots, QDs), silica, polymers, surfactants, lipids, and many different mixing of two or more of them. Moreover, it is possible, in many cases, to derivatize their surface with different capping agents (receptors, chemosensors, DNA strains, etc…) to introduce whatever functionality desired.[9] Among the different nanoparticles listed above properly modified gold nanoparticles (AuNPs) and silica nanoparticles can be seen as very interesting options for solving important analytical problems including those related to medical diagnosis and imaging.

Gold nanoclusters, even if already known and used for their iridescent colours since centuries before Christ, have gained great importance only in last decades in biology and medicine: their possible applications when functionalized with biomolecules in sensing, diagnostics and therapeutics are really outstanding.[10,11] In this context, a new generation of sensing materials using soft donor atoms such as sulphur have been used for decorating gold nanoparticles (AuNPs).[1,9,12,13]

On the other hand, because of the favourable chemical, optical and toxicological properties of silica,[14] incorporation of fluorescent chemosensors in monodisperse silica nanoparticles yielded a new group of fluorescent materials with improved properties, such as higher affinity, versatility and sensitivity, also thanks in some case, to signal amplification processes.[15]

Although some examples of decorated nanoparticles with peptides has been reported recently for heavy metal ion detection [16], this is the first time in which highly fluorescent (oligo)thienyl-benzo[*d*]oxazole derivatives are incorporated as fluorophores into emissive nanoparticle devices.

Following our ongoing research project on bio-inspired fluorescent chemosensors using amino acids as building blocks, we have already explored thiophene and bithiophene rings as new sulphur-donor chelating units within an amino acid core.[17] The resulting highly fluorescent unnatural heterocyclic alanine derivatives (Φ_F = 0.26 to 0.80) showed a noticeable quenching upon complexation with paramagnetic Cu^{2+} and Ni^{2+} metal ions and with diamagnetic Hg^{2+} ions. A negligible interaction with other important biological metal ions such as Zn^{2+}, Ca^{2+} and Na^{+} was also observed.[17]

In the present paper we report the synthesis of seven new emissive peptide-based compounds, **L1**-**L7**, containing an alanine, cysteine or tryptophan as building blocks, combined with two synthetic amino acids, [2-(thien-2'-yl)benzo[*d*]oxazol-5-yl]-L-alanine (BOT) and [2-(bithien-2'-yl)benzo[*d*]oxazol-5-yl]-L-alanine (BOTT) (Scheme 7.1). The

(oligo)thienyl-benzo[*d*]oxazole chromophore was used as emissive unit in all cases. All compounds were characterized by elemental analysis, melting point, MALDI-TOF-MS spectrometry, infrared, UV-vis absorption, fluorescence emission, ^{1}H and ^{13}C NMR spectroscopy. Their interaction with several mono- and divalent metal ions was followed by spectroscopic techniques. Gold and silica nanoparticles decorated with these new peptides were synthesized and characterized by fluorescence spectroscopy, dynamic light scattering (DLS), and transmission electronic microscopy (TEM). The complexation ability of the silica nanoparticles in solution was also investigated.

7.4 - Experimental Section

7.4.1 - Synthesis of peptides

The synthesis and characterization of the parent compound **L** was previously described (See Scheme 7.1).[17a,17b]

L1. **Boc-BOT-Cys(Bzl)-OMe.**

Boc-BOT-OH,[17] (0.13 g, 3.26×10^{-4} mol) was dissolved in distilled DMF (2 ml), cooled in an ice bath, followed by the addition of HOBt (0.04 g, 3.26×10^{-4} mol) and DCC (0.07 g, 3.26×10^{-4} mol). The mixture was stirred in an ice bath during 30 minutes. In a separate flask, thionyl chloride (0.20 ml, 2.60×10^{-2} mol) was added drop wise with stirring to methanol (10 ml), cooled in an ice bath, followed by the addition of Boc-Cys(Bzl)OH (0.81 g, 2.60×10^{-2} mol). The solution was refluxed at boiling temperature for 2 h. The solvent was evaporated under reduce pressure, yielding an oil. The oil was triturated with diethyl ether leading to a white solid (HCl.H-Cys-OMe).

In a next step, HCl.H-Cys-OMe (0.09 g, 3.26×10^{-4} mol) was neutralized with triethylamine (43 μl, 3.26×10^{-4} mol) in distilled DMF for 30 minutes. The solution was filtered and the filtrate was added to the previous mixture containing Boc-BOT-OH. The final mixture was stirred for 1 h in an ice bath and 1 h at room temperature. The solvent was evaporated under reduced pressure and the residue was treated with cooled acetone, to remove *N,N'*-dicyclohexylurea (DCU) through filtration. The solvent was evaporated and the residue purified by column chromatography with silica gel (eluent: CH_2Cl_2/MeOH 100:1, 100:2). The fractions were combined and the product **L1** was obtained as a solid.

Yellow solid (0.14 g, 75 %), melting point = 94-97ºC, $C_{30}H_{33}N_3O_6S_2$. $3/2CH_3CH_2OCH_2CH_3$, FW= 706.9

Elemental Analysis: (Found: C, 61.4; H, 6.4; N, 6.4; S, 9.6 % CHNS requires: C, 61.2; H,

6.8; N, 6.0; S, 9.1).

IR (NaCl windows): v (NH st) (cm^{-1})= 3300; v (COO^- st) (cm^{-1})= 1730, v (C=O) (cm^{-1})= 1696; v (C=C benzene) (cm^{-1})= 1663; v (-CH_2 δ) (cm^{-1})= 1453; v (-CH_3 δ) (cm^{-1})= 1369; v (thiophene) (cm^{-1})= 3061 (CH st), 1534 (CH γ), 746 (CH δoop).

NMR Spectrum:

δ_H ($CDCl_3$, 300 MHz): 1.41 (s, 9H, $C(CH_3)_3$), 2.74-2.94 (m, 2H, β-CH_2 Cys), 3.19 (d, J= 6.3 Hz, 2H, β-CH_2 BOT), 3.65 (s, 2H, CH_2 Bzl), 3.70 (s, 3H, OCH_3), 4.42 (m, 1H, α-H Cys), 4.72-4.78 (m, 1H, α-H BOT), 5.00 (d, J=5.7 Hz, 1H, NH BOT), 6.62 (d, J=7.5 Hz, 1H, NH Cys), 7.18-7.30 (m, 7H, 5 × Ph-*H*, H6 and H4'), 7.45 (d, J=8.4 Hz, 1H, H7), 7.55 (d, J=1.2 Hz, 1H, H4), 7.57 (dd, J=1.2 and 5.1 Hz, 1H, H5'), 7.91 (dd, J=1.2 and 2.4 Hz, 1H, H3').

δ_C ($CDCl_3$, 75.4 MHz): 28.26 ($C(\underline{C}H_3)_3$), 33.40 (β-CH_2 Cys), 36.49 (CH_2 Bzl), 37.65 (β-CH_2 BOT), 52.40 (OCH_3), 53.41 (α-C Cys), 53.85 (α-C BOT), 80.05 ($\underline{C}(CH_3)_3$), 110.53 (C7), 119.73 (C4), 127.02 (C4''), 126.68 (C6), 128.55 (C2'' and C6''), 128.62 (C4'), 128.77 (C2), 128.97 (C3'' and C5''), 130.51 (C3'), 131.22 (C5'), 133.08 (C5), 138.12 (C1''), 141.14 (C3a), 149.17 (C7a), 155.28 (C=O Boc), 159.55 (C2'), 170.87 (C=O BOT), 171.00 (C=O Cys).

L2. **Boc-BOT-Cys(Bzl)- OH**

The precursor Boc-BOT-Cys(Bzl)-OMe, **L1**, (0.14 g, 2.43×10^{-4} mol) was dissolved in 1,4-dioxane (1 ml) in an ice bath, and aqueous sodium hydroxide 1M solution (0.36 ml, 1.5 eq., 3.65×10^{-4} M) was added dropwise. The mixture was stirred at room temperature for 3h. The pH was adjusted to 2-3 by addition of aqueous $KHSO_4$ 1M solution and extracted with ethyl acetate (3 × 10 ml). After drying with anhydrous sodium sulphate and evaporation of the solvent, the residue was triturated with diethyl ether and a solid was obtained.

White solid (0.10 g, 71 %), melting point = 149-151 ºC , $C_{29}H_{31}N_3O_6S_2$, FW= 581.7.

Elemental Analysis: (Found: C, 61.2; H, 5.5; N, 7.1; S, 10.6 %. CHNS requires: C, 59.9; H, 5.4; N, 7.2; S, 11.0).

IR (NaCl windows): v (NH st) (cm^{-1})= 3300; v (OH) (cm^{-1})= 3423; v (COO^- st) (cm^{-1})= 1730, v (C=O) (cm^{-1})= 1696; v (C=C benzene) (cm^{-1})= 1663; v (-CH_2 δ) (cm^{-1})= 1453; v (-CH_3 δ) (cm^{-1})= 1369; v (thiophene) (cm^{-1})= 3061 (CH st), 1534 (CH γ), 746 (CH δoop).

NMR Spectrum:

δ_H (DMSO-d_6, 300 MHz): 1.24 (s, 9H, $C(CH_3)_3$), 2.69-2.88 (m, 2H, β-CH_2 Cys), 3.09-3.15 (m, 2H, β-CH_2 BOT), 3.78 (s, 2H, CH_2 Bzl), 4.24-4.30 (m, 1H, α-H BOT), 4.45-4.51 (m, 1H, α-H Cys), 6.99 (d, J=8.7 Hz, 1H, NH BOT), 7.22-7.36 (m, 7H, 5 × Ph-*H*, H6 and H4'), 7.63 (d, J=8.7 Hz, 1H, H7), 7.66 (br s, 1H, H4), 7.92-7.95 (m, 2H, H3' and H5'), 8.36 (d,

J=7.8 Hz, 1H, NH Cys).

δ_C (DMSO-d_6, 75.4 MHz): 28.22 (C($\underline{C}H_3)_3$), 32.23 (β-CH_2 Cys), 35.49 (CH_2 Bzl), 37.38 (β-CH_2 BOT), 52.00 (α-C Cys), 55.98 (α-C BOT), 78.05 ($\underline{C}(CH_3)_3$), 110.03 (C7), 120.14 (C4), 126.82 (C4''), 126.88 (C6), 128.37 (C3'' and C5''), 128.62 (C4'), 128.91 (C2), 128.98 (C2'' and C6''), 130.40 (C3'), 131.83 (C5'), 135.22 (C5), 138.24 (C1''), 141.34 (C3a), 148.69 (C7a), 155.26 (C=O Boc), 158.42 (C2'), 171.80 (C=O BOT), 172.00 (C=O Cys).

L3. Boc-Cys(Bzl)-Ala-BOT-OMe

Synthesis of Boc-Cys(Bzl)-Ala-OMe **(1)**

Thionyl chloride (2.5 ml, 3.40×10^{-2} mol) was added dropwise with stirring to methanol (20 ml), cooled in an ice bath, followed by the addition of L-alanine (3g, 3.36×10^{-2} mol). The solution was refluxed at boiling temperature for 2 h. The solvent was evaporated under reduce pressure, yielding a brown solid. The crude was washed with diethyl ether leading a white solid (HCl.H-Ala-OMe).

In a separate flask, Boc-Cys(Bzl)-OH (0.25 g, 8.03×10^{-4} mol) was dissolved in distilled DMF (2 ml), cooled in an ice bath, followed by the addition of HOBt (0.11 g, 8.14×10^{-4} mol) and DCC (0.16 g, 7.75×10^{-4} mol). The mixture was stirred in an ice bath during 30 minutes (solution A).

Finally, HCl.H-Ala-OMe (0.11 g, 7.89×10^{-4} mol) was neutralized with triethylamine (0.11 ml, 8.03×10^{-4} mol) in distilled DMF for 30 minutes. The solution was filtered and the filtrate was added to the solution A. The mixture was stirred 1 h in an ice bath and 1 h at room temperature. The solvent was evaporated under reduced pressure and the residue was treated with cooled acetone, to remove DCU through filtration. The solvent was evaporated and residue purified by column chromatography with silica gel (eluent: $CHCl_3$). The fractions were combined and the product **1** was obtained as a solid.

White solid (0.30 g, 87 %), melting point = 93-95 ºC, $C_{19}H_{28}N_2O_5S$, FW= 396.5

Elementar Analysis: (Found: C, 57.6; H, 7.2; N, 7.0; S, 7.9 % CHNS requires: C, 57.6; H, 7.1; N, 7.1; S, 8.1)

NMR Spectrum:

δ_H ($CDCl_3$, 400 MHz): 1.40 (d, J=7.2 Hz, 3H, β-CH_3 Ala), 1.46 (s, 9H, $C(CH_3)_3$), 2.76-2.78 (m, 1H, β-CH_2 Cys), 2.85-2.90 (m, 1H, β-CH_2 Cys), 3.74 (s, 3H, OCH_3), 3.75 (s, 2H, CH_2 Bzl), 4.22-4.27 (m, 1H, α-H Cys), 4.56 (m, 1H, α-H Ala), 5.30-5.35 (br s, 1H, NH Cys), 6.91 (d, J= 6.0 Hz, 1H, NH Ala), 7.31-7.34 (m, 5H, 5 × Ph-*H*).

δ_C ($CDCl_3$, 100 MHz): 18.25 (β-CH_3 Ala), 28.22 (C($\underline{C}H_3)_3$), 33.65 (β-CH_2 Cys), 36.45 (CH_2 Bzl), 48.19 (α-C Ala), 52.43 (OCH_3), 53.64 (α-C Cys), 80.32 ($\underline{C}(CH_3)_3$), 127.17 (C4''), 128.55 (C2'' and C6''), 128.97 (C3'' and C5''), 137.84 (C1''), 155.28 (C=O Boc), 170.16 (C=O Cys), 172.83 (C=O Ala).

Synthesis of **Boc-Cys(Bzl)-Ala-OH (2)**

Boc-Cys(Bzl)-Ala-OMe **(1)** (0.21 g, 5.5×10^{-4} mol) was dissolved in 1,4-dioxane (3.4 ml), in an ice bath, and sodium hydroxide 1M aqueous solution (0.80 ml, 1.5 eq., 8.0×10^{-4} M) was added dropwise. The mixture was stirred at room temperature for 3h. The pH was adjusted to 2-3 by addition of $KHSO_4$ 1M aqueous solution and extracted with ethyl acetate (3 × 10 ml). After drying with anhydrous sodium sulphate and evaporation of the solvent, the residue was triturated with diethyl ether and a solid was obtained.

White solid (0.21 g, 87 %), $C_{18}H_{26}N_2O_5S$, FW= 382.5

NMR Spectrum:

δ_H ($CDCl_3$, 300 MHz): 1.43 (s, 12H, $C(CH_3)_3$ and β-CH_3 Ala), 2.75-2.78, (m, 2H, β-CH_2 Cys), 3.71 (s, 2H, CH_2 Bzl), 4.35-4.37 (br s, 1H, α-H Cys), 4.52-4.57 (m, 1H, α-H Ala), 5.62-5.65 (br s, 1H, NH Cys), 7.20-7.30 (m, 6H, 5 × Ph-*H* and NH Ala).

δ_C ($CDCl_3$, 75.4 MHz): 17.95 (β-CH_3 Ala), 28.10 ($C(\underline{C}H_3)_3$), 33.50 (β-CH_2 Cys), 36.21 (CH_2 Bzl), 48.20 (α-C Ala), 53.48 (α-C Cys), 80.49 ($\underline{C}(CH_3)_3$), 127.03 (C4''), 128.42 (C2'' and C6''), 128.85 (C3'' and C5''), 137.64 (C1''), 155.67 (C=O Boc), 170.73 (C=O Cys), 175.08 (C=O Ala).

Synthesis of **Boc-Cys(Bzl)-Ala-BOT-OMe (L3)**

Boc-Cys(Bzl)-Ala-OH **(2)** (0.19g, 5.09×10^{-4} mol) was dissolved in distilled DMF (2 ml), cooled in an ice bath, followed by the addition of HOBt (0.08 g, 5.09×10^{-4} mol) and DCC (0.11 g, 5.09×10^{-4} mol). The mixture was in an ice bath during 30 minutes. The ligand **L** (0.15 g, 5.09×10^{-4} mol) was then added and the solution was stirred for 1 h in an ice bath and 1 h at room temperature. The solvent was evaporated under reduced pressure and the residue was treated with cooled acetone, to remove DCU through filtration. The solvent was evaporated and the residue submitted to column chromatography with silica gel (eluent: $CHCl_3$/MeOH 100:1). The fractions were combined and the product was obtained as a solid.

Pale orange solid (0.14 g, 42 %), melting point = 140-142 ºC, $C_{33}H_{38}N_4O_7S_2$, FW= 666.8.

Elemental Analysis: (Found: C, 59.6; H, 5.7; N, 8.4; S, 9.3 % CHNS requires: C, 59.4; H, 5.7; N, 8.4; S, 9.6).

IR (NaCl Windows): v (NH st) (cm^{-1})= 3300; v (C=O aliphatic ester) (cm^{-1})= 1751; v (COO-) (cm^{-1})= 1734; v (C=O st) (cm^{-1})= 1695; v (O-C=N, C=N derivatives) (cm^{-1})= 1690; v (C=C benzene) (cm^{-1})= 1669; v (-CH_2 δ) (cm^{-1})= 1457; v (-CH_3 δ) (cm^{-1})= 1366; v (thiophene) (cm^{-1})= 3100 (CH st), 1534 (CH γ).

NMR Spectrum:

δ_H ($CDCl_3$, 400 MHz): 1.34 (d, J=6.8 Hz, 3H, β-CH_3 Ala), 1.43 (s, 9H, $C(CH_3)_3$), 2.75-2.77 (m, 1H, β-CH_2 Cys), 2.84-2.89 (m, 1H, β-CH_2 Cys), 3.15-3.20 (m, 1H, β-CH_2 BOT), 3.24-

3.29 (m, 1H, β-CH_2 BOT), 3.70-3.72 (d, J=5.6 Hz, 2H, CH_2 Bzl), 3.73 (s, 3H, OCH_3), 4.24-4.27 (m, 1H, α-H Cys), 4.42-4.47 (m, 1H, α-H Ala), 4.84-4.88 (m, 1H, α-H BOT), 5.41 (d, J=7.2 Hz, 1H, NH Cys), 6.84-6.89 (m, 2H, NH Ala and NH BOT), 7.11-7.13 (dd, J= 1.6 and 8.4 Hz, 1H, H6), 7.19-7.22 (m, 1H, H4'), 7.27-7.31 (m, 5H, 5 × Ph-*H*), 7.46 (d, J=8.4 Hz, 1H, H7), 7.48 (d, J=1.6 Hz, 1H, H4), 7.59 (dd, J= 1.2 e 5.2 Hz, 1H, H5'), 7.97-7.98 (br d, J= 2.8 Hz, 1H, H3').

δ_C ($CDCl_3$, 100 MHz): 17.74 (β-CH_3 Ala), 28.24 (C($\underline{C}H_3)_3$), 33.66 (β-CH_2 Cys), 36.51 (CH_2 Bzl), 37.70 (β-CH_2 BOT), 49.10 (α-C Ala), 52.47 (OCH_3), 53.53 (α-C Cys), 53.65 (α-C BOT), 80.38 ($\underline{C}(CH_3)_3$), 110.49 (C7), 119.89 (C4), 126.66 (C6), 127.20 (C 4''), 128.60 (C4'), 128.94 (C2'' and C6''), 130.80 (C3'), 131.01 (C5'), 133.10 (C5), 137.91 (C1''), 141.18 (C3a), 149.39 (C7a), 155.35 (C=O Boc), 159.38 (C2 and C2'), 170.60 (C=O Cys), 171.35 (C=O Ala and C=O BOT).

L4. Boc-BOT-Cys(Bzl)-Trp(ZNO_2)-OMe

Boc-BOT-Cys(Bzl)-OH (**L2**), (0.07g, 1.25×10^{-4} mol) was dissolved in distilled DMF (2 ml), cooled in an ice bath, followed by the addition of HOBt (0.02 g, 1.48×10^{-4} mol) and DCC (0.03 g, 1.45×10^{-4} mol). The mixture was stirred in an ice bath during 30 minutes. Then, NH_2-Trp(ZNO_2)-OMe (0.05g, 1.26×10^{-4} mol) was added and the solution was stirred for 1h in an ice bath and 1 h at room temperature. The solvent was evaporated under reduced pressure and the residue was treated with cooled acetone, to remove DCU through filtration. The solvent was evaporated and the residue submitted to column chromatography with silica gel (ethyl acetate/hexane 1:1 followed by ethyl acetate/MeOH 200:1). The fractions were combined and the product was obtained as a solid. The final product was recrystallized from methanol.

White solid (0.49 g, 51 %), melting point = 198-200ºC, $C_{49}H_{50}N_6O_{12}S_2$, FW= 979.1.

Elemental Analysis: (Found: C, 61.4; H, 5.2; N, 8.4; S, 6.7 % CHNS requires: C, 61.2; H, 5.0; N, 8.7; S, 6.7).

IR (NaCl windows): v (NH st) (cm^{-1})= 3311; v (NH st tryptophan) (cm^{-1})= 3054,2984; v (COO^- st) (cm^{-1})= 1738, v (C=O) (cm^{-1})= 1687; v (C=C benzene) (cm^{-1})= 1634; v (-CH_2 δ) (cm^{-1})= 1450; v (-CH_3 δ) (cm^{-1})= 1392,1367; v (thiophene) (cm^{-1})= 3054 (CH st), 1525 (CH γ), 1422, 1433, 739 (CH δoop).

NMR Spectrum:

δ_H (DMSO-d_6, 400 MHz): 1.21 (s, 9H, $C(CH_3)_3$), 2.55-2.60 (m, 1H, β-CH_2 Cys), 2.66-2.78 (m, 2H, β-CH_2 Cys and β-CH_2 BOT), 2.98-3.03 (m, 1H, β-CH_2 BOT), 3.10-3.21 (m, 2H, β-CH_2 Trp), 3.57 (s, 3H, OCH_3), 3.74 (s, 2H, CH_2 Bzl), 4.18-4.24 (m, 1H, α-H Cys), 4.57-4.67 (m, 2H, α-H BOT and α-H Trp), 5.48 (s, 2H, CH_2 ZNO_2), 6.89 (d, J=8.8 Hz, 1H, NH BOT), 7.20-7.33 (m, 11H, 5 × Ph-*H* Bzl, 2 × H2' and H4' ZNO_2, H6 BOT, H2 and H5 Trp),

7.54-7.61 (m, 3H, H4 and H7 BOT, H4 Trp), 7.67-7.73 (m, 3H, H6 Trp, H2'' and H6'' Bzl), 7.89 (dd, J= 1.2 and 3.6 Hz, 1H, H3'), 7.92 (dd, J= 1.2 and 4.8 Hz, 1H, H5'), 8.03 (d, J= 8.4 Hz, 1H, NHCys), 8.21 (d, J=8.8 Hz, 2H, 2 × H3' ZNO_2), 8.69 (d, J= 7.2 Hz, NH Trp).

δ_C (DMSO-d_6, 100 MHz): 26.31 (β-CH_2 BOT), 27.99 (C($\underline{C}H_3)_3$), 33.07 (β-CH_2 Cys), 35.25 (β-CH_2 BOT), 37.35 (CH_2 Bzl), 51.99 (OCH_3), 52.15 (α-C BOT and α-C Trp), 55.95 (α-C Cys), 66.68 (CH_2 ZNO_2), 78.06 ($\underline{C}(CH_3)_3$, 109.90 (C7 BOT), 114.67 (C3 Trp), 116.71 (C7 Trp), 119.13 (C4 Trp), 120.5 (C4 BOT), 123.03 (C5 Trp), 123.62 (C3' ZNO_2), 123.88 (C6 Trp), 124.71 (C2 Trp), 126.72 (C6 BOT), 126.77 (C 4''), 128.27 (C3'' and C5''), 128.56 (C4'), 128.64 (C2'' and C6''), 128.83 (C2), 128.94 (C2' ZNO_2), 130.04 (C3a Trp), 130.31 (C3'), 131.76 (C5'), 134.77 (C5 BOT), 135.13 (C7a Trp), 138.33 (C1''), 141.28 (C3a BOT), 142.97 (C1' ZNO_2), 147.23 (C4' ZNO_2), 148.61 (C7a BOT), 155.17 (C=O Boc), 158.35 (C2'), 170.26 (C=O Cys), 171.41 (C=O Trp and C=O BOT).

L5. H-BOTT-OMe

Compound **L5** was obtained by removal of the Boc group from the previously published compound **A**. Compound **A** was dissolved in 1 ml of dichloromethane and 1ml of TFA and stirred during 2 hours. The solution was evaporated under pressure, yielding a green salt. The solid residue was dissolved in aqueous solution (pH=8) and extracted with ethyl acetate (3× 5mL). After drying with anhydrous magnesium sulphate and evaporation, compound **L5** was isolated as a yellow solid.[17]

Yellow solid (0.06 g, 90 %), $C_{19}H_{16}N_2O_3S_2$, FW = 384.1

Elemental Analysis: (Found: C, 59.6; H, 4.4; N, 7.7; S, 15.5 %. CHNS requires: C, 59.4; H, 4.2; N, 7.3; S, 16.7).

NMR Spectrum:

δ_H (DMSO, 400 MHz): 3.06-3.15 (m, 2H, β-CH_2 BOTT), 3.49 (s, 2H, NH_2), 3.70 (s, 3H, OCH_3), 4.32-4.36 (m, 1H, α-H BOTT), 7.16-7.18 (m, 1H, H4''), 7.23 (d, J=3.6 Hz, 1H, H4'), 7.49-7.60 (m, 8H, 5 × Ph-*H*, H3'', H5'', H6), 7.70 (d, J= 8.4 Hz, 1H, H7), 7.80 (d, J= 1.6 Hz, 1H, H4), 7.90 (d, J= 4.0 Hz, 1H, H3').

δ_C ($CDCl_3$, 100 MHz): 38.81 (β-CH_2 BOTT), 52.60 (OCH_3), 57.8 (α-C BOTT), 110.64 (C7), 120.26 (C4), 125.21 (C4'), 125.89 (C5''), 125.96 (C3''), 126.18 (C6), 126.84 (C2'), 127.35 (C4''), 128.67 (C3'), 131.68 (C5), 135.00 (C2''), 141.63 (C5'), 141.69 (C3a), 149.26 (C7a), 158.13 (C2).

IR (NaCl Windows): ν (C=O aliphatic ester) (cm^{-1})= 1751; ν (COO-) (cm^{-1})= 1734; ν (C=O st) (cm^{-1})= 1695; ν (O-C=N, C=N derivatives) (cm^{-1})= 1690; ν (C=C benzene) (cm^{-1})= 1669; ν (-CH_2 δ) (cm^{-1})= 1457; ν (-CH_3 δ) (cm^{-1})= 1366; ν (thiophene) (cm^{-1})= 3100 (CH st), 1534 (CH γ).

UV-Vis spectra (dichloromethane, λ nm): 366 nm, log ε ≈ 3.9.

Emission spectra (dichloromethane): λ_{exc} =366 nm, λ_{emis} = 440 nm.
Electrospray (ESI) calc.(found) %: [**1**]H^+, 385.06 (385.06) 100%.

L6. Boc-BOTT-Cys(Bzl)-OMe

Boc-BOTT-OH (**B**) (0.11 g, 2.41×10^{-4} mol) was dissolved in freshly distilled DMF (2 ml), cooled in an ice bath, followed by the addition of HOBt (0.03 g, 2.41×10^{-4} mol) and DCC (0.05 g, 2.41×10^{-4} mol). The mixture was stirred in an ice bath during 30 minutes.
HCl .H-Cys(Bzl)-OMe (0.06 g, 2.41×10^{-4} mol) was neutralized with triethylamine (32 µl, 2.41×10^{-4} mol) in freshly distilled DMF for 30 minutes. The mixture was filtered, and the filtrate was added to **B** solution. The solution was stirred for 1h in an ice bath, and 1h at room temperature. The solvent was evaporated under reduced pressure and the residue was treated with cooled acetone, to remove DCU through filtration. The solvent was evaporated and the residue submitted to column chromatography with silica gel (eluent: ethyl acetate/hexane 2.3). The fractions were combined and the product was obtained as a stable solid.
Yellow solid (0.13 g, 70 %), melting point = 181-183 ºC, $C_{34}H_{35}N_3O_6S_3$, FW = 677.8
Elemental Analysis: (Found: C, 60.3; H, 5.2; N, 6.1; S, 14.0 %. CHNS requires: C, 60.2; H, 5.2; N, 6.2; S, 14.2).
NMR Spectrum:
δ_H ($CDCl_3$, 400 MHz): 1.42 (s, 9H, $C(CH_3)_3$), 2.78-2.89 (m, 2H, β-CH_2 Cys), 3.20 (d, J= 6.4 Hz, 2H, β-CH_2 BOTT), 3.66 (s, 2H, CH_2 Bzl), 3.70 (s, 3H, OCH_3), 4.41-4.43 (m, 1H, α-H BOTT), 4.73-4.77 (m, 1H, α-H Cys), 4.99-5.02 (br s, 1H, NH Cys), 6.61 (d, J= 7.2 Hz, 1H, NH BOTT), 7.07-7.09 (m, 1H, H4''), 7.20-7.33 (m, 8H, 5 × Ph-*H*, H3'', H5'', H6), 7.23 (d, J=3.6 Hz, 1H, H4'), 7.44 (d, J= 8.4 Hz, 1H, H7), 7.54 (d, J= 1.6 Hz, 1H, H4), 7.79 (d, J= 4.0 Hz, 1H, H3').
δ_C ($CDCl_3$, 100 MHz): 28.24 ($C(\underline{C}H_3)_3$), 33.37 (β-CH_2 Cys), 36.55 (CH_2 Bzl), 38.22 (β-CH_2 BOTT), 51.67 (α-C Cys), 52.61 (OCH_3), 55.85 (α-C BOTT), 80.37 ($\underline{C}(CH_3)_3$), 110.39 (C7), 120.36 (C4), 125.47 (C4'), 125.10 (C5''), 125.93 (C3''), 126.38 (C6), 127.23 (C4'''), 127.45 (C2'), 128.17 (C4''),128.56 (C3''' and C5'''), 128.89 (C2''' and C6'''), 130.68 (C3'), 133.25 (C5), 136.24 (C2''), 137.60 (C1'''), 142.33 (C5'), 142.47 (C3a), 149.64 (C7a), 155.23 (C=O Boc), 159.02 (C2), 170.66 (C=O Cys), 170.88 (C=O BOTT).
IR (NaCl windows): v (NH st) (cm^{-1})= 3300; v (OH) (cm^{-1})= 3423; v (COO^- st) (cm^{-1})= 1731, v (C=O) (cm^{-1})= 1696; v (C=C benzene) (cm^{-1})= 1663; v (-CH_2 δ) (cm^{-1})= 1453; v (-CH_3 δ) (cm^{-1})= 1369; v (thiophene) (cm^{-1})= 3061 (CH st), 1534 (CH γ), 746 (CH δoop).
UV-Vis spectra (dichloromethane, λ nm): 366 nm, log ε ≈ 3.95.
Emission spectra (dichloromethane): (λ_{exc} =366 nm, λ_{emis} = 440 nm).
MALDI-TOF-MS calc.(found): [**2**LNa]$^+$, 700.1(700.03) 10%, [**2**-BocNa]$^+$, 599.2 (599.9)

45%.

L7. Boc-Cys(Bzl)-Ala-BOTT-OMe

Boc-Cys(Bzl)-Ala-OH (**2**) (0.12g, 3.14×10^{-4} mol) was dissolved in freshly distilled DMF (2 ml), cooled in an ice bath, followed by the addition of HOBt (0.045 g, 3.33×10^{-4} mol) and DCC (0.064 g, 3.10×10^{-4} mol). The mixture was stirred in an ice bath during 30 minutes. **L5** (0.11 g, 2.99×10^{-4} mol) was added and the final mixture was stirred for 1h in an ice bath, follow by other 1h at room temperature. The solvent was evaporated under reduced pressure and the residue was treated with cooled acetone, to remove DCU through filtration. The solvent was evaporated and the residue submitted to column chromatography with silica gel (eluent: ethyl acetate/hexane, 1:1). The fractions were combined and the product was obtained as a solid. The final product was recrystallized from methanol.

Yellow solid (0.06 g, 26 %), melting point = 162-166 ºC, $C_{37}H_{40}N_4O_7S_3$, FW = 748.9

Elementar Analysis: (Found: C, 59.5; H, 5.5; N, 7.2; S, 12.9 % CHNS requires: C, 59.3; H, 5.4; N, 7.5; S, 12.8).

NMR Spectrum:

δ_H (DMSO-d_6, 300 MHz): 1.16-1.18 (d, J=6.9 Hz, 3H, β-CH_3 Ala), 1.37 (s, 9H, $C(CH_3)_3$), 2.43-2.48 (m, 1H, β-CH_2 Cys), 2.65-2.71 (m, 1H, β-CH_2 Cys), 2.99-3.07 (m, 1H, β-CH_2 BOTT), 3.12-3.20 (m, 1H, β-CH_2 BOTT), 3.59 (s, 3H, OCH_3), 3.69 (s, 2H, CH_2 Bzl), 4.11-4.19 (m, 1H, α-H Cys), 4.24-4.33 (m, 1H, α-H Ala), 4.49-4.56 (m, 1H, α-H BOTT), 6.97 (d, J=8.4 Hz, 1H, NH Ala), 7.14-7.24 (m, 6H, 5 × Ph-*H* and H4''), 7.46 (d, J=3.9 Hz, 1H, H4'), 7.52 (dd, J= 1.2 and 3.9 Hz, 1H, H3''), 7.58 (d, J= 1.2 Hz, 1H, H4), 7.62 (d, J= 8.7 Hz, 1H, H7), 7.65 (dd, J= 1.2 and 6.0 Hz, 1H, H5''), 7.87 (d, J= 3.9 Hz, 1H, H3'), 7.99 (d, J= 7.2 Hz, 1H, NH Cys), 8.33 (d, J= 7.5 Hz, 1H, NH BOTT).

δ_C (DMSO-d_6, 75.4 MHz): 18.34 (β-CH_3 Ala), 28.15 ($C(\underline{C}H_3)_3$), 33.54 (β-CH_2 Cys), 35.21 (CH_2 Bzl), 36.42 (β-CH_2 BOTT), 47.91 (α-C Ala), 51.92 (OCH_3), 53.63 (α-C Cys), 53.80 (α-C BOTT), 78.28 ($\underline{C}(CH_3)_3$), 110.26 (C7), 119.85 (C4), 125.25 (C4'), 125.97 (C3''), 126.48 (C2'), 126.72 (C4'''), 126.76 (C6), 127.36 (C5''), 128.28 (C3''' and C5'''), 128.75 (C4''), 128.86 (C2''' and C6'''), 131.48 (C3'), 134.16 (C5), 135.15 (C2''), 138.35 (C1'''), 141.50 (C5'), 141.54 (C3a), 148.89 (C7a), 155.27 (C=O Boc), 158.02 (C2), 170.11 (C=O Cys), 171.61 (C=O BOTT), 172.06 (C=O Ala).

IR (NaCl Windows): v (NH st) (cm^{-1})= 3300; v (C=O aliphatic ester) (cm^{-1})= 1751; v (COO-) (cm^{-1})= 1734; v (C=O st) (cm^{-1})= 1695; v (O-C=N, C=N derivatives) (cm^{-1})= 1690; v (C=C benzene) (cm^{-1})= 1669; v (-CH_2 δ) (cm^{-1})= 1457; v (-CH_3 δ) (cm^{-1})= 1366; v (thiophene) (cm^{-1})= 3100 (CH st), 1534 (CH γ).

UV-Vis spectra (dichloromethane, λ nm): 366 nm, log ε ≈ 4.0.

Emission spectra (dichloromethane): λ_{exc} =366 nm, λ_{emis} = 440 nm. MALDI-TOF-MS calc.(found) %: [**3**-Boc]H^+, 649.1(649.5) 20%; [**L**-Boc-Bzn]H^+.MeOH, 633.2(633.4) 25%; $[C_{22}H_{21}N_3O_4S_2H]^+$, 456.1 (456.5) 35%; $[C_{19}H_{16}N_2O_3S_2H]^+$, 385.1 (385.5) 100%. (See MALDI-TOF-MS fragments in scheme 7.2.)

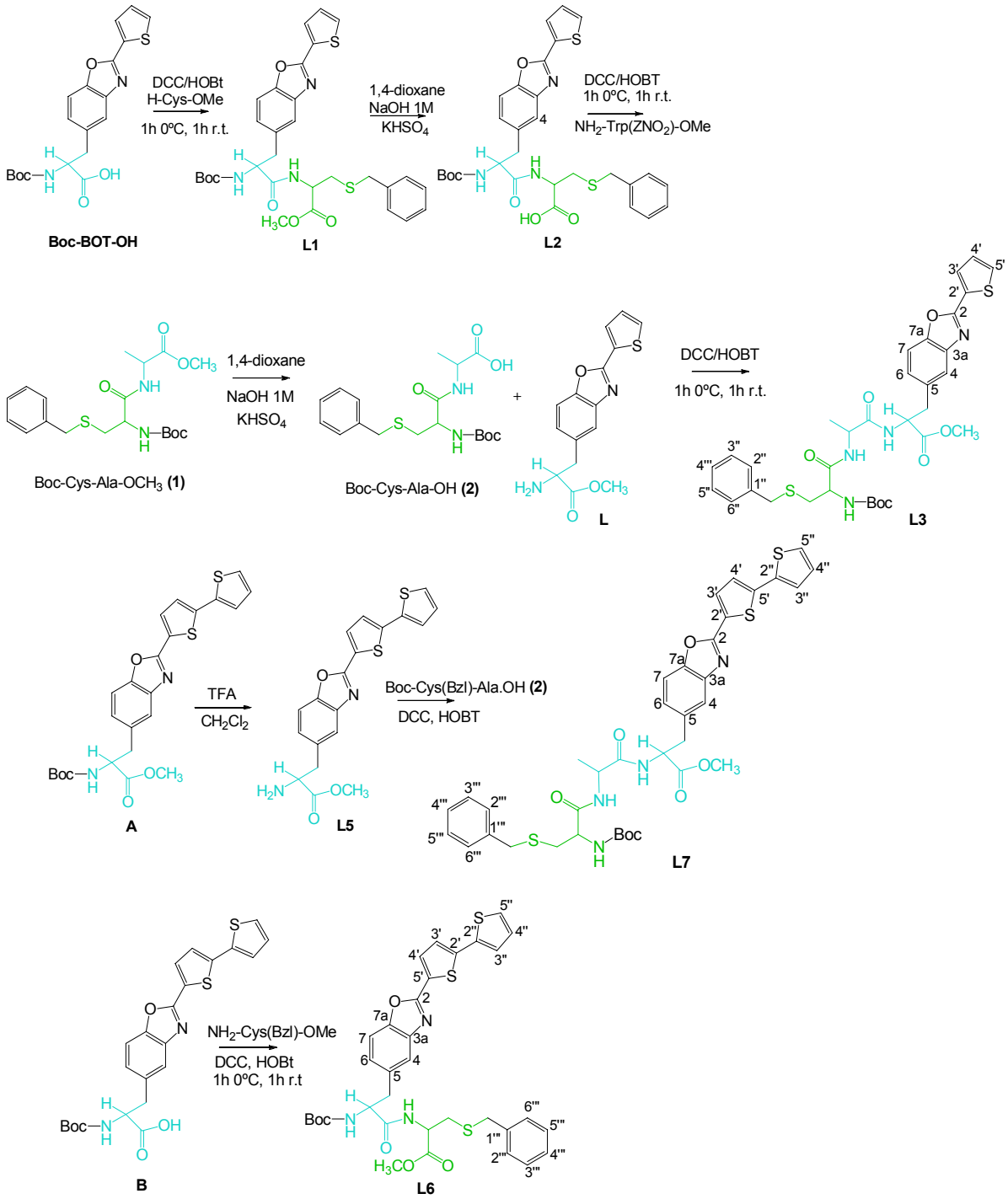

Scheme 7.1. Synthesis of peptides **L** to **L7**.

7.4.2 - Synthesis of Gold nanoparticles

Ligand **L** (0.008g, 2.62×10^{-5} mol) was dissolved in dry dichloromethane, followed by the addition of dithiobis(succinimidylpropionate) (DSP, 0.011 g, 2.72×10^{-5} mol). The solution was stirred at room temperature overnight. The mixture was extracted with milliQ water (3 $\times$ 3 ml), and the organic phase was dried with sodium sulphate and filtered. The filtrated solution was evaporated and dried under vacuum pressure resulting in a pale yellow solid **(a)**. $HAuCl_4$ (0.0876 mmol) was dissolved in 10 ml of milliQ water giving a yellow solution and 0.41 mmol of tetraoctylammonium bromide (TOAB, 98%) were dissolved in 10 ml of CH_2Cl_2. 1 ml of the gold solution was added to 1 ml of CH_2Cl_2 solution of TOAB. The mixture was stirred until the water phase was decoloured and the organic phase made deeply red by the complete phase transfer of the gold ions. The two solutions were then separated and 0.005 mmol of **(a)** were added to the organic phase and 1 ml of milliQ water containing 1.1 mmol of $NaBH_4$ were stirred leading to the reduction of the $[AuCl_4]^-$ ions and causing a colour change from red to brown which confirmed the formation of gold nanoparticles. The solution of nanoparticles was extracted three times with water, and isolated by precipitation with methanol and centrifugation. The absence of free ligand **L** in the final product was confirmed by the absence of its fluorescence.

Colour: dark red. UV-Vis in dichloromethane (λ nm): Bands at 316 nm and 520 nm, log $\varepsilon_{316} \approx 4.44$, log $\varepsilon_{520} \approx 2.84$. Emission spectra in dichloromethane (λ_{exc} =316nm, λ_{emis} = 394 nm).

Dynamic Light Scattering: 4.2 nm

TEM: 2.4 nm

Ligand **L3** (0.010g, 1.53×10^{-5} mol) was stirred in TFA/dichloromethane solution (1:1, 1 mL) at room temperature for 2 h. The solvent was evaporated and the oily residue was dissolved in dichloromethane followed the addition of triethylamine. Water miliQ was added to the solution and therefore extracted three times with dichloromethane. The solution was evaporated under reduce pressure, yielding a solid residue **(b)**. Solid **b (**0.013 mmol) was dissolved in 2ml of dried dichloromethane, followed by the addition of DSP (0.013 mmol). The solution was stirring at room temperature overnight. The mixture was extracted with miliQ water (3 $\times$ 3 ml), and the organic phase was dried with sodium sulphate and filtered. The filtrated solution was evaporated and dried under vacuum pressure, resulting solid **(c)**.

$HAuCl_4$ (0.0876 mmol) was dissolved in 10 ml of miliQ water giving a yellow solution and 0.41 mmol of TOAB 98% were dissolved in 10 ml of CH_2Cl_2. 1 ml of the gold solution was added to 1 ml of CH_2Cl_2 solution of TP. The mixture was stirred until the water phase was decoloured and the organic phase made deeply red by the complete phase transfer of the gold ions. Both solutions were then separated and 0.005 mmol of **(c)** were added to the

organic phase and 1 ml of miliQ water containing 1.2 mmol of $NaBH_4$ were stirred leading to the reduction of the $[AuCl_4]^-$ ions and causing a colour change from red to brown which confirmed the formation of gold nanoparticles.

The solution of nanoparticles was extracted three times with water, and isolated by precipitation with methanol and centrifugation. The absence of the free ligand, **L3**, in the final product was confirmed by the absence of the intrinsic fluorescence.

Colour: dark red. UV-Vis in dichloromethane (λ nm): Bands at 316 nm and 520 nm, log $\varepsilon_{316} \approx 4.60$, log $\varepsilon_{520} \approx 2.80$. Emission spectra in dichloromethane (λ_{exc} = 316nm, λ_{emis} = 396nm).

Dynamic Light Scattering: 15.1 nm.

TEM: 3.3 and 9.8 nm.

7.4.3 - Synthesis of the decorated silica nanoparticles with compounds L5 to L7.

Compound **L5** (0.01 mmol) was dissolved in 1 ml of dichloromethane under stirring followed by the addition of triethylamine (0.02 mmol) and the linker 3-isocyanotopropyl-triethoxysilane (0.02 mmol). The mixture was kept under stirring during 2 days. The complete reaction, substitution of the amino group by the silane derivative, was evidenced by TLC (eluent: ethyl acetate). The solvent, dichloromethane, was evaporated by vacuum pressure yielded a yellow powder.

In a cap tube, the yellow product obtained was dissolved in 0.5 ml of ethanol, 0.5 ml of Milli-Q distilled water, 0.5 ml of CH_3COOH and mixed with 0.680 mL of commercial Ludox. This mixture was stirred at 80ºC during 2 days. Then, 200 μl of the sample were dissolved in 1 mL of dichloromethane and centrifuged at 8600 rpm, at 21ºC, for 10 minutes. The pellet was washed three times with ethanol (1mL x 3), and then dissolved in 0.5 mL of absolute ethanol.

Compounds **L6** and **L7**, were dissolved in dichloromethane/TFA (1:1), stirred for 2 hours and evaporated to dryness. The syntheses of the silica nanoparticles with compounds **L6** and **L7** followed the same procedure detailed above for **L5**.

7.4.4 - Photophysical Measurements

Absorption spectra were recorded on a Perkin Elmer lambda 45 and JASCO 650 spectrophotometers and fluorescence emission on a Perkin Elmer LS55. The linearity of the fluorescence emission vs. concentration was checked in the concentration used (10^{-4} – 10^{-6} M). A correction for the absorbed light was performed when necessary. The spectrometric characterizations and titrations were performed as follows: the stock solutions of the compounds (*ca*. 10^{-3} M) were prepared by dissolving an appropriated amount of the complex in a 10 ml volumetric flask and diluting to the mark with absolute ethanol. The solutions were prepared by appropriate dilution of the stock solutions up to

10^{-5} – 10^{-6} M. Titrations of the ligands **L1**, to **L7** were carried out by the addition of microliter amounts of standard solutions of the ions in absolute ethanol. All the measurements were performed at 298 K. The absorption and fluorescence spectra were also performed in microsamples using a NANODROP spectrophotometer ND-1000 and spectrofluorimeter ND-3300. The linearity of the fluorescence emission vs. concentration was checked in the concentration used (10^{-4} – 10^{-6} M).

Luminescence quantum yields were measured using a solution of quinine sulphate in sulphuric acid (0.5M) as a standard ([ϕ] = 0.54) [18] and were corrected for different refraction indexes of solvents.

Luminescence lifetime measurements were carried out by using a Time Correlated Single Photon Counting Apparatus by Edinburg Instruments, as previously described.[19]

7.4.5 - MALDI-TOF-MS measurements

The MALDI mass spectra of the soluble samples (1 or 2 μg/μL) such as the metal salts were recorded using the conventional sample preparation method for MALDI-MS. 1μL were put on the sample holder on which the chelating ligand had been previously spotted. The sample holder was inserted in the ion source. Chemical reaction between the ligand and metal salts occurred in the holder and complexed species were produced.
The MALDI-TOF-MS analysis have been performed in a MALDI-TOF-MS model voyager DE-PRO biospectrometry workstation equipped with a nitrogen laser radiating at 337 nm from Applied Biosystems (Foster City, United States) at the REQUIMTE, Chemistry Department, Universidade Nova de Lisboa. The acceleration voltage was 2.0×10^{4} kV with a delayed extraction (DE) time of 200 ns. The spectra represent accumulations of 5×100 laser shots. The reflectron mode was used. The ion source and flight tube pressures were less than 1.80×10^{-7} and 5.60×10^{-8} Torr, respectively.

7.4.6 - Physical measurements

Elemental analyses were carried out by the REQUIMTE DQ, Universidade Nova de Lisboa Service on a Thermo Finnigan-CE Flash-EA 1112-CHNS, on a a Fisons Instruments EA1108 microanalyser at the Universidade de Vigo or at Centro de Química, Universidade do Minho on a Leco CHNS 932 instrument. Infrared spectra were recorded in NaCl windows using Bio-Rad FTS 175-C spectrophotometer. NMR spectra were obtained on a Varian Unity Plus Spectrometer at an operating frequency of 300 MHz for ^{1}H NMR and 75.4 MHz for ^{13}C NMR or a Bruker Avance III 400 at an operating frequency of 400 MHz for ^{1}H NMR and 100.6 MHz for ^{13}C NMR using the solvent peak as internal reference at 25 ºC. All chemical shifts are given in ppm using δ_H Me_4Si = 0 ppm as reference and *J* values are given in Hz. Assignments were made by comparison of

chemical shifts, peak multiplicities and *J* values and were supported by spin decoupling-double resonance and bidimensional heteronuclear HMBC and HMQC correlation techniques.

7.4.7 - Particles Size Distribution

The nanoparticles size distributions were measurement using the dynamic light scattering, a Malvern Nano ZS instrument with a 633 nm laser diode in the University of Bologna (Italy) and in the University of Vigo, Faculty of Science of Ourense.

7.4.8 - TEM measurements

For TEM investigations a drop of nanoparticle in dichloromethane solution was transferred onto holey carbon foils supported on conventional copper microgrids. A Philips CM 100 transmission electron microscope operating at 80 kV was used at the University of Bologna, Italy.

7.4.9 - Chemicals and Starting Reagents

$Cu(CF_3SO_3)_2$, $Ni(BF_4)_26H_2O$, $Ag(BF_4)$, $Zn(CF_3SO_3)_2$, $Cd(ClO_4)_26H_2O$ $Hg(CF_3SO_3)_2$, $Pb(CF_3SO_3)_2$, salts have been purchased from Strem Chemicals, Sigma Aldrich and Solchemar. Thionyl chloride, DCC (N,N'-Dicyclohexylcarbodiimide), Boc-Cys(Bzl)-OH, NH_2-Trp(ZNO_2)-OMe were from Fluka. HOBt (1-Hydroxybenzotriazole) was purchased from Senn Chemicals. Triethylamine, sodium hydroxide, anhydrous sodium sulphate, DSP (dithiobis(succinimidylpropionate), Tetraoctylammonium bromide (TOAB), L-alanine, $HAuCl_4$, $NaBH_4$, TFA (trifluoracetic acid) and all the solvents used were from Sigma Aldrich. $KHSO_4$ and Chromatography silica gel were from Merck. All were used without further purification.

7.5 - Results and Discussion

7.5.1 - Synthesis of Peptides

The synthesis of peptides **L1**, **L3** and **L4** were carried out by standard DCC/HOBt amino acid coupling procedures while peptide **L2** was obtained from **L1** by cleavage of the ester protecting group by a basic hydrolysis at the carboxylic acid terminal. Tripeptide **L3** was obtained by coupling of **L** [17] with Boc-Cys(Bzl)-Ala-OH (**2**) and tripeptide **L4** was obtained by coupling of **L2** and H-Trp(ZNO_2)-OMe (See Scheme 7.1).

Particularly, the synthesis of the emissive alanine derivative **L5** was carried out by removal of the *N-tert*-butyloxycarbonyl (Boc) protecting group from ligand **A**.[17] Dipeptide **L6** was obtained by reaction between **B** and H-Cys(Bzl)-OMe. Tripeptide **L7**

was obtained by a standard DCC/HOBt coupling reaction between precursor (**2**) (Boc-Cys(Bzl)-Ala-OH) and **L5**.
All compounds synthesized were obtained in a good to moderated yield: 75%(**L1**); 71%(**L2**); 42%(**L3**); 51%(**L4**); 90% (**L5**); 70% (**L6**) and 26% (**L7**).

All compounds were characterized by elemental analysis, ^{1}H and ^{13}C NMR, infrared spectroscopy, MALDI-TOF-MS, melting point, UV-vis absorption and fluorescence emission spectroscopy
The MALDI-TOF-MS spectra showed peaks corresponding to [**L1**]H^+ at 596.5, [**L2**]H^+ at 582.5, [**L3**]H^+ at 667.5 confirming the integrity of the studied peptides The Electrospray (ESI) spectra for **L5** show the peak [**L5**]H^+, 385.06 (385.06) 100%. The MALDI-TOF-MS spectra for the bithienyl dipeptide **L6** shows peaks for [**L6**] Na^+, 700.1(700.03) 10%, [**L6**-Boc]Na^+, 599.2 (599.9) 45%, while the tripeptide **L7** shows several peaks; among them, the ones corresponding to [**L7**-Boc]H^+, 649.1(649.5) 20% and [**L7**-Boc-Bzn]H^+.MeOH, 633.2(633.4) 25% as the most interesting.

The IR spectra of compounds **L1** - **L4**, **L6** and **L7** presented a band at 3300 cm^{-1} assignable to the amide NH, as well as a band at *ca* 1750-1650 cm^{-1} related to the urethane, ester, amide and carboxylic acid carbonyl groups. The ^{1}H NMR spectra of compounds **L1** - **L4**, **L6** and **L7** presented the characteristic signals of the amino acid backbone NH and α-H and side chain β-CH_3 (for Ala) or β-CH_2 (for BOT, BOTT, Cys and Trp). The signals due to the heterocyclic ring present at the BOT, BOTT, and Trp side chains (thiophene, benzo[*d*]oxazole and indole, respectively) were also visible. In the ^{13}C NMR spectra, the formation of the amide linkage was also confirmed by the appearance of the signal due to the amide carbonyl group at about 170-175 ppm.

7.5.2 - Photophysical Studies

The most significant photophysical data of the synthesized compounds are gathered in table 7.1. The absorption and emission bands of **L1** – **L4** are all centred at 316 nm and 396 nm, respectively, and they can be attributed to the thienyl-benzo[*d*]oxazole chromophore. **L4** presents an additional absorption in the 250-300 nm region, due to the insertion of a tryptophan residue. The absorption and emission bands of the bithienyl-benzo[*d*]oxazole derivatives **L5** - **L7**, centred at 366 nm and 440 nm respectively, are both remarkably red shifted compared with the previous family of compounds, as expected because of their increased conjugation. As an example of the two classes of compounds, figure 7.1 shows the absorption, emission and excitation spectra in dichloromethane of **L3** (7.1A) and **L7** (7.1B). The same photophysical characterization was performed also in absolute ethanol for all compounds, and only small differences could be observed. The absorption band of these species can be assigned to the π-π*

transition centred on the chromophoric units.[16] The perfect match between the absorption and excitation spectra, moreover, rules out in all cases the presence of any emissive impurity.

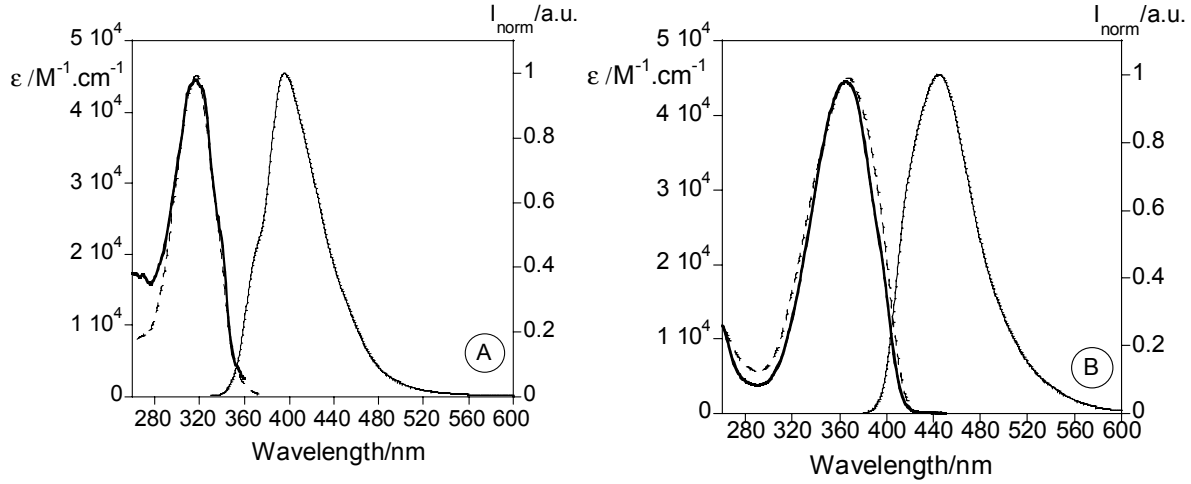

Figure 7.1**.** Room temperature absorption (bold line), normalized emission (full line, λ_{excL3} = 316 nm; λ_{excL7} = 366 nm) and excitation spectra (dotted line, λ_{emL3} = 396 nm; λ_{emL7} = 440 nm) of compound **L3** (A) and **L7** (B) in dichloromethane.

The fluorescence quantum yields of **L1-L4**, **L6** and **L7** measured in dichloromethane and in absolute ethanol are in general very high, with higher values in the latter solvent (Table 7.1). It has to be noted, however, that the addition of a tryptophan to obtain the tripeptide **L4** caused a strong decrease of the quantum yield. This quenching, accompanied by a parallel shortening of the excited state lifetime, can be probably attributed to an electron transfer process, since the alternative possibility based on the occurrence of a resonance energy transfer from the singlet excited state of the indole to the thienyl-benzo[*d*]oxazole chromophore is not allowed for thermodynamic reasons.[17] On the contrary, the coincidence between the absorption and excitation spectra of **L4** indicates the occurrence of a very efficient energy transfer process in the opposite direction.

As expected, the selective deprotection of the carboxylic group of the amino acid residue, which lies far apart from the chromophoric unit, had only a minor influence on the fluorescence quantum yields.

Table 7.1. Optical data for **L1**-**L4**, **L6** and **L7** in dichloromethane and absolute ethanol.

	UV-vis		Fluorescence		
	λ_{exc} (nm)	Log ε	λ_{em} (nm)	t (ns)	ϕ
L1	316[a]	4.29[a]	394[a]		0.26[a]
	316[b]	4.28[b]	384[b]	1.5[b]	0.44[b]
L2	316[a]	4.29[a]	395[a]		0.29[a]
	316[b]	4.29[b]	384[b]	1.5[b]	0.46[b]
L3	316[a]	4.64[a]	396[a]		0.31[a]
	316[b]	4.32[b]	384[b]	1.5[b]	0.71[b]
L4	316[a]	4.49[a]	395[a]		0.08[a]
	316[b]	4.26[b]	384[b]	≤ 0.6[b]	0.06[b]
L6	366[a]	4.29[a]	440[a]		0.26[a]
	366[b]	4.28[b]	440[b]	1.5[b]	0.44[b]
L7	366[a]	4.29[a]	440[a]		0.29[a]
	366[b]	4.29[b]	440[b]	1.5[b]	0.46[b]

[a] Dichloromethane solution. [b] Absolute ethanol solution.

7.5.3 - Spectrophotometric and spectrofluorimetric titrations and metal sensing effect

The investigation of the sensing ability of compounds **L1**-**L4**, **L6** and **L7** was carried out by UV-vis absorption and fluorescence emission studies in abs. ethanol solutions for Cu^{2+}, Ni^{2+}, Ag^{+}, Zn^{2+}, Cd^{2+}, Hg^{2+} and Pb^{2+}. The most significant data are gathered in Table 7.2.

Table 7.2. Complexation constants for peptides **L2**-**L4**, and **L7** in the presence of Ag^{+}, Cu^{2+}, Ni^{2+} and Hg^{2+} in absolute ethanol.

Peptides	Metals	Constants M:L
L2	Ag^{+}	1:1 – 4.87 ± 0.01
		2:1 – 8.04 ± 0.05
	Cu^{2+}	1:1 – 7.45 ± 0.28
		2:1 – 13.99 ± 0.43
	Ni^{2+}	2:1 – 8.54 ± 0.03
	Hg^{2+}	2:1 – 10.43± 0.01
L3	Ag^{+}	1:1 – 4.74 ± 0.18
		2:1 – 8.88 ± 0.22
	Hg^{2+}	2:1 – 11.81 ± 0.07
L4	Hg^{2+}	1:1 – 7.06 ± 0.22
		2:1 – 12.47 ± 0.21
L7	Hg^{2+}	1:1 – 4.49 ± 0.21
		2:1 – 8.90 ± 0.08

L1 showed spectral changes only upon addition of Hg^{2+}, that led to an emission quenching of *ca.* 88 % with a relatively low association constant (Figure S7.1; log β (M:L – 1:1) = 8.97±0.01, and log β (M:L – 2:1) = 13.42 ± 0.01). A significantly different behaviour was observed for **L2**, presenting a carboxylic complexing function instead of an ester. In this case no changes were observed in the absorption spectra in the presence of metal ions, suggesting that the ground state of the peptides is not affected by complexation, that instead induces strong changes in the excited state with a decrease of the fluorescence intensity of *ca.* 20%, 60% and 100%, upon addition of Ag^{+}, Ni^{2+} and Cu^{2+} (see figure 7.2) respectively. All titration data were fitted using SPECFIT program,[20] suggesting also the formation of dinuclear complexes with molar ratio M:L; 2:1. The spectral response observed for these metal titrations, compared with the results previously published for ligand **L**,[17] supports the hypothesis that the complexation takes place in two steps, the first one involving the unprotected carboxylic group and the amine of the amino acid. The association constants follow the trend $Cu^{2+} > Ni^{2+} > Ag^{+}$, that can be easily explained taking into account that the more available donor atoms present in this dipeptide system are nitrogens and oxygens. On the other hand, Hg^{2+} gave an

emission quenching of 75% with an association constant of (Figure S7.2, log β (M:L – 2:1) = 10.43± 0.01).

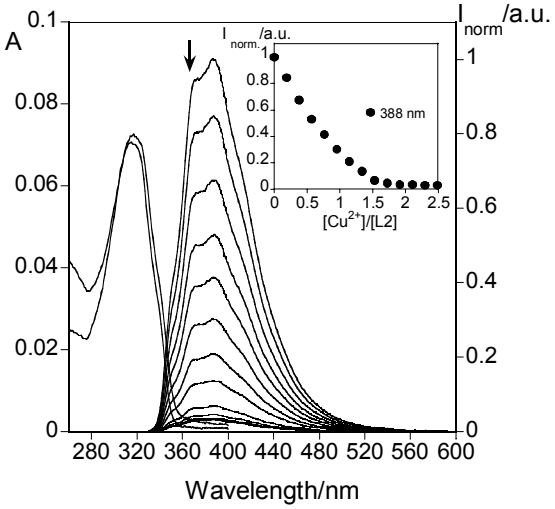

Figure 7.2. Absorption and emission spectra of **L2** in the presence of Cu^{2+} in absolute ethanol solution. The inset shows the intensity of emission as a function of $[Cu^{2+}]/[\mathbf{L2}]$ at 388 nm. (T=298K, [**L2**] = 3.22×10^{-6} M, λ_{exc} = 316 nm).

In compound **L3**, insertion of an additional alanine between the chromophore and the cysteine leads to an elongation of the spacer between the receptor and the signalling units. This has interesting effects on the complexation ability of this compound. Figure 7.3 shows the absorption (A) and the emission (B) spectra of **L3** upon addition of increasing amounts of Hg^{2+}.

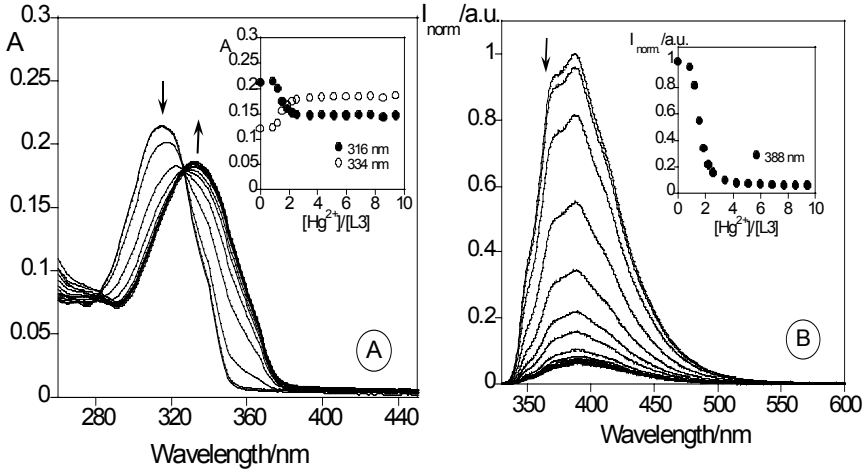

Figure 7.3. Spectrophotometric (A) and spectrofluorimetric titration (B) of **L3** in the presence of Hg^{2+} in abs. Ethanol solution. The inset represents the absorption at 316 nm and 334 nm (A), and the emission (B) at 388 nm, as a function of $[Hg^{2+}]/[\mathbf{L3}]$. (T=298K, [**L3**] = 8.8×10^{-6} M, λ_{exc} = 316 nm).

In particular, the addition of the first equivalent of Hg^{2+} did not induce any change in the spectra of **L3**, while the addition of a second equivalent caused a significant absorption change, with an isosbestic point at 328 nm, and an emission quenching of 95%. This can suggest the complexation of the first metal ion by the peptide far from the chromophore, and a second complexation processes involving the donor atoms present on the chromophore[17]

All the results discussed so far show that the insertion of alanine moieties on going from **L1** to **L3** leads to a higher affinity and sensitivity towards Hg^{2+} ions, and this is of particular interest for the design of more and more efficient chemosensors.

Among the other cations studied, only Ag^{+} induced some spectral changes, namely a red shift in the absorption spectra of 6 nm (λ =316 – 322 nm) and a 65% quenching of the emission intensity (data not shown), but with smaller association constants.

With the aim to introduce an additional chromophore in the peptide skeleton to enrich the photophysical properties, an emissive tryptophan unit was added to **L3**, yielding the tripeptide **L4**. In this case, the absorption spectra after the addition of increasing amounts of Hg^{2+} did not show any change, while the fluorescence intensity is again strongly quenched (by *ca.* 80%, figure S7.3). It has to be noted that the estimated association constant (2:1; M:L) with Hg^{2+} for **L4** is the highest observed with Hg^{2+} among all the peptides reported here. Interestingly, a relative enhancement of the fluorescence of 14% for Ag^{+} and of 23% for Zn^{2+} was also observed, while no changes were recorded for other metal ions (Cu^{2+}, Ni^{2+}, Cd^{2+}, and Pb^{2+}).

Compound **L6**, a dipeptide containing the bithienyl-benzo[*d*]oxazole chromophore, showed changes upon addition of various metal ions, namely $Cu^{2+,}$ Zn^{2+}, Ag^{+}, and Hg^{2+} only in the emission spectra. In particular, addition of one equivalent of Cu^{2+} or Hg^{2+} induces a quenching on the fluorescence emission *ca.* of 20%. On the other hand, addition of Zn^{2+} or Ag^{+} to **L6** induced a small emission increase of *ca.* of 12% and 14%.

As already observed for the series **L1** - **L3**, the insertion of an alanine moiety into the backbone of **L6** to give **L7** changed dramatically its response to the presence of transition metal ions. In particular, the addition of Ag^{+} ions (Figure S7.4) induced a small decrease and a red shift ($\Delta\lambda$ =11 nm) in the absorption spectra, and an increase of 45% of the intensity of the emission, that is also red-shifted ($\Delta\lambda$ =15 nm). As it can be seen from figure 7.4, the addition of Hg^{2+} induced even more pronounced spectral changes. In particular, as already observed for **L3**, the first equivalent of Hg^{2+} did not induce any spectral change, while the second equivalent caused a decrease in the absorbance in the range of 366-383 nm, and an increase at higher wavelength, with an isosbestic point at λ = 383 nm. The colour of the solution changed consequently from colourless to yellow. The strong quenching (92%) of the fluorescence emission is also accompanied by a large red shift in the emission band from 440 to 480 nm. This result is of interest since it makes

L7 a ratiometric chemosensor. As far as the association constants of **L6** and **L7** are concerned, unfortunately it was only possible to obtain the formation constant for compound **L7** with Hg^{2+} (log β_{11} (M:L – 1:1) = 4.49±0.21, and log β_{11} (M:L – 2:1) = 8.90 ± 0.08), indicating that the introduction of the second thiophene ring reduced the affinity towards these ions.

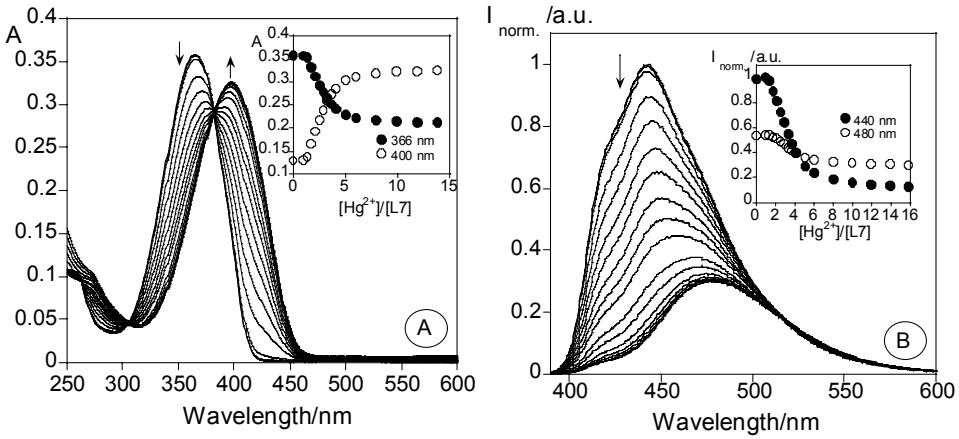

Figure 7.4. Spectrophotometric (A) and spectrofluorimetric (B) titration of **L7** in the presence of Hg^{2+} in absolute ethanol solution. The inset represents the absorption at 366 nm and 400 nm (A), and the emission (B) at 440 nm and 480 nm, as a function of $[Hg^{2+}]/[\mathbf{L7}]$. (T=298K, [**L7**] = 7.69×10^{-6}M, $[Hg(CF_3SO_3)_2]$=3.76×10^{-3}M, λ_{exc} = 366 nm).

7.5.4 - MALDI-TOF-MS Studies

In order to explore the possible applications of these new species as MALDI-TOF-MS active matrices, peptides **L1** - **L4** were studied directly, without the help of any other external organic matrix.

To perform the metal titrations, two different strategies were explored: a dried droplet solution and a layer-by-layer deposition sample preparation. First, two solutions containing compound **(L1** or **L3)** (1 µL) and the metal salt (1 µL) were mixed and shake and then applied in the MALDI-TOF-MS sample holder. The second method consisted of a layer by layer deposition of different solutions: i) a solution of peptides **L1** or **L3** was spotted in the MALDI-TOF-MS plate and then dried in vacuum; subsequently, 1 µL of the solution containing the metal salt was placed on the sample holder and dried. Finally, the plate was then inserted in the ion source. For this second case, the complexation reaction between the ligand and the metal salts occurred in the holder, and the complex species were produced in gas phase.

In general, the peaks corresponding to the protonated ligand and several fragments were perfectly observed (See table 7.3, scheme 7.2)

Table 7.3. MALDI-TOF-MS peaks of free compounds **L1** to **L7**.

Peptides	Species	MALDI-TOF-MS calc.(found)%
L1	LH^+	596.7(596.5) 25%
	$LH^+.5H_2O$	686.7(686.4) 68%
	[L-Boc] H^+	496.6(496.4) 40%
	$C_{11}H_7NOS.\ Na^+$	225(225.6) 100%
L2	LH^+	582.7(582.5) 25%
	[L-Boc] H^+	482.6(482.5) 5%
	$C_{11}H_7NOS.\ Na^+$	225(225.6) 100%
	[L-Boc. H]$^{2+}$	242.8(242.5) 50%
L3	LH^+	667.8(667.5) 10%
	[L-Boc] H^+	567.8(567.5) 55%
	$C_{15}H_{14}N_2O_3S.H^+$	303 (303.5) 100%
L4	LNa^+	984(983.6) 20%
	[L-Boc] Na^+	884(884.5) 15%
	$C_{34}H_{33}N_5O_3S_2.H^+$	625 (625.8) 98%
	$C_{35}H_{33}N_5O_5S_2.H^+$	669(669.8) 85%
	$C_{11}H_7NOS.H^+.CH_3CN$	243.2(243.5) 100%
L5	LH^+	385.06(385.06) 100%
L6	LNa+	700.1(700.03) 10%
L7	[L-Boc]Na+	599.2(599.9) 45%
	[L-Boc]H+	649.1(649.5) 20 %
	[L-Boc-Bzn]H+MeOH	633.2(633.4) 25%
	$[C_{22}H_{21}N_3O_4S_2H]^+$	456.1 (456.5) 35%
	$[C_{19}H_{16}N_2O_3S_2H]^+$	385.1 (385.5) 100%

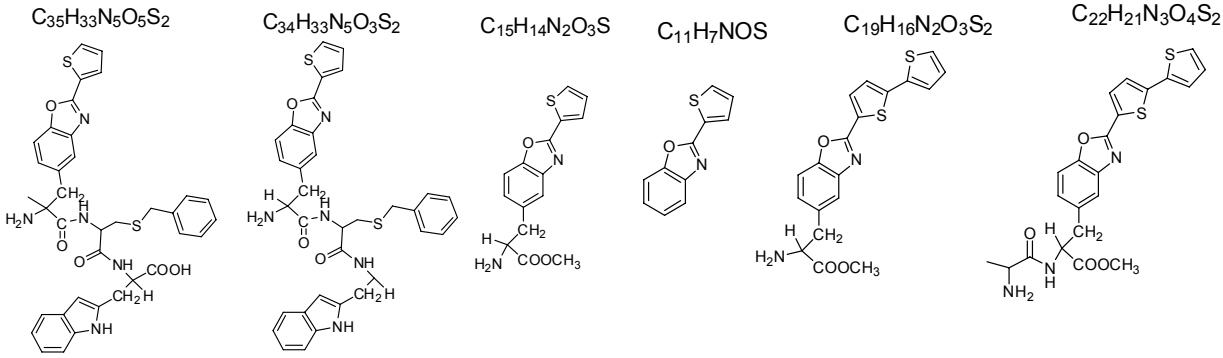

Scheme 7.2. Fragments of the ligands obtained on MALDI-TOF-MS.

Compounds **L1** and **L3** were also titrated with one or two equivalent of Ag^+, Cu^{2+} or Hg^{2+}

(Table 7.4). The formation of the mononuclear and dinuclear complexes was followed by the appearance of several peaks attributable to the metal complexes. The detected intense peaks especially upon addition of Cu^{2+} or Hg^{2+}, confirming the affinity trends observed in solution.

Table 7.4**.** MALDI-TOF-MS most important peaks of compounds **L1** and **L3** in the presence of 1 or 2 equivalents of Ag^{+}, Cu^{2+} and Hg^{2+}.

Peptides	Metal	Species	MALDI-TOF-MS calc.(found)%
L1	Ag^{+}	L1 Ag^{+}	702.7(702.6) 53%
		$(L1.2AgBF_4)^{+}$	897.3(897.5) 15%
	Cu^{2+}	$L1.2Cu^{2+}.3CF_3SO_3^{-}Na^{+}$	589.5(589.4) 30%
	Hg^{2+}	$L1H^{+}2Hg(CF_3SO_3)_4\ Na^{+}$	809 (809.6) 15%
L3	Ag^{+}	L3 Ag^{+}	775(775.5) 35%
		$[L3 –Boc.\ Ag]^{+}$	675(675.4) 60%
	Cu^{2+}	$L3H^{+}.2Cu^{2+}.3CF_3SO_3^{-}.H_2O$	629.5(629.5) 100%
		$L3.2Cu^{2+}.3CF_3SO_3^{-}Na^{+}$	631.9(631.5) 80%
		$L3H^{+}.2Cu^{2+}.4CF_3SO_3^{-}$ $.CH_3CH_2OH.Na^{+}$	730(729.6) 55%
	Hg^{2+}	$L3H^{+}.Hg(CF_3SO_3^{-})\ 2H_2O.Na^{+}$	538.5(538.5)50%

7.5.5 - Gold nanoparticles and TEM measurements

In order to study the effect of the peptide length in stabilizing AuNPs, amino acid **L** (Boc-BOT-OH) and **L3** (tripeptide Boc-Ala-Cys(Bzl)-BOT-OMe) were selected for the synthesis of decorated AuNPs. In general, the synthetic procedure of AuNPs was based on the reduction of $AuCl_4^{-}$ in dichloromethane with $NaBH_4$, in the presence of the compound derivatize with a suitable cross-linker dithiobis(succinimidylpropionate) (DSP) (See Scheme 7.3).

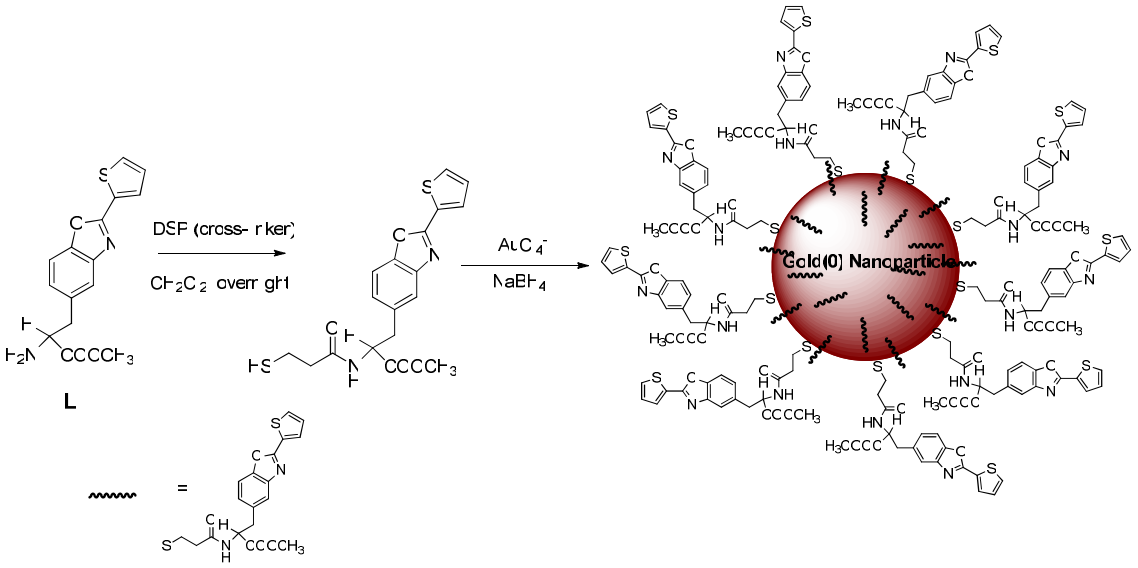

Scheme 7.3. General synthesis of decorated AuNPs

The formation of the nanoparticles could be followed by the appearance of the gold plasmonic resonance band centred at 520 nm (see figure 7.5A), accompanied by a colour change from orange/yellow to dark red. The size of the nanoparticles were measured by dynamic light-scattering (DLS) and TEM. The AuNPs prepared using **L** showed a hydrodynamic diameter measured by DLS of *ca.* 4.2 nm, while the nanoparticles obtained with compound **L3** showed larger hydrodynamic diameter of *ca*. 15.0 nm. TEM images of the nanoparticles with compound **L** showed a core radius of *ca.* 2.4 nm being monodispersed (See figure 7.5B), while for the ones with compound **L3** we observed a polydispersed distribution with a core diameter between 3.3 and 9.8 nm. This result could probably be due to some π-π stacking interaction between the thienyl-benzo[*d*]oxazole moieties present in the **L3** peptide and to its possibility to form different flexible conformers on the gold nanoparticle surface due to its longer peptide chain.

In both cases, as far as emission properties are concerned, we observed a complete quenching after their binding to the gold core. From one side, these results probe the total absence of free ligand in solution, but from the other side the fluorescence suppression observed in both nanoparticles unfortunately prevented any further studies using the synthesized nanoparticles as fluorescent metal ion chemosensors.

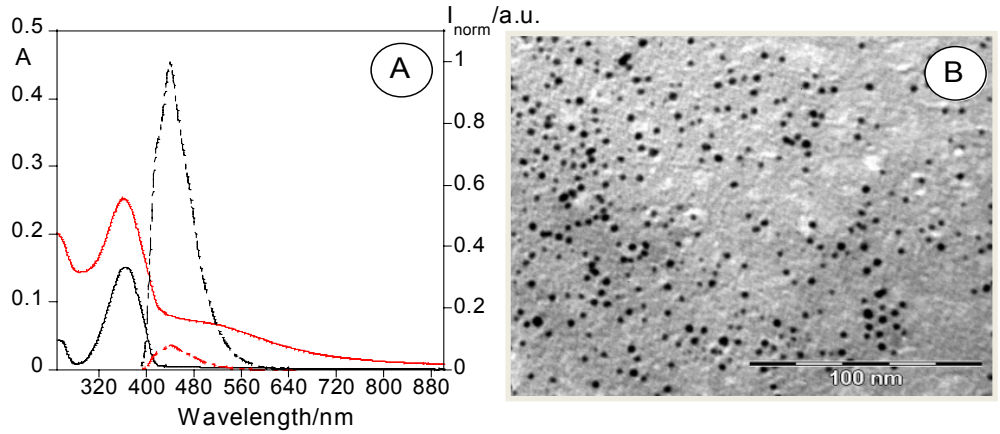

Figure 7.5. (A) Absorption (full line) and emission (dotted line) spectra of **L** (black line) and its gold(0) nanoparticles (red line) in dichloromethane. (T=298K, λ_{exc} = 316 nm). (B) TEM picture of AuNPs functionalized with **L**

7.5.6 - Silica nanoparticles obtained by surface derivatization.

The first strategy followed to combine the peptides with transparent silica nanoparticles was to derivatize **L6** or **L7** with an alkoxysilane group, and then to anchor them to the surface of commercial Ludox silica nanoparticles, since it had already been demonstrated that this is a useful method to modify the nanoparticles surface (see Scheme 7.4).[21]

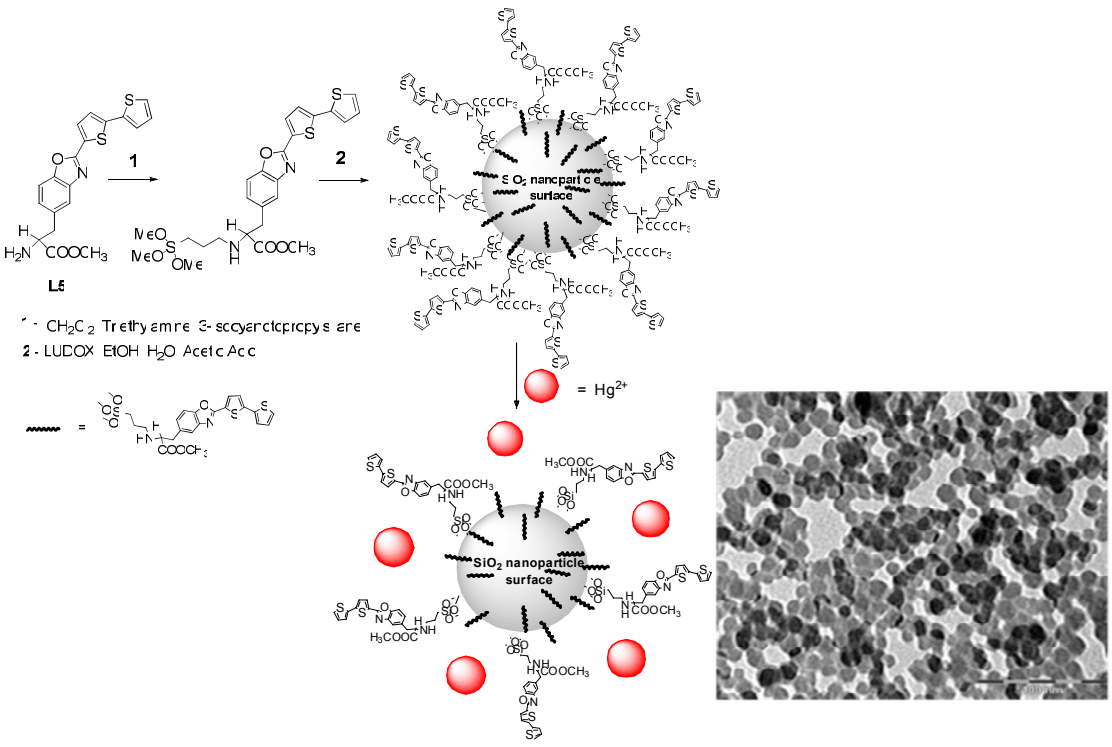

Scheme 7.4. General Synthetic pathway for silica nanoparticles. TEM image of silica nanoparticles with compound **L5** in absolute ethanol.

These synthesis were made by using different compound:Ludox ratios. An average number of 94, 29 and 27 molecules of **L5**, **L6** and **L7** compounds per nanoparticle of Ludox, respectively, were possible to determinate. The absorption and emission spectra of the derivatize nanoparticles were very similar to the ones of the free ligands because, from one hand, the silica nanoparticles are totally transparent to the visible light and inert to electron-transfer processes,[14] and, from the other hand, the photophysics of these peptides was scarcely affected by the environment, as previously discussed. The size of all nanoparticles obtained was measured by dynamic light-scattering. Sizes between 150 nm for **L5**, 665 nm for **L6** and 6900 nm for **L7** were observed, demonstrating that the derivatization with the peptides induced the aggregation of the Ludox nanoparticles, aggregation that became more pronounced by increasing the length of the peptide chain, as was observed above for AuNPs.

In order to apply these fluorescent probes as new sophisticate metal ion chemosensors for bioapplications, the characterization of nanoparticles with peptides **L5** to **L7** was also performed by the absorption and emission fluorescence spectra obtained in the NanoDrop instruments in order to study the application and reproducibility in mL sample as new proteomics platforms. Two mL of each nanoparticles were used in each experiment. In Figure S7.5 are reported the spectrofluorimetric titration of the silica nanoparticles with compound **L5** in the presence of Ag^{+} (A) and Hg^{2+} (B). In both cases the absorption spectra were not affected by the metal ion. On the other hand, the fluorescence intensity was quenched by 20% and 80% upon addition of Ag^{+} or Hg^{2+}, respectively. The affinity to Hg^{2+} ions was increased in the case of the nanoparticles decorated with compound **L6** (see Figure 7.6, Panel B).

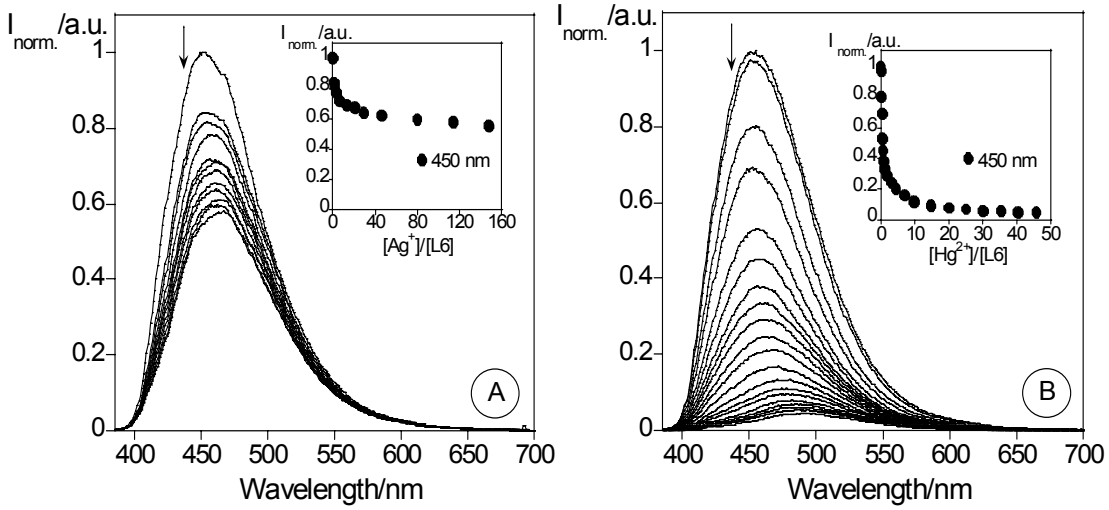

Figure 7.6. Spectrofluorimetric titration of silica nanoparticles of compound **L6** (ratio 1:1, ligand-ludox), with the addition of Ag^{+} (A) and Hg^{2+} (B) in absolute ethanol. The inset

represents the emission at 450 nm, as a function of $[Ag^+]/[\mathbf{L6}]$ (A) and as a function of $[Hg^{2+}]/[\mathbf{L6}]$. (**[L6]** = 7.71×10^{-6} M, λ_{exc} = 368 nm, T=298K).

It is interesting to note that contrary to observed for the free compounds **L5** and **L6**, when titrated with Ag^+, the increase on the emission intensity was changed for the nanoparticles decorated with the same compounds to an emission quenching; this quenching was probably due to the short distance between the chromophores around the nanoparticles. Addition of 5 equivalents of Hg^{2+} to the nanoparticles with **L7**, showed an emission quenching of 90%, at the same time a blue shift from 460 to 440 nm was observed, as shown in Figure 7.7.

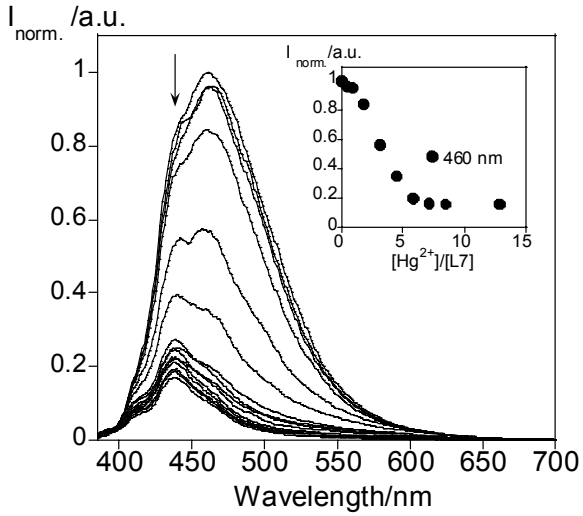

Figure 7.7. Spectrofluorimetric titration of silica nanoparticles of compound **L7** (ratio 1:1, ligand-ludox), with the addition of Hg^{2+} in dichloromethane. The inset represents the emission at 460 nm, as a function of $[Hg^{2+}]/[\mathbf{L7}]$. (**[L7]** = 2.14×10^{-6} M, λ_{exc} = 373 nm, T=298K).

Interestingly, it was possible to observe a decrease on the nanoparticle size upon addition of Hg^{2+} namely from 665 nm to 46 nm for **L6**, and from 6936 nm to 57 nm for **L7**. These results shows that complexation of Hg^{2+} ion induced a decrease on the aggregation of the nanoparticles, reducing the π-π^* interaction between the (bi)thienyl-benzo[*d*]oxazole chromophores.

Comparing the free compounds **L5** to **L7**, and those linked to the nanoparticles, it could be concluded that the nanoparticles of compounds **L5** and **L6** were more sensitive for Hg^{2+}, resulting in a more intensive quenching with the same amount of metal ion. However, in compound **L7** the sensitivity was practically not affected.

7.5.7 - The use of core/shell water soluble silica nanoparticles

We have recently developed a new one-pot approach for the synthesis of water-soluble core-shell dye-doped silica nanoparticles (CSNPs) based on the preparation of micelles of Pluronic F127 in water.[22] The final material is a versatile multi-compartment system characterized by a high water solubility, stability, and brightness. Most interestingly, we have very recently demonstrated the possibility to host in the outer PEG shell water insoluble dyes, that are able to give rise to very efficient energy transfer processes with the molecules hosted in the core, if present.[23] In an attempt to make the peptides operate in water, 10^{-4} M DMSO solutions of **L3** - **L5** were prepared. Small aliquots (1 to 10 microliters) of such solutions were then injected in 2.5 mL of a water dispersion containing CSNPs 10^{-7} M (Scheme 7.7). Despite their poor solubility in pure water, when the CSNPs were present, the peptides became soluble and visible in the absorption and emission spectra, which matched the ones of the same compounds in absolute ethanol. In addition, contrary to what was observed for the same compounds in abs. ethanol (in which the anisotropy was almost negligible), in CSNPs the emissions showed a higher anisotropy (> 0.2), clearly confirming that the peptides were located in the outer hydrophobic PEG shell of the nanoparticles, where they experienced a reduced rotational freedom, forming the system **Lx**@NPs.

Among all the peptides studied, **L3** showed, in these conditions, the most pronounced changes upon addition of both Ag^{+} and Hg^{2+}, as it can be seen from Figure 7.8. Although the association constants are smaller than those previously discussed, it is important to note, in this latter case, the use of water as solvent.

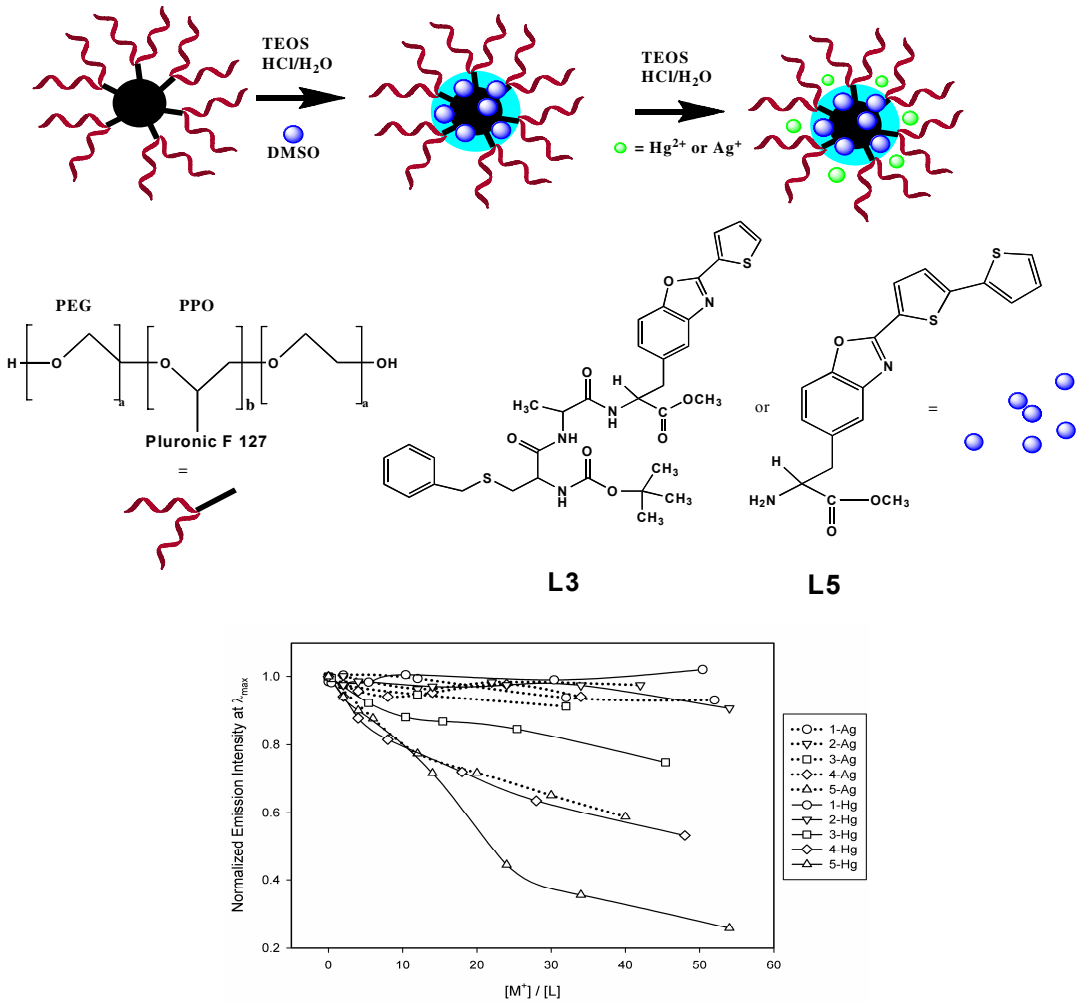

Figure 7.8. Water-soluble core-shell dye-doped silica nanoparticles decorated with **L3** or **L5** in the presence of Ag^{+} and Hg^{2+}.

7.6 - Conclusions

A new family of bio-inspired fluorescent peptide-based chemosensors, **L1** to **L7**, was successfully synthesized and characterized. All compounds have been studied by elemental analyses, MALDI-TOF-MS spectrometry, infrared, ^{1}H and ^{13}C NMR, UV-vis, and emission fluorescence spectroscopy.

These peptides showed in general high relative fluorescence quantum yields. Their study as fluorescent chemosensors was performed in ethanol solutions and in gas phase, using absorption and fluorescence emission spectroscopy and MALDI-TOF mass spectrometry. In all cases, the strongest affinity and sensitivity were observed in the presence of the heavy and pollutant Hg^{2+} ions. The results showed that the insertion of an alanine residue on going from **L1** to **L3** and from **L6** to **L7** increased the affinity towards Hg^{2+} ions thanks to a higher flexibility, an interesting result for the design of more and more efficient chemosensors.

Stable non-emissive gold(0) nanoparticles decorated with systems **L** and **L3** were successfully obtained using the Brust strategy.[24] TEM measurements showed monodispersed nanoparticles with a diameter of 2.4 nm for the **L** system and more polydispersed nanoparticles with a diameter between 3.3 and 9.8 nm for the **L3** one.

In addition, three groups of silica nanoparticles were successfully obtained with peptides **L5** - **L7** by covalently linking them to the surface of commercial Ludox. In these cases, due to the inert nature of silica, the nanoparticles resulted to be highly luminescent, in line with the behaviour of the starting peptides. These new hybrid systems were able to efficiently complex Hg^{2+} and Ag^{+} ions, with a concomitant quenching of the fluorescence intensity.

Finally, we were able to dissolve the studied peptides in water inserting them in the outer PEG shell of silica core/PEG shell nanoparticles recently developed in our laboratories. In these conditions, **L3** was able to signal the presence in water of Hg^{2+} and Ag^{+} ions, enlarging the possibilities offered by this family of bio-inspired chemosensors.

7.7 - Acknowledgements

We would like to thank Xunta de Galiza (Spain) for project 09CSA043383PR (Biomedicine) and the University of Vigo for projects INOU UVIGO/VICOU/K914-122P64702/2009 and UVIGO/VICOU/K912-122P64702/2009. Thanks to the FCT-MCTES/FEDER (Portugal) through national project PDTC/QUI/66250/2006 (FCOMP-01-0124-FEDER-007428). Financial support from MIUR (PRIN and FIRB projects) and from Fondazione Cassa di Risparmio in Bologna is also gratefully acknowledged. E. O. thanks FCT/Portugal for a PhD

grant (SFRH/BD/35905/2007), and Fundação Calouste Gulbenkian for the Prize 2008 in Excellence in Research (Estímulo à Creatividade e a Qualidade na Actividade de Investigação). C.L. and J.L. thank Xunta de Galicia for the Isidro Parga Pondal Research Program. C.L. thanks the Royal Society of Chemistry for a Journal Grant for International Authors 2008. The NMR spectrometer Bruker Avance III 400 is part of the National NMR Network and was purchased within the framework of the National Program for Scientific Re-equipment, contract REDE/1517/RMN/2005 with funds from POCI 2010 (FEDER) and FCT.

7.8 - Electronic Supplementary Information (ESI) available.

Spectrophotometric and spectrofluorimetric titrations of **L1**, **L2** and **L4**, with Hg^{2+} in absolute ethanol and **L7** in the presence of Ag^{+}. Spectrofluorimetric titration of silica nanoparticles of compound **L5** with the addition of Ag^{+} and Hg^{2+} in absolute ethanol; TEM images of gold silica nanoparticles with compound **L3** and **L6**.

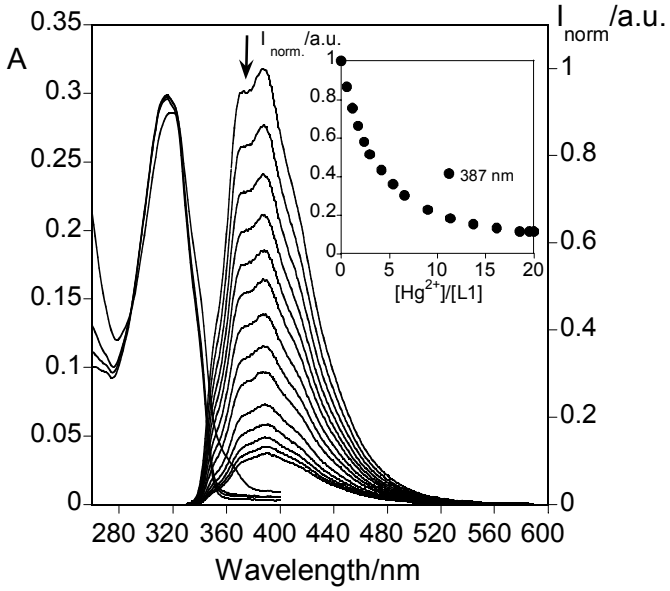

Figure S7.1 Absorption and emission spectra of **L1** in the presence of Hg^{2+} in abs. ethanol solution. The Inset represents the intensity of emission as a function of $[Hg^{2+}]/[\mathbf{L1}]$ at 387 nm. (T=298K, [**L1**] = 1.26×10^{-5} M, λ_{exc} = 316 nm).

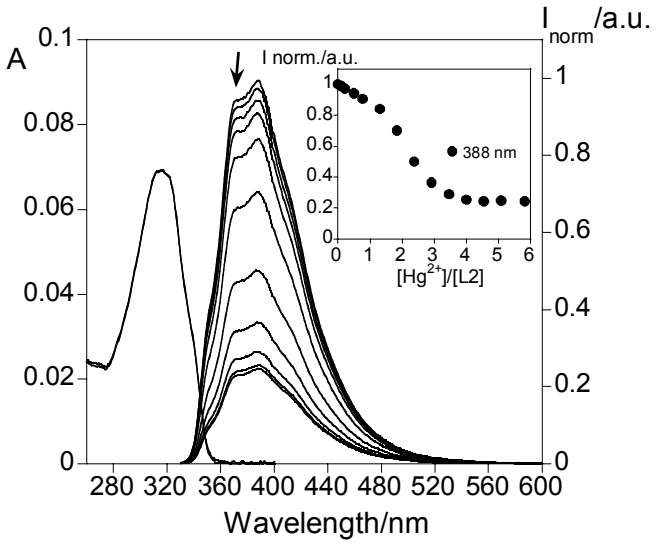

Figure S7.2 Absorption and emission spectra of **L2** in the presence of Hg^{2+} in absolute ethanol solution. The inset shows the intensity of emission as a function of $[Hg^{2+}]/[\mathbf{L2}]$ at 388 nm. (T=298K, [**L2**] = 3.22×10^{-6} M, λ_{exc} = 316 nm).

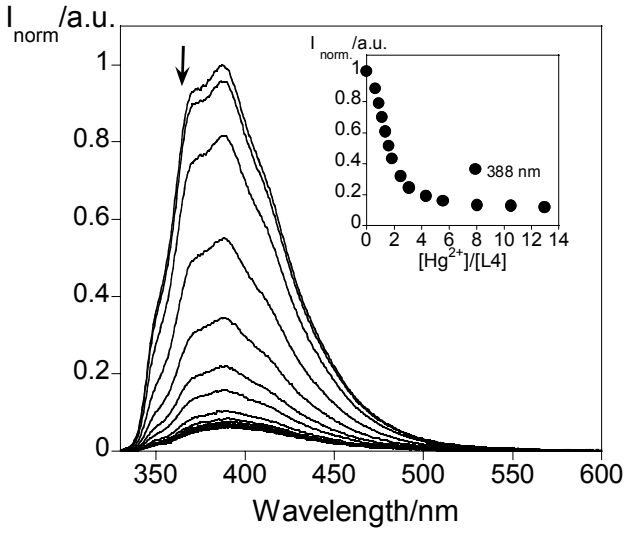

Figure S7.3 Absorption and emission spectra of **L4** in the presence of Hg^{2+} in abs. ethanol solution. The inset represents the intensity of emission as a function of $[Hg^{2+}]/[\mathbf{L4}]$ at 388.5 nm. (T=298K, [**L4**] = 1.22×10^{-5} M, λ_{exc} = 316 nm).

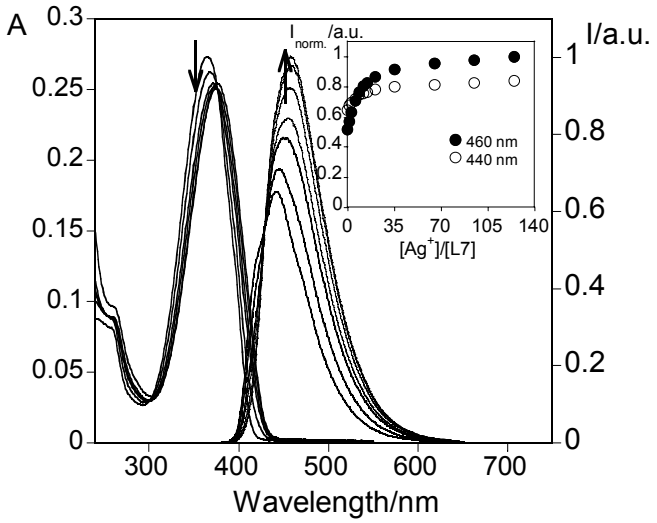

Figure S7.4 Spectrophotometric and spectrofluorimetric titration in absolute ethanol of compound **L7** with addition of an ethanolic solution of $Ag(BF_4)$. [**L7**]= 7.69×10^{-6} M, [$Ag(BF_4)$] = 5.70×10^{-3} M, T=298 K, λ_{exc} = 366 nm. The inset shows the intensity of emission as a function of [Ag^+/[**L7**] at 440 and 460 nm.

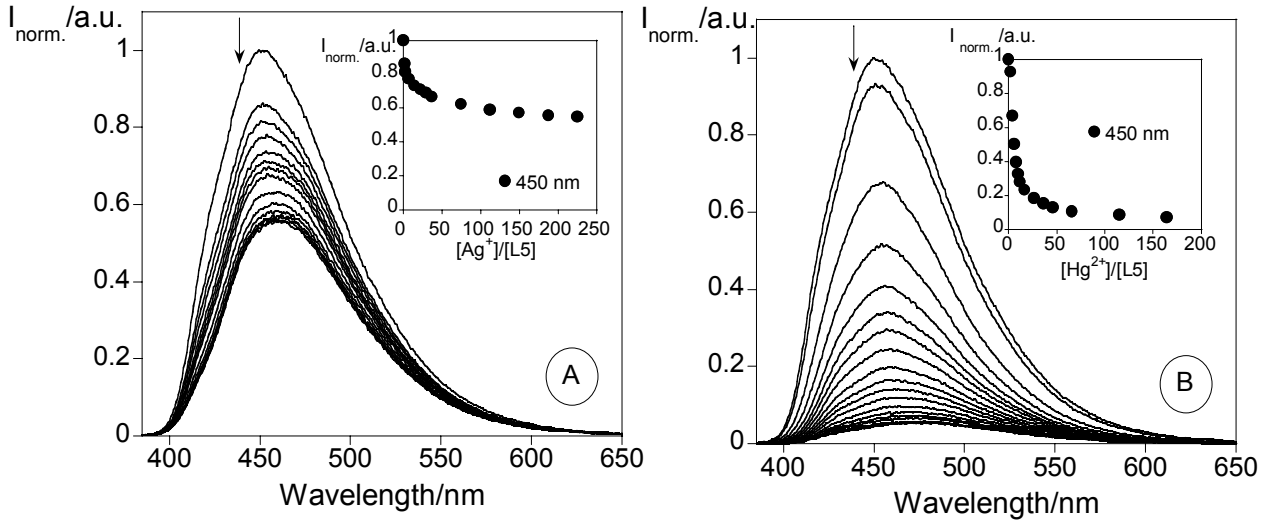

Figure S7.5 Spectrofluorimetric titration of silica nanoparticles of compound **L5** with the addition of Ag^+ (A) and Hg^{2+} (B) in absolute ethanol. The inset represents the emission at 450 nm, as a function of [Ag^+]/[**L5**] (A) and as a function of [Hg^{2+}]/[**L5**]. ([L5] = 8.45×10^{-6} M, λ_{exc} = 368 nm, T=298K).

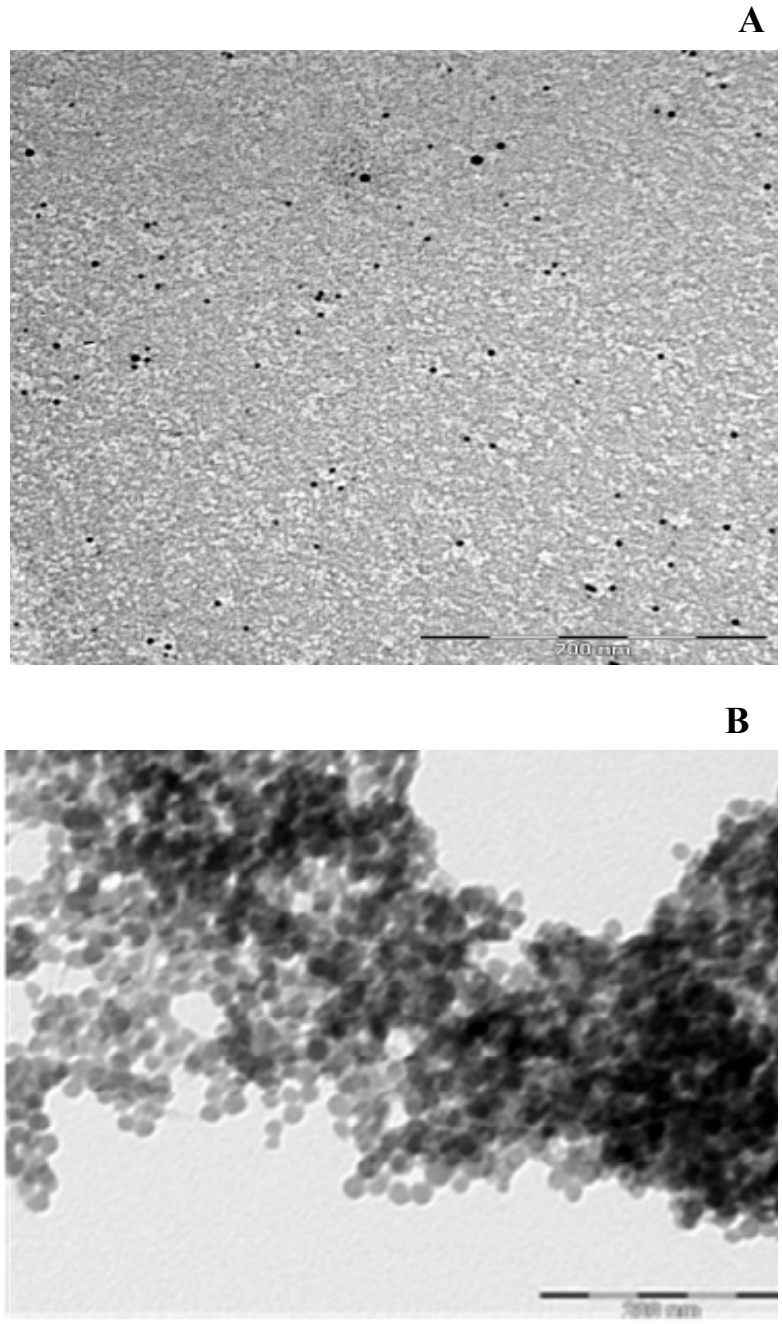

Figure S7.6 TEM image of gold nanoparticles (A) and silica nanoparticles (B) with compounds **L3** in dichloromethane and **L6** in absolute ethanol.

7.9 - References

(1) (a) Czarnik, A.W. *Acc. Chem. Res.* **1994**, *21*, 302-308; Lodeiro, C.; Pina, F. *Coord. Chem. Rev.* **2009**, *253*, 1353-1383. (b) Lodeiro, C.; Capelo, J. L.; Mejuto, J. C.; Oliveira, E.; Santos, H. M.; Pedras, B.; Nuñez, C. *Chem. Soc. Rev*. **2010**, *39*, 2948-2976.

(2) (a) Ulijn, R. V.; Smith, A. M. *Chem. Soc. Rev*. **2008**, *37*, 664-675. (b) Cavalli, S.; Albericio, F.; Kros, A. *Chem. Soc. Rev.* **2010**, *39*, 241-263. (c) Sawada, T.; Takahashi, T.; Mihara, H. *J. Am. Chem. Soc.* **2009**, *131*, 14434-14441.

(3) (a) Guzow, K.; Milewska, M.; Wróblewski, D.; Gieldón, A.; Wiczk, W. *Tetrahedron* **2004**, *60*, 11889-11894. (b) Milewska, M.; Skwierawska, A.; Guzow, K.; Szmigiel, D.; Wiczk, W. *Inorg. Chem. Commun*. **2005**, *8*, 947-950.

(4) Joshi, B. P.; Cho, W-M.; Kim, J.; Yoon, J.; Lee, K-H; *Bioorg. Med. Chem. Lett.* **2007**, *17*, 6425-6429.

(5) Zheng, Y.; Cao, X.; Orbulescu, J.; Konka, V.; Andreopoulos, F. M.; Phan, S. M.; Leblanc, R. M.; *Anal. Chem.* **2003**, *75*, 1706-1712.

(6) Li, Y.; Yang, M. *J. Am. Chem. Soc.*, **2005**, *127*, 3527-3530.

(7) McGrath, M. E.; Sprengeler, P. A.; Hill, C. M.; Martichonok, V.; Cheung, H.; Somoza, J. R.; Palmer, J. T.; Janc, J. W. *Biochemistry* **2003**, *42*, 15018-15028.

(8) Prodi, L. *New J. Chem.* **2005**, *29*, 20-31.

(9) Bonacchi, S.; Genovese, D.; Juris, R.; Mancin, F.; Montalti, M.; Prodi, L.; Rampazzo, E.; Zaccheroni, N.; in *Handbook of Porphyrin Science*, ed. Kadish, K. M.; Smith, K. M.; Guilard, R.; World Scientific, New York **2010**, Vol. 12, Ch. 5.

(10) (a) Boisselier, E.; Astruc, D. *Chem. Soc. Rev.* **2009**, *38*, 1759-1782. (b) Aili, D.; Stevens, M. M. *Chem. Soc. Rev.* **2010**, *39*, 3358-3370. (c) Klajn, R.; Stoddart, J. F.; Grzybowski, B. A. *Chem. Soc. Rev.* **2010**, *39*, 2203-2237. (d) Bunz, U. H. F.; Rotello, V. M. *Angew. Chem. Int. Ed.* **2010**, *49*, 3268-3279. (e) Giljohann, D. A.; Seferos, D. S.; Daniel, W. L.; Massich, M. D.; Patel, P. C.; Mirkin, C. A. *Angew. Chem. Int. Ed.* **2010**, *49*, 3280-3294. (f) Liu, S. Q.; Z. Tang, Y. *J. Mat. Chem.* **2010**, *20*, 24-35.

(11) (a) Vial, St.; Mansuy, C.; Sagan, S.; Irinopoulou, T.; Burlina, F.; Boudou, J.-P.; Chassaing, G.; Lavielle, S. *ChemBioChem.* **2008**, *9*, 213-2119. (b) Knecht, M. R.; Scthi, M. *Anal. Bioanal. Chem.* **2009**, *394*, 33-46. (c) Wang, Z.; Ma, L. *Coord. Chem. Rev.* **2009**, *253*, 1607-1618.

(12) (a) Montalti, M.; Prodi, L.; Zaccheroni, N.; Beltrame, M.; Morotti, T.; Quici, S. *New J. Chem.* **2007**, *31*, 102-108. (b) Montalti, M.; Zaccheroni, N.; Prodi, L.; O'Reilly, N.;. James, S. L. *J. Am. Chem. Soc.* **2007**, *129*, 2418-2419. (c) Montalti, M.; Prodi, L.; Zaccheroni, N.; Battistini, G. *Langmuir* **2004**, *20,* 7884-7886. (d) Montalti, M.; Prodi, L.; Zaccheroni, N.; Baxter, R.; Teobaldi, G.; Zerbetto, F. *Langmuir* **2003**, *19,* 5172-5174.

(13) He, X.; Liu, H.; Li, Y.; Wang, S.; Li, Y.; Wang, N.; Xiao, J.; Xu, X.; Zhu, D. *Adv. Mater.* **2005**, *17*, 2811-2815.

(14) (a) Burns, A.; Ow, H.; Wiesner, U. *Chem. Soc. Rev.* **2006**, *35*, 1028-1042. (b) Wang, L.; Wang, K. M.; Santra, S.; Zhao, X. J.; Hilliard, L. R.; Smith, J. E.; Wu, J. R.; Tan, W. H. *Anal. Chem.* **2006**, *78*, 646-654. (c) Yong, K. T.; Roy, I.; Swihart, M. T.; Prasad, P. N. *Mater. Chem.* **2009**, *19*, 4655-4672.

(15) (a) Burns, A.; Sengupta, P.; Zedayko, T.; Baird, B.; Wiesner, U. *Small* **2006**, *2*, 723–726. (b) Arduini, M.; Rampazzo, E.; Manicn, F.; Tecilla, P.; Tonellato U. *Inorg. Chim. Acta* **2007**, *360*, 721-727. (c) Doussineau, T.; Shulz, A.; Lapresta-Fernandez, A.; Moro, A.; Körsten, S.; Trupp, S.; Mohr, G. J. *Chem. Eur. J.* DOI: 10.1002/chem.201000829. (d) Montalti, M.; Prodi, L.; Zaccheroni, N. *J. Mater. Chem.* **2005**, *15*, 2810–2814. (e) Bonacchi, S.; Rampazzo, E.; Montalti, M.; Prodi, L.; Zaccheroni, N.; Mancin, F.; Teolato, P. *Langmuir* **2008**, *24*, 8387-8392. (f) Zanarini, S.; Rampazzo, E.; Ciana, Della L.; Marcaccio, M.; Marzocchi, E.; Montalti, M.; Paolucci, F.; Prodi, L. *J. Am. Chem. Soc.* **2009**, *131*, 2260-2267. (g) Seo, S.; Lee, H. Y.; Park, M.; Lim, J. M.; Kang, D.; Yoon, J.; Jung, J. H. *Eur. J. Inorg. Chem.* **2010**, 843-847.

(16) (a) Si, S.; Kotal, A.; Mandal, T. K. *J. Phys. Chem. C.*, **2007**, *111*, 1248-1255. (b)

(17) (a) Costa, S. P. G.; Oliveira, E.; Lodeiro, C.; Raposo, M. M. M. *Sensors*, **2007**, *7*, 2096-2114. (b) Costa, S. P. G.; Oliveira, E.; Lodeiro, C.; Raposo, M. M. M. *Tetrahedron Lett.* **2008**, *49*, 5258-5261. (c) Oliveira, E.; Costa, S. P. G.; Raposo, M. M. M.; Lodeiro, C.; *Inorg. Chim. Acta*., **2010**, in press.

(18) (a) Berlman, I. B.; *Handbook of Fluorescence Spectra of Aromatic Molecules*, 2nd ed.; Academic Press: New York, **1971**. (b) Montalti, M.; Credi, A.; Prodi, L.; Gandolfi, M. T.; *Handbook of Photochemistry*, 3rd Ed. Taylor & Francis, Boca Raton, **2006**.

(19) (a) Friggeri, A.; Montalti, M.; Dolci, L. S.; Prodi, L.; Zaccheroni, N.; Stuart, M. C. A.; van Bommel, K. J. C. *Langmuir* **2006**, *22*, 2299-2303. (b) Montalti, M.; Prodi, L.; Zaccheroni, N.; Battistini, G.; Marcuz, S.; Mancin, F.; Rampazzo, E.; Tonellato, U. *Langmuir* **2006**, *22*, 5877-5881.

(20) SPECFIT/32 Global Analysis System, v. 3.0; Spectrum Software Associates, Malborough, MA, U.S.A.

(21) Montalti, M.; Prodi, L.; Zaccheroni, N.; Falini, G. *J. Am. Chem. Soc*. **2002,** *124*, 45, 13540-13546.

(22) Zanarini, S.; Rampazzo, E.; Bonacchi, S.; Juris, R.; Marcaccio, M.; Montalti, M.; Paolucci, F.; Prodi, L. *J. Am. Chem. Soc.* **2009**, *131*, 14208–14209.

(23) Rampazzo, E.; Bonacchi, S.; Juris, R.; Montalti, M.; Genovese, D.; Zaccheroni, N.; Prodi, L.; Rambaldi, D. C.; Zattoni, A.; Reschiglian, P. *J. Phys. Chem. B*, DOI: 10.1021/jp1023444.

(24) Brust, M.; Fink, J.; Bethell, D.; Schiffrin D. J.; Kiely, C. *J. Chem. Soc., Chem. Commun.*, **1995**, 1655-1656.

Chapter 8

General Conclusions

"All my life through, the new sights of Nature made me rejoice like a child"
Marie Curie

1.- A new poly-oxa-aza macrocyclic ligand provided with an anthracene emissive pendant arm was fully characterized. The photophysical characterization shows **L** as a good example of proton and metal ion chemosensor. (Chapter 2)

2.- The complexation capability of **L** towards alkaline and alkaline earths metal ions (M= Na^+, K^+, Li^+, Ca^{2+}, Mg^{2+}), as well as transition and post-transition metal ions (M= Cr^{3+}, Cu^{2+}, Zn^{2+}, Cd^{2+}, Hg^{2+} and Al^{3+}) was studied by UV-vis and fluorescence emission measurements in methanol and mixtures methanol-water. (Chapter 2)

3.- The results suggest that the anthracene ligand **L** is an effective complexation molecular device for several divalent metal ions of biological importance as well as for Al^{3+} and Cr^{3+}, both metals of great relevance in medicine and environmental chemistry.
A very promising result was observed for Al^{3+} and Cr^{3+}; the CHEF founded effect in both cases could be used as a starting point to developed a more efficiently fluorescence chemosensor based on macrocyclic ligands for these metals. (Chapter 2)

4.- Three new emissive molecular probes **1** to **3** derived from 15-crown-5-monoaza macrocyclic ligands bearing a furyl, aryl or thienyl 4,5-disubstituted imidazole system were successfully studied and used for the synthesis of Cu^{2+} and Hg^{2+} metal complexes. (Chapter 3)

5.- Through the photophysical studies, the furyl derivative compound **1** was found to be the most emissive system, ϕ = 0.87. (Chapter 3)

6.- The interaction with several metal ions (Na^+, Ca^{2+}, Cu^{2+}, Ni^{2+} e Hg^{2+}) and anions (F^-) was explored by absorption and emission spectroscopy. (Chapter 3)

7.- Compounds **2** and **3** reveals an important enhancement of the fluorescence emission in the presence of Ca^{2+}, Ni^{2+} and Cu^{2+}, being compound **3**, containing the thiophene ring, the most emissive with a quantum yield of 0.79 in the presence of one equivalent of Cu^{2+} and Ca^{2+}. (Chapter 3)

8.- Compound **3** showed a fluorescence and colorimetric chemosensorial properties for Cu^{2+}.(Chapter 3)

9.- The X-Ray structures of the ligands **2** and **3** were obtained and resolved. (Chapter 3)

10.- A new family of highly emissive alanine derivatives (**2a**-**2g**), containing a benzoxazole moiety as chromophore and bearing thiophene or trimethoxybenzaldehyde as pendant-arm were photophysically characterized by absorption and fluorescence emission spectroscopy. (Chapter 4)

11.- The interactions with Cu^{2+}, Ni^{2+} and Hg^{2+} as well as, alkaline and alkaline-earths metals were studied in absolute ethanol. The stronger interaction and the highest complexation constanst were obtained for Hg^{2+} ions. (Chapter 4)

12.- Six different heteroaromatic alanines derivatives bearing (oligo)thiophene units (**4a-c to 6a-c**) were studied in solution by absorption and fluorescence emission techniques. These compounds show high values of relative fluorescence quantum yields since 0.03 to 0.55 as a function of the number of thiophene rings located in the pendant arm. (Chapter 5)

13.- Several Cu^{2+}, Ni^{2+} and Hg^{2+} metal complexes were synthesized with four selected ligands reported in chapter 4. All analytical and spectroscopic data confirms the formation of mononuclear or dinuclear metal complexes. DFT calculations show that the first metal ion interacts with the aminoacid residue and the second metal goes directly to the chromophore. (Chapter 6)

14.- Starting from the single alanine emissive precursors reported in chapter 4 and 5, three new dipeptides (**L1, L2** and **L6**) and three new tripeptides (**L3, L4** and **L7**) compounds were synthesized and fully characterized. Alanine, cysteine and tryptophan were selected from the 20 natural aminoacids to create the chelatant peptide chain. (Chapter 7)

15.- All peptides were explored as new bio-inspired chemosensors in the presence of transition and post-transition metal ions. (Cu^{2+}, Ni^{2+}, Zn^{2+}, Cd^{2+}, Hg^{2+}, Pb^{2+} and Ag^{+}).
The best performance was obtained with Cu^{2+}, Ni^{2+}, Hg^{2+} and Ag^{+}. These results suggest the importance of the sulphur atoms in these ligands. (Chapter 7)

16.- With respect to the peptide chain, increasing the length increased the selectivity to Hg^{2+}. (Chapter 7)

17.- By $NaBH_4$ reductive method several gold(0) nanoparticles were synthesized with (**L1**-**L4**) peptides. In all cases the fluorescence emission was quenched. Through dynamic light scattering and transmission electron microscopy (TEM) monodispersed or polydispersed nanoparticles with sizes between *ca.* 2.4 nm to 9.8 were obtained depending on the peptide used. (Chapter 7)

18.- We also conclude that increasing the peptide chain increase the aggregation degree of the nanoparticles. (Chapter 7)

19.- Emissive silica nanoparticles synthesized from commercial Ludox® nanoparticles, were obtained and decorated *via* a silane spacer with compounds **L5**-**L7** . (Chapter 7)

20.- All Silica nanoparticles obtained were studied as more sophisticate chemosensors in the presence of metal ions. Strong selective for Ag^{+} and Hg^{2+} was observed. (Chapter 7)